5-2017

Impact of Using Spatially Distributed Soils Information on Flood Hydrograph Simulation with HEC-HMS

Matthew J. Nelson
University of Nebraska-Lincoln, matt_nelson21@yahoo.com

Impact of Using Spatially Distributed Soils Information on Flood Hydrograph Simulation with HEC-HMS

By

Matthew J. Nelson

A THESIS

Presented to the Faculty of

The Graduate College at the University of Nebraska

In Partial Fulfillment of Requirements

For the Degree of Master of Science

Major: Civil Engineering

Under the Supervision of Professor

Ayse Kilic

Lincoln, NE

May 2017

IMPACT OF USING SPATIALLY DISTRIBUTED SOILS INFORMATION ON FLOOD HYDROGRAPH SIMULATION WITH HEC-HMS

Matthew J. Nelson, M.S.

University of Nebraska, 2017

Advisor: Ayse Kilic

Hydrologic rainfall-runoff models employ numerical equations to simulate the soil absorption of rainfall and resulting runoff. A number of methods have been developed to model these processes, but the parameters used to define these methods can be difficult to directly measure due to the variable nature of soil properties. They often rely on estimation of hydraulic and hydrologic parameters and calibration to produce accurate results.

A challenge with runoff method parameterization is the need for oversimplification using a lumped modeling approach. While distributed hydrologic modeling techniques are now available, distributed runoff methods are limited in use due to the tradition of lumped modeling and lack of widely available runoff parameter datasets. This study sought to define modeling parameters for three runoff methods based on physical soil data contained within the Soil Survey Geographic (SSURGO) database for lumped and distributed modeling approaches. These parameters were defined for 1-foot and 3-foot soil depths for estimating controlling influences on infiltration. The methods investigated are the Deficit and Constant method, the Green and Ampt method, and the SCS Curve Number method.

The Salt Creek Basin located in southeast Nebraska was the pilot basin for this study. The basin was modeled using the Hydrologic Engineering Center-Hydrologic Modeling System (HEC-HMS) software package. The model was adapted to the basin using ArcGIS and the HEC-GeoHMS extension. Three different precipitation events were modeled with the simulated

runoff hydrographs at seven locations compared to the observed data to assess the model performance.

Several trends in the quality of loss parameters were observed. First, Deficit and Constant and Green and Ampt runoff methods produced runoff hydrographs that closely matched observations. Second, distributed loss parameters for these two methods produced more accurate results than their lumped counterparts. Third, the shallower soil depth parameters produced marginally better hydrographs than their counterparts. Finally, the SCS Curve Number method was able to produce accurate peak flow and runoff volume estimates, but performed poorly with the hydrograph timing.

Acknowledgements

First and foremost I would like to thank my adviser Dr. Ayse Kilic for the support and guidance through this study effort. She was able to give me the independence to explore this topic on my own and provide guidance when dealing with the complicated nature of this process. Dr. Kilic's depth of understanding and passion for hydrology have shone through and provided me with the determination to complete this study. I thank my committee members, Dr. Yusong Li and Dr. Suat Irmak for their willingness to provide feedback for this project and my thesis defense. Many thanks to the Civil Engineering Department at the University of Nebraska for providing a flexible framework to complete my studies and achieve my graduate degree.

I would like to thank everyone at the U.S. Army Corps of Engineers – Omaha District who provided assistance in a variety of ways. I would like to thank the Water Management Office for providing all of the observed precipitation and hydrograph data necessary to complete this study. I thank Ms. Jessica Batterman for her help in thinking through some of the modeling complications and data discrepancies as well as her advice for putting the report together. I am grateful to Ms. Kellie Bergman for being willing to work with my complicated schedule and for supporting my time away from the office me to pursue this degree.

I thank my wonderful children Isaiah and Chloe for always being a source of joy and laughter during this stressful period.

I especially would like to thank my amazing wife Ashley for her continuous support, encouragement, and understanding. She has been an unbelievable partner in this journey and has always helped me keep my perspective and move toward my goal all while pursuing her own important profession. Without her, this project would have been simply impossible.

Contents

List of Figures

List of Tables

Chapter 1 Introduction

1.1 Background

Hydrologic modeling is the application of numerical procedures designed to simulate the physical processes that occur within a watershed. Hydrologic modeling can be used for a variety of purposes ranging from drought monitoring, evapotranspiration calculations, water balance, and water rights determination. One of the most common uses is in the determination of rainfall runoff and flood discharge during precipitation events. Such information is critical in the design of any structures intended to protect and defend communities near water bodies. While hydrologic models are useful, any simulated product is a simplification of real-world processes, and as a result, leave room for error in a variety of ways.

Many processes involved in hydrology vary both temporally and spatially. Temporal variation is generally a result of rainfall, and can be accounted for in a hydrologic simulation. Spatial variability, however, is much more difficult to incorporate. In the early days of hydrologic modeling, data and computational limitations led to the use of lumped parameter models for hydrologic calculations (Paudel et al., 2009). Lumped models treat a drainage area as a single homogenous element resulting in a single runoff hydrograph (Jones, 2014). These lumped models seek to define the average value for each variable within the hydrologic modeling processes chosen. Such values may include the precipitation depth, soil infiltration rate, soil porosity, average slope of the catchment, etc. Their long history and ease of use led to their adoption as standard practice in the field of hydrology, and a majority of modeling systems used in practice today are simple lumped parameter models (Butts et al., 2004). While useful and able to produce meaningful results, a significant shortcoming of lumped modeling is the parameter values being based on empirical analysis and not on physical soil properties (Reed et

al., 2004). This limits the use of lumped models to gauged watershed with a long enough record of observed data with no significant changes to the watershed conditions (Reed at al., 2004).

As computational power and geospatial data availability improved, distributed hydrologic modeling was introduced as a way to improve the sensitivity of hydrologic modeling to spatial variations of elements such as precipitation, soil infiltration, and surface runoff (Paudel et al., 2009). The introduction of geographic information systems (GIS) led to the ability of handing large spatial datasets for parameter estimation and to the development of automated hydrologic modeling applications (Bradley, 2003). However, the implementation of these capabilities through the use of GIS into the field of hydrology has been slow. (Paudel, Nelson et al., 2009). A significant issue with the use of distributed hydrologic modeling is the vast amount of data needed to define all modeling parameters in a geospatial context (Paudel, 2010). These large data requirements result in a significant computational burden in both the development of distributed hydrologic models as well as their solving of the equations for each modeling process (Paudel, 2010). This in turn has stunted the acceptance and use of hydrologic models that account for spatial variability (Sui and Maggio, 1999).

Both lumped and distributed hydrologic models have their importance within the field of hydrology. Lumped models, because of their few parameters and simplified approach, are easy to use and calibrate to observed events. However, their reliance on empirical data analysis and inability to account for spatial variability provide significant limitations in their applications (Paudel, 2010). Conversely, distributed models are able to account for the spatial variability, but require a significant amount of data and computational power in order to do so. Deciding which model structure to use depends on what the goals of the modeling application entail (Paudel, 2010).

Regardless of which modeling structure is chosen, a hydrologic model will only be able to produce meaningful results if the data and parameters used for the simulation are reliable and accurate. There are many methods available to define the parameters in the hydrologic modeling process, some based on direct measurement of different variable and elements, and others inferring values based on similarities to other modeled watersheds. Precipitation data can be directly measured using rain-gauges like those employed by the United States Geological Survey (USGS), or from radar estimates like those made available by the National Land Data Assimilation Service (NLDAS) and Next Generation Rada (NEXRAD) used by the National Weather Service (NWS). Transform parameters can be derived from certain physical aspects of the watershed such as the slope and longest flow path to the watershed outlet (Hydrologic Engineering Center, 2010). However, much focus has been on the development of soil infiltration and loss parameters.

Many approaches have been used to derive hydrologic loss parameters. One approach was to simply borrow the derived and calibrated values from neighboring catchments (Mosley, 1981; Vandewiele and Elias, 1995). However, the inherent spatial variability of hydrological behavior from catchment to catchment was deemed too severe to be reliable (Post et al., 1998; Beven et al., 2000). Another strategy is known as parameter regionalization. This approach relates basin characteristics and model parameters in a statistical manner. The process involves the calibration of many gauged watersheds with similar characteristics and derive a statistical regression relationship between these catchment characteristics and the model parameters necessary to produce accurate runoff hydrographs. The relationships can then be applied to new or ungauged watersheds to establish the necessary parameter values (Wagener et al., 2006).

A third technique is to derive modeling parameters from physical property information such as porosity, field capacity, wilting point, percentage forest cover, etc. This method would allow the implementation of the parameter derivation procedure to any location, provided the soil information was made available. Two such databases for the entire continental United States are the Soil Survey Geographic (SSURGO) database and its coarser resolution predecessor the State Soil Geographic (STATSGO) dataset (Soil Survey Staff, 2016). Information contained within these datasets include geology, topography, vegetation, and climate information in addition to the physical and chemical soil properties, soil interpretations, and qualitative soil descriptions (Soil Survey Staff, 2016). Sets of average hydrologic modeling parameters have been developed using physical soil horizon information or soil texture class or both (Rawls et al., 1983), but have yet to be distributed in a geospatial context. One concern with the use of physically based model parameterization is one of scale (Beven et al., 2000). The scale at which measurements are made, such as within a laboratory with small soil samples, is different from the scale at which the information is applied, such as across an entire watershed (Wagener et al., 2006).

1.2 Problem Statement

The determination of accurate hydrologic modeling parameters is crucial to the reliability of the simulation results. However, no method has proven to be totally reliable in parameter determination and a large part of hydrologic modeling still relies on subjective, expert assessment and adjustment of parameter estimates, greatly limiting their reproducibility (Andersen et al., 2006). A physically based method for determining hydrologic model parameters that uses readily available GIS soil data could provide an objective and reproducible solution that would eliminate the need for expert oversight.

SSURGO soil data provides coverage for the continental United States and provides a plethora of soil information, both quantitative and qualitative. From this information, a wide variety of physically based hydrologic modeling parameters can be calculated. Previous work done by Rawls et al (1983) used similar soil database information to derive average parameter values for the Green and Ampt loss method based on soil texture classification. This paper will seek to follow a similar format, but define the parameters for multiple other loss methods as well as use the geospatial computational power of GIS to generate distributed grids of these hydrologic parameters.

1.3 Objective

The goal of this research can be broken down into two main objectives:

1. The first objective is to develop a method for defining hydrologic loss parameter values for three different loss methods based on soil data contained within the SSURGO database. Such a method would allow for derivation of parameter values in watershed where no observed data is available for model calibration. The three loss methods are:
    - Deficit and Constant Loss method
    - Green and Ampt method
    - SCS Curve Number method

    Each of the physically based loss methods will be tested at two different soil depths, 1-foot and 3-foot, to determine the impact this parameter has on sensitivity and accuracy of results. The hypothesis is that a reasonably accurate set of hydrologic loss parameters can be developed for each of the selected loss methods for use in hydrologic modeling, and that the shallower soil depth (1-foot) parameters will provide a more accurate runoff hydrograph than those of the deep soil (3-foot).

2. The second objective is to create spatially variable datasets for each of the selected loss method parameters to compare the difference in simulated runoff between lumped and distributed modeling techniques. The hypothesis is that the spatial variability of soil properties will be more accurately represented in the distributed hydrologic model resulting in runoff hydrographs that more closely match observed results.

The testing of the two objectives will require the generation of 10 different loss parameter datasets. All necessary modeling parameters for these methods were derived from the SSURGO database or supplementary datasets from the National Land Cover Database (NLCD). These datasets will be tested using the Hydrologic Engineering Center's (HEC) Hydrologic Modeling Software (HEC-HMS). A complete list of the loss methods to be test is shown below in Table 1 - 1.

Table 1 - 1. Study Loss Methods

	Lumped versus Distributed	Hydrologic Loss Method	Soil Depth
1	Lumped	Deficit and Constant Loss	1 Foot
2			3 Foot
3		Green and Ampt	1 Foot
4			3 Foot
5		SCS Curve Number	
6	Distributed	Deficit and Constant Loss	1 Foot
7			3 Foot
8		Green and Ampt	1 Foot
9			3 Foot
10		SCS Curve Number	

Chapter 2 Literature Review

Many techniques have been developed in the field of hydrology for estimating loss parameters for use in hydrologic modeling. Relevant literature was found in three major categories: estimation of loss parameters based on regionalized comparability, the use of physical soil data in the determination of loss parameters, and the effect of using distributed hydrologic modeling techniques to account for soil property spatial variability.

2.1 Regionalized Hydrologic Parameterization

The process known as parameter regionalization is the process of relating catchment characteristics and model parameters in a statistical manner (Wagener et al, 2006). The process involves the application of a hydrologic model to a large number of gauged catchments and derive regression equations defining the relationship between model characteristics and model parameters (Wagener et al, 2006). One of the most comprehensive approaches to parameter regionalization is a project known as The Model Parameter Estimation Experiment (MOPEX). MOPEX is a project aimed at developing techniques for a priori parameter estimation in hydrologic modeling (Duan et al, 2006). Several international workshops were held as part of the MOPEX project, the findings of which were published by Duan et al (2006). The results of this experiment were mixed causing the author to describe the a priori parameter estimation procedures as “problematic and need improvement.” The results produced could be vastly improved through calibration. The recommendations were to conduct more research to develop the relationship between model parameters and catchment characteristics and to investigate the transferability of these parameters from one basin to another.

Wagener et al (2006) also sought to test the effectiveness of parameter regionalization by way of a case study of 10 catchments located in southeast England. His study sought to establish how local parameters were correlated with catchment characteristics as well as how

these parameters were represented in the regionalized dataset. His results showed that the regionalization of parameters resulted in only a few parameters showing a significant correlation with catchment characteristics. He also noted the inherent error introduced depending on the model structure selected for study and how this error can negatively affect the regionalization process. He concludes that a procedure is necessary for the development of parameters for ungauged watersheds, but care must be taken in the selection and calibration of regionalized parameter datasets.

Merz and Blöschl (2003) conducted their own regionalization study using 308 catchments in Austria to define relationships between catchment characteristics and 11 calibration parameters. The regionalized parameter simulations were then compared to the performance of a model that simply used the average parameter values for its immediate neighboring basins, generally thought to be a poor means of estimating model parameter values. However, just the opposite was demonstrated. While both the regionalization and neighboring-value techniques both saw a drop in the model performance, the regionalization method performed much worse, forcing the conclusion that “Apparently, spatial proximity is a better surrogate of unknown controls on runoff dynamics than catchment attributes” (Merz and Blöschl 2003).

Another study by Ao et al (2006) used parameter regionalization in hydrologic model called the Block-wise TOPMODEL with the Muskingum-Cunge routing method (BTOPMC). The study utilized the parameters generated by the MOPEX project without any adjustment and found the results cannot satisfactorily simulate rainfall and that significant adjustment had to be made through calibration.

2.2 Physically Based Hydrologic Parameterization

While some rely on regionalization for determining parameters at a large scale, another technique involves using physical soil information contained within soil databases to develop necessary model parameters. One of the most well-known instances of defining hydrologic modeling parameters from physical soil information was a study performed by Rawls et al (1983). The results from this study have been reproduced many times in other publications and have become the standard of practice for initial parameterization in the field of hydrologic engineering (Reinartz, 2016). This study used a comprehensive collection of soils data available as of 1978 covering 34 states. In total, approximately 1,200 soils containing over 5,000 horizons were analyzed with each set including detailed descriptions, particle sizes, densities, porosities, mineralogies, chemical data, and water retention information. From this massive dataset, Rawls was able to establish a relationship between soil texture and the Green and Ampt parameter values. This study was then updated by Saxton and Rawls (2006) to make use of the larger availability of soils data compared to the 1978 soils data, and also developed regression equations that would allow for the adjustment of loss parameters based on other not previously considered soil characteristics such as salinity, compaction, and gravel content.

Koren et al (2000) developed a procedure to use information within the State Soil Geographic (STATSGO) database to define soil parameters. His work used the Sacramento Soil Moisture Accounting model (SAC-SMA) used as the official forecasting tool of the National Weather Service, which uses 16 unique parameters in its hydrologic modeling algorithm. Of these parameters, 11 were defined based on soil texture information within the STATSGO database. While the STATSGO database is coarse in terms of spatial resolution, it was the only comprehensive soil database available at the time, and the parameter values determined were deemed as a reasonable approximation, although still requiring manual calibration to produce

accurate runoff results. Koren's efforts were improved upon by Anderson et al (2006) and Zhang et al (2006), both of whom sought to advance the model parameter derivation strategy using the finer-resolution Soil Survey Geographic (SSURGO) database. The same parameter set was re-derived using SSURGO and simulations were conducted for six basins within the Ohio River Basin comparing the results of the STATSGO parameters vs the SSURGO parameters. The results showed the higher resolution, SSURGO-based parameters were able to predict streamflow runoff as well or better than the STATSGO parameters for the six basins. The study also suggested the move to SSURGO-based a priori parameter estimates as distributed hydrologic modeling develops and the need for small-scale flash flood basin modeling becomes necessary.

Ficklin et al (2014) developed a study to test the effects of aggregating soil property information across multiple survey areas to perform hydrologic analysis. The study utilized the Soil and Water Assessment Tool (SWAT) with three different sets of hydrologic parameters determined from physical soils data to model the Shasta Lake watershed in southern Oregon and northern California. All three sets of hydrologic parameters used soil type identifiers from different soil data sources to define the parameters. The first set was determined using the low-resolution STATSGO database while the other two sets were determined using the SSURGO database, one using the Map Unit (MUKEY) as the soil type identifier, the other using the soil taxonomy (TAXSUB) as the soil type identifier. The parameters were then area-weighted to define average subbasin values, and the model was run to determine the effectiveness of each parameter set in predicting streamflow. The study was able to show that the parameter set using the soil taxonomy SSURGO data, thought to be the most representative of soil conditions, was able to best match the observed runoff hydrographs when compared to the MUKEY and STATSGO strategies.

Another study conducted by Livneh et al (2015) sought to compare the impacts of much coarser soil databases in the long term trends of the Mississippi River Basin. The two databases used were the digital general soil map of the USA (STATSGO2) and the Food and Agriculture Organization (FAO)-based harmonized world database. The modeling focused on the major flood and drought events during 1988, 1993, and 2012 as well as annual and seasonal water fluxes. Overall, the STATSGO2 simulations showed more extreme responses to both the flood and drought events while the coarser harmonized world soil database showed much more attenuation and dampening of significant events due to a larger water capacity. The model concluded that the finer-resolution STATSGO2 database provided more favorable results and recommended further study into the effects of the even finer-resolution SSURGO database.

Finally, in 2016, Reinartz sought to define infiltration parameters for the Green and Ampt method to be used in a fully-distributed GSSHA model. The goal of the study was to develop and understanding of how soil parameterization affects the evaluation of best management practice (BMPs) associated with drainage. The study utilized a multi-layered approach for the Green and Ampt method and used the SSURGO database to define hydrologic parameters based on soil texture classification. No results of the parameterization as the study was meant to establish a framework for future testing studies.

2.3 Distributed Modeling Techniques

Several authors have commented on the increased modeling capabilities made possible by distributed hydrologic modeling. In his research, Paudel (2010) sought to establish the credibility of distributed hydrologic modeling as a superior alternative to the traditional lumped approach. He compared the two methods and noted the relative strengths and weaknesses of both, summarized in Table 2 - 1.

Table 2 - 1. Relative Strengths and Weaknesses of Lumped and Distributed Hydrologic Models

Model	Relative Strengths and Weaknesses
Lumped	- Ease in development but inefficient to represent the spatial variation - Ease in calibration but does not work well with other storms - Fewer parameters but these parameters are not related to watershed physics - Incapable of simulating scenario as these models cannot simulate the overland flow path
Distributed	- Complex in development but represents the spatial variation efficiently - Complex in calibration but work well with other storms - Require a lot of parameters and the parameters are physically based - Efficiently simulate scenario as these models simulate the overland flow path

Note: Retrieved from "An examination of distributed hydrologic modeling methods as compared with traditional lumped parameter approaches" by M Paudel, 2010, *All Theses and Dissertations.* Paper 2219. Copyright 2010 by Murari Paudel

This study was able to illustrate this superiority through a series of case studies using the lumped and distributed modeling capabilities within HEC-HMS as well as the fully-distributed Gridded Surface Subsurface Hydrologic Analysis (GSSHA) model. These case studies showed that distributed modeling was able produce more accurate simulation results not only for its ability to account for spatial variability in hydrologic parameters, but also for its ability to change over-time as a watershed becomes more developed. In Paudel et al (2009), he was able to use HEC-HMS to demonstrate the effectiveness of a quasi-distributed runoff method known as the Modified Clark (ModClark) model to account for spatial variation of loss parameters within a watershed. Then, in Paudel et al (2011), he used GSSHA to show the distributed modeling capability of accounting for land use change over time. Finally, Paudel was able to identify a few common hurdles causing the adoption of distributed modeling to be slowed, specifically issues related to the stream and 2D grid interaction, order of work flow, and initial model parameterization.

Reed et al (2004) presented the results from the Distributed Model Inter-comparison Project (DMIP) study, which compared the results from distributed model simulations compared to both the observed runoff and the lumped model simulations for twelve different watersheds.

The results were mixed with some lumped parameter models outperforming the distributed counterparts, some models produced equal results, and still other distributed models showed vast improvements over the lumped models. This inconsistent result was attributed to the lack of established parameter estimation and calibration techniques for distributed modeling, especially when compared to lumped modeling.

A major shortcoming in the field of distributed modeling was noted by Malone et al (2015) regarding model parameterization. He observed that a large body of literature had been developed in recent years touting the use and development of distributed hydrologic models, but very little had been devoted to the establishment of general parameterization guidelines to use in the application of these models. As a result, he laid out a seven key guidelines for the estimation of soil parameters and their calibration to improve model performance.

One technique for defining Green and Ampt Parameters for use in distributed hydrologic modeling was developed by Reinartz (2016). As mentioned above, he defined parameters for use in a fully-distributed GSSHA model based on soil texture classifications contained within the SSURGO database. The effectiveness of these parameters were not yes discussed as the values were to be used in future evaluation of best management practices in land drainage in Minnesota.

2.4 Benefits of Research

Based on the results of work completed by other researchers, the prospect of determining uncalibrated hydrologic loss parameters from physical soil characteristics seems superior to the application of regionalized parameters from similar basins. Furthermore, the use of physical soils data have been used and compared in their ability to forecast rainfall runoff. However, these research efforts all focus on the use of soil type classifications and correlating

typical value tables to define hydrologic parameter rather than using the physical data to define the parameters directly.

Furthermore, while the potential benefits of complex distributed models has been discussed, there is very little literature discussing the development of model parameters for distributed modeling techniques. This particular shortcoming, mentioned by Paudel (2010), Malone (2015), and Reinartz (2016), has proven to be a significant road-block in the acceptance and common use of distributed modeling techniques.

This research effort seeks to fill both of these apparent knowledge gaps. The first will be examined by evaluating a technique of directly measuring hydrologic loss parameter from the SSURGO soil database for three different loss methods. The second will be addressed by developing a process for model parameter generation in a spatially distributed format for the same loss methods.

Chapter 3 Methodology

3.1 Overview

This study was completed through the use of three primary pieces of software: a Geographic Information System (GIS) platform by ESRI[tm] named ArcGIS, a hydrologic tool used in conjunction with ArcGIS called HEC-GeoHMS, and the Hydrologic Engineering Center – Hydrologic Modeling System (HEC-HMS). ArcGIS was used extensively to both develop the hydrologic model as well as generate the loss parameters for both limped and distributed simulations. HEC-GeoHMS provided the tools to be used in the ArcGIS environment to analyze the terrain data and to create the necessary files for a HEC-HMS model. HEC-HMS is the main computational engine capable of performing complex hydrologic simulations using a variety of different methods for all phases of hydrologic modeling.

The GIS datasets for this study were all downloaded from the internet and are freely available to the public. The National Hydrography Dataset (NHD) is part of the United States Geological Survey (USGS) *The National Map* initiative, which is a collaborative project between the USGS and several other public agencies to provide a variety of geospatial datasets. The NHD was used to obtain a 10-meter resolution digital elevation model (DEM) as well as stream centerline information. Soil data was obtained from the Soil Survey Geographic (SSURGO) database, which is maintained by the USDA National Resource Conservation Service (NRCS). Precipitation datasets are based on the Next-Generation Radar (NEXRAD) datasets generated by the National Weather Service (NWS). These gridded precipitation data are created by the NWS and reformatted by the U.S. Army Corps of Engineers (USACE) to be compatible with the HEC-HMS software.

ArcGIS in conjunction with Geo-HMS was used to develop the HMS model for the Salt Creek Basin, Nebraska. The process began with the 10-meter DEM data and applied a series of

operations to generate a stream network and subbasin delineation. Once complete, the data were formatted and exported to the HEC-HMS software. ArcGIS was also used to develop the runoff parameter datasets for all methods being tested, including both the lumped and distributed datasets.

HEC-HMS was used to conduct the hydrologic simulations based on the data generated from ArcGIS. The HMS modeling framework and the runoff parameter datasets were used in conjunction with the gridded precipitation to generate rainfall runoff hydrographs at several observation locations. These simulated hydrographs were then compared to the corresponding observed hydrographs to analyze how well the model performed.

3.2 Study Location

The location selected for this modeling effort is the Salt Creek basin located in southeast Nebraska in the area surrounding the city of Lincoln. Salt Creek flows in a generally northeast direction before depositing into the Platte River at Ashland, Nebraska. A six mile stretch of the creek flows through the city of Lincoln, Nebraska which has a population of approximately 268,000 residents. The basin covers portions of Cass, Lancaster, and Saunders counties and has a drainage area of 1,640 square miles stretching approximately 63 miles from north to south and 38 miles from east to west (Brodnicki, 1983). The relative location of this watershed is shown in Figure 3 - 1.

The range of elevation for the basin ranges from 1,060 feet above mean sea level at the mouth of the creek up to 1,690 feet above mean sea level in the uppermost headwaters (USACE, 1978). The DEM for this basin can be seen in Figure 3 - 2. The Salt Creek Basin is made up mostly of loess deposits at the higher elevations and alluvium in the bottomlands (Brodnicki, 1983). In terms of soil texture, this results in clay loam, silty clay loam, and silty loam composing most of the basin. The nature of this material has resulted in characteristic low tolling hills and well

defined stream channels. Bedrock consisting of sandstone, limestone and shale lies at an average depth of 200 feet below the surface, but is exposed in a few areas near major streams (Burgess, 1906). A map of the soil texture can be seen in Figure 3 - 3.

The Salt Creek Basin is primarily rural with most of the land being cultivated for agricultural use. The agriculture is diversified with fields being used to grow crops, such as corn and soy beans, as well as to raise livestock. Climate conditions as well as soil type are favorable for these land uses. The City of Lincoln, Nebraska lies in the center of the Salt Creek basin and is the only major industrial and urban development center in the Salt Creek Basin (USACE, 1983). A map of the land use for the Salt Creek Basin is shown in Figure 3 - 4.

The climate of the Salt Creek Basin can be described as temperate and continental (Brodnicki, 1983). Mean annual precipitation is approximately 28 inches with a majority of this precipitation occurring as rainfall. This rainfall accounts for 25 inches (~80%) of the total precipitation and occurs at evenly distributed intervals during the growing season from March to October. This pattern makes for ideal conditions for plant growth, where the pattern of precipitation tends to follow patterns of evapotranspiration. The remaining precipitation falls as snow and rain during the winter months.

The Salt Creek Basin has several observed hydrologic data locations throughout the basin. A network of 17 stream gauges and 10 reservoir elevation gauges are able to provide a total of 27 observed flow measurements (USACE, 1978). Additionally, 22 of these gauge locations monitor precipitation. The size of the individual drainage areas for each of the reservoirs ranges between 5.4 and 88.7 square miles. These reservoirs are relatively unimpeded in terms of upstream catchments diversions, making them ideal candidates for the testing of runoff calculations. A map of the basin, with locations of stream gauges and reservoirs, is shown in Figure 3 - 5.

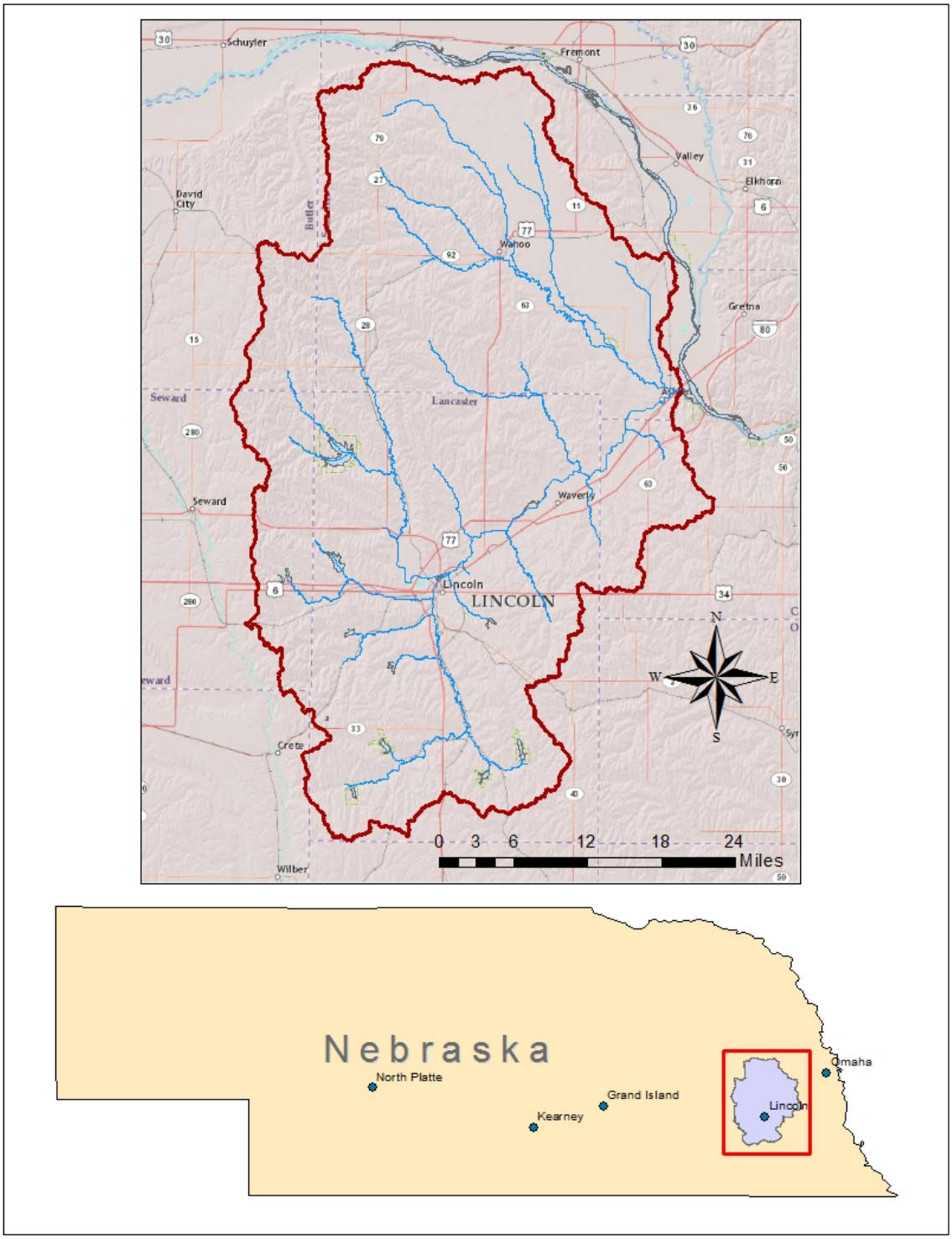

Figure 3 - 1. The Salt Creek Watershed

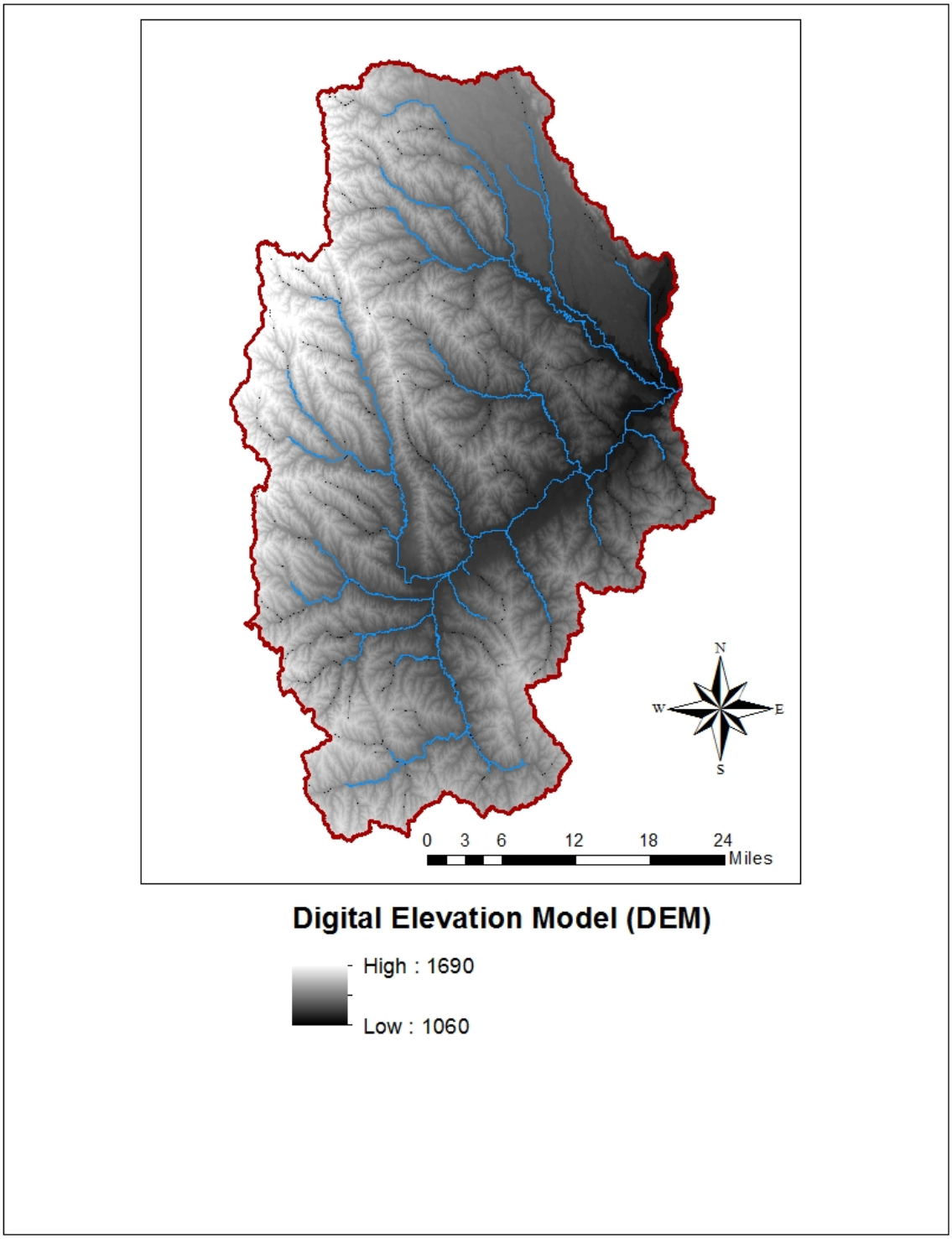

Figure 3 - 2. Digital Elevation Model for the Salt Creek Basin.

Obtained from USGS National Elevation Dataset (USGS 2016)

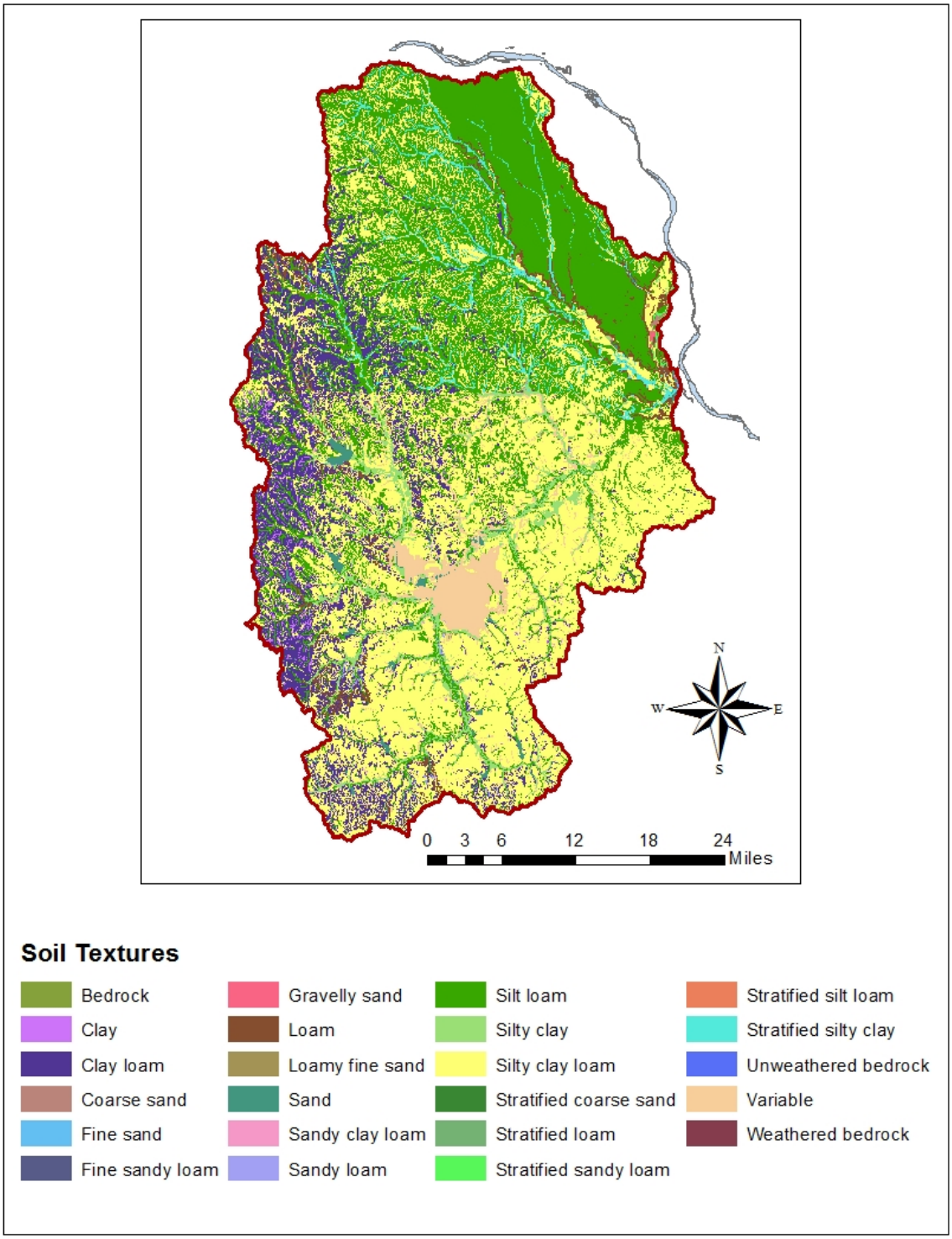

Figure 3 - 3. SSURGO Soil Textures in Salt Creek Basin.

Obtained From SSURGO Database (Soil Survey Staff, 2016)

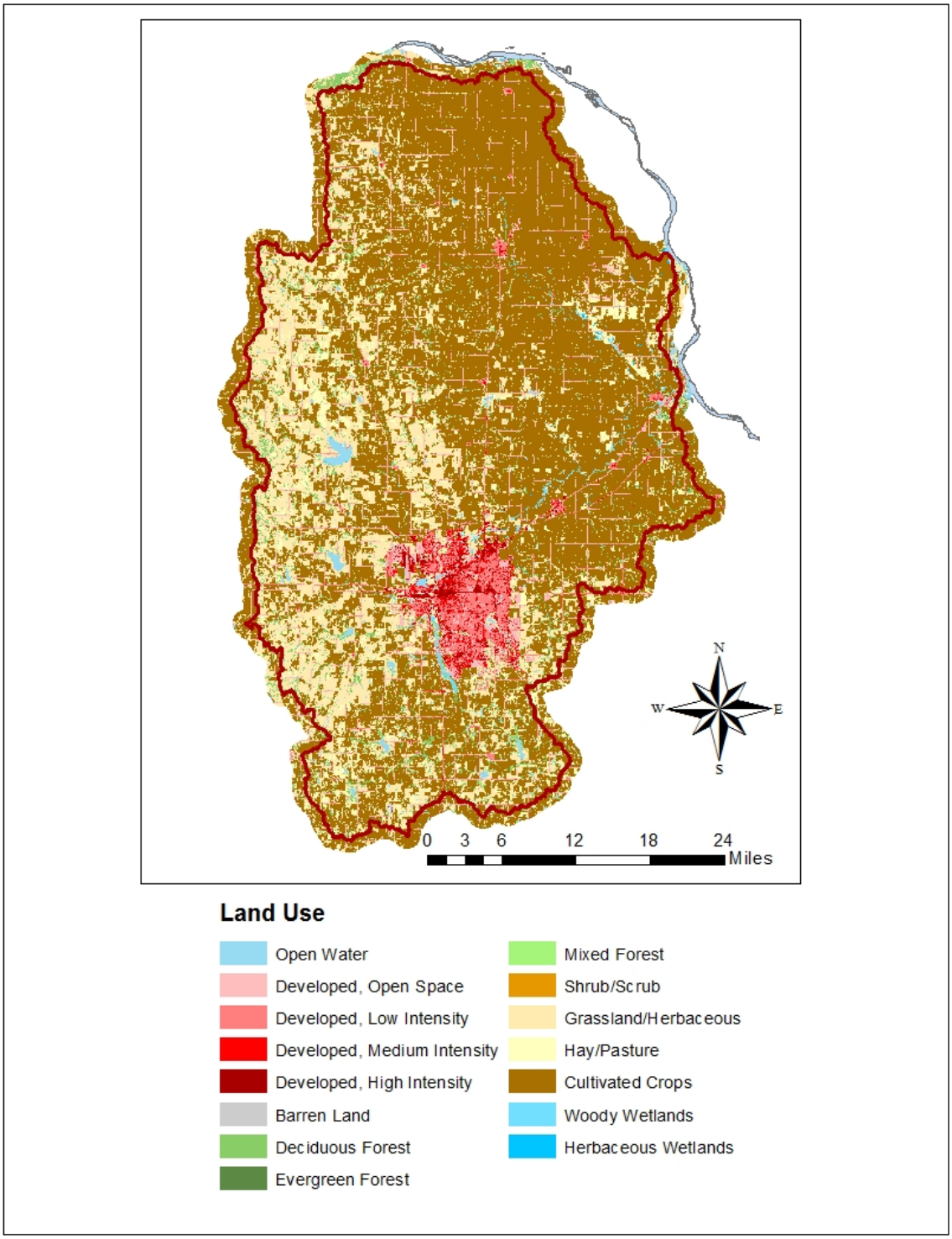

Figure 3 - 4. Land Use for the Salt Creek Basin

Obtained from 2011 National Land Cover Database (Homer et al, 2015)

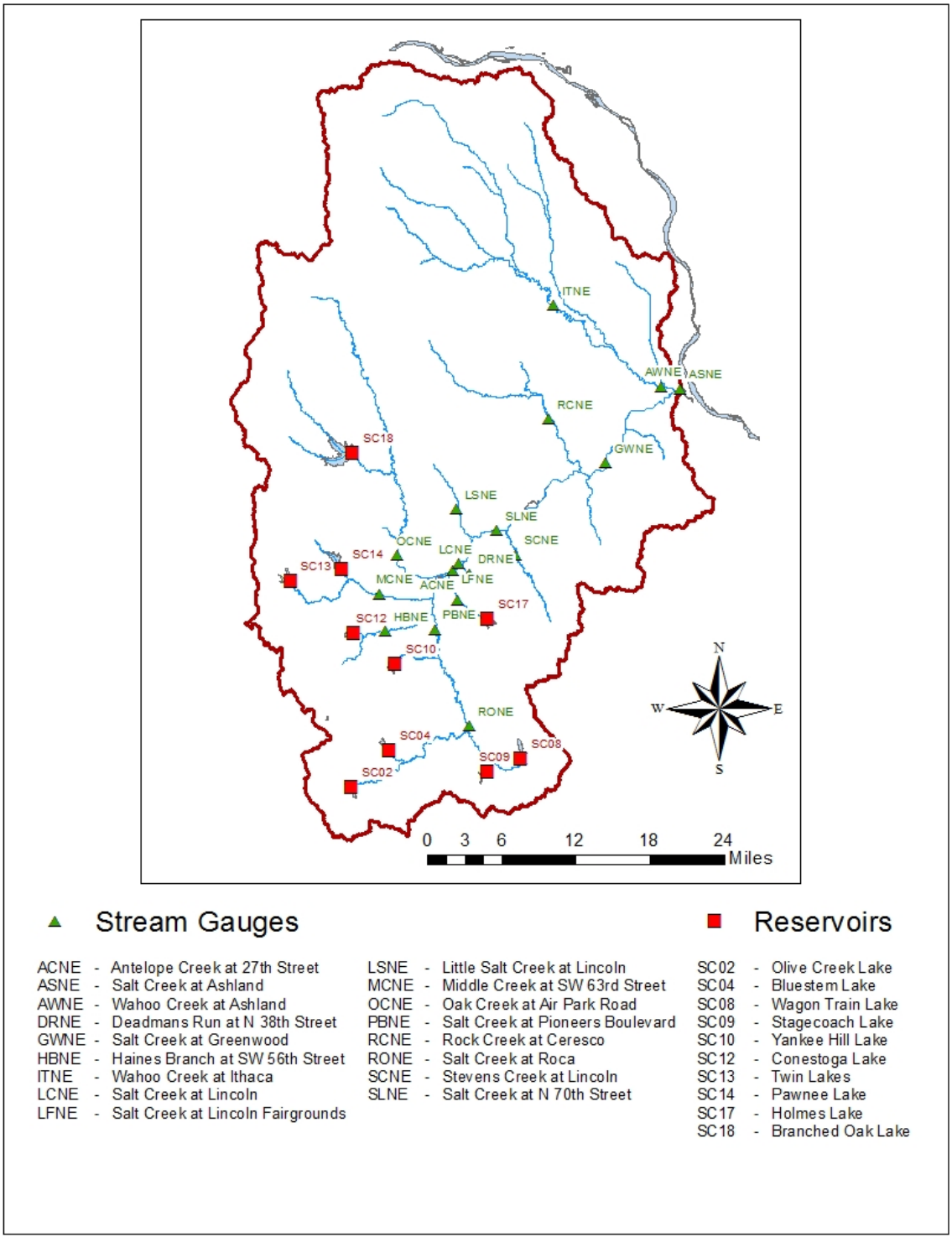

Figure 3 - 5. Stream Gauges and Reservoir Locations in the Salt Creek basin study area.

3.3 Model Development

ArcGIS and the hydrologic plug-in HEC-GeoHMS have been used extensively to develop hydrologic models (Baumann 2011, Ogden 2011). The processes used by this software have become industry standards, and while a variety of hydrologic modeling programs are available, most use this same process to develop the model (Maidment, 2002; Paudel 2010). The procedure beings with a "pre-processing" phase in which the HEC-GeoHMS commands manipulate the provided DEM data to generate the necessary datasets for watershed delineation. Once complete, the model development phase begins in which the user can manipulate the default watershed alignment to create a custom delineation suited for the modeler's needs. Finally, the model is ready to be parameterized and exported to the HEC-HMS.

3.3.1 Pre-processing

The pre-processing phase is a standard practice in hydrologic modeling and applications that use the ESRI ArcMAP Spatial Analysis Tools – Hydrology package, and is used to generate a hydrologic model layout from DEM data. The ESRI process uses a total of 10 steps to generate the modeling framework. The full process is explained in *Arc Hydro: GIS for Water Resources* (Maidment, 2002). These steps are described below with figures for each step included in Appendix A:

1. DEM Reconditioning uses the stream locations obtained from the NHD to "burn" the stream alignment into the DEM. This is done by decreasing the elevation of every DEM grid cell that touches the stream centerline, ensuring that the subsequent processes will respect the stream lines and not malfunction due to DEM resampling errors
2. "Fill sinks" is a process that guarantees that every cell within the DEM has a downstream path toward the watershed outlet. This is done by analyzing each grid

cell and its eight neighboring cells and increases any cell elevation that is completely surrounded by eight elevated values. This process is visualized below in Figure 3 - 6:

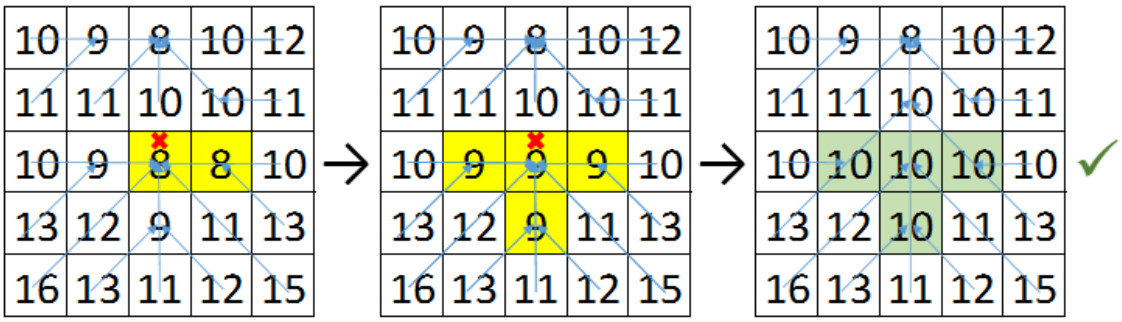

Figure 3 - 6. Fill Sinks Process. Adapted from Arc Hydro: GIS for Water Resources *(Maidment, 2002).*

3. The Flow Direction grid is created by using the eight-point pour model to determine the direction of steepest descent for each grid cell. Each grid cell is assigned a value indicating the direction flow runoff would take. Much like a compass, the eight-point pour model has the following eight possible directions:

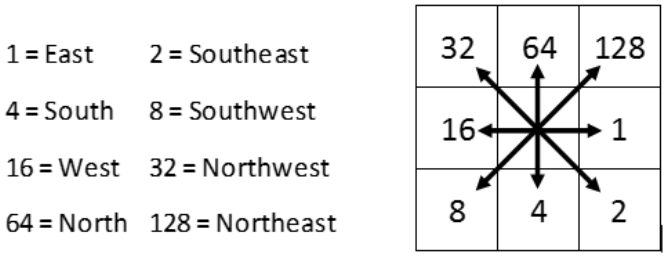

Figure 3 - 7. Eight-Point Pour Model for Flow Direction Grid. Adapted from Arc Hydro: GIS for Water Resources *(Maidment, 2002).*

A small sample of this process is shown below in Figure 3 - 8:

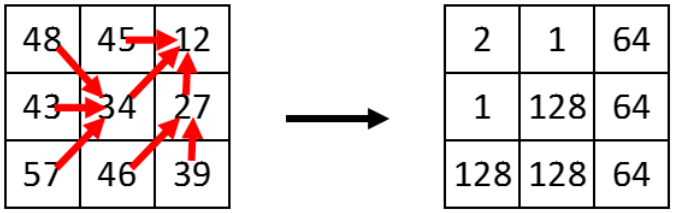

Figure 3 - 8. Flow Direction Process. Adapted from Arc Hydro: GIS for Water Resources *(Maidment, 2002).*

4. The Flow Accumulation Grid is then generated by calculating the number of upstream grid cells for each grid cell in the DEM. Upstream drainage area at a given cell can then be calculated by multiplying the Flow Accumulation grid value by the grid cell area. A small sample of the process is shown in Figure 3 - 9:

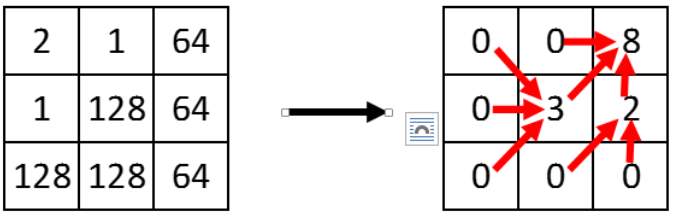

Figure 3 - 9. Flow Accumulation Process. Adapted from Arc Hydro: GIS for Water Resources *(Maidment, 2002).*

5. The Stream Definition grid is produced by using the Flow Accumulation grid in conjunction with a stream threshold value. This threshold value indicates the minimum number of cells that must flow to a point to be considered to be part of the stream network. The process uses the flow accumulation grid and assigns a value of 1 or 0 indicating whether the flow accumulation to that point exceeds the threshold required to form a stream, and to be part of the stream network, or falls below the threshold and is not part of the stream, respectively. The threshold must be set low enough to provide adequate stream definition for the basin but not too low resulting in an overly complex network. In this application, a threshold of 5,000 cells was used.
6. The Stream Segmentation grid breaks the Stream Definition network at each confluence and assigns unique values for each portion of the stream.
7. Catchment Grid Delineation generates a unique subbasin for each stream segment based on the Flow Direction grid. By using each cell in a given segment, the flow directions can be back calculated to determine the member subbasin and

corresponding stream segment corresponding to each individual cell within the DEM.

8. Catchment Polygon Processing is used to convert the Catchment Grid from a raster format to a vector format. This step generates a polygon feature class with a unique entry for each catchment. This process insures hydraulic continuity during the streamflow routing processes. The Drainage Line Processing completes the same raster-to-vector conversion for the Stream Segment Grid, resulting in a polyline feature class.
9. The Adjoint Catchment Processing is used to aggregate upstream subbasins at every stream confluence. During the raster-to-vector conversion, rounding errors sometimes produce extra unnecessary subbasin polygons. This step dissolves these polygons into their original catchment.
10. The Slope grid is created from the original DEM dataset, where the slope for each cell is generated individually.

The completion of these 10 steps completes the model pre-processing of the initial DEM and NHD stream alignment. Through this process, ArcGIS and HEC-GeoHMS are able to generate the geometry and terrain models necessary to generate hydrologic models. In this study, the models were created for the Salt Creek Basin.

3.3.2 Model Set-up with HEC-GeoHMS

Once the pre-processing step is completed, the data produced are used as the starting point for model development, where multiple hydrologic models can be created from the same pre-processing data without having to regenerate the entire process. Each of the individual model developments are referred to as “projects” within the HEC-GeoHMS framework. Model Development utilizes the Basin Processing, Characteristics, and Parameters processes within

HEC-GeoHMS to customize subbasin delineations, define physical properties of the watershed, and assign hydrologic parameters, respectively.

1. Basin Processing is used to manipulate the default watershed layout generated during preprocessing to meet the needs of the modeler. The Subbasin Merge and Split tools are used to modify the default catchment delineations. For this project, the modified delineation was based on the location of reservoir elevation gauges and stream flow gauges, since this is where observed hydrographs were collected and compared with modeling results. The subbasins were realigned such that each subbasin outlet had one of these gauges at its mouth. This was done so that simulated results could be directly compared to observed data for the same event to determine how well the model predicts runoff.

   The process involves using the subbasin merge tool to combine all catchments upstream of a particular gauge, including the subbasin containing all upstream areas that envelope the particular gauge. The subbasin divide tool was applied at the gauge to split the subbasin into two, resulting in a single continuous subbasin upstream of each gauge. An example of this process is shown in Figure 3 - 10:

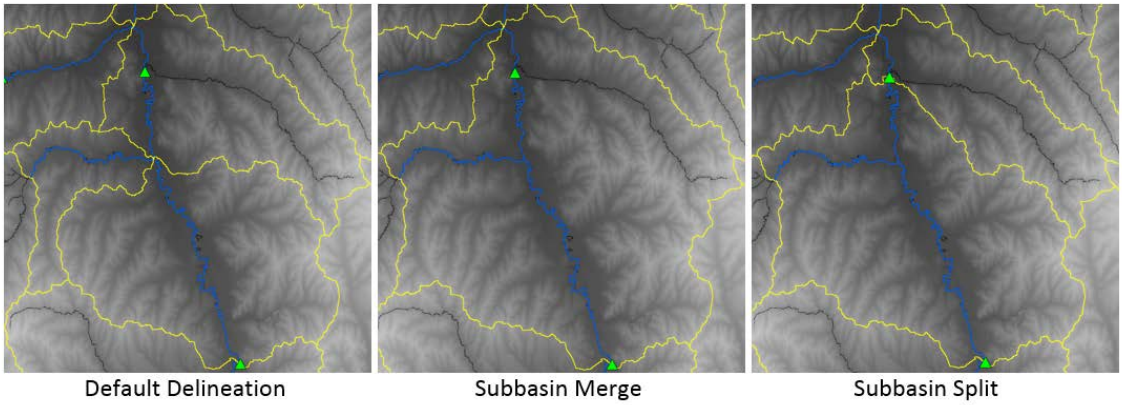

Figure 3 - 10. Subbasin Merge and Split Process for an example subbasin in the Salt Creek study area.

The Salt Creek Basin contains 17 stream gauges and 10 reservoir elevation gauges used for hydrologic data collection. These 27 locations provide enough definition to reasonably apply lumped modeling procedures for each subbasin. However, due to irregular shaping, seven of the 27 subbasins were divided again, resulting in 34 total subbasins within the watershed. The final subbasin layout is shown in Figure 3 - 11.

2. The Characteristics procedure in HEC-HMS is used to describe the physical nature of all the elements within the model. These values are obtained for each applicable element within the Salt Creek Basin and are useful pieces of information when it comes to estimation of certain hydrologic parameters. The parameters include river length and slope, basin slope, the longest flow path from the hydraulically most distant point in the subbasin to the outlet, the subbasin centroid, subbasin centroid elevation, and the subbasin centroid flow path to the outlet of the subbasin. The results from all of these processes can be found in Appendix A.
3. The Hydrologic Parameters procedure of HEC-HMS is used to assign the hydrologic modeling techniques to be employed in the model and to assign parameter values to be directly imported into HEC-HMS. The modeling techniques to be defined are the runoff method, transform method and routing method. This study uses a variety of runoff methods listed previously, but these varieties will be described and parameterized in the Section 3.4 - Modeling Methods. The transform method, which convert the rainfall runoff to the watershed hydrograph, is the Modified Clark (ModClark) method. The Mod-Clark method is a quasi-distributed unit hydrograph model developed by the Hydrologic Engineering Center for use within HEC-HMS for distributed modeling (Hydrologic Engineering Center, 2010). The selected routing

method, which translates runoff within streams from an upstream outlet to a downstream outlet, is Muskingum routing (McCarthy, 1938; Nash, 1959).

4. The Grid Cell Processing procedure is used to define the Standard Hydrologic Grid (SHG) framework used within the distributed modeling schema. The hydrologic loss calculations are completed on a grid cell-by-grid cell basis, and then routed to the outlet using the ModClark method. This project uses a 2,000 meter grid cell resolution to match the precipitation gridded datasets available for this study. A map showing the SHG for the Salt Creek Basin is shown in Figure 3 - 12.
5. The final step is to prepare the data for import to the HEC-HMS software. The steps include the assignment of a units system, a data check for hydrologic connectivity and consistency, assignment of coordinates, creation of background map files, and generation of the HEC-HMS basin file. For this project, English units were selected to remain consistent with the precipitation data, the observed hydrograph data and common usage within the USACE. No errors were detected, and the creation of the background maps was done for the subbasin layout as well as the stream centerlines.

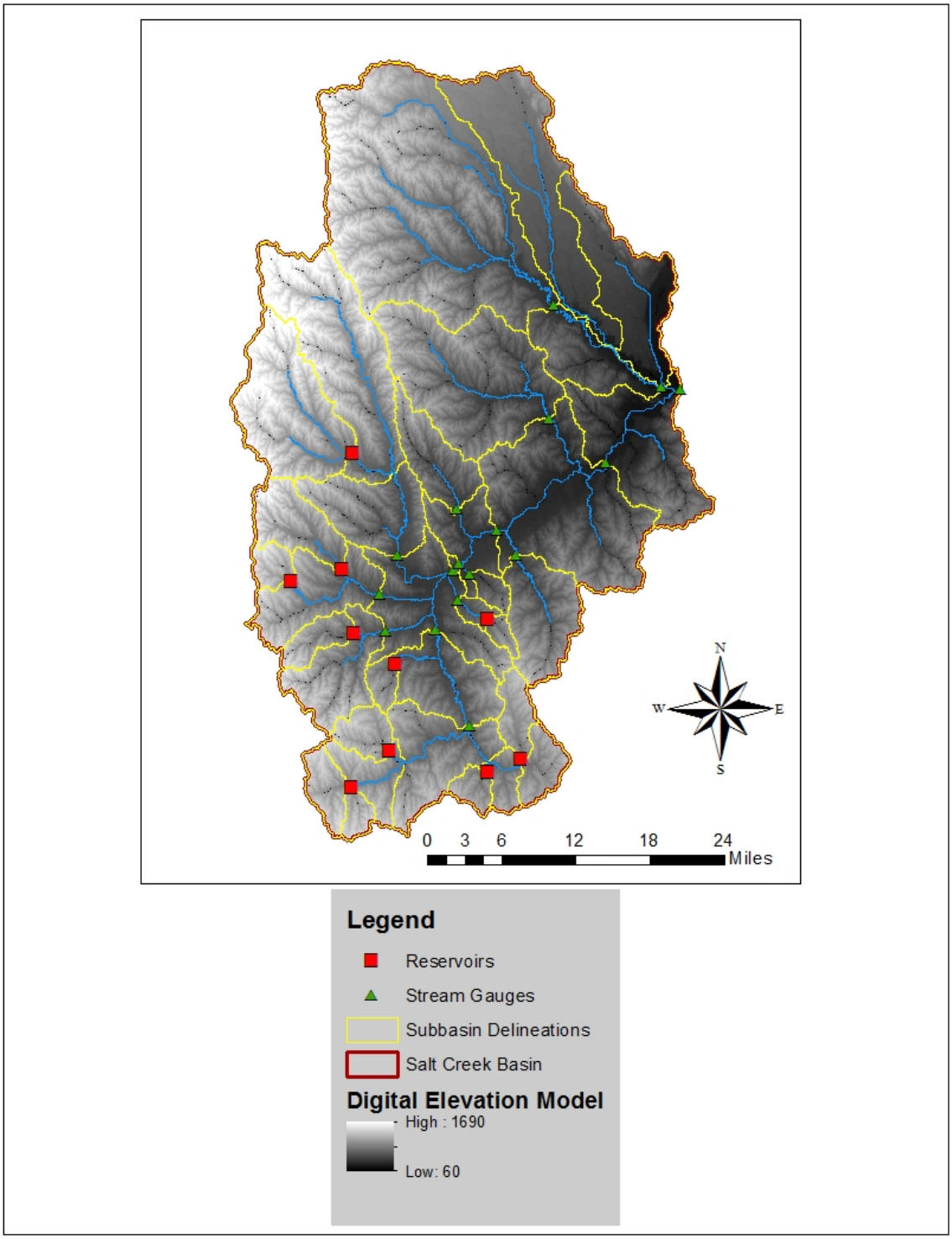

Figure 3 - 11. Subbasin Delineations for Salt Creek Basin

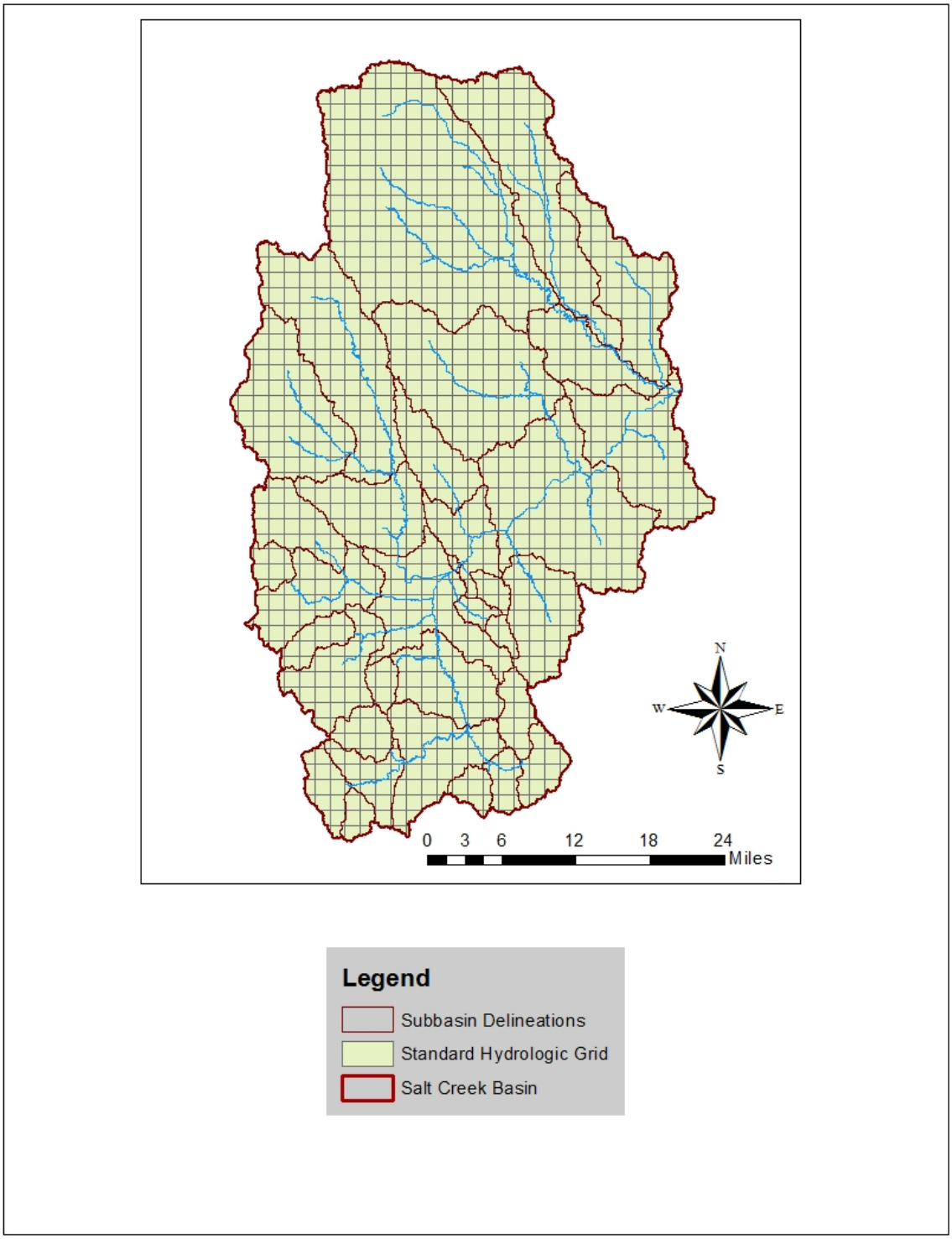

Figure 3 - 12. Standard Hydrologic Grid for Salt Creek Basin using 2000 m grid cells.

3.4 Modeling Methods

Hydrologic modeling methods are mathematical models used to simulate the physical processes that occur during a precipitation event. They can be broken into three main groups: rainfall-runoff methods, used to describe the water that infiltrates into the soil and water that runs off the surface to streams, transform methods used to describe how the precipitation excess translates into a runoff hydrograph, and routing methods, used to define how water moves within a stream channel. This study focuses on the impact that different runoff models have on the shape of a runoff hydrograph. Therefore, a variety of runoff models were evaluated using a single transform and routing method. Methods are described in the following section.

3.4.1 Rainfall-runoff Methods

The runoff methods refer to the modeling techniques used to quantify and simulate the amount of rainfall that infiltrates into the soil and the amount that is converted to runoff. This is an important step in estimating the total volume of expected runoff at each observation location. This study evaluated three different runoff methods and discusses their application in a distributed model.

3.4.1.1 Deficit and Constant Loss

The Deficit and Constant Loss method (Hydrologic Engineering Center, 2000) is one of the simpler methods for estimating runoff. The underlying principle is that the maximum infiltration rate remains constant regardless of precipitation rate, volume, or initial conditions. Therefore, the runoff volume, R, for any given time-step, can be directly estimated given the rate of precipitation, P, and the maximum infiltration rate, I (Hydrologic Engineering Center, 2000):

$$R = \begin{cases} P - I & if\ P > I \\ 0 & otherwise \end{cases} \quad (3\text{-}1)$$

Where R, P, and I are all measured in terms of depth (in) for the measured time step. Both the P and I values are determined by multiplying their rates of precipitation (in/hr) and infiltration (in/hr), respectively, by the time interval.

An initial deficit, D, is added to the model to represent the volume available for rainfall interception and depression storage. Rainfall interception is a result of the absorption of water due to land cover, such as plants within the watershed, while depression storage is a result of low lying areas within the topography that collect water prior to allowing for any runoff. Using this logic, the runoff volume at each time step can be calculated as:

$$R = \begin{cases} 0 & if \sum P < D \\ P - I & if \sum P - \sum I > D \; and \; P > I \\ 0 & if \sum P - \sum I > D \; and \; P < I \end{cases} \quad (3\text{-}2)$$

Where R, P, I, and D are all measured in terms of depth (in) for the measured time step. Both the P and I values are determined by multiplying their rates of precipitation (in/hr) and infiltration (in/hr), respectively, by the time interval.

As the watershed approaches a saturated condition, the initial deficit approaches zero, implying that the soil column has no available room to store the precipitation volume. If the watershed is dry, the initial deficit will increase up to the maximum deficit. The constant loss rate is typically associated with the infiltration capacity of the soil defined by its hydraulic conductivity.

The modeling framework also allows for the initial deficit to grow during periods of no precipitation through the use of a recovery rate. Throughout the simulation, the moisture deficit within the soil layer is tracked continuously and is computed as the initial deficit less the precipitation depth plus the rate of recovery for each time step. The recovery rate is intended to simulate the impact of evapotranspiration on drying of the surface soil layers, and the

percolation of water to the groundwater layer, or some fraction thereof. If no recovery rate is specified, this process is ignored. There is also an upper limit to the deficit at which point the soil column is virtually empty of moisture. This is known as the maximum deficit, M (Hydrologic Engineering Center, 2000)

The deficit and constant loss model requires the input of two modeling parameters and one initial condition. These parameters are based on the physical properties of the soils found within the modeled watershed and the moisture condition prior to the simulation. These parameters are:

• Infiltration Rate	(in/hr)	Modeling parameter
• Maximum Deficit	(in)	Modeling Parameter
• Initial Deficit	(in)	Initial Condition

This project will seek to define the constant loss rate and the maximum deficit by using the soil data provided within the SSURGO database. This process is described in Section 3.5.2.

3.4.1.2 Green and Ampt

The Green and Ampt model of soil infiltration is an approximate, but theoretical, model based on the application of Darcy's law (Green & Ampt 1911; Wurbs and James, 2002). The advantage of this modeling technique lies in its use of physically based parameters in the calculation of runoff volume. However, estimating accurate parameter values can be difficult, especially in ungauged watersheds.

The Green and Ampt infiltration model was first developed to simulate ponded infiltration through a homogeneous soil with a uniform initial water content. Water is assumed to push through the soil as piston flow with a sharply defined barrier between the wetted and unwetted soil known as a wetting front. The equation for determining Green and Ampt rate of infiltration is:

$$f = K\left[1 + \frac{(\phi - \theta_i)S_f}{F}\right] \quad (3\text{-}3)$$

Where f is the infiltration rate (in/hr) at any particular time, K is the saturated hydraulic conductivity (in/hr), ϕ is the soil porosity (in^3/in^3), θ_i is the initial water content (in^3/in^3), S_f is the effective suction at the wetting front (in), and F is the accumulated infiltration (in) at any particular time.

In the equation, the infiltration rate f at any given time step is dependent on the total accumulated infiltration volume F, meaning that both values change over time. Because both f and F are unknown, there is no deterministic solution for this equation. Instead, an iterative process must be completed for each time step of interest, estimating both f and F at each time step. Because of the computationally intensive procedure, hydrologic modeling software designed for the process such as HEC-HMS prove a valuable resource.

As the watershed approaches a saturated condition, the difference between saturated and initial soil water contents will approach zero implying that the infiltration rate will be reduced to match the saturated hydraulic conductivity of the soil. If the watershed is dry, the difference between initial and saturated water contents will increase, which will in turn increase the influence that the wetting front suction has on the total infiltration rate.

The Green and Ampt loss model requires the input of three modeling parameters, and one initial condition, the initial moisture content. These parameters are based on the physical properties of the soils found within the modeled watershed and the moisture condition prior to the simulation. These parameters are:

- Saturated Hydraulic Conductivity (in/hr) Modeling parameter
- Saturated Soil Water Content (in^3/in^3) Modeling Parameter
- Wetting Front Suction Head (in) Modeling Parameter
- Initial Soil Water Content (in^3/in^3) Initial Condition

This project will seek to define the saturated soil water content, wetting front suction, and hydraulic conductivity by using the soil data provided within the SSURGO database. This process is described in Section 3.5.2. The Green and Ampt method has been shown to provide highly accurate estimates of infiltration of water into homogeneous soil, provided that it is parameterized accurately (Freyberg et al, 1980; Van Mullen 1991; Ma, 2010).

3.4.1.3 SCS Curve Number

The SCS Curve Number method is widely used in the field of hydrology due to its simplicity of application (Hawkins and Hjemfelt, 1985; Woodward et all, 2003; Mishra, 2013). The basic equation used for this method is:

$$R = \begin{cases} 0 & if\ P \leq I_a \\ \dfrac{(P - I_a)^2}{P - I_a + S} & if\ P > I_a \end{cases} \tag{3-4}$$

Where R is the depth of rainfall runoff (in), P is the depth of rainfall (in), I_a is the initial abstraction of rainfall (in), and S is the total potential retention of water needed to fully saturate the soil column (in). The initial abstraction, being the sum of all losses prior to the beginning of runoff, is highly variable from watershed to watershed. However, data from many small watersheds yields the following empirical relationship (Woodward et al., 1999):

$$I_a = 0.2S \tag{3-5}$$

Finally, for the standardization of this equation's application and for the streamlining of the process, the potential retention is given in the form of a dimensionless runoff curve number (CN) (Woodward et al., 1999):

$$CN = \frac{1000}{S + 10} \tag{3-6}$$

The CN process eliminates all of the physically based properties related to the soil within the watershed and enables the estimation of runoff volume given only precipitation and a curve number. The curve number is related to the type of vegetation cover, general soil type, and

hydrologic condition of the watershed (Hawkins et al., 1985). Typically, the curve numbers are organized first by land use, as this is generally straightforward to define based on the name (pasture, commercial and business, residential). From there, the numbers are further subdivided into four groups based on soil classification and expected runoff characteristics (Wurbs and James, 2002):

- Group A: soil has high infiltration rate with a low potential for runoff. This classification is typically for well-drained sand, loess, and gravel
- Group B: soil has a moderate infiltration rate and consists primarily of moderately fine to moderately coarse textured soils such as sandy loam
- Group C: soil has a slow infiltration rate and consists of fine textures oils such as clay loam, shallow sandy loam and some clays
- Group D: soil has a high potential for runoff with a very slow infiltration rate. This classification is typically for swelling and plastic clays as well as soils with a high permanent water table.

Curve Numbers also vary with antecedent moisture condition (AMC). AMC is categorized into three main categories defined as dry, average, and wet (AMC I, II, and III). Curve numbers are typically defined in terms of the average condition, AMC II, and tend to be used under this condition. However, if information is available to suggest the need to use either AMC I or AMC III, the following equations can be used (Hawkins et al., 1985):

$$CN(AMC\ I) = \frac{4.2 * CN(AMC\ II)}{10 - 0.058 * CN(AMC\ II)} \tag{3-7}$$

$$CN(AMC\ III) = \frac{23 * CN(AMC\ II)}{10 + 0.13 * CN(AMC\ II)} \tag{3-8}$$

The CN for a watershed will vary between the values of 0 and 100. Based on Equation 3-6, a CN of 100 corresponds to a potential retention of 0, meaning that all of the precipitation will be converted to runoff volume. While a CN of 100 is almost impossible to achieve, a good example would be a small concrete parking lot. Conversely, a CN of 0, while mathematically impossible, would suggest a high potential retention with no possibility of runoff. An example of this would be a gravelly soil with extremely high permeability and no layering.

This study sought to define the curve number based on information provided in the SSURGO database as well as the National Land Cover Database (NLCD) provided by the Multi-Resolution Land Characteristics Consortium (MRLCC) (Soil Survey Staff, 2016). This process is described in Section 3.6.

3.4.2 Transform Methods

The transform method for a hydrologic model describes how the excess precipitation from any location in a watershed is translated into a runoff hydrograph for a subbasin. This is typically done through the use of a unit hydrograph. For this study, the ModClark method, which is a modified version of the Clark Unit Hydrograph Method, was used for runoff transformation. To understand the use of ModClark, the Clark method is first explained.

3.4.2.1 Clark Synthetic Unit Hydrograph

The Clark Synthetic Unit Hydrograph method is based on the concept of a time-area relationship through a linear reservoir. The two critical processes are the translation of rainfall runoff from its point of origin to the watershed outlet and the attenuation of that runoff as it is collected throughout the watershed. In order to utilize this methodology, the time of concentration, t_c, is required. This value is the travel time from the most hydraulically remote point in the basin to the outlet. Also, the time-area relationship must be established between travel time and contributing watershed area. However, as determining t_c is difficult, establishing an accurate time-area relationship is even more difficult. To simplify the Clark method, the Hydrologic Engineering Center developed the following synthetic time-area relationship (Hydrologic Engineering Center, 2008):

$$\frac{A_c}{A} = \begin{cases} 1.414\left(\frac{t}{t_c}\right)^{1.5} & for\ t \le \frac{t_c}{2} \\ 1 - 1.414\left(1 - \frac{t}{t_c}\right)^{1.5} & for\ t \ge \frac{t_c}{2} \end{cases} \quad (3\text{-}9)$$

Where A_c represents the cumulative watershed area (ac) contributing at time t (hrs), and A represents the total watershed area (ac), and t_c represents the time of concentration (hrs). Application of this portion of the Clark model requires only the time of concentration.

The next phase is to develop the linear reservoir routing relationship. Generally speaking, a linear reservoir is a modeling technique that uses a direct relationship between the storage within a reach, S, and the outflow hydrograph, O, by way of a storage coefficient, R:

$$S = R \cdot O \tag{3-10}$$

Where S is the storage (ft^3), R is the storage coefficient (hrs), and O is the reservoir outflow (cfs). In terms of the Clark method application, this storage coefficient, R, is an index of the temporary attenuation of runoff in the watershed as it drains towards the basin outlet point (Sabol, 1988). R has units of time (hrs), but it doesn't have an exact physical meaning in terms of a measurable feature. Clark indicated that R can be computed as the flow at the inflection point on the falling limb of the hydrograph divided by the time derivative of flow, but it's mostly thought of as a calibration parameter (Sabol, 1988).

To utilize this method with the simplifications provided by way of the HEC time-area relationship approximation, the only input parameters required are t_c and R. There are a variety of ways to determine the values for these two parameters. Time of concentration was determined using the procedure outlined in the United States Department of Agriculture's (USDA) Natural Resources Conservation Service (NRCS) Technical Release 55 (TR-55). TR-55 is entitled "Urban Hydrology for Small Watersheds" (Cronshey, 1986) and contains, among other things, a method that describes the time of concentration as the sum of all the travel times for consecutive components of the drainage conveyance system (Cronshey, 1986). The three main components for this conveyance are sheet flow, shallow concentrated flow, and open channel flow.

The storage coefficient R is a difficult parameter to estimate even if recorded hydrograph information is available (Sabol, 1988). Sabol (1988) determined an empirical relationship for calculating R based on the time of concentration for a watershed. This equation is:

$$\frac{T_c}{R} = 1.46 - 0.0867\frac{L^2}{A} \quad (3\text{-}11)$$

Where T_c is the time of concentration (hrs), R is the basin storage coefficient (hrs) L is the longest flow path (ft) for a drainage area and A is the drainage area (ft^2). This equation was used to estimate R for each subbasin within this study. Calculations for all model parameters are shown in Appendix B – Hydrologic Parameter Calculations.

3.4.2.2 ModClark

The ModClark method is a method for applying the Clark Unit Hydrograph method in a quasi-distributed fashion enabling the model to account for spatial differences in rainfall and infiltration losses (Paudel et al., 2009). Rainfall runoff is calculated for each grid cell and is then lagged based on travel time to the defined subbasin outlet and routed through a linear reservoir. The key difference between ModClark and Clark is the value for time of concentration. For each grid cell, the time of concentration value is adjusted based on the relative distance to the subbasin outlet using Equation 3-12 (Hydrologic Engineering Center, 2000):

$$t_{cell} = t_c \frac{d_{cell}}{d_{max}} \quad (3\text{-}12)$$

Where t_{cell} = time of travel for a cell (hrs), t_c = time of concentration for the watershed (hrs), d_{cell} = travel distance from a cell to the outlet (ft), and d_{max} = travel distance for the cell that is most distant (ft).

The results from each cell within a drainage area are combined to produce the final runoff hydrograph. If the precipitation pattern and the loss methods are uniform across all grid

cells, the result from a ModClark transform model will produce an identical result to that of a Clark transform (Paudel et al., 2009).

3.4.3 Routing Method

Hydrologic routing is the method of moving discharge from the outlet of one subbasin through a channel network to the outlet of the next subbasin downstream (Hydrologic Engineering Center, 2010). Within the Salt Creek Basin HEC-HMS model, there are a total of 28 reaches connecting upstream subbasin outlets to downstream outlets. For this study, the Muskingum method was chosen.

The Muskingum routing method (McCarthy, 1938; Nash 1959, Wurbs and James, 2002) is a popular routing method used within the Hydrologic and Hydraulic community in the United States. It is based on the assumption that the storage volume in a stream reach at any instant in time is a linear function of the weighted inflow and outflow of the reach. The method accounts for the tendency of a hydrograph to flatten out (reducing its peak discharge) as it travels downstream, and to lengthen in time. The variable discharge-storage equation is (Chow, 1959; Tung, 1985):

$$S = K(xI + (1 - x)O) \tag{3-13}$$

Where S is the storage volume within the reach (ft^3), I is the instantaneous inflow volume into the reach (cfs), O is the corresponding outflow value (cfs), and K and x are the two Muskingum parameters defining the storage-flow relationships. The weighting factor x is a dimensionless number ranging between the values of 0 and 0.5 and is indicative of the influence that inflow versus outflow has on the storage volume. The parameter K is a proportionality constant and is often close to the travel time within the modeled reach (hr).

By applying a derivative with respect to time to the above equation, the following relationship is derived for the outflow of the reach at the following time step (McCarthy 1938):

$$O_{t+\Delta t} = C_1 I_{t+\Delta t} + C_2 I_t + C_3 O_t \quad (3\text{-}14)$$

In which:

$$C_1 = \frac{0.5\Delta t - Kx}{K - Kx + 0.5\Delta t} \quad (3\text{-}15)$$

$$C_2 = \frac{0.5\Delta t + Kx}{K - Kx + 0.5\Delta t} \quad (3\text{-}16)$$

$$C_3 = \frac{K - Kx - 0.5\Delta t}{K - Kx + 0.5\Delta t} \quad (3\text{-}17)$$

$$C_1 + C_2 + C_3 = 1 \quad (3\text{-}18)$$

The use of the Muskingum routing method only requires the input of two parameters: x and K. While the value of x can mathematically vary between 0 and 0.5, x will almost always fall between the values of 0.1 and 0.3 for naturally occurring river systems (Wurbs and James, 2002). Also, values for K can be assigned based on the travel time within the reach, which can be estimated from observed hydrographs at the upstream and downstream ends of the reach. Additionally, values for K should meet the requirement of $K/3 \leq \Delta t \leq K$ (Maidment 1993). If this relationship is not valid, the reach should be subdivided, or the time step altered. A violation of this relationship may result in unrealistic negative dips in the computed hydrographs.

For this study, the value of K was estimated based on the application of Manning's equation (Manning, 1890; Chow, 1959; Maidment, 1993) to each river segment. The Manning's roughness (n) value and hydraulic radius are estimated based on aerial imagery and the slope of the river segments as measured during the pre-processing phase. The value of K was estimated for each reach by combining this information with a standard travel time equation. For the x parameter, an average value of 0.25 was assigned to all reaches. More details for the Muskingum parameter estimation are available in Appendix B.

3.4.4 Distributed Computational Framework

This study sought to determine the impact that the different runoff methods and their means for parameterization have on the resulting runoff hydrograph. The three methods previously described and listed in Table 1 - 1 were applied in both a lumped and distributed fashion, and the resulting runoff hydrographs were compared to the observed hydrographs at the subbasin outlets. A grid-based computational scheme was used to calculate the rainfall runoff for both lumped and distributed computations. Doing so allowed the model to use the exact same gridded precipitation data and ModClark transform method, isolating the impact of each runoff model on the results.

When applying a lumped parameter to the model, the same loss parameters were used for every grid-cell computation within a given subbasin. Whether at the mouth of the basin with a soil composition of mostly alluvial sands or at the very headwaters, the same parameter values were applied. When applying distributed parameters, the loss parameters varied within the basin and experienced different infiltration rates and runoff volumes. In both cases, the runoff was routed to the subbasin outlet using the same ModClark hydrograph transform parameters.

3.5 Parameter Estimation from SSURGO

The prediction of rainfall runoff parameters for catchments without the use of observed streamflow data and calibration is a significant challenge in the field of hydrology (Wagener et al., 2006). Hydrologists have developed methods of estimation based on similar characteristics between gauged and ungauged watersheds through a process called parameter regionalization, and some have tried to establish relationships between physical characteristics of the soil and the hydrologic modeling parameters. The problem with the latter solution has been the lack of comprehensive soil data and the spatial variability of soil properties. This study attempts to leverage the comprehensive Soil Survey Geographic (SSURGO) database and generate loss parameters for all methods.

The Soil Survey Geographic (SSURGO) Database contains soil data that have been collected over the past 100 years (Soil Survey Staff, 2016). This information is maintained by the Natural Resources Conservation Service, a branch of the United States Department of Agriculture. The data have been obtained by manual surveys conducted via ground surveys that observed the properties of the soil and was occasionally tested in labs to obtain more specific properties. This information was then organized and can be displayed in either a tabular format or as a map (Soil Survey Staff, 2016).

SSURGO datasets are composed of geospatial data, tabular data, and metadata describing how the data were obtained. The extent of the individual datasets tends to include information for an entire county, although they may consist of multiple counties, or even parts of several counties combined. While much of the SSURGO data represents measured data points, there are also many qualitative aspects of the soil that are recorded as well, such as soil texture. As a result, a difference in opinion as to how to classify a certain soil could yield

unnatural boundaries of soil features. This can be seen in Figure 3 - 3 with a notable shift from “silty clay loam” to “silt clay” occurring along the Lancaster-Saunders county line.

Gridded SSURGO (gSSURGO) is similar to the standard SSURGO data, but is instead stored within a file geodatabase. Doing so allows for the storage of much more data, leading to the product being available with statewide extents rather than based on county. Also stored within gSSURGO is a higher resolution 10-meter raster dataset version of the map unit data. The tabular data included within gSSURGO is an identical match to that of SSURGO.

One goal of this study was to develop a method that can use the information within SSURGO, and by extension gSSURGO, to derive the parameters necessary for the hydrologic simulations, with the end goal being a single parameter value for each subbasin in the HEC-HMS model. As a result, only select information contained in SSURGO was used, with other data sources supplementing the information as needed.

3.5.1 SSURGO Data Structure

SSURGO data is the highest resolution soils data product that is distributed by the NRCS. The data are compiled as scales ranging from 1:12,000 to 1:63,360 and are available for most areas within the United States (Soil Survey Staff, 2016). The resolution of the SSURGO database is based on the map unit, which describes an area dominated by one or more major soil types and named according to taxonomic classification of the dominant soils (Soil Survey Staff, 2016).

The data are downloaded from the SCS Web Soil Survey (WSS) which provides an interactive map displaying the availability of SSURGO data for the contiguous United States. The data are available for download by county, and with a known area of interest with the corresponding counties, the user can proceed directly to the download soils tab (Soil Survey Staff, 2016). For this study, SSURGO data were necessary for seven Nebraska counties: Butler, Cass, Gauge, Lancaster, Saline, Saunders, and Seward counties.

SSURGO datasets were obtained from the SCS contain spatial data, tabular data, and metadata for the study area. Once downloaded, the data for the seven counties were combined into a single dataset and clipped to the Salt Creek Basin using ArcGIS. The resulting map from this process is shown in Figure 3 - 13.

While the individual map units do describe an area dominated by a particular soil group, these map units are not homogenous in their soil properties. Map units can be made up of anywhere from one to three “components” which are thought to have similar properties. These components can then be broken down into a series of layers referred to as “horizons,” each of which is thought to be completely homogenous. The depth of each horizon varies from component to component.

The data for the map units, components, and horizons are stored in their own tables within the SSURGO data structure and can be related to one another via “keys”. The map unit key is denoted in the field “mukey” which can be found in both the map unit and component table as a way of matching the map unit to its components. In the same way the component key is denoted by the field “cokey” and relates each component to its horizons in the chorizon table. A graphic showing this information is shown in Figure 3 - 14.

Due to the spatial variability of soil properties within each map unit and the vertical variability of properties within each component, the physical information necessary to define the loss parameters for this study are stored within the horizon information. However, since there are multiple horizons within a component and multiple components within a map unit, the data must be carefully aggregated to properly represent the soil properties. The procedure involves first calculating each loss parameter for each horizon and then using a series of weighted averages to calculate the average parameter value for each map unit.

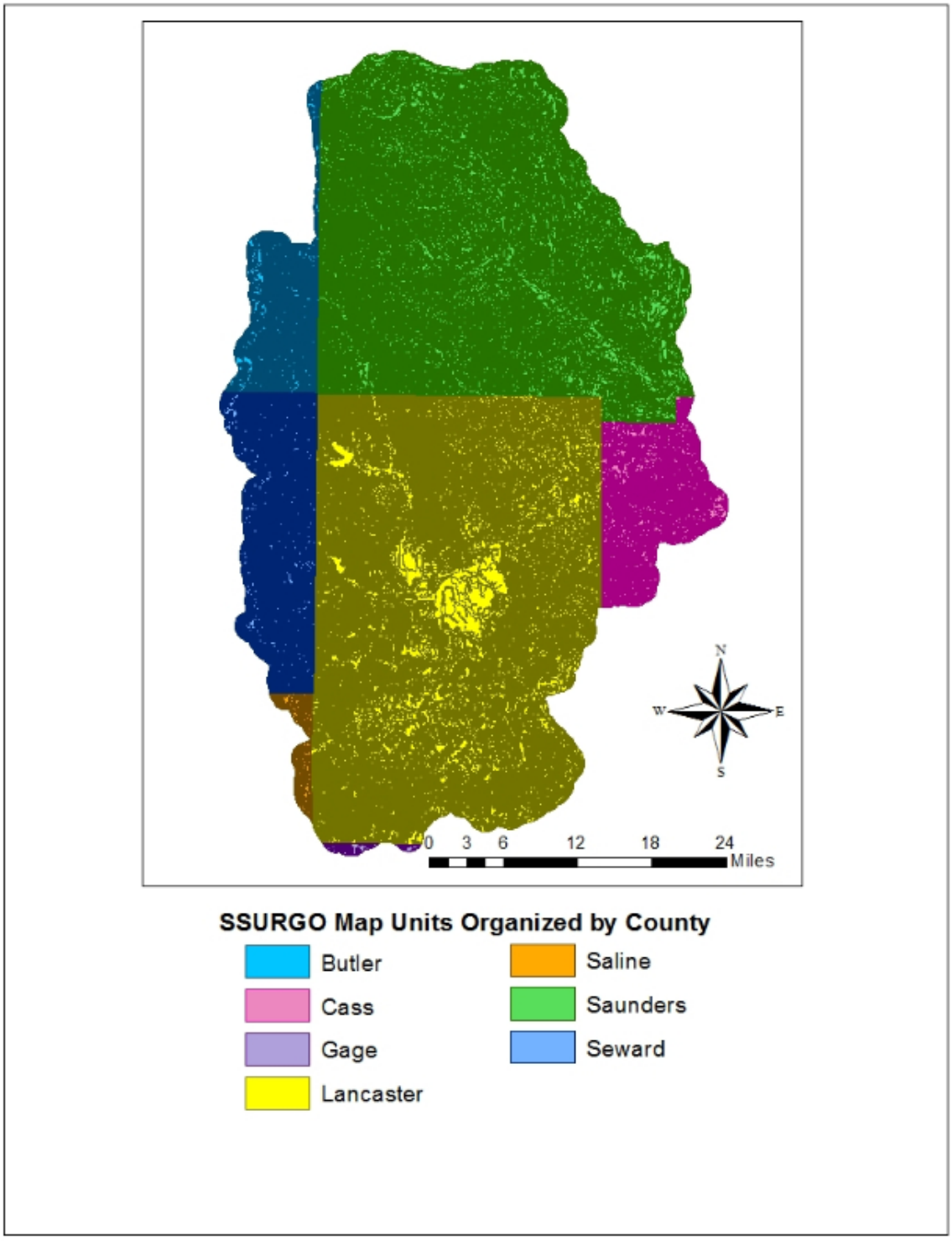

Figure 3 - 13. SSURGO Map Units by County within Salt Creek Basin

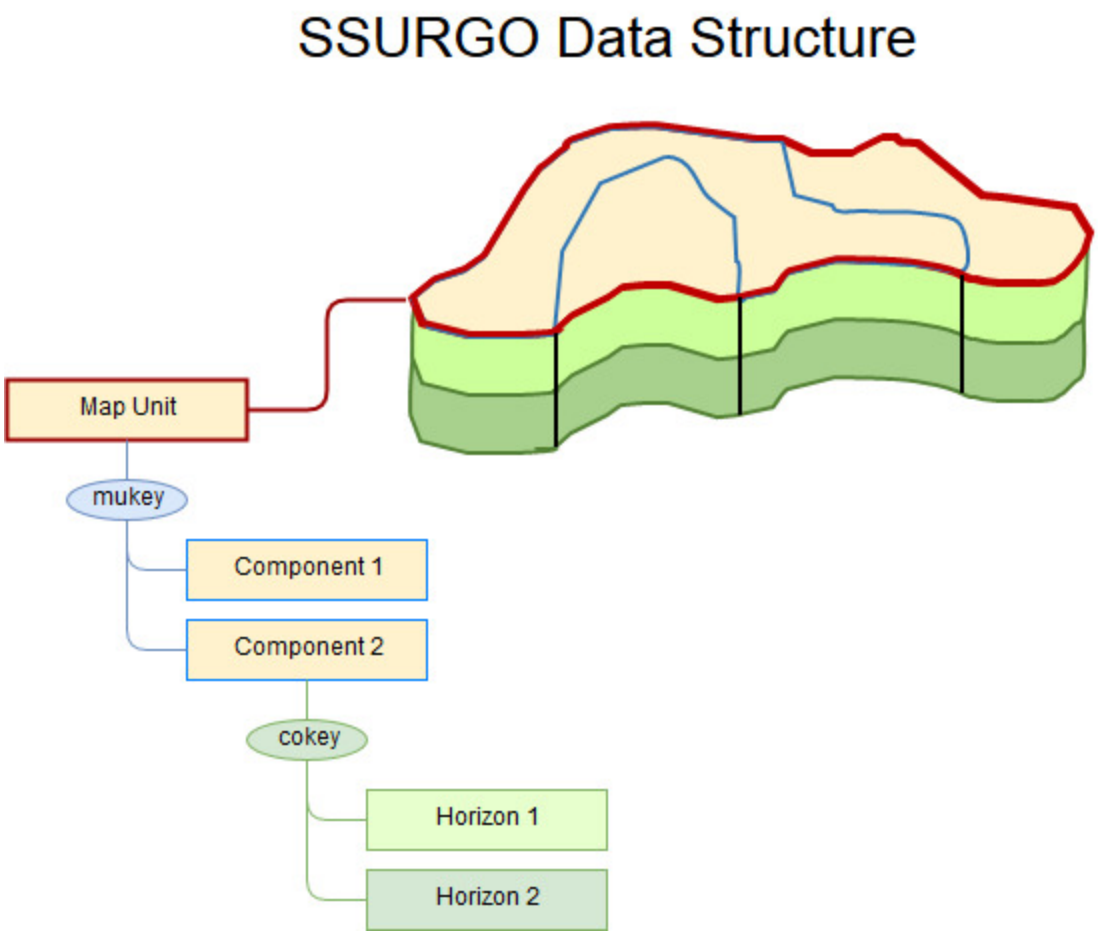

Figure 3 - 14. SSURGO data structure

3.5.2 Parameter Estimation for SSURGO Horizons

The chorizon table contains a plethora of physical soils information for each horizon. This study focused on the information necessary to define the parameters for the runoff methods. The necessary fields and descriptions (Soil Survey Staff, 2016) are listed in Table 3-1.

Table 3 - 1. Chorizon Table Fields Used in the Calculation of Loss Parameters

Field	Units		Description
	Given	English	
Hzdept_r	cm	In	The average distance from the ground surface to the upper boundary of the soil horizon
Hzdepb_r	cm	In	The average distance from the ground surface to the lower boundary of the soil horizon
Hzthk_r	cm	In	Measures the average soil horizon thickness (hzdepb_r - hzdept_r)
Ksat_r	mm/hr	In/hr	The average saturated hydraulic conductivity for the soil horizon
Texture	N/A	N/A	Gives the symbol associated with a particular soil texture
Texdesc	N/A	N/A	Describes the soil texture qualitatively with standard soil classifications (sand, clay, loam, etc.)
Wfifteenbar_r	cm^3/cm^3	in^3/in^3	The average volumetric water content measured at 15 bars (1500 kPa). This is used to estimate the permanent wilting point of the soil (USDA 2017)
Dbthirdbar_r	g/cm^3	lb/in^3	The oven dry weight of the less than 2 mm soil material per unit volume of soil at a water tension of 1/3 bar. Represents the horizon bulk density (USDA 2017)
Partdensity	g/cm^3	lb/in^3	Mass per unit of volume (not including pore space) of the solid soil particle. Represents the soil particle density (USDA 2017)

One necessary piece of information necessary for this study and not stored within the SSURGO database is the information for wetting front suction head. A study completed by Rawls et al. (1983) determined the average values for Green and Ampt parameters based on soil texture. This study is well known in the field of hydrologic engineering and is considered standard practice in its use of soil texture information to define parameters to use in hydrologic modeling (Reinartz, 2016). To incorporate the wetting front suction head values into this study, a field was added to the chorizon table titled “Suction” and the fields were populated based on the soil texture and the values from Rawls et al. (1983). The table of values can be found in Appendix B, Table B - 7.

Field	Units		Description
	Given	English	
Suction	cm	in	Average wetting front suction based on soil type

3.5.2.1 Deficit and Constant Loss

The Deficit and Constant Loss method is a simplified modeling technique based on the physical characteristics of the watershed. The method requires the input of two modeling parameters:

- Infiltration Rate (IR)
- Maximum Deficit (MD)

Hydraulic Conductivity is the easier of the two parameters to determine from SSURGO data as it is directly given by the ksat_r field.

$$IR = Saturated\ Hydraulic\ Conductivity = ksat\_r \quad (3\text{-}19)$$

Where IR is the infiltration rate (in/hr) and ksat_r is the SSURGO-given saturated hydraulic conductivity (in/hr).

Maximum Deficit is a more nuanced in its definition. The first step is to define the Porosity for each soil horizon. The parameter is not directly defined within the SSURGO table, but can be calculated by using the bulk density and particle density information. The ratio of the volume composed of solids to the total volume within a particular soil horizon is equal to the bulk density divided by the particle density. Following this logic, the volume of voids, or porosity, is equal to the solids ratio subtracted from one as in equation 3-20 (Soil Survey Staff, 2016).

$$Porosity = 1 - \frac{Bulk\ Density}{Particle\ Density} = 1 - \frac{dbthirdbar\_r}{partdensity} \quad (3\text{-}20)$$

Where Porosity is the ratio of total volume of voids per unit volume of soil (in^3/in^3), Bulk Density, represented by dbthirdbar_r from SSURGO, is the ratio of the oven dry weight of soil per unit volume of soil (lb/in^3), and Particle Density, represented by partdensity from SSURGO, is the mass of soil particles per unit volume of soil particles (lb/in^3).

Once the porosity is defined for each horizon, the next step is to determine the total amount of interstitial space within the defined soil column known as the saturation capacity

(SatCap). This can be determined by multiplying the porosity of the soil horizon by the horizon thickness, hzthk_r.

$$SatCap = Porosity \cdot Layer\ Thickness = Porosity \cdot hzthk\_r \quad (3\text{-}21)$$

Where SatCap is the total volume of voids within the horizon (in), Porosity is the ratio of total volume of voids per unit volume of soil (in^3/in^3), and hzthk_r is the SSURGO-given average horizon thickness (in).

Saturation Capacity describes the total space within the soil layer, but this volume is not completely available for water storage. Often times, the shape of soil particles themselves hold water and are not able to release the moisture. As a result, the space available to hold incoming rainfall must be reduced by some amount. This residual term is commonly referred to as the permanent wilting point and is often estimated as the volume of water occupied at a pressure of -15 bar (Saxton and Rawls, 2006). SSURGO provides the data necessary to estimate this information. The field wfifteenbar_r provides a volumetric percentage of water at wilting point in soil for each soil horizon. Dividing this value by 100 and then multiplying by horizon thickness yields the wilting capacity (WiltCap) of the soil horizon:

$$WiltCap = \frac{Wilt\ Water\ Content}{100} \cdot Layer\ Thickness = \frac{wfifteenbar\_r}{100} \cdot hzthk\_r \quad (3\text{-}22)$$

Where WiltCap is the volume of voids per unit volume unavailable for precipitation storage (in), wfifteenbar_r is the SSURGO-given average volumetric water content measured at 15 bars (1500 kPa) used to estimate the permanent wilting point of the soil (in^3/in^3), and hzthk_r is the SSURGO-given average horizon thickness (in).

Finally, the Maximum Deficit, or the volume available to store rainfall volume, is calculated as the difference between the saturation capacity and the wilting capacity:

$$MD = Saturation\ Capacity - Wilting\ Capacity = SatCap - WiltCap \quad (3\text{-}23)$$

Where MD is the maximum volume available to store precipitation volume (in), SatCap is the total volume of voids within the horizon (in), and WiltCap is the volume of voids per unit volume unavailable for precipitation storage (in).

With both parameters defined for each horizon, what remains is to use weighted averages to generalize the parameter to the component, map unit, and subbasin levels. This process is outlined in Section 3.5.4.

3.5.2.2 Green and Ampt

The Green and Ampt loss method is a more rigorous physical model designed to take into account the actual process of water moving down through the soil column. The method requires the input of three modeling parameters:

- Hydraulic Conductivity (K)
- Saturated Content (SC)
- Wetting Front Suction Head (S)

As with the Deficit and Constant Loss method, the hydraulic conductivity is straightforward to estimate from the SSURGO data as it is directly given by the ksat_r field:

$$K = ksat\_r \tag{3-24}$$

Where IR is the infiltration rate (in/hr) and ksat_r is the SSURGO-given saturated hydraulic conductivity (in/hr).

Saturated Content is similar to hydraulic conductivity in its estimation. This parameter specifies the water holding capacity of the soil column in terms of volumetric ratio. It is often assumed to be equivalent to the total soil porosity (Hydrologic Engineering Center, 2008), which is a parameter already defined in the table:

$$SC = Porosity \tag{3-25}$$

Where SC and Porosity are both the ratio of the total volume of voids per unit volume of soil (in^3/in^3).

Finally, wetting front suction is a parameter already defined in the table:

$$S = Suction \tag{3-26}$$

where S is the characteristic wetting front suction head (in) for each soil type as defined by Saxton et al. (1983).

With all three parameters defined for each horizon, what remains is to use weighted averages to generalize the parameter to the component, map unit, and subbasin levels. This process is outlined in the Section 3.5.4.

3.5.3 Soil depth variance

Before the horizon parameters were combined using weighted averaging techniques, the dataset was doubled to allow for the development of parameter values for different soil depths: 1-foot and 3-foot. This process was done to see what impact if any the depth of the soil would have on the hydrologic modeling. The 1-foot soil depth is possibly more applicable for describing rainfall runoff parameters that are generally most impacted by the near-surface soil conditions, while the 3-foot depth is typical for long range modeling efforts involved in soil moisture accounting, for example, root zone soil water contents for agricultural crops.

To perform this analysis, the values contained within the hzdept_r and hzdepb_r fields were altered so that no number would exceed the desired depth of the soil profile. Since these two categories are measured from the surface, the values had to either be less than or match their corresponding desired depth: 12 inches for the 1-foot soil column, 36 inches for the 3-foot soil column. Any values greater than the desired depth was reduced to the desired depth. The value in the hzthk_r field was then adjusted to reflect the truncated distance. An example of this operation is shown in Table 3 - 2 and Table 3 - 3:

Table 3 - 2. Example Horizon Depth Alteration for 1-Foot Soil Depth

CHKEY	Hzdept_r (in)	Hzdepb_r (in)	Hzthkr (in)
1516489	0	5	5
1516490	5	20	15
1516491	20	50	30
		TOTAL	**50 in**

→

CHKEY	Hzdept_r (in)	Hzdepb_r (in)	Hzthkr (in)
1516489	0	5	5
1516490	5	12	7
1516491	12	12	0
		TOTAL	**12 in**

Table 3 - 3. . Example Horizon Depth Alteration for 3-Foot Soil Depth

CHKEY	Hzdept_r (in)	Hzdepb_r (in)	Hzthkr (in)
1516489	0	5	5
1516490	5	20	15
1516491	20	50	30
		TOTAL	**50 in**

→

CHKEY	Hzdept_r (in)	Hzdepb_r (in)	Hzthkr (in)
1516489	0	5	5
1516490	5	20	15
1516491	50	36	16
		TOTAL	**36 in**

Manipulating the data in this way did not remove the superfluous entries from the table for deeper soil depths, but it did render them irrelevant during the depth-weighted average computations that occurred during the parameter aggregation phase. A layer with a depth of zero had no impact on the calculation of the average parameter value.

3.5.4 Parameter Aggregation

The general framework for deriving hydrologic modeling parameters from the SSURGO database information relies heavily on the computing power within the ArcGIS software. For the distributed modeling approach, the end goal is to obtain a raster dataset containing the hydrologic parameter values for each 10m grid cell currently assigned to a single map unit value. For the lumped parameter modeling approach, the end goal is to obtain an average value for each hydrologic modeling input for each subbasin. However, each subbasin is composed of several map units, each of which is composed of different components, which are then further divided into horizons. A representation of this breakdown is shown in Figure 3 - 15 below and will be used to track the aggregation process:

<table>
<tr><td rowspan="18">subbasin</td><td rowspan="9">map unit 1</td><td rowspan="3">component 1</td><td>chorizon 1</td></tr>
<tr><td>chorizon 2</td></tr>
<tr><td>chorizon 3</td></tr>
<tr><td rowspan="3">component 2</td><td>chorizon 4</td></tr>
<tr><td>chorizon 5</td></tr>
<tr><td>chorizon 6</td></tr>
<tr><td rowspan="3">component 3</td><td>chorizon 7</td></tr>
<tr><td>chorizon 8</td></tr>
<tr><td>chorizon 9</td></tr>
<tr><td rowspan="9">map unit 2</td><td rowspan="3">component 4</td><td>chorizon 10</td></tr>
<tr><td>chorizon 11</td></tr>
<tr><td>chorizon 12</td></tr>
<tr><td rowspan="3">component 5</td><td>chorizon 13</td></tr>
<tr><td>chorizon 14</td></tr>
<tr><td>chorizon 15</td></tr>
<tr><td rowspan="3">component 6</td><td>chorizon 16</td></tr>
<tr><td>chorizon 17</td></tr>
<tr><td>chorizon 18</td></tr>
</table>

Figure 3 - 15. Example Diagram of SSURGO Data Structure

In order to obtain the proper hydrologic parameter values, a weighted average approach was used within each layer of the data structure. The desired hydraulic parameters was first generated at the chorizon level and was then summarized at the component level by a layer depth-weighted average. The map unit average value was then computed by a weighted average based on each component's percentage of the map unit. Finally, the subbasin value was determined based on an area-weighted average of the map units within the subbasin.

3.5.4.1 Component Parameters with Depth-Weighted Average

The calculation of the soil parameters began with the chorizon table. To generalize these values from the horizon level to the component level required different operations for the parameters. For the volume based parameters, a simple sum of all soil horizons yielded the desired result as shown in equation 3-27. These parameters are Saturation Capacity, Wilting Capacity, and Maximum Deficit.

$$P_{co} = \sum P_{ch} \tag{3-27}$$

Where P_{co} is the hydrologic parameter value average for the component and P_{ch} is the hydrologic parameter value for the chorizon element. This process was applied for all layers up to the specified soil depth (1-foot or 3-foot).

For the other parameters, an average weighted parameter had to be developed for the whole column. The weighting factor to move from the horizon level to the component level is the horizon depth. Once the parameter was determined for each chorizon element, a depth weighted average was applied to generate a best estimate for the entire component:

$$P_{co} = \frac{\sum(P_{ch} \times hzthk\_r_{ch})}{\sum hzthk\_r_{ch}} \quad (3\text{-}28)$$

This used the same variables as defined in equation 3-27 with hzthk_r_{ch} representing the horizon thickness (in). The denominator of this equations should be equal to the soil column depth for each table. This calculation was where the elements beyond the desired depths (1-foot and 3-foot) were essentially eliminated from consideration. By multiplying the parameter value by a depth of zero, the influence in the weighting equation also became zero.

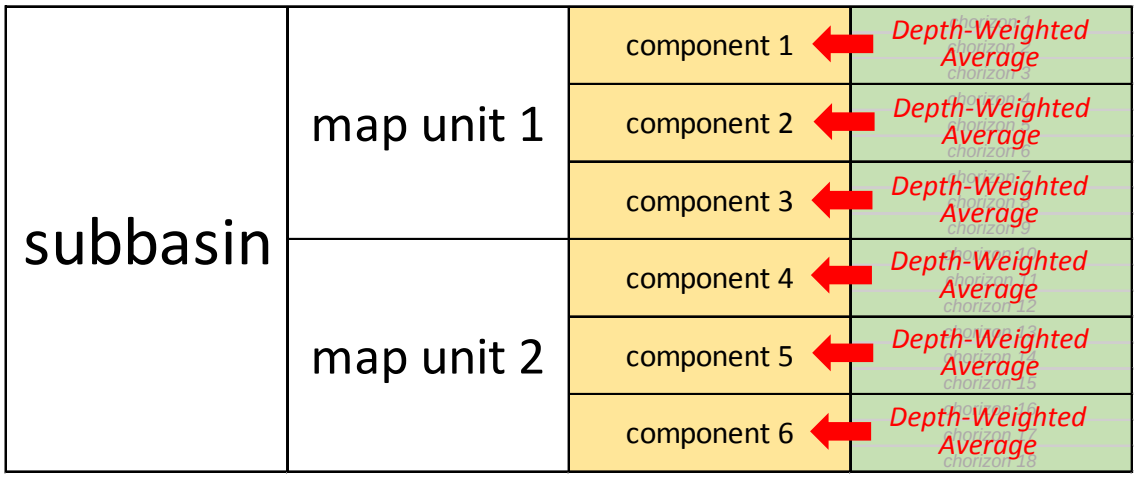

3.5.4.2 Map Unit Parameters with Percent-Weighted Average

The next phase in the parameter aggregation was to find the map unit weighted average for each parameter value. The weighting factor to move from the component level to the map unit level is the percentage of the map unit made up by each component. This information is stored in the comppct_r field in the component data table. With this data in hand, the equation for percent-weighted average can be performed and is shown in equation 3-29:

$$P_{mu} = \frac{\sum(P_{co} \times comppct\_r_{co})}{\sum comppct\_r_{co}} \quad (3\text{-}29)$$

Where P_{mu} is the hydrologic parameter value average for the map unit, P_{co} is the hydrologic parameter value for the component element, and $comppct\_r_{co}$ is the component percentage (%). The denominator of this equation should be equal to 100%.

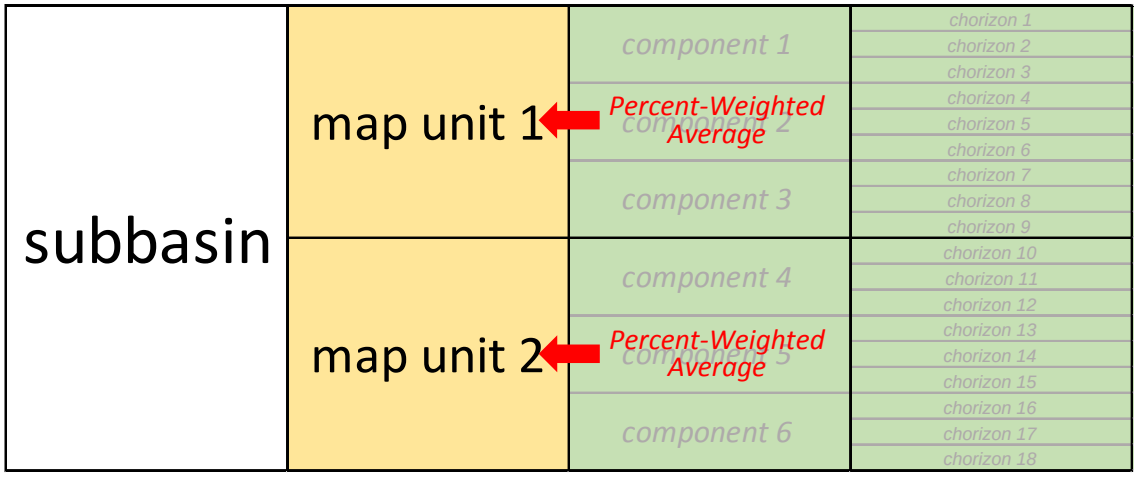

At this point in the procedure, the paths for the lumped and distributed parameter calculations diverge. Because the map unit parameter values have been defined and the map unit serves as the base unit for SSURGO datasets, these parameters are ready to be applied to both raster and vector datasets.

For lumped parameterization, one more weighted average was applied to move from the map unit scale to the subbasin scale. Once complete, the values were then ready to be used in the lumped-parameter hydrologic modeling to test their efficacy in estimating rainfall runoff.

For distributed parameterization, the parameter aggregation stops at the map unit level, and the map unit average parameter values are used to create grid-based version of the parameters. The process involved using the raster-based map unit grid downloaded for the state of Nebraska and clipped to the Salt Creek basin and combining it with the parameter tables to generate a raster grid for each hydrologic parameter. This process will be described further in Section 3.5.5.

3.5.4.3 Subbasin Average Parameters with Area-Weighted Average

The last phase in the lumped parameter aggregation was to find the subbasin weighted average for each parameter value. Because the map unit shapefiles were included with the SSURGO data download, some geospatial techniques could be used to derive the parameter values based on the polygon geometries.

Up to this point, all of the numerical manipulation was performed with datasets that were within the SSURGO dataset. As a result, all of the information was already linked by the map unit key and component key. The subbasin delineations, however, are not part of SSURGO and were derived using the processes outlined in Model Development Section 3.3.2. To rectify these different data sources, the data layers were overlaid using ArcGIS intersect tool to associate each map unit with its corresponding subbasin. For map units that overlap into multiple subbasins, the map units were be split along the subbasin boundaries and treated as separate polygons during the weighted averaging.

From this point, the procedure is similar to that of the percent weighted averaging. The weighting factor to move from the map unit level to the subbasin level is the area of each map unit. The equation for area-weighted average is:

$$P_{sub} = \frac{\sum(P_{mu} \times Area_{mu})}{\sum Area_{mu}} \quad (3\text{-}30)$$

Where P_{sub} is the hydrologic parameter value average for the subbasin, P_{mu} is the hydrologic parameter value for the map unit, and $Area_{mu}$ is the map unit area (ac). The denominator of this equation should be equal the subbasin area.

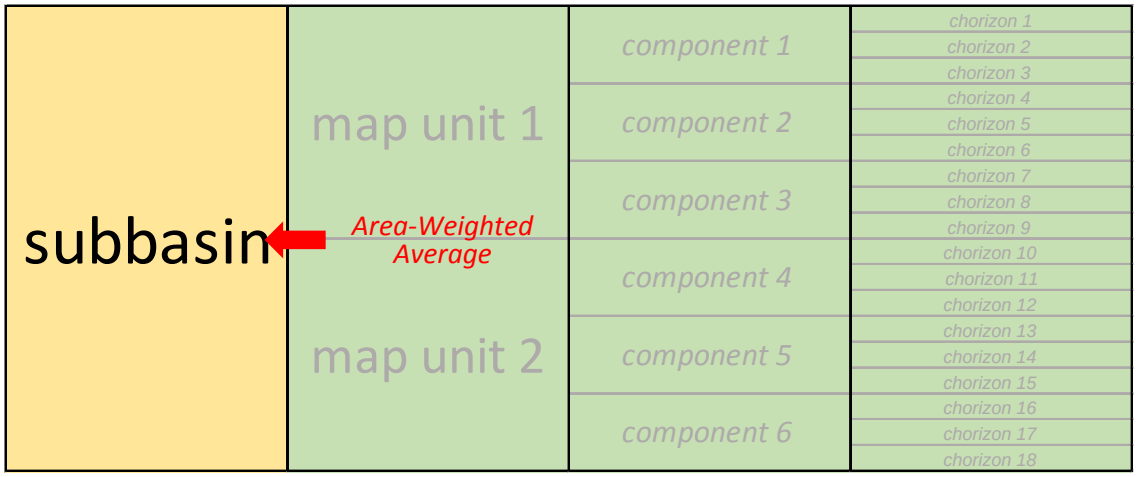

A complete table with each calculated subbasin parameter value is shown in Appendix B. Additionally, maps displaying the parameter values to be used in the hydrologic modeling for both the 1-foot and 3-foot soil depths are shown in Figure 3 - 16 through Figure 3 - 23.

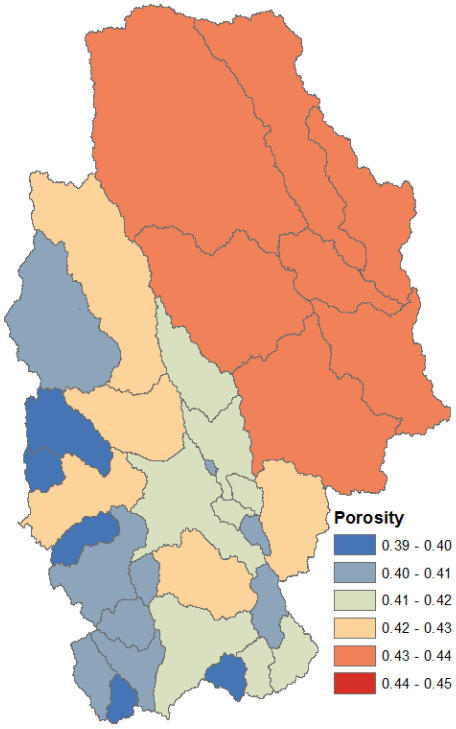

Figure 3 - 16. Average Subbasin Porosity for 1-Foot Soil Depth

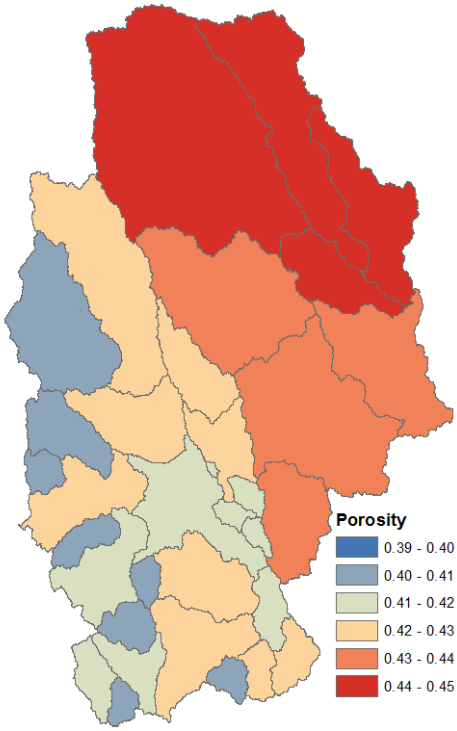

Figure 3 - 17. Average Subbasin Porosity for 3-Foot Soil Depth

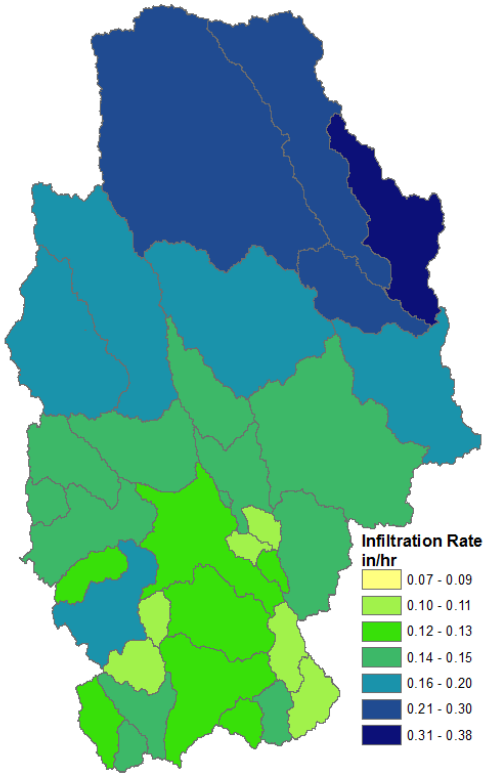

Figure 3 - 18. Average Subbasin Infiltration Rate for 1-Foot Soil Depth

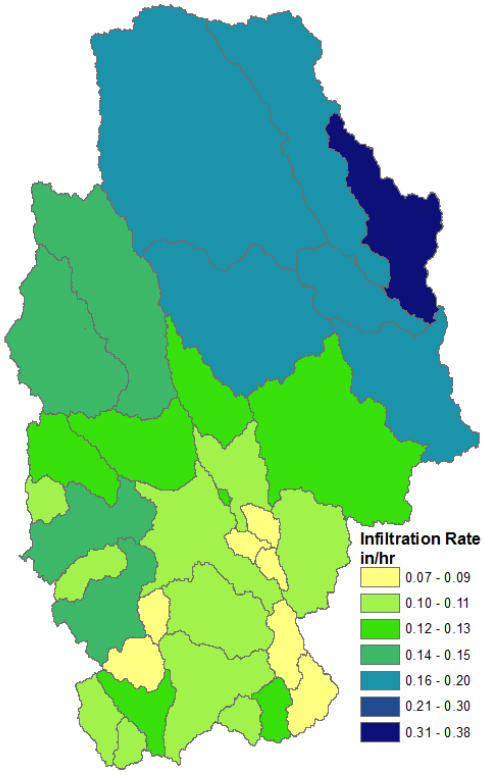

Figure 3 - 19. Average Subbasin Infiltration Rate for 3-Foot Soil Depth

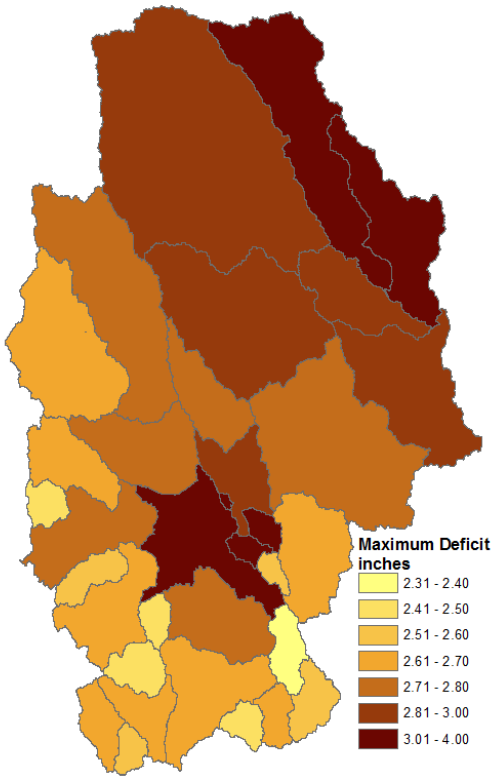

Figure 3 - 20. Average Subbasin Maximum Deficit for 1-Foot Soil Depth

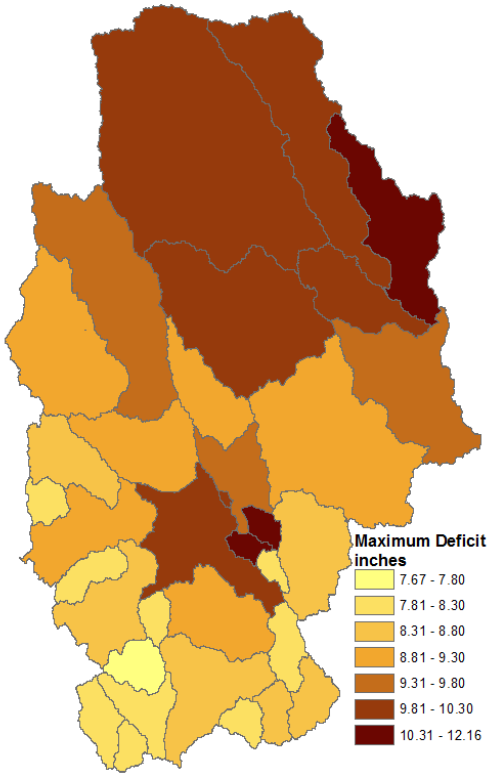

Figure 3 - 21. Average Subbasin Maximum Deficit for 3-Foot Soil Depth

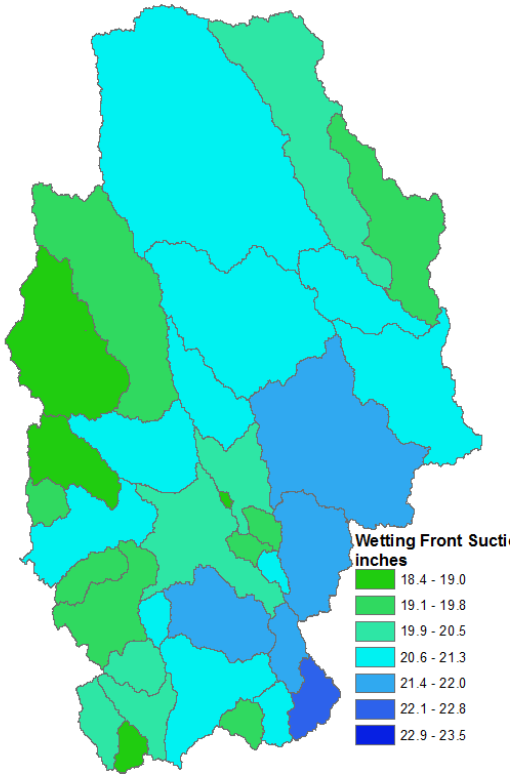

Figure 3 - 22. Average Subbasin Wetting Front Suction Head for 1-Foot Soil Depth

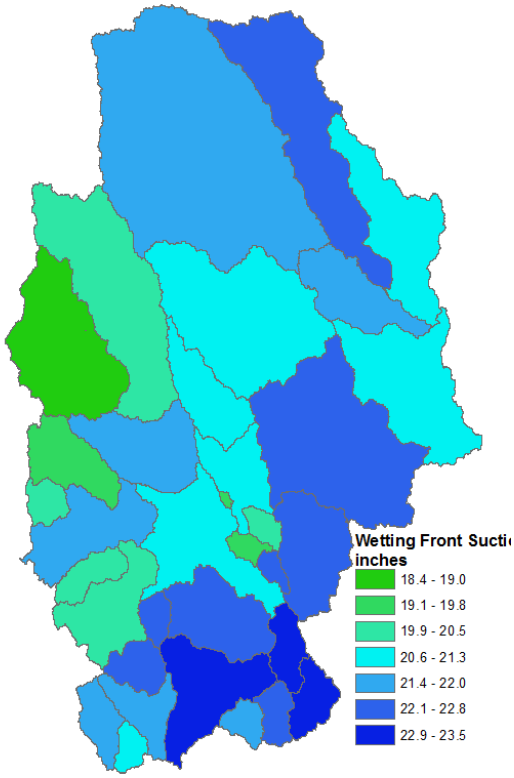

Figure 3 - 23. Average Subbasin Wetting Front Suction Head for 3-Foot Soil Depth

3.5.5 Distributed Parameterization using gSSURGO

The generation of distributed hydrologic parameters involves the association of the Salt Creek Basin map unit raster with the average map unit parameters computed in Section 3.5.4.2. This procedure is completed using ArcGIS and involves joining the map unit tabular information to the map unit raster dataset and performing a reclassify command to generate each parameter raster.

The gSSURGO raster dataset is a 10-meter gridded version of the SSURGO map unit polygons. The cell value assigned to each grid cell is the map unit number. The reclassify command uses a lookup table to change each grid cell value from the map unit number to whichever parameter is specified in the command. The result is a 10-meter raster dataset for each hydrologic parameter.

This reclassify command is used to generate a raster data set for porosity/saturated content, infiltration rate, maximum deficit, and wetting front suction. The entire process was completed twice to generate parameters for both the 1-foot soil depth and the 3-foot soil depth. The results of this analysis are shown in Figure 3 - 24 through Figure 3 - 31.

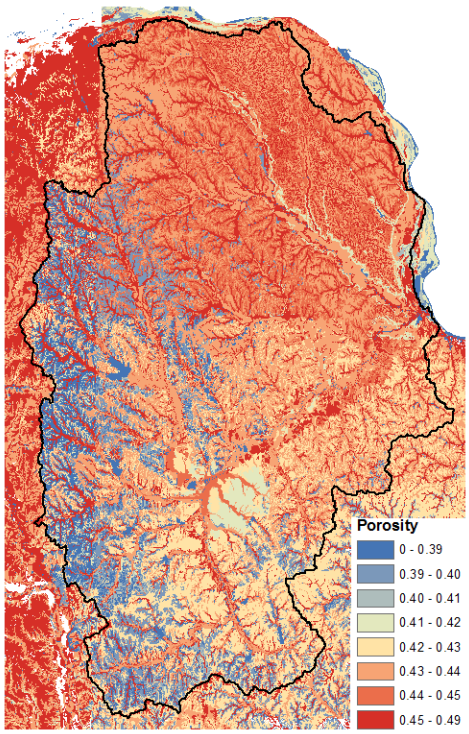

Figure 3 - 24. Distributed Porosity for 1-Foot Soil Depth

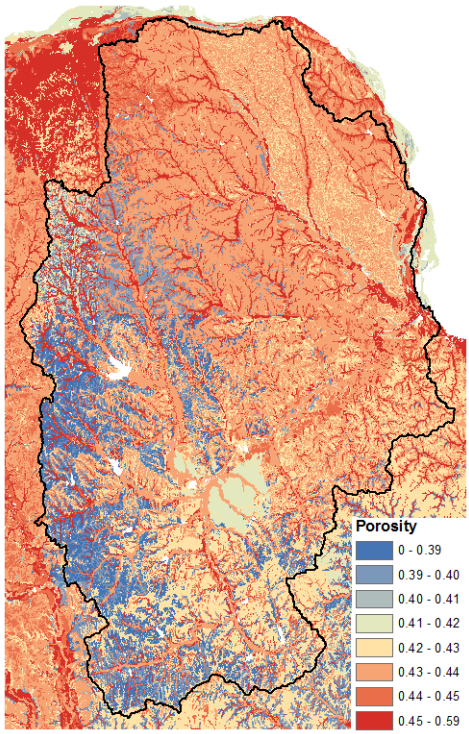

Figure 3 - 25. Distributed Porosity for 3-Foot Soil Depth

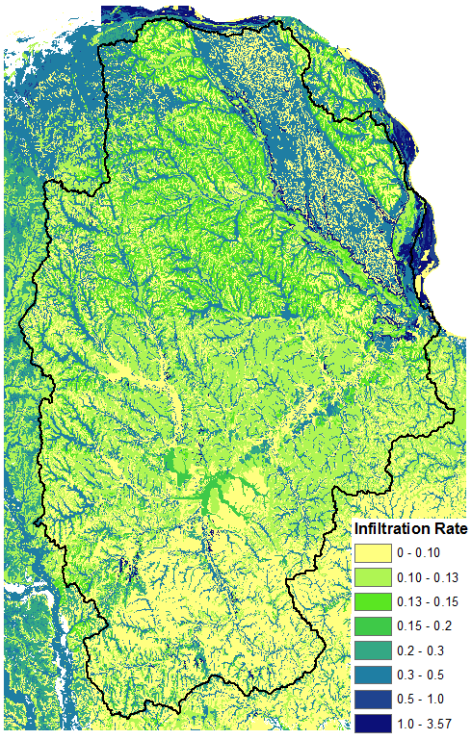

Figure 3 - 26. Distributed Infiltration Rate for 1-Foot Soil Depth

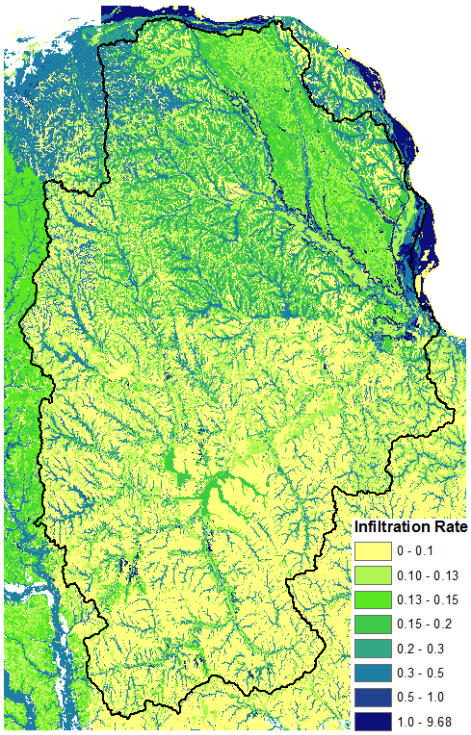

Figure 3 - 27. Distributed Infiltration Rate for 3-Foot Soil Depth

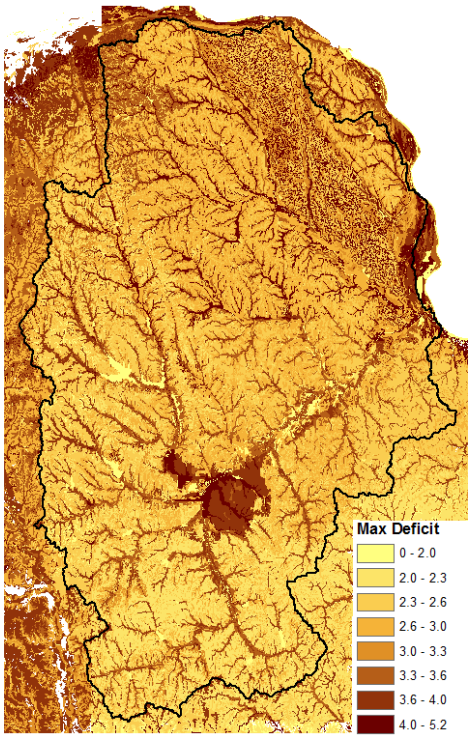

Figure 3 - 28. Distributed Maximum Deficit for 1-Foot Soil Depth

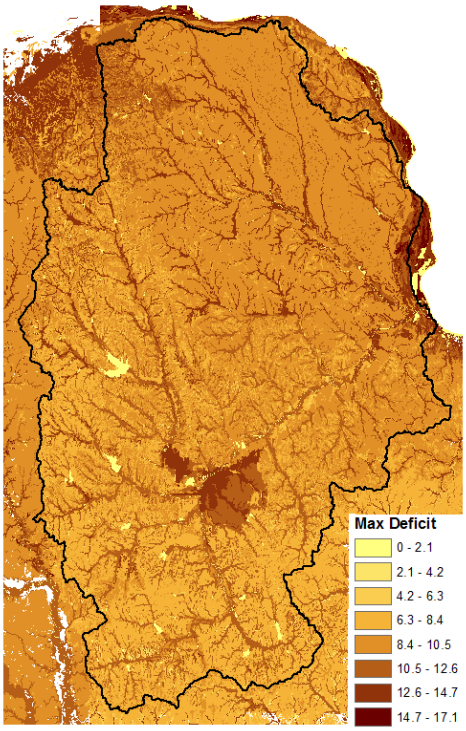

Figure 3 - 29. Distributed Maximum Deficit for 3-Foot Soil Depth

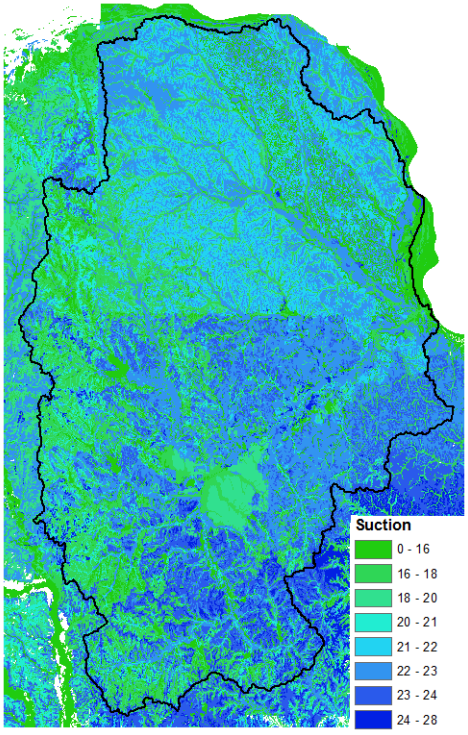

Figure 3 - 30. Distributed Wetting Front Suction Head for 1-Foot Soil Depth

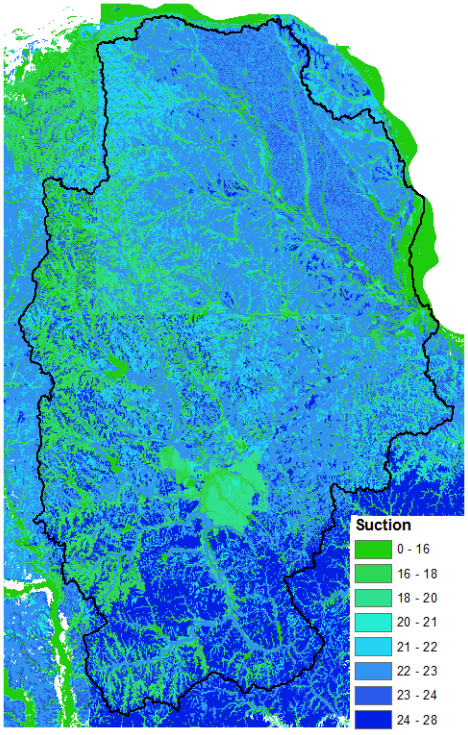

Figure 3 - 31. Distributed Wetting Front Suction Head for 3-Foot Soil Depth

3.6 SCS Curve Number Parameterization

The SCS Curve Number method is different from the other two loss methods in that it doesn't rely solely on the physical properties of the soil, but also looks at how the land is being used to determine the runoff volume. The use of this method requires only one variable:

- The SCS Curve Number

However, the determination of the SCS Curve Number relies on three different factors:

- Hydrologic Group Classification
- Land Use Classification
- Antecedent Moisture Condition

3.6.1 Hydrologic Group Classification

The Hydrologic Group Classification is a variable that is stored within the component table in the SSURGO database. Since the hydrologic groups are taken from the component layer, they are the same regardless of soil depth meaning that this analysis only needs to be completed once. A map of the hydrologic soil group for the study area is shown in Figure 3 - 32.

3.6.2 Land Use Classification

The Land Use Classification was obtained by downloading the NLCD 2011 dataset from the MRLC website (Homer, 2015). This product is available for the entire United States including Alaska, Hawaii, and Puerto Rico. This dataset provides a 30 meter raster grid containing values that assign each grid cell into one of 16 land cover classes. A brief description for each of these classes is shown in Table 3 - 4.The raster dataset was clipped to the extents of the Salt Creek Basin and is shown in Figure 3 - 33.

A table of curve numbers was for each of the 16 land use classifications and each of the four hydrologic groups was created to enable the generation of a curve number grid. The curve numbers selected for this study, also listed in Table 3 - 4, were obtained from the USDA Technical Report 55 (TR-55).

Table 3 - 4. Curve Numbers

NLCD		TR-55 Hydrologic Soil Group				
Class/Value	Classification Description	Cover Description	A	B	C	D
11	Open Water	N/A	100	100	100	100
12	Perennial Ice/Snow	N/A	100	100	100	100
21	Developed, Open Space	Open Space (Good)	39	61	74	80
22	Developed, Low Intensity	Residential - 1/2 acre	54	70	80	85
23	Developed, Medium Intensity	Residential - 1/8 acre	77	85	90	92
24	Developed, High Intensity	Commercial & Business	89	92	94	95
31	Barren Land (Rock/Sand/Clay)	Fallow - Bare Soil	77	86	91	94
41	Deciduous Forest	Oak-Aspen (Good)	30	30	41	48
42	Evergreen Forest	Woods (Good)	30	55	70	77
43	Mixed Forest	Woods (Fair)	36	60	73	79
51	Dwarf Scrub	Brush (Fair)	35	56	70	77
52	Shrub/Scrub	Brush (Fair)	35	56	70	77
71	Grassland/Herbaceous	Pasture, Grassland (Fair)	49	69	79	84
81	Pasture/Hay	Meadow	30	58	71	78
82	Cultivated Crops	Row Crops - SR (Good)	67	78	85	89
90	Woody Wetlands	Wetlands	100	100	100	100
95	Emergent Herbaceous Wetlands	Wetlands	100	100	100	100

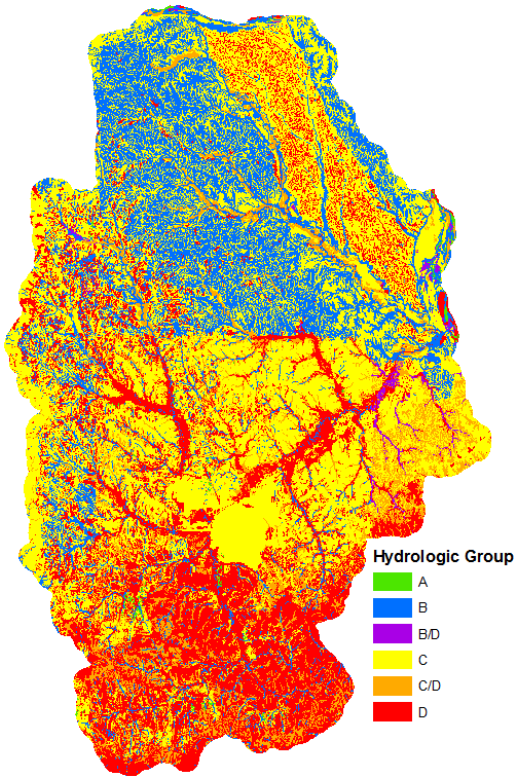

Figure 3 - 32. Hydrologic Group for Salt Creek Basin

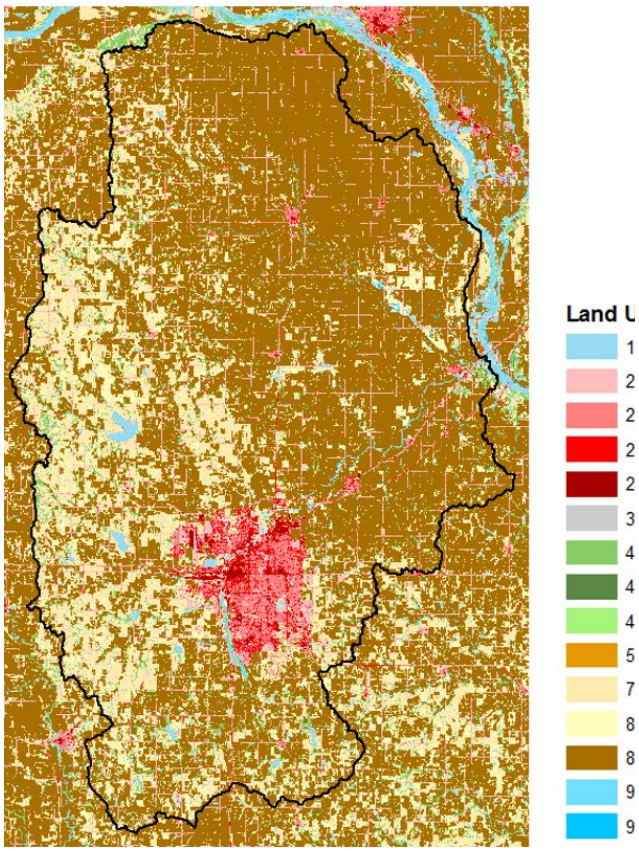

Figure 3 - 33. Land Use Classification for Salt Creek Basin

3.6.3 Curve Number Grid Generation

The framework for generating a SCS curve number grid is a feature that is included within HEC-GeoHMS. The tool combined the input of a Hydro DEM, a soil land use polygon, and a curve number lookup table to generate a Curve Number Grid for the Salt Creek Basin. The process overlaid the land use and hydrologic group information and extracted a curve number based on the provided lookup table. Most locations in the watershed have only a single hydrologic group making the lookup procedure fairly straightforward. For the cells with multiple hydrologic groups, namely with a “B/D” or a “C/D” classification, the algorithm averaged the two corresponding curve numbers based on the land use value. The resulting raster dataset from this procedure matched the resolution of the land cover dataset, which is 30-meters. The resulting Curve Number Grid is shown in Figure 3 - 34.

3.6.4 Subbasin Average Curve Numbers

One final step for this dataset was to compute an average curve number for each subbasin within the Salt Creek basin. This was necessary to be able to run the SCS Curve Number method for the lump-sum parameter framework. These average values were obtained by using the Zonal Statistics tool within ArcGIS. By using the Curve Number Grid as the input raster and the Salt Creek Subbasins as the summary shapefile, an average curve number for the entire subbasin was obtained. A complete table of each subbasin curve number can be found in Appendix B. A map showing the results of this procedure is shown in Figure 3 - 35.

3.6.5 Antecedent Moisture Condition Variations

Both of the Curve Number datasets generated represent average soil moisture conditions (AMC II). Equations 3 - 7 and 3 - 8 were then applied to generate datasets to represent dry antecedent conditions (AMC I) as well as wet antecedent conditions (AMC III). The resulting Curve Number values can be seen in Appendix B, Table B - 6.

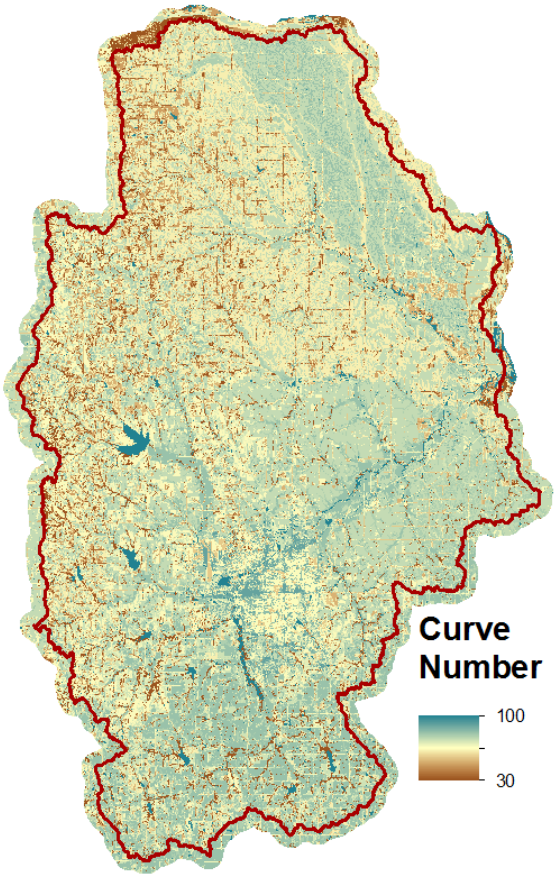

Figure 3 - 34. Distributed Curve Number for the Salt Creek Basin

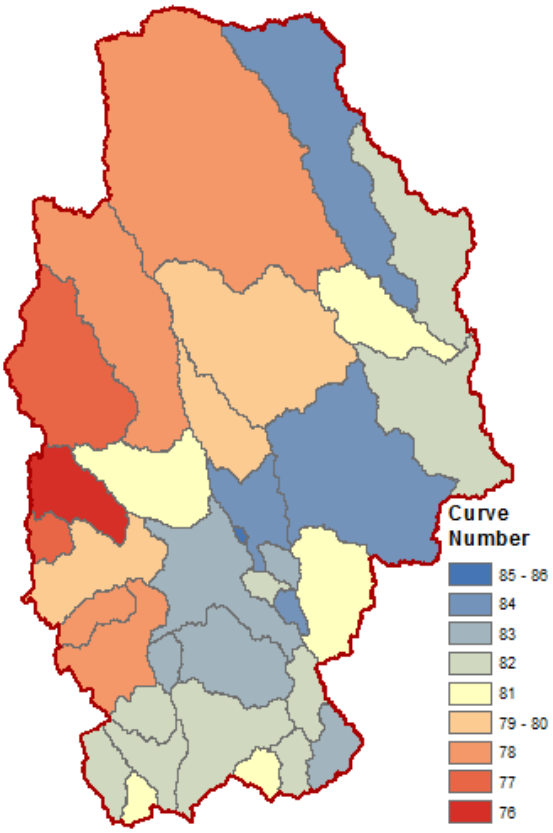

Figure 3 - 35. Average Subbasin Curve Numbers for the Salt Creek Basin

3.7 Precipitation Datasets

One of the most important factors in a hydrologic model is the precipitation dataset. In order to use a distributed hydrologic model, gridded precipitation is required. For this study, the precipitation data was acquired from the U.S. Army Corps of Engineers (USACE) Corps Water Management System (CWMS) database.

The precipitation product that is stored within the CWMS database is based on the Next Generation Radar (NEXRAD) hourly gridded precipitation shapefiles generated by the National Weather Service (NWS). These precipitation data are quality-controlled, multi-sensor precipitation estimates generated from the River Forecast Centers (RFCs) within the NWS (National Weather Service, 2017). The files are originally produced in a special binary format

designed specifically for NWS data storage called XMRG and are projected in the Hydrologic Rainfall Analysis Project (HRAP) grid coordinate system. This data is stored on the internet and is free to download from the NWS website (National Weather Service, 2017). While this is an efficient means of storing vast amounts of information, it does not present the data in a manner that is readily available to the end user and for ingestion into ArcGIS and HEC-HMS.

To simplify the use of this gridded information, USACE has set up an automatic routine which pulls in hourly precipitation and converts the XMRG files into the Hydrologic Engineering Center Data Storage System (HEC-DSS) format. The benefit of using the USACE precipitation data is that it is nicely organized for each month for the past several years and it has already been converted to the necessary format to be used within the HEC-HMS software.

3.7.1 Storm Selection

In order to get an accurate test for the effectiveness of the derived loss parameters, significant precipitation events were modeled. The events selected for this study were chosen based on several criteria including observed hydrographs and availability of observed hydrologic data. The first level of screening involved a visual inspection of the elevation hydrographs at several reservoir locations and the flow hydrographs at several stream gauge locations. Each large increase in the reservoir elevation and flow hydrographs was flagged as a potential candidate for analysis. An example elevation hydrograph from Salt Creek Dam site 10 – Yankee Hill Lake is shown in Figure 3 - 36 with potential storms dated and circled.

The second level of screening involved the ready availability of gridded precipitation data. While USACE has an efficient operation of database storage for DSS precipitation now, this system did not exist more than five years ago. As a result, much more data analysis and preparation would be involved if a storm was chosen for a time period outside of the data stored within the CWMS database. Also, there are times when the stream of precipitation data

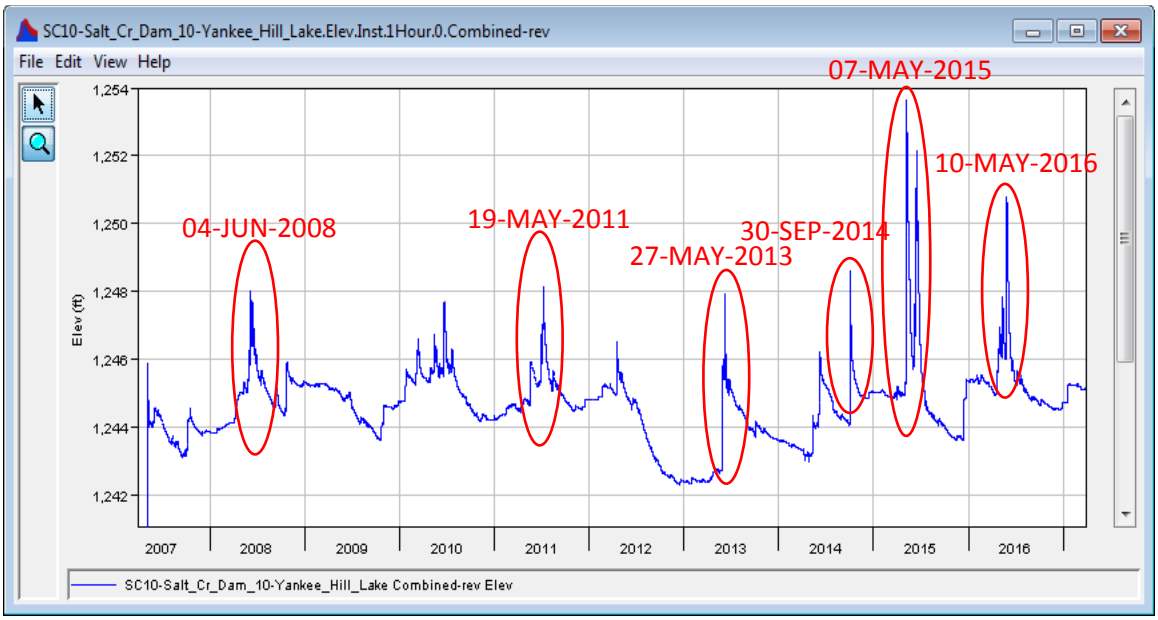

Figure 3 - 36. Observed Elevation Data for Salt Creek Dam Site 10 - Yankee hill Lake during 2007-2016

from NWS to USACE was interrupted due to IT security updates. This unfortunately occurred during the summer months of 2013 meaning that no gridded precipitation was available for the large event that occurred on May 27, 2013.

The last level of screening involved the availability of observed hydrograph data for selected events. Flow hydrographs are rarely measured directly. Instead, the river stage is measured directly and related to flow by way of a rating curve. For reservoir inflow hydrographs within the Salt Creek Basin, the inflow hydrograph is one step further removed. The reservoirs operate in “fill-and-spill” mode, meaning that they have an uncontrolled weir that passes flow when the elevation exceeds the weir crest. As a result, a direct relationship can be derived relating pool elevation to reservoir outflow. The inflow is then calculated by using the standard continuity equation shown in equation 3-31 (Chow et al, 1988).

$$\frac{dS}{dt} = I(t) - O(t) \tag{3-31}$$

Where dS/dt is the change in storage over time step t (cfs), I(t) is the rate of inflow over time step t (cfs), and O(t) is the rate of outflow over time step t (cfs). For application to the reservoirs, both storage and outflow are measured every hour and inflow is then calculated.

This method of flow hydrograph observation is well established and commonly used by the U.S. Geological Survey. However, stream gauges are sometimes taken out of commission for maintenance purposes or faulty equipment and sometimes can even be damaged during a significant precipitation event. As a result, storms were only selected with continuous observed hydrographs throughout the event.

This three-tiered screening process led to the selection of three major precipitation and runoff events for this study:

- September 30, 2014
- May 7, 2015
- May 10, 2016

Maps showing the total precipitation for these three events were generated and are shown in Figure 3 - 37 through Figure 3 - 39. All three storms had significant spatial variability in precipitation depths over the basin.

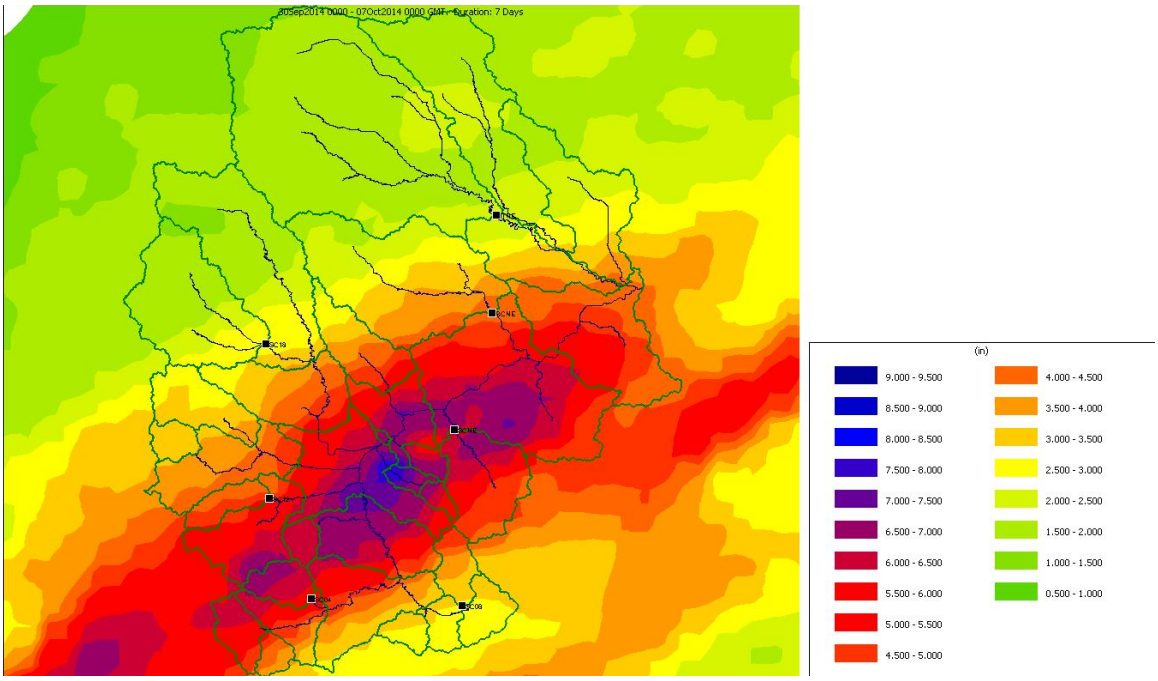

Figure 3 - 37. Salt Creek Basin Gridded Precipitation for September 30, 2014 Event

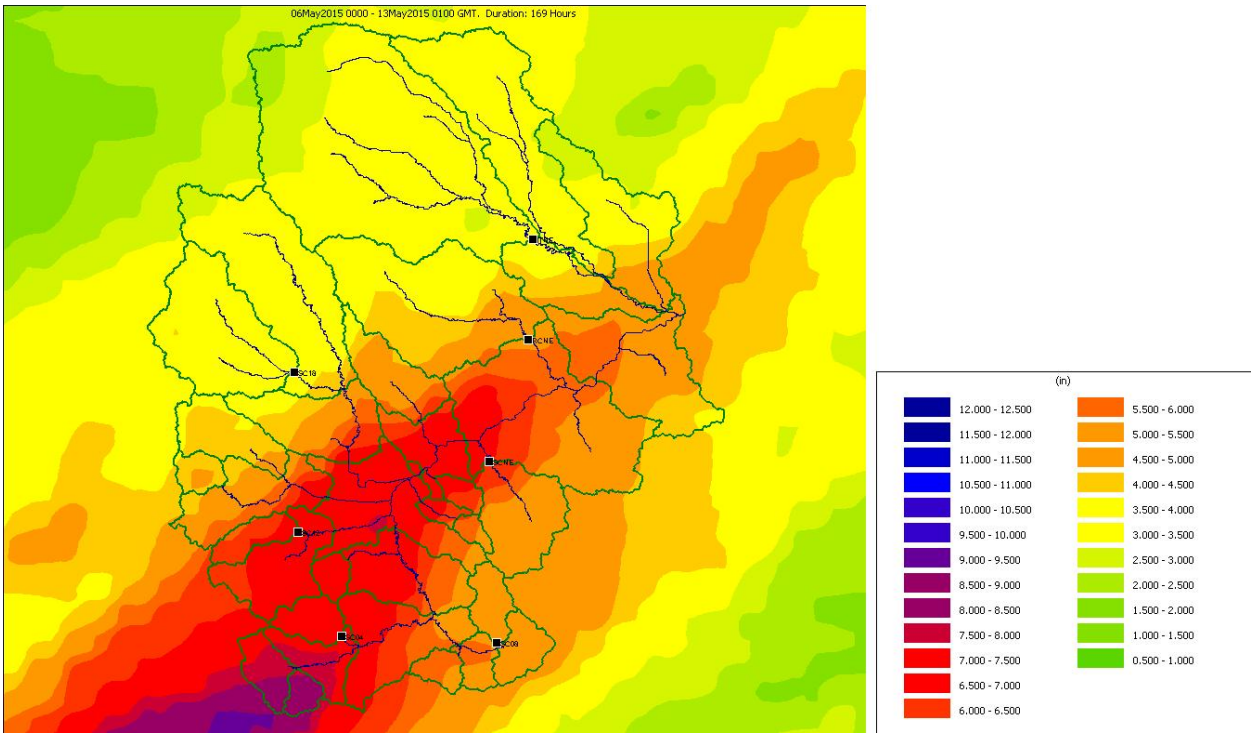

Figure 3 - 38. Salt Creek Basin Gridded Precipitation for May 7, 2015 Event

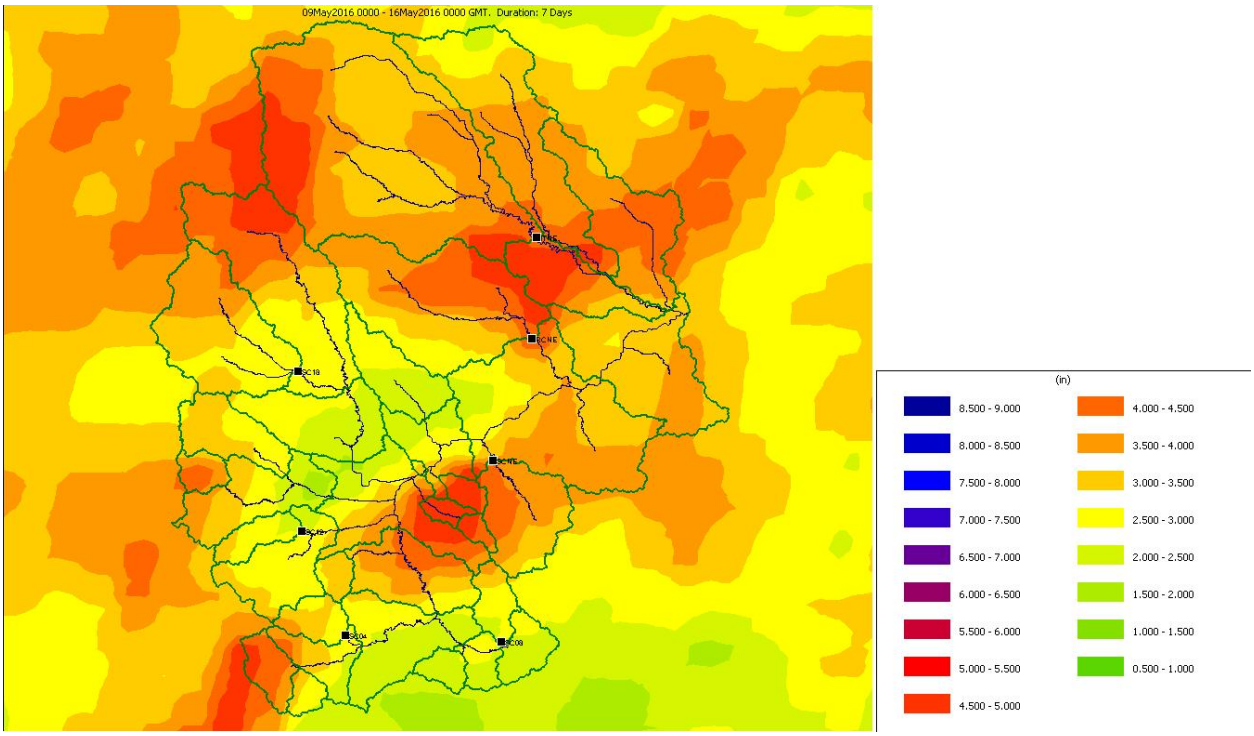

Figure 3 - 39. Salt Creek Basin Gridded Precipitation for May 10, 2016 Event

3.7.2 Gridded Precipitation Verification

Before using the gridded precipitation products in the hydrologic simulations, a data quality check was performed using reported rain gauge data and HEC-MetVue, a program developed by the Hydrologic Engineering Center for visualization and manipulation of meteorological datasets. The program uses a triangulated irregular network (TIN) computational format to process the gridded data and develop average precipitation measurements for a subbasin. HEC-MetVue can also allow for the point measurement on a series of precipitation grids to develop a rainfall hyetograph for a particular location. This capability was used at six rain gage locations for the Salt Creek Basin, which were chosen to cover the entire basin. The total observed rainfall volume from the rain gauge was compared to the gridded precipitation values at the same location and the percent differences between the two numbers were determined. The results from this analysis are shown in Table 3 - 5.

Table 3 - 5. Observed vs Gridded Precipitation Comparison

Gauge Location	30-Sep-14				7-May-15				10-May-16			
	Obs	Grid	Diff		Obs	Grid	Diff		Obs	Grid	Diff	
	(in)	(in)	(in)	(%)	(in)	(in)	(in)	(%)	(in)	(in)	(in)	(%)
SC04	4.94	5.276	0.336	7%	7.03	7.361	0.331	5%	2.48	2.675	-0.195	8%
SC08	2.71	2.926	0.216	8%	5.47	5.376	-0.094	-2%	2.11	2.504	-0.394	19%
SC12	4.60	4.903	0.303	7%	6.50	6.940	0.440	7%	*Gauge out of commission*			
SC18	2.45	2.697	0.247	10%	3.26	3.490	0.230	7%	2.67	2.855	-0.185	7%
SCNE	6.29	6.507	0.217	3%	6.90	6.506	-0.394	-6%	4.76	4.540	0.220	-5%
ITNE	2.04	2.138	0.098	5%	3.60	3.636	0.036	1%	6.15	6.270	-0.120	2%

The results from this comparison show that there is a good correspondence between the observed rain gauge data and the gridded precipitation product. The largest percentage error was -19%, but this value is skewed, based on the relatively small rainfall depth measured. Thus the actual error is less than 0.4 inches difference between the observed and gridded precipitation. The largest absolute error was 0.44 inches occurring at Salt Creek Dam Site 12 – Conestoga Lake, but this is a small percent error due to the large values of precipitation data measured (6.5 inches). Based on this comparison, the USACE gridded precipitation data was judged to be accurate in regards to traceability to gauge measurements and can be confidently used to the HEC-HMS model.

3.8 Hydrologic Simulation using HEC-HMS

HEC-HMS is the Hydrologic Modeling System developed by the U.S. Army Corps of Engineers Hydrologic Engineering Center. The program is designed to model the complete hydrologic processes for a watershed including precipitation, infiltration, unit hydrographs, and hydrologic routing. This study takes advantage of the distributed modeling capabilities within HEC-HMS to test the efficacy of the distributed loss parameter datasets created in Section 3.5 and Section 3.6.

3.8.1 Model Set-up

The hydrologic model structure used within HEC-HMS can be broken down into four main components. These four components work together to specify the different aspects of the hydrologic simulation. The components are the Basin Model, Meteorologic Model, Control Specifications, and Supporting Data.

The Basin Model is used to represent the geography of the watershed and to define the stream network (Hydrologic Engineering Center, 2016). Various elements such as subbasins, routing reaches, junctions, and reservoirs work together to mimic the layout of the watershed. The watershed uses a node and link system to represent the different elements and how they are connected hydrologically. For this study, a total of 10 Basin Models were generated, one for each runoff-lumping-soil depth method evaluated. The only difference between all 10 models is the runoff method-lumping-soil depth combination, meaning that the transform and routing methods as well as the parameters values that define them are identical.

The Meteorologic Model is used to simulate all of the atmospheric conditions for a watershed. This includes precipitation, evapotranspiration, and snowmelt (Hydrologic Engineering Center, 2016). For this study, three different Meteorologic Models were generated to represent each of the three selected storms. Because of the short duration of the storms and their time of occurrence, evapotranspiration and snow-melt were not included.

The Control Specifications are used to define the computational time window for a simulation. The start and end times as well as the computational time-step are required inputs for a simulation to run. For this study, the time window for each event was always one week beginning a day before the bulk of the precipitation and ending seven days later. A time step of one hour was chosen to match the resolution of both the gridded precipitation data as well as the observed flow hydrographs. It should be noted that while the run time for each simulation

was 1 week, the resulting hydrographs shown in Appendix C are trimmed time-wise to show more detail for the portion of the hydrograph directly responding to the precipitation.

The Supporting Data includes all sets of information used to compute and evaluate the hydrologic simulations. Examples include Time-Series data such as observed precipitation, streamflow, and reservoir elevation hydrographs, Paired Datasets such as storage-discharge and storage-elevation relationships for reservoirs, and gridded datasets such as gridded precipitation and distributed loss parameters. For the Time-Series Data and Paired Data, the information can either be stored in a DSS file external to the HEC-HMS model and referenced to the file location or can be entered manually. Any gridded datasets have to be stored in an external DSS file.

3.8.2 Gridded Data Import

The use of distributed modeling techniques within HEC-HMS requires the use of the gridded datasets. The Grid Data Manager is used to organize and store all gridded datasets that will be used in the modeling process. Throughout this study, a wide variety of gridded datasets were generated including precipitation, several runoff parameters, and curve numbers. However, each of these datasets had to first be resampled to match the resolution of the Standard Hydrologic Grid (SHG) computed in Section 3.3.2 and reformatted into DSS format to be readable by HEC-HMS.

The SHG resolution was chosen to be 2,000 meters to match the resolution of the coarsest dataset, the precipitation dataset. As a result, no resampling needed to be done to the precipitation data. The resolution for all runoff parameters matched the 10 meter map unit raster dataset from the gSSURGO database. The Curve Number Grid was generated primarily off of the land use dataset and therefore matched that resolution of 30 m.

The HEC-GeoHMS toolbar contains a set of commands that can be applied to raster datasets to both resample the data and to convert the files into DSS format. The resampling

works like the zonal statistics command of ArcGIS, creating a field within the grid cell file and populating with the average value for all cells from the original raster dataset that fall within the resampled grid cells. This information was then converted first to an ASCII delimited file and then into a DSS grid file using commands within the HEC-GeoHMS toolbar (Hydrologic Engineering Center, 2016). Once complete, the data was ready to be imported and used within HEC-HMS.

3.8.3 Treatment of Initial Conditions

The only parameter left to define before hydrologic simulations could begin was the initial conditions for each loss method. These parameters include the initial deficit for the Deficit and Constant Loss method, the Initial Content for the Green and Ampt method, and the initial abstraction and antecedent moisture condition for the SCS Curve Number method. Up to this point, no observed flow information had been used for calibration purposes. This is because the goal of this study was to determine hydrologic modeling parameters without relying on calibration techniques using observed data. However, in order to evaluate the effectiveness of this technique, all other variables had to be treated in such a way as to standardize their impact on the simulated results. Two approaches were used in order to set initial conditions

In the first approach, an iterative process was used that involved tuning the initial conditions for each method up or down until the simulated hydrograph runoff volume matched that of the observed hydrograph. This meant finding the ideal initial condition for the initial deficit, initial water content, and the initial abstraction for the Deficit and Constant, Green and Ampt, and SCS Curve Number methods, respectively. It's important to note that the AMC II curve number for each simulation. Setting the initial conditions in this way equalized and diminished the impacts of the initial condition parameters on the runoff hydrograph across all simulations. Doing so allowed the peak flow rate and the time of peak to be the primary

impacted outcomes so that these could be compared and their difference quantified without the results being skewed by a poorly chosen initial condition that caused total runoff volumes to vary among methods.

In the second approach, the initial conditions were not optimized and were instead set based only on information available prior to the beginning of the precipitation event. By looking at the observed precipitation for several weeks before the simulation events, the moisture conditions were determined to be dry, average, or wet. Based on this decision, the initial conditions were set using the following table:

	Initial Conditions			
Moisture Condition	**Initial Deficit (% of Max Deficit)**		**Initial Water Content (% of Saturated Content)**	**Antecedent Moisture Condition Classification**
	1 ft Soil	3 ft Soil		
Dry	75%	25%	50%	AMC I
Average	50%	17%	75%	AMC II
Wet	25%	10%	95%	AMC III

The parameters for the initial deficit and initial water content were selected based on the physical properties of the soil. The range of percentages differ due to the fact that the maximum deficit already accounts for the wilting point water content, where the saturated water content does not. As a result, the Green and Ampt initial water content percentages are skewed higher than the Deficit and Constant initial deficit values. Also, neither method use a fully saturated soil (0% initial deficit or 100% initial water content) in order to account for other naturally occurring losses in the basin, such as detention ponds that attenuate water. For the SCS Curve Number method, the curve number will be adjusted based on antecedent moisture condition instead of adjusting the initial abstraction. Instead, the traditional value of initial abstraction of 20% of the total potential retention. This represents the more traditional approach when using the SCS Curve Number method.

Setting the initial conditions in this way is more representative of real-time flood forecasting. Prior to a precipitation event, the exact initial condition cannot be known and will instead rely on knowledge of the basin prior to the precipitation. This approach will represent a more fair approach when comparing the runoff methods as well as provide another metric for evaluation in the total runoff volume.

3.8.4 Observation Locations

Due to the relatively large size of the Salt Creek Basin and the large number of observed hydrographs available for comparison, it was unpractical and unnecessary to evaluate model results at all locations. Furthermore, the use of hydrologic routing and the inaccuracy of the parameters involved would probably have skewed the evaluation of the loss parameters by introducing other uncertain variables into the analysis. For these reasons, a small subset of gauged locations was selected as the observation. The first criterion for selecting these locations was that their catchment area be the most upstream subbasin along their drainage path. This ensured that the runoff hydrograph produced at the subbasin outlet was a product of only that subbasin and did not include flow routed from another upstream location. From there, subbasins were chosen to represent locations from across the basin as well as a wide range of drainage areas. A map showing the locations of selected gauges is shown in Figure 3 - 40.

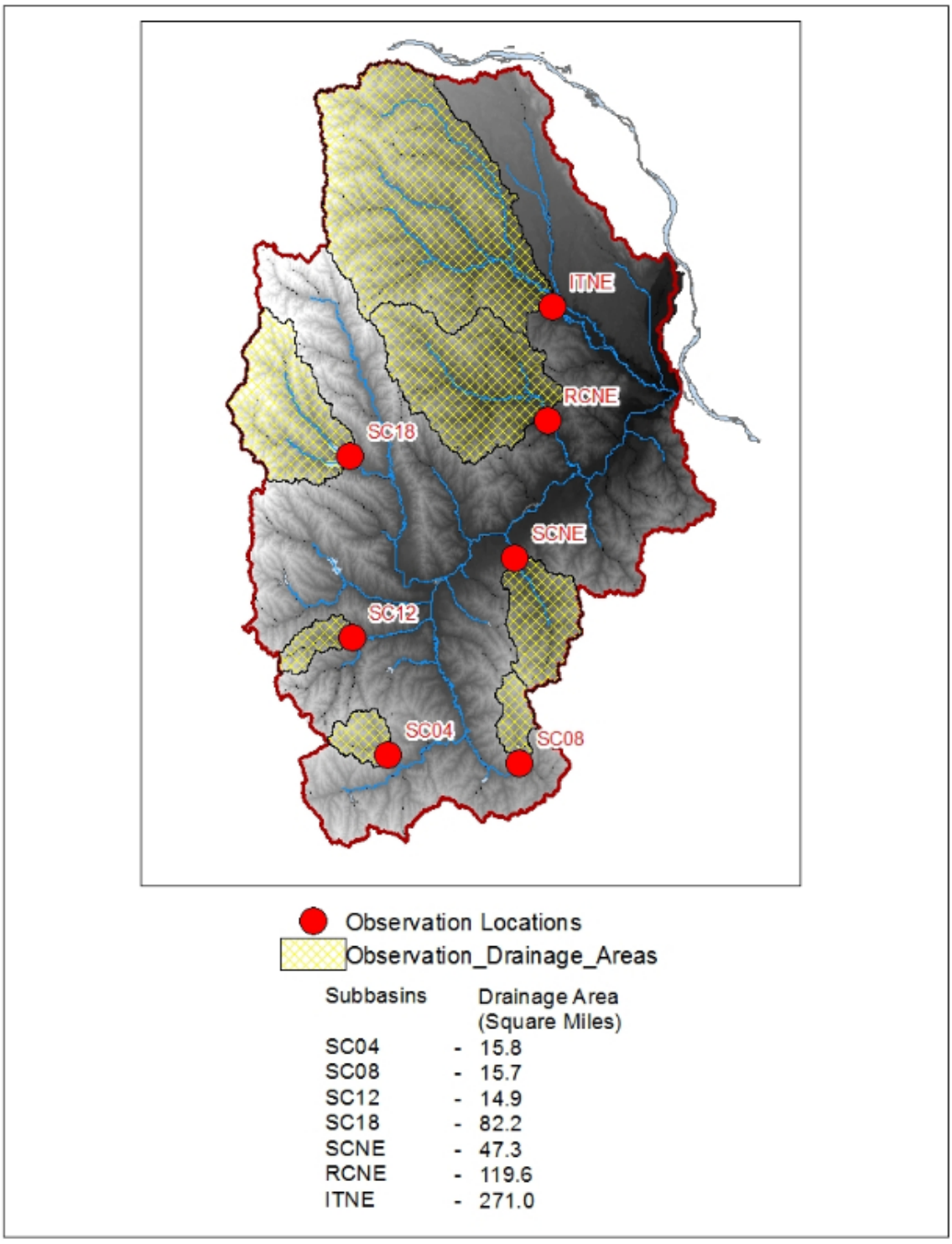

Figure 3 - 40 Flow Observation Locations for the Salt Creek Basin

Chapter 4 Results

This study was driven by two primary objectives. The first was to determine whether information in the SSURGO database could be used to dependably derive loss parameters for use in hydrologic modeling of runoff hydrographs. The second objective was to determine if using a spatially distributed loss parameter gridded datasets would improve overall model performance as compared to the use of lumped parameterizations. The hypothesis was that accounting for spatial variability in soil parameters can provide for a more sensitive and accurate simulated runoff hydrograph.

4.1 Simulated Runoff Hydrographs

When comparing simulated versus observed hydrographs, three main factors were considered to determine model accuracy. These were the peak flow, time to peak, and total runoff volume.

Two approaches were used to set the initial condition. For this the first approach, the total runoff volumes between the observed and simulated hydrographs were made equal to one another by adjusting the initial soil moisture condition for each simulation run. This was done to eliminate the impact of uncertainty or error in estimating initial condition on total runoff volume and to produce a balanced apples to apples comparison of the peaks and durations of runoff hydrographs. In the second approach, the initial conditions were not optimized and were instead set based only on information available prior to the beginning of the precipitation event. By looking at the observed precipitation for several weeks before the simulation events, the moisture conditions were determined to be dry, average, or wet. Bot methods for determining initial condition are described further in Section 3.8.3.

The three selected storms were simulated using each of the 10 different runoff-lumping-soil depth methods described earlier. The resulting hydrographs from these simulations were

plotted against the observed hydrographs. A typical hydrograph for each observation location is shown in the following discussion. The optimized initial conditions hydrographs are shown in Section 4.2 with the full set of simulation results presented in Appendix C. for the non-optimized initial conditions, the typical hydrographs can be found in Section 4.3 with the full set of simulation results presented in Appendix D.

4.2 Simulated Runoff Hydrographs – Optimized Initial Conditions

4.2.1 SC04 – Salt Creek Dam Site 4 – Bluestem Lake

The simulation results for the May 10, 2016 event for Salt Creek Dam Site #4 – Bluestem Lake with Optimized Initial Conditions are shown in Figure 4 - 1. Included in the figure are the basin average rainfall hyetograph and runoff hydrographs for the observed event as well as 10 different runoff-lumping-soil depth combinations.

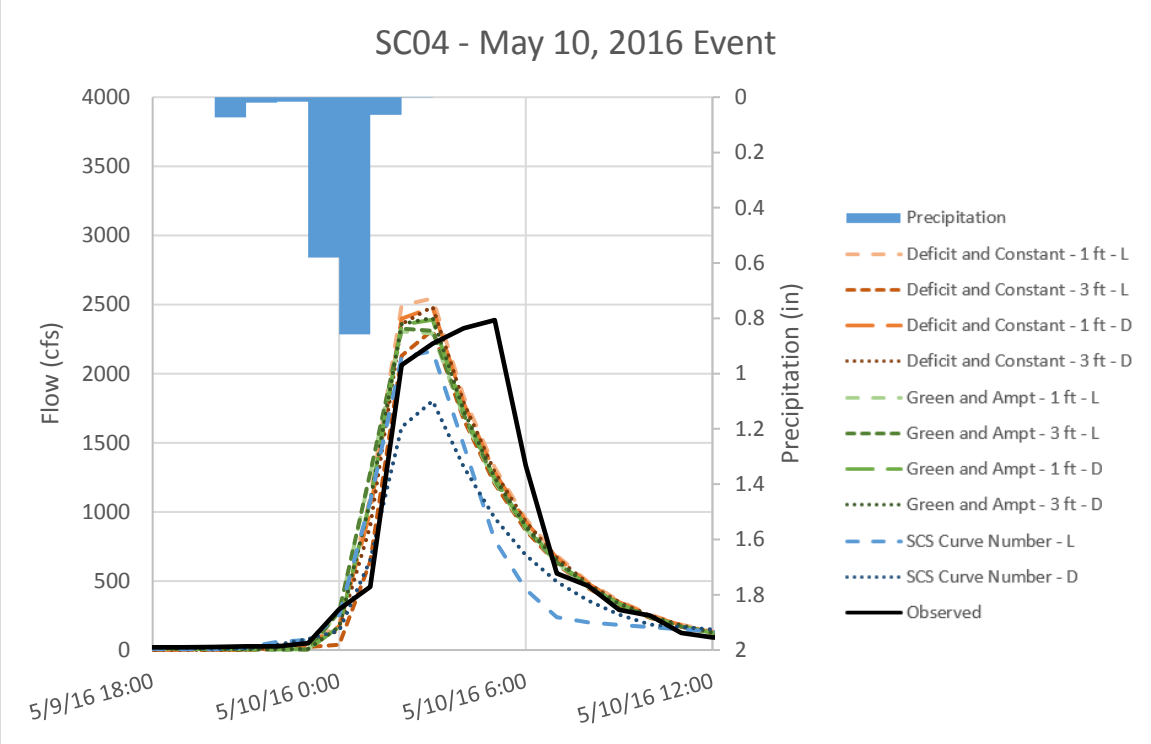

Figure 4 - 1. Comparison of Simulation Results for May 10, 2016 Event at Salt Creek Dam Site 04 - Bluestem Lake Optimized Initial Conditions

The resulting hydrographs at this location are relatively similar for all 10 simulated modeling combinations. The peak of the simulated hydrographs all occurred before the observed hydrograph peak by approximately 3 hours. Also, most of the methods over-predicted the peak flow rate, although by a small margin. The exception to this was for the lumped and distributed SCS Curve number methods, which substantially under-predicted the peak flow rate. These discrepancies could be due to inaccuracies in the implied rates of infiltration for the drainage area, allowing the runoff to travel to the watershed outlet instead of being infiltrated into the soil. The shape of the hydrograph could be adjusted by increasing the infiltration rate and decreasing the initial condition, resulting in no net change to runoff volume. Another major factor affecting results could be inaccuracy in the transform parameters. While the TR-55 method for determining time of concentration is fairly extensive, it is only an approximation and could be improved through model calibration.

Results for all three precipitation events showed the same trends as the event described above. The simulated peak flows and times to peak were above and ahead of observed results, respectively, by similar margins. This consistency across multiple events is promising, showing that the model may be able to accurately predict future runoff with slight adjustments to a few parameters.

4.2.2 SC08 – Salt Creek Dam Site 8 – Wagon Train Lake

The simulation results for the May 7, 2015 event for Salt Creek Dam Site #8 – Wagon Train Lake with Optimized Initial Conditions are shown in Figure 4 - 2. Included in the figure are the basin average rainfall hyetograph and runoff hydrographs for the observed event as well as 10 different runoff methods.

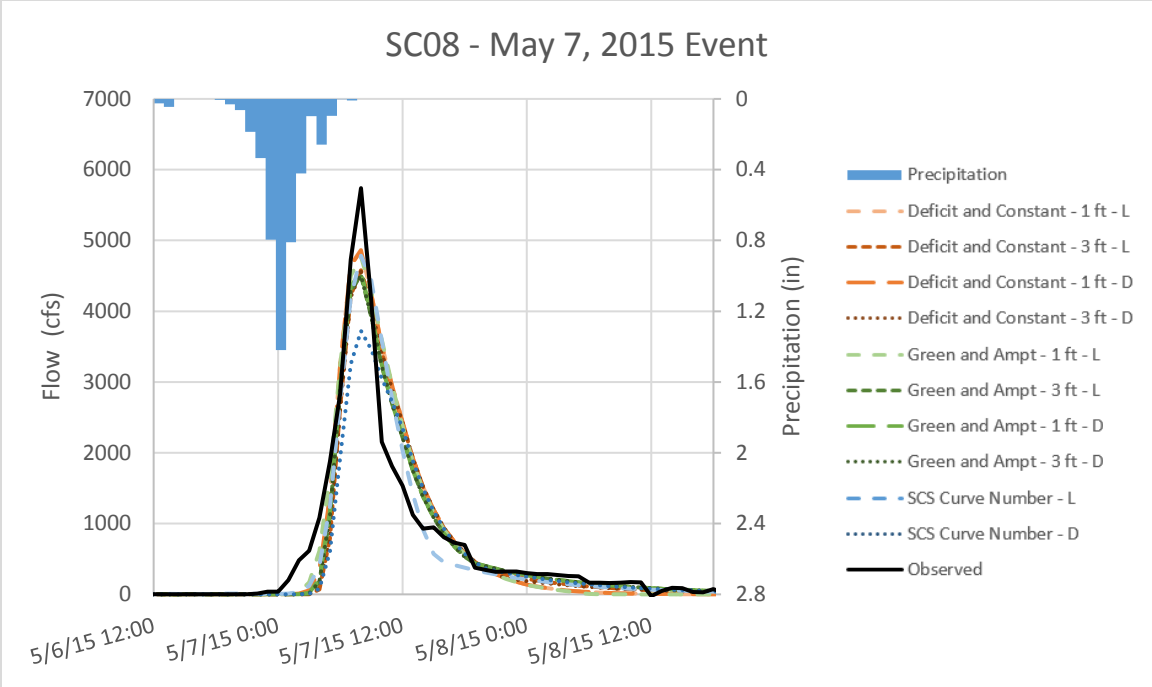

Figure 4 - 2. Comparison of. Simulation Results for May 7, 2015 Event at Salt Creek Dam Site 08 - Wagon Train Lake Optimized Initial Conditions

The resulting hydrographs at the SC08 location were relatively similar for all 10 simulated runoff methods. The time of peak for the simulated hydrographs all matched the observed time of peak well. This indicates that the transform parameters are likely a good fit for this subbasin. The peak flow rate, however, was under-predicted by all loss methods, and the recession limb of the simulated results decreased more slowly than the observed. Additionally, there was a lag between the rising limb of the observed and the simulated results. This pattern of results indicates that the infiltration rate was likely too low and the initial condition too high. This could be rectified by increasing either the hydraulic conductivity or wetting front suction head parameter values in the Green and Ampt method and decreasing the initial condition in the CN method, resulting in no net change in simulated runoff volume.

The results for all three events show a wide range of results. This is likely due to the relatively small precipitation amounts experienced within the drainage basin when compared to the other observation locations.

4.2.3 SC12 – Salt Creek Dam Site 12 – Conestoga Lake

The simulation results for the September 30, 2016 event for Salt Creek Dam Site 12 – Conestoga Lake with Optimized Initial Conditions are shown in Figure 4 - 3. Included in the figure are the basin average rainfall hyetograph and runoff hydrographs for the observed event as well as 10 different runoff methods.

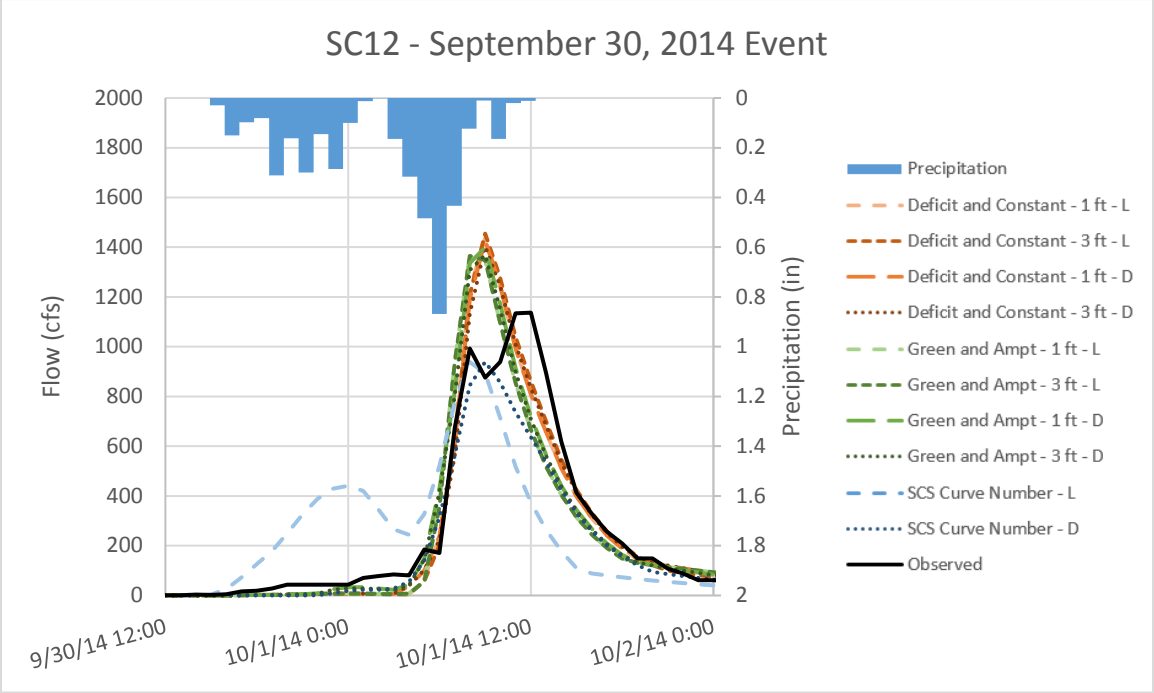

Figure 4 - 3. Comparison of Simulation Results for Sept. 30, 2014 Event at Salt Creek Dam Site 12 - Conestoga Lake Optimized Initial Conditions

The results for this simulation show similar results for the Deficit and Constant Loss and Green and Ampt methods, with the SCS Curve Number showing some deviation from the other two. All 10 methods predicted a time to peak approximately 4 hours before the observed peak. The peak flow for most methods was simulated higher than the observed hydrograph, with both of the Curve Number simulations under-predicting the peak flow. The Curve Number performed especially poorly for this observation location. Even with the initial abstraction reduced to zero, the Curve Number method was unable to match the inflow volume or peak discharge. This must

be due to inaccuracy in the Curve Number values or the CN number method, indicating that the CN values should be increased.

The results for this observation location could only be completed for two of the three selected storms. This is because the reservoir was evacuated in the winter of 2015 for lake rehabilitation and the observation gauge was turned off.

4.2.4 SC18 – Salt Creek Dam Site 18 – Branched Oak Lake

The simulation results for the May 7, 2015 event for Salt Creek Dam Site 18 – Branched Oak Lake with Optimized Initial Conditions are shown in Figure 4 - 4. Included in the figure are the basin average rainfall hyetograph and runoff hydrographs for the observed event as well as 10 different runoff methods.

The results from this simulation show a large degree of variability between the different loss methods. The relative accuracy for peak flow and time to peak relative to the observed hydrograph varied significantly, with some results predicting high flows and early peaks and others predicting low flows with late peaks. This observation location inflow hydrograph was calculated poorly and contains unrealistic jumps in flow rate. This is due to a lack of accuracy within the CWMS database used to compute the inflow hydrograph based on observed elevation data.

The trend of poor observed data is seen for all three precipitation events, making this location difficult to match hydrograph data. However, the data are still usable, as the peak flow rates and inflow volumes are still considered to be correct.

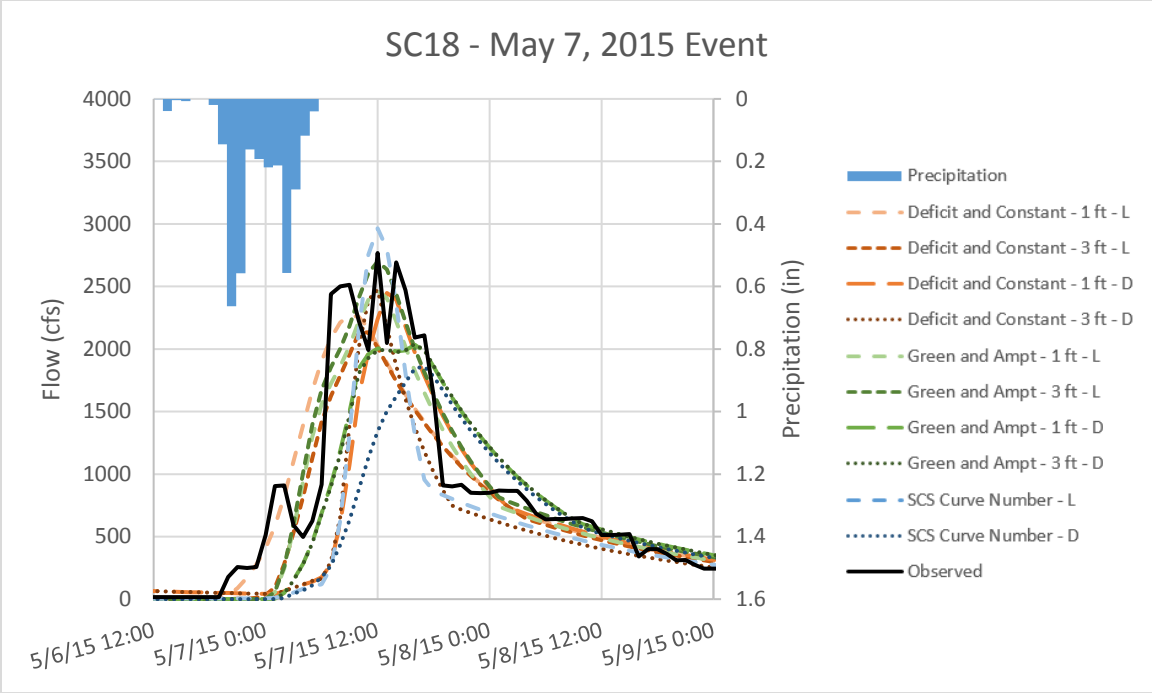

Figure 4 - 4. Comparison of Simulation Results for May 7, 2015 Event at Salt Creek Dam Site 18 - Branched Oak Lake Optimized Initial Conditions

4.2.5 SCNE – Stevens Creek at Lincoln

The simulation results for the May 10, 2016 event for Stevens Creek at Lincoln with Optimized Initial Conditions are shown in Figure 4 - 5. Included in the figure are the basin average rainfall hyetograph and runoff hydrographs for the observed event as well as 10 different runoff methods.

The results from this simulation show an excellent match between the observed hydrograph and the simulated results. The peak flows for nine of the 10 method combinations are within 10% of the observed peak, with only the lumped SCS Curve Number method having a large discrepancy. The timing for all of the simulations was a perfect match to the observed data.

The trend of excellent runoff results does extend to the other two precipitation events. The results for the May 7, 2015 event show a good match in both peak flow and time to peak.

However, the simulated results from the September 30, 2014 event show an earlier predicted peak flow that is higher than the observed data.

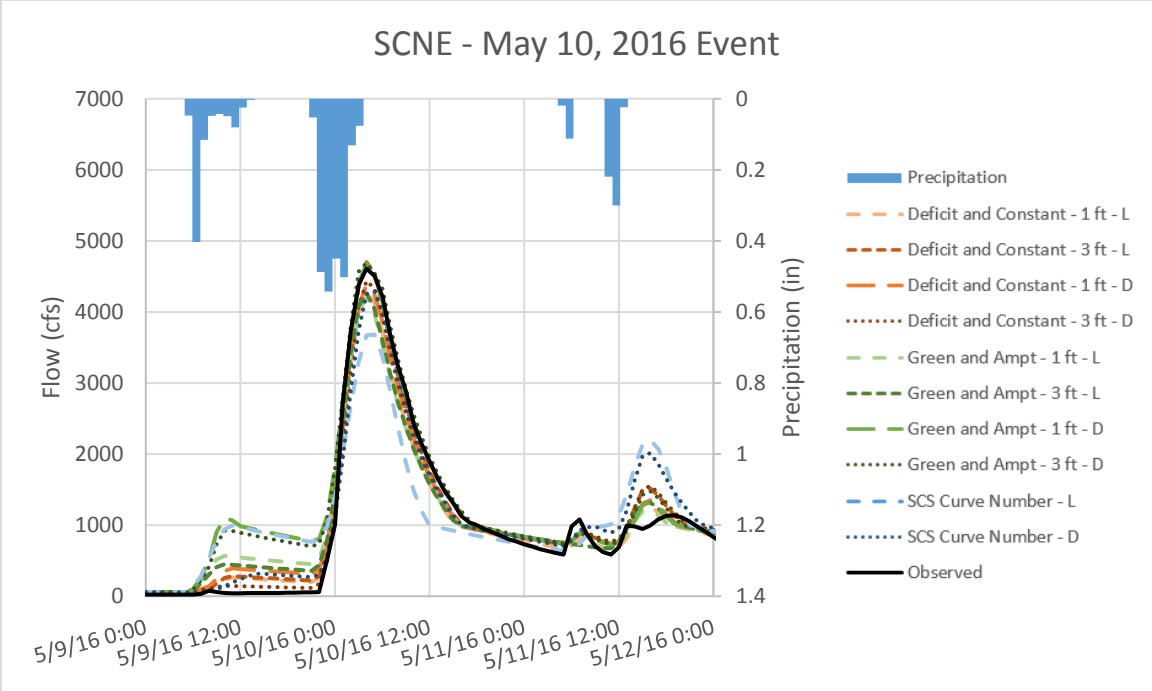

Figure 4 - 5. Comparison of Simulation Results for May 10, 2016 Event at Stevens Creek at Lincoln Stream Gauge Optimized Initial Conditions

4.2.6 RCNE – Rock Creek at Ceresco

The simulation results for the September 30, 2014 event for Stevens Creek at Lincoln with Optimized Initial Conditions are shown in Figure 4 - 6. Included in the figure are the basin average rainfall hyetograph and runoff hydrographs for the observed event as well as 10 different loss methods.

The results from this simulation show a variety of calculated peak flows and times to peak. Overall, the Deficit and Constant Loss Methods perform the best, matching the ascending limb of the hydrograph very well and staying the closest to the observed hydrographs peak flow. This simulation also clearly shows a particular short-coming of the Green and Ampt method. The initial condition specifies an initial water content within the soil column, but does not have away

for including precipitation volume lost to depression and temporary storage within the basin. As a result, even the slightest amount of rainfall will produce runoff when in reality, such precipitation should be absorbed by the soil or held within depressions, ditches and storage ponds. The result of this model inaccuracy is seen on the front end of the hydrograph, with the Green and Ampt methods showing a minor surge in runoff when the observed hydrograph did not.

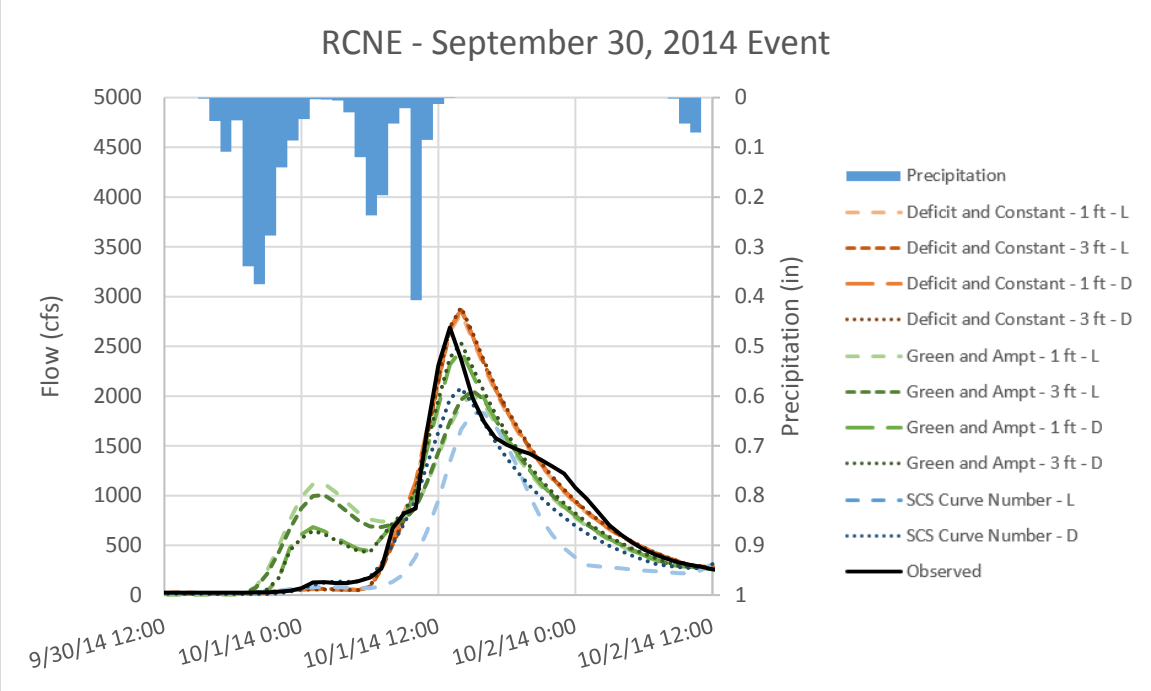

Figure 4 - 6. Comparison of Simulation Results for September 30, 2014 Event at Rock Creek at Ceresco Stream Gauge Optimized Initial Conditions

Furthermore, because this flow volume was calculated early in the simulation and the total flow volume was forced to match the observed, the predicted peak flow for Green and Ampt tended to be lower than that of Deficit and Constant.

The results at this observation location for all the other precipitation events are varied. Overall, the peak flows tended to be higher than the observed flows, with a later time to peak, but the degrees to which these values deviate from the observed are different.

4.2.7 ITNE – Wahoo Creek at Ithaca

The simulation results for the May 10, 2016 event for the Wahoo Creek at Ithaca with Optimized Initial Conditions with are shown in Figure 4 - 7. Included in the figure are the basin average rainfall hyetograph and runoff hydrographs for the observed event as well as 10 different loss methods.

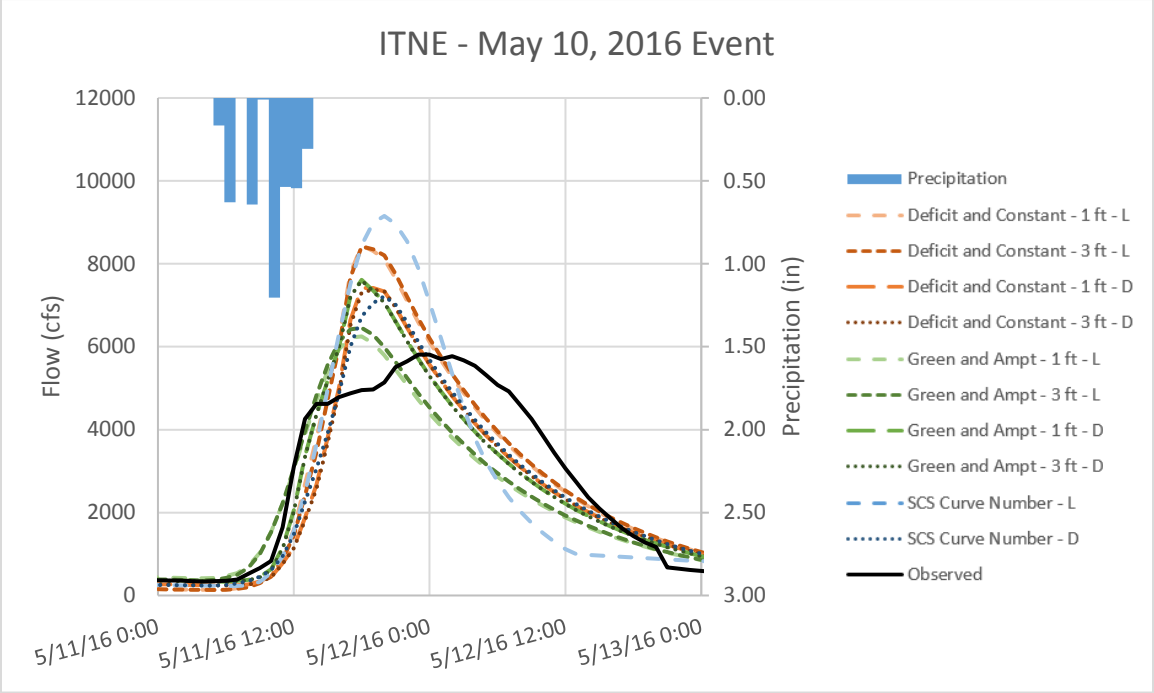

Figure 4 - 7. Comparison of Simulation Results for May 10, 2016 Event at Wahoo Creek at Ithaca Stream Gauge Optimized Initial Conditions

The results from this simulation show an early estimated peak flow from all method combinations that was higher than the observed peak flow for all loss methods. The shape of the hydrograph looks to show some attenuation of the flow as it moved toward the subbasin outlet resulting in a drawn-out and smoother peak. The HEC-HMS model may not be able to accurately account for that as this is the largest subbasin within the model.

This trend was for peaks to be both early and high as compared to the observed data as seen for every simulation at this observation location.

4.3 Simulated Runoff Hydrographs – Non-Optimized Initial Conditions

4.3.1 SC04 – Salt Creek Dam Site 4 – Bluestem Lake

The simulation results for the May 10, 2016 event for Salt Creek Dam Site #4 – Bluestem Lake with Non-Optimized Initial Conditions are shown in Figure 4 - 8. Included in the figure are the basin average rainfall hyetograph and runoff hydrographs for the observed event as well as 10 different runoff-lumping-soil depth combinations.

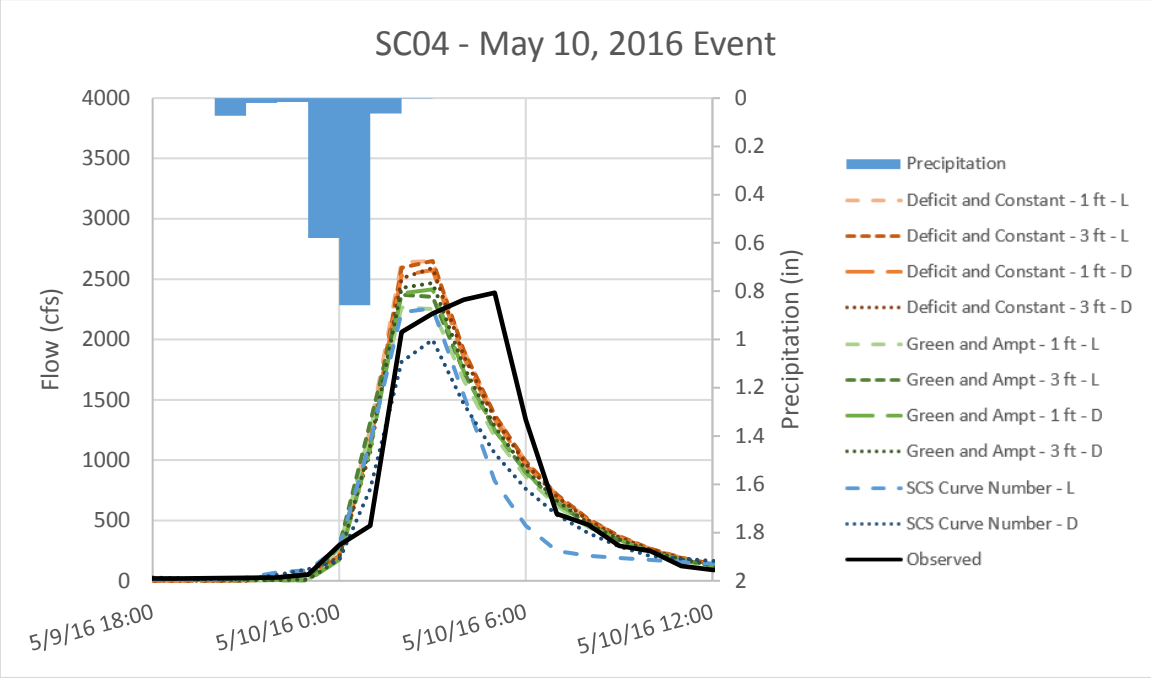

Figure 4 - 8. Comparison of. Simulation Results for May 10, 2016 Event at Salt Creek Dam Site 04 - Bluestem Lake Non-Optimized Initial Conditions

As with the optimized initial conditions, the resulting hydrographs at this location are relatively similar for all 10 simulated modeling combinations. The peak of the simulated hydrographs all occurred before the observed hydrograph peak by approximately 3 hours. The methods were all close to the peak flow rate with some occurring slightly above and others slightly below. SCS Curve Number performed markedly better with the non-optimized initial conditions for both lumped and distributed methods. The shape of the hydrograph could be

improved by adjusting rates of infiltration and initial condition as well as tuning the transform parameters.

Once again, the same trends were seen for all three precipitation events. The simulated times to peak were early by the same margin for all methods when compared to the observed hydrograph. This consistency across multiple events is promising, showing that the model may be able to accurately predict future runoff with slight adjustments to a few parameters.

4.3.2 SC08 – Salt Creek Dam Site 8 – Wagon Train Lake

The simulation results for the May 7, 2015 event for Salt Creek Dam Site #8 – Wagon Train Lake with Non-Optimized Initial Conditions are shown in Figure 4 - 9. Included in the figure are the basin average rainfall hyetograph and runoff hydrographs for the observed event as well as 10 different runoff methods.

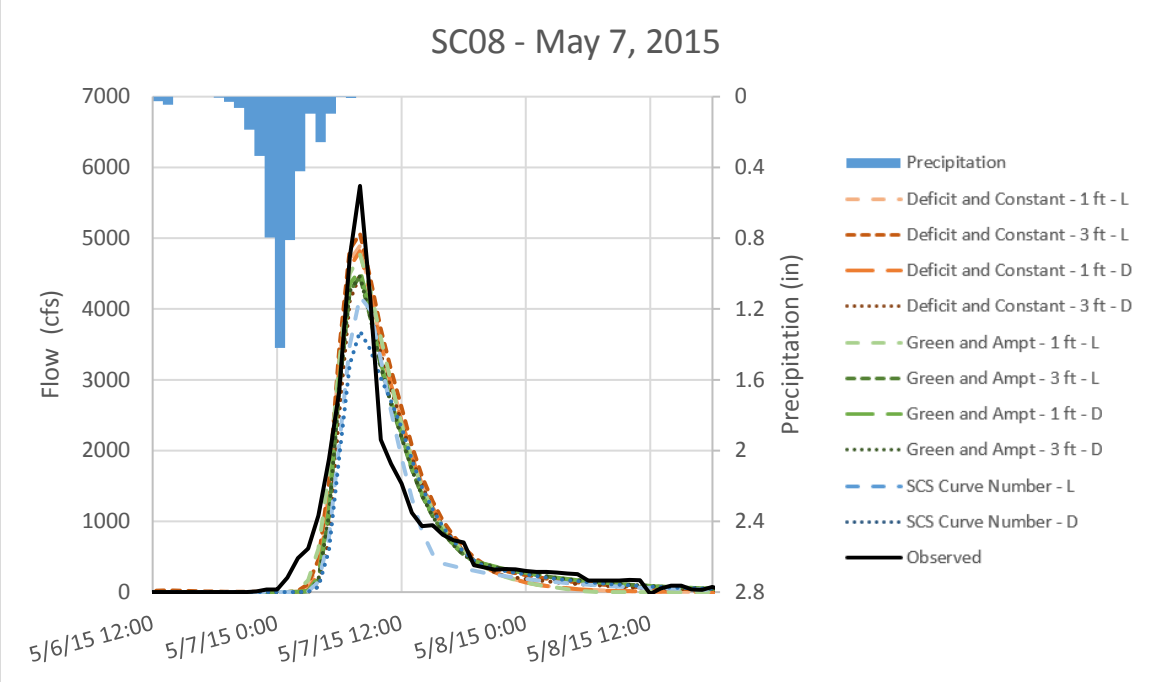

Figure 4 - 9. Comparison of. Simulation Results for May 7, 2015 Event at Salt Creek Dam Site 08 - Wagon Train Lake Non-Optimized Initial Conditions

The resulting hydrographs at the SC08 location were relatively similar for all 10 simulated runoff methods. Once again, the time of peak for the simulated hydrographs all

matched the observed time of peak indicating that the transform parameters are a good fit for this subbasin. The peak flow rate, however, was under-predicted by all loss methods, and the recession limb of the simulated results decreased more slowly than the observed. Additionally, there was a lag between the rising limb of the observed and the simulated results indicating that the infiltration rate was likely too low and the initial condition too high.

The results for all three events show a wide range of results. This is likely due to the relatively small precipitation amounts experienced within the drainage basin when compared to the other observation locations.

4.3.3 SC12 – Salt Creek Dam Site 12 – Conestoga Lake

The simulation results for the September 30, 2016 event for Salt Creek Dam Site 12 – Conestoga Lake with Non-Optimized Initial Conditions are shown in Figure 4 - 10. Included in the figure are the basin average rainfall hyetograph and runoff hydrographs for the observed event as well as 10 different runoff methods.

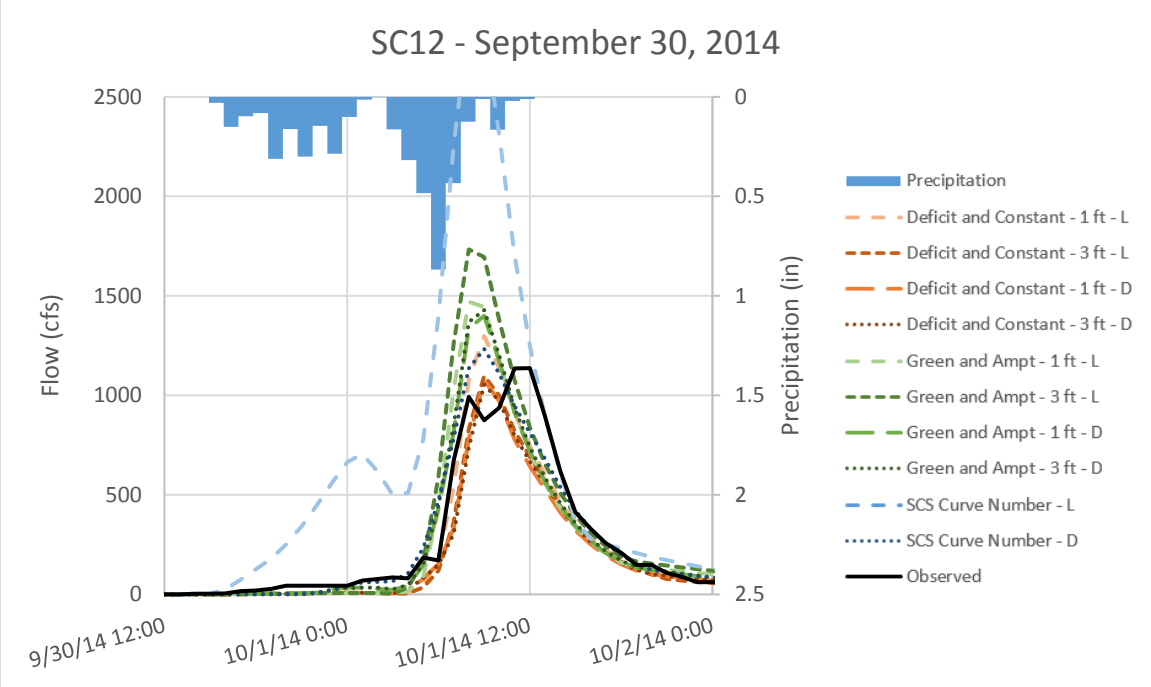

Figure 4 - 10. Comparison of Simulation Results for Sept. 30, 2014 Event at Salt Creek Dam Site 12 - Conestoga Lake Non-Optimized Initial Conditions

The results for this simulation show a wide variety between all ten methods. All methods predict the time to peak occurring 2 – 3 hours early, but the peak simulated flows are widely spread. Generally speaking, the Deficit and Constant method slightly under-predicts the peak flow-rate while Green and Ampt slightly over-predicts. The SCS curve number shows a large discrepancy between the lumped and distributed methods. The distributed method only slightly over-predicts peak flow, while the lumped method greatly over-predicts.

The results for this observation location could only be completed for two of the three selected storms. This is because the reservoir was evacuated in the winter of 2015 for lake rehabilitation and the observation gauge was turned off.

4.3.4 SC18 – Salt Creek Dam Site 18 – Branched Oak Lake

The simulation results for the May 7, 2015 event for Salt Creek Dam Site 18 – Branched Oak Lake are shown in Figure 4 - 11. Included in the figure are the basin average rainfall hyetograph and runoff hydrographs for the observed event as well as 10 different runoff methods.

The results from this simulation show a large degree of variability between the different loss methods. Much like with the optimized initial conditions, the relative accuracy for peak flow and time to peak relative to the observed hydrograph varied significantly, with some results predicting high flows and early peaks and others predicting low flows with late peaks. This observation location inflow hydrograph was calculated poorly and contains unrealistic jumps in flow rate. This is due to a lack of accuracy within the CWMS database used to compute the inflow hydrograph based on observed elevation data.

The trend of poor observed data is seen for all three precipitation events, making this location difficult to match hydrograph data. However, the data are still usable, as the peak flow rates and inflow volumes are still considered to be correct.

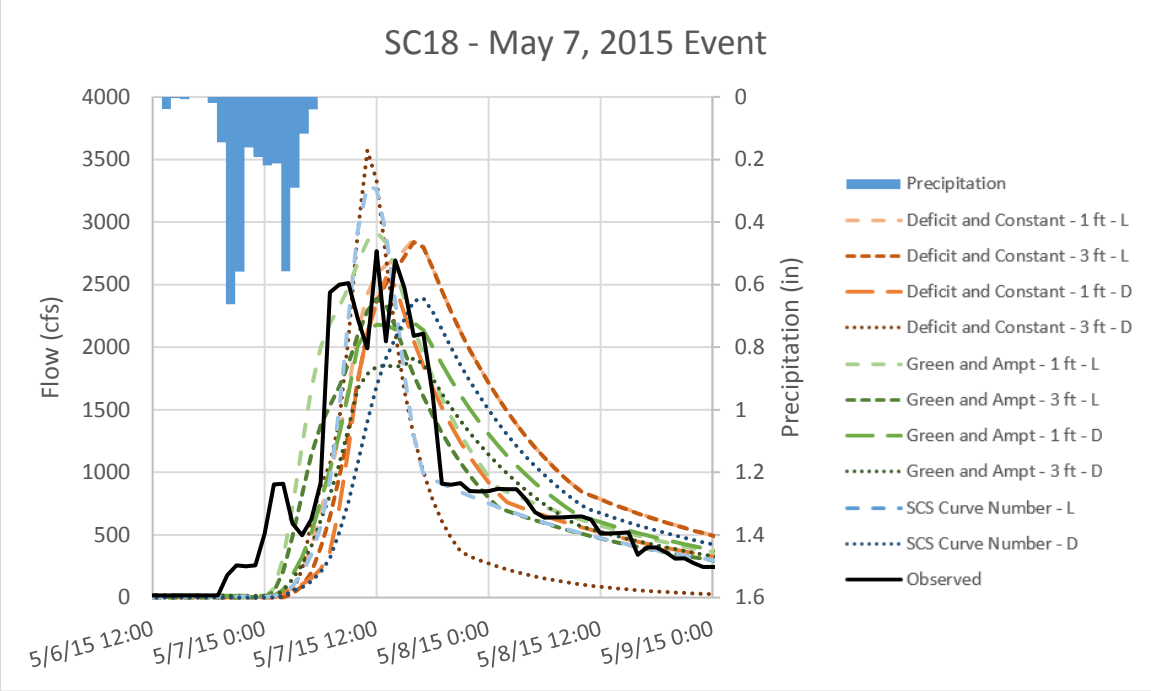

Figure 4 - 11. Comparison of Simulation Results for May 7, 2015 Event at Salt Creek Dam Site 18 - Branched Oak Lake Non-Optimized Initial Conditions

4.3.5 SCNE – Stevens Creek at Lincoln

The simulation results for the May 10, 2016 event for Stevens Creek at Lincoln with Non-Optimized Initial Conditions are shown in Figure 4 - 12. Included in the figure are the basin average rainfall hyetograph and runoff hydrographs for the observed event as well as 10 different runoff methods.

The results from this simulation show a good match between the observed hydrograph and the simulated results. Once again, the timing for all simulated hydrographs matches perfectly with the observed data. The peak flow rates show a range of discrepancy, with most under-predicting the peak flow.

The trend of excellent runoff results does extend to the other two precipitation events. The results for the May 7, 2015 event show a good match in both peak flow and time to peak. However, the simulated results from the September 30, 2014 event show an earlier predicted peak flow that is higher than the observed data.

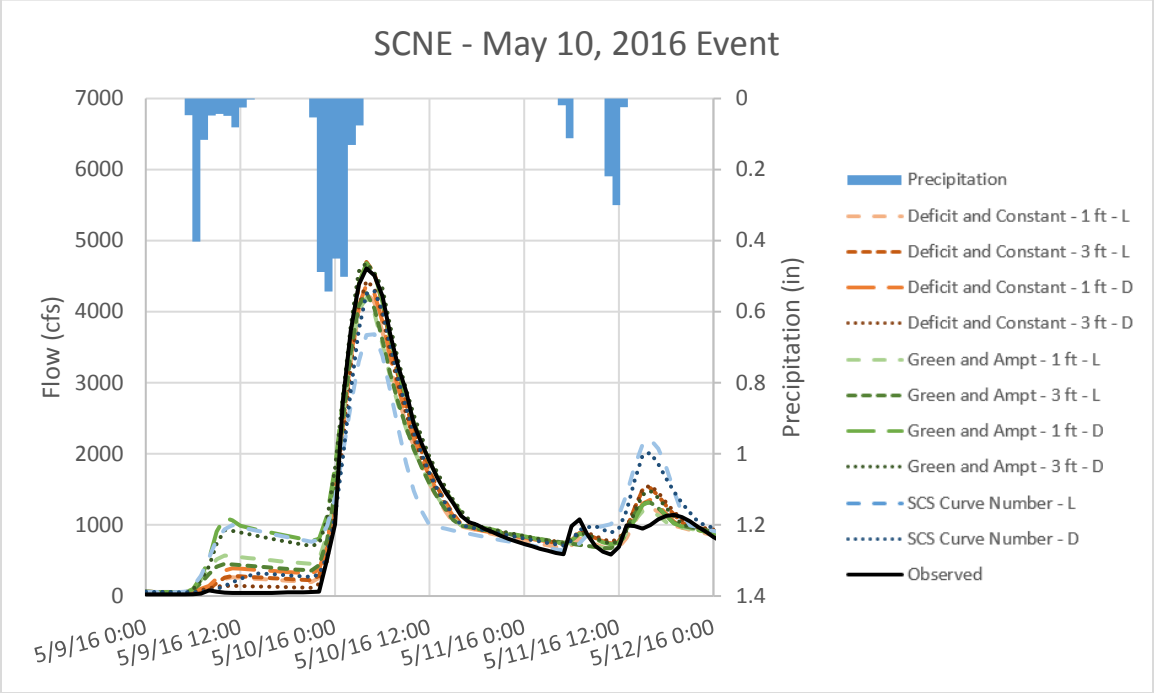

Figure 4 - 12. Comparison of Simulation Results for May 10, 2016 Event at Stevens Creek at Lincoln Stream Gauge Non-Optimized Initial Conditions

4.3.6 RCNE – Rock Creek at Ceresco

The simulation results for the September 30, 2014 event for Stevens Creek at Lincoln are shown in Figure 4 - 13. Included in the figure are the basin average rainfall hyetograph and runoff hydrographs for the observed event as well as 10 different loss methods.

As with the optimized initial conditions, the results show a variety of peak flows and times to peak. Deficit and Constant method does the best job of matching the overall shape of the hydrograph matching the ascending limb of the hydrograph and being the closest on peak flow. The Green and Ampt method shows a surge of runoff at the front end of the simulation the does not appear in the observed hydrograph, again due to the method's inability to accurately account for an initial loss due to terrain depressions and storage ponds.

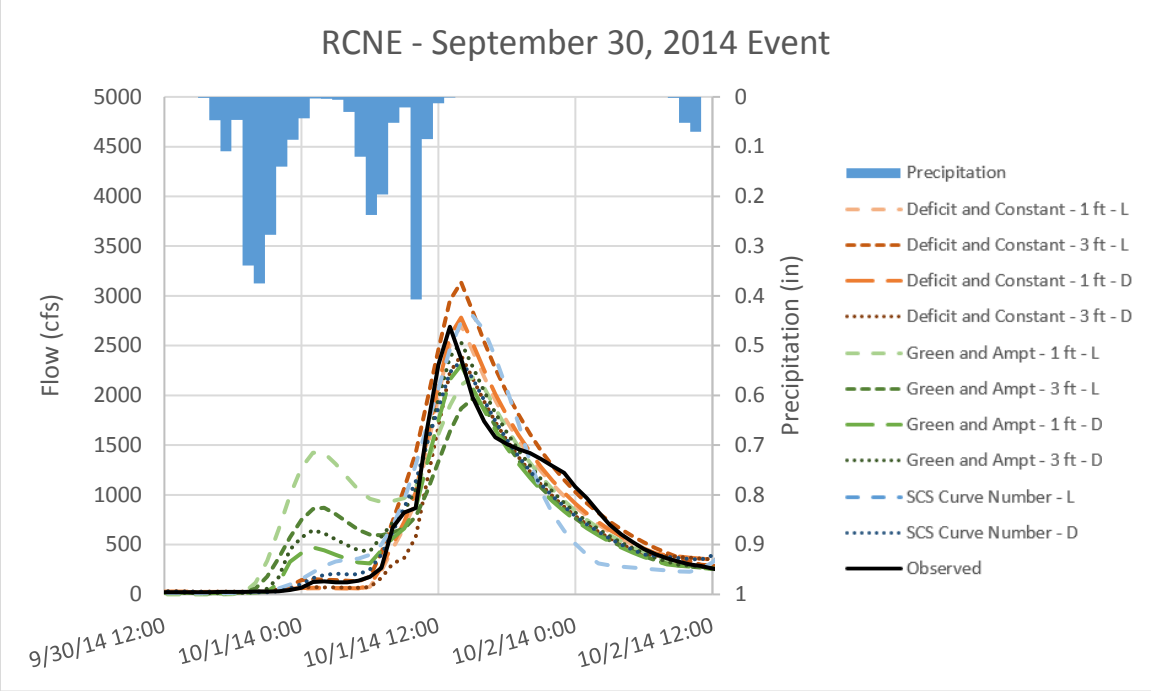

Figure 4 - 13. Comparison of Simulation Results for September 30, 2014 Event at Rock Creek at Ceresco Stream Gauge Non-Optimized Initial Conditions

The results at this observation location for all the other precipitation events are varied. Overall, the peak flows tended to be higher than the observed flows, with a later time to peak, but the degrees to which these values deviate from the observed are different.

4.3.7 ITNE – Wahoo Creek at Ithaca

The simulation results for the May 10, 2016 event for the Wahoo Creek at Ithaca Stream Gauge are shown in Figure 4 - 14. Included in the figure are the basin average rainfall hyetograph and runoff hydrographs for the observed event as well as 10 different loss methods.

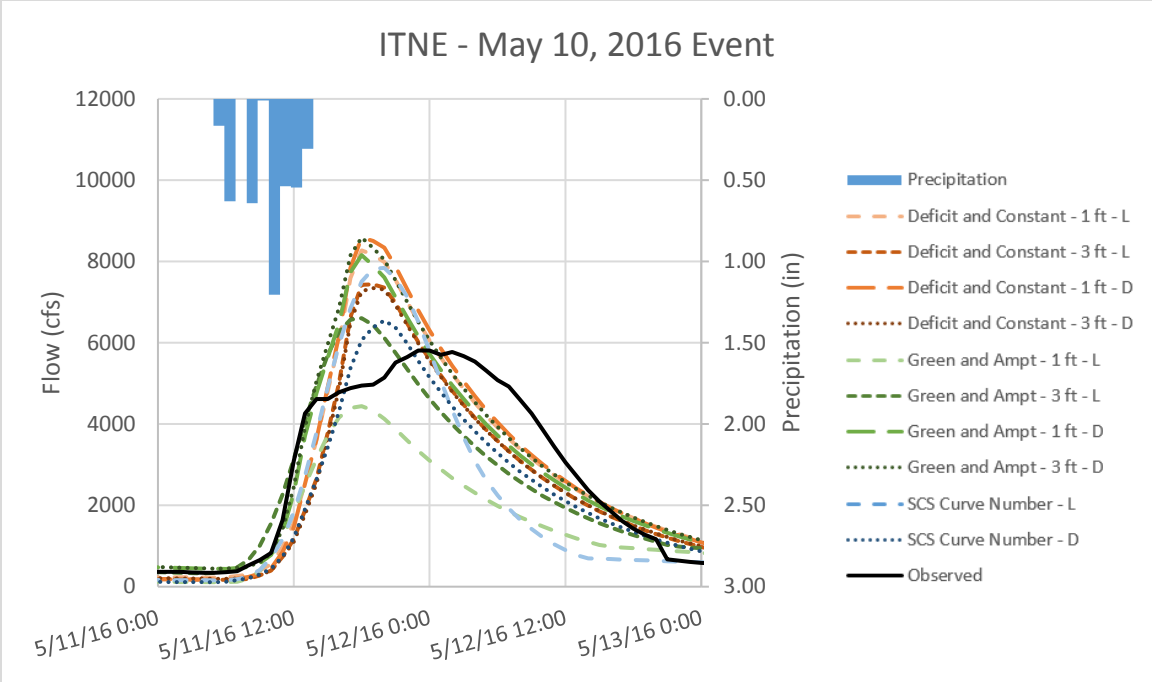

Figure 4 - 14. Comparison of Simulation Results for May 10, 2016 Event at Wahoo Creek at Ithaca Stream Gauge Non-Optimized Initial Conditions

The results from this simulation show an early estimated peak flow from all method combinations that was higher than the observed peak flow for all loss methods. The shape of the hydrograph looks to show some attenuation of the flow as it moved toward the subbasin outlet resulting in a drawn-out and smoother peak. The HEC-HMS model may not be able to accurately account for that as this is the largest subbasin within the model.

This trend was for peaks to be both early and high as compared to the observed data as seen for every simulation at this observation location.

4.4 Analysis Metrics

Two variables were used to evaluate the effectiveness of each loss method on the resulting runoff hydrographs: peak flow and time to peak. Two metrics were used to compare the results: regression analysis and Normalized Root Mean Square Error (NRMSE).

4.4.1 Regression Analyses

A regression analysis was performed to compare simulated and observed data for both the peak flow rate, measured in cfs, and the time to peak, measured in hours from the beginning of the simulation. The procedure involved plotting observed versus simulated flow values and fitting a linear regression line to the data. The coefficient of determination (R^2) was then calculated based on Equation 4-1.

$$R^2 = \frac{\sum(\hat{y} - \bar{y})^2}{\sum(y - \bar{y})^2} \quad (4\text{-}1)$$

Where $\hat{y}$ represents the regression line value, $\bar{y}$ represents the average value for the dataset, and y represents the measured value. The coefficient of determination was used to measure the goodness of fit for simulated data versus observed data. Its value can range between 0 and 1 with 0 representing no correlation between two datasets and a value of 1 indicating a perfect match.

For this analysis, all observed versus simulated data points for peak flow, time to peak, and total runoff volume were collected for all simulations in the analysis. The data were then organized based on initial condition approach and loss method and the linear regression equation and coefficient of determination were determined for each method. The full set of regression analyses are shown in Figure 4 - 15 through Figure 4 - 26 with the first six figures showing results for optimized initial conditions while the last six showing results for non-optimized initial conditions.

After the analyses were complete for each initial condition and loss method, the results were collected and summarized into tables for comparison. The results for peak flow, time to peak, and runoff volume for optimized initial conditions are shown in Table 4 - 1 through Table 4 - 3, respectively, while the results for the same parameters with non-optimized initial conditions are shown Table 4 - 4 through Table 4 - 6, respectively.

Figure 4 - 15. Peak Flow Regression Analyses - Lumped Parameterization - Optimized Initial Conditions

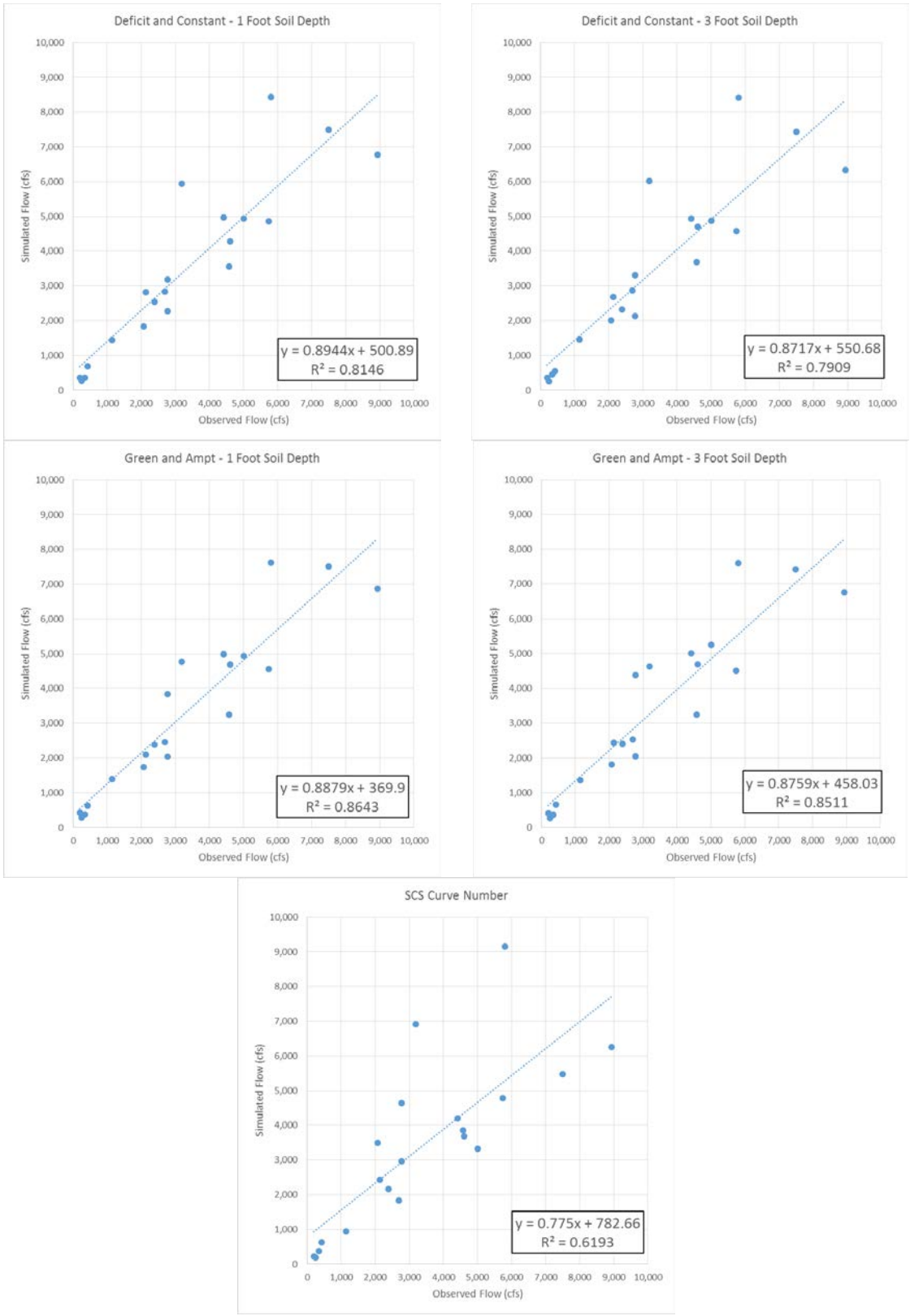

Figure 4 - 16. Peak Flow Regression Analyses – Distributed Parameterization – Optimized Initial Conditions

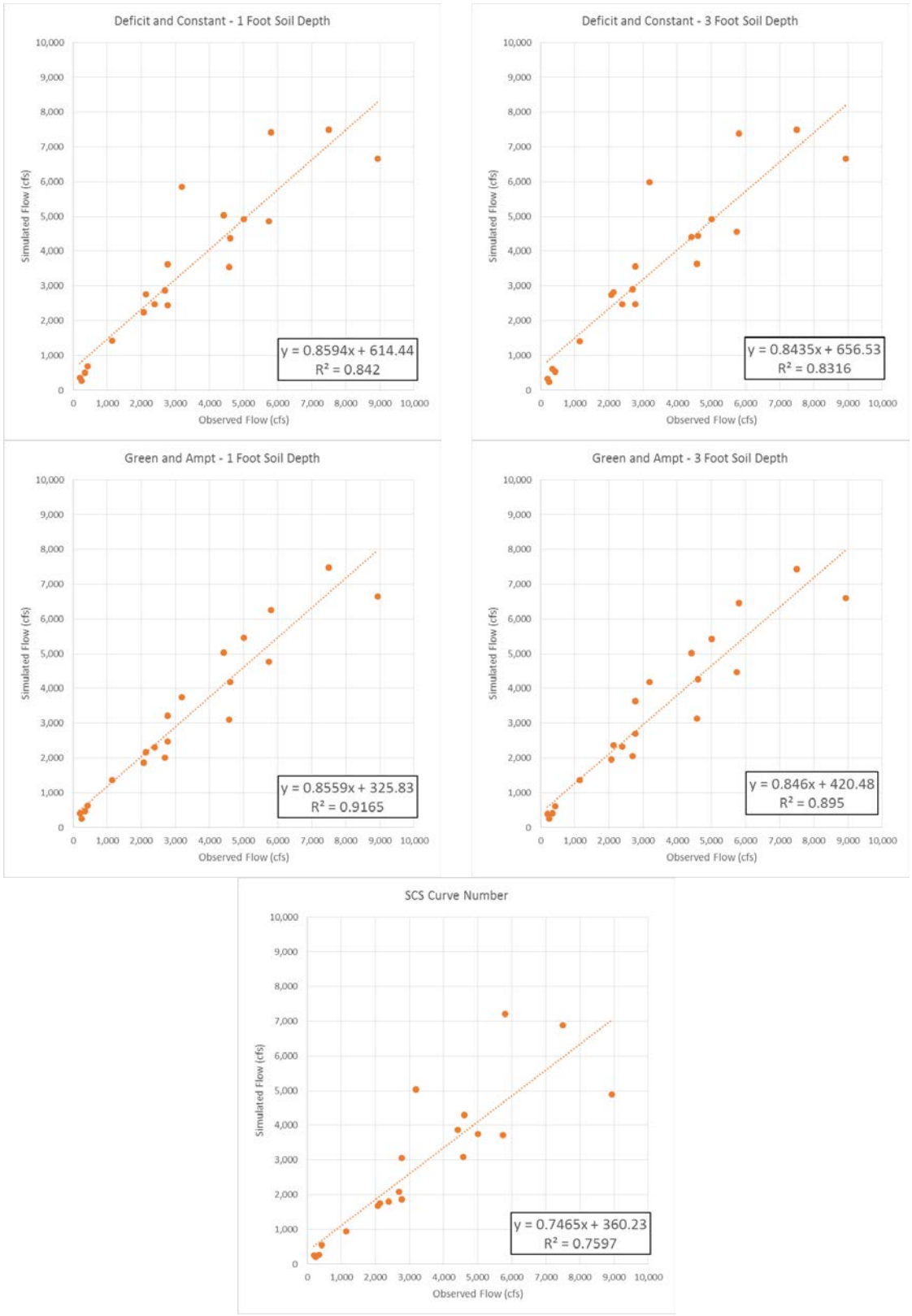

Figure 4 - 17. Time to Peak Regression Analyses – Lumped Parameterization – Optimized Initial Conditions

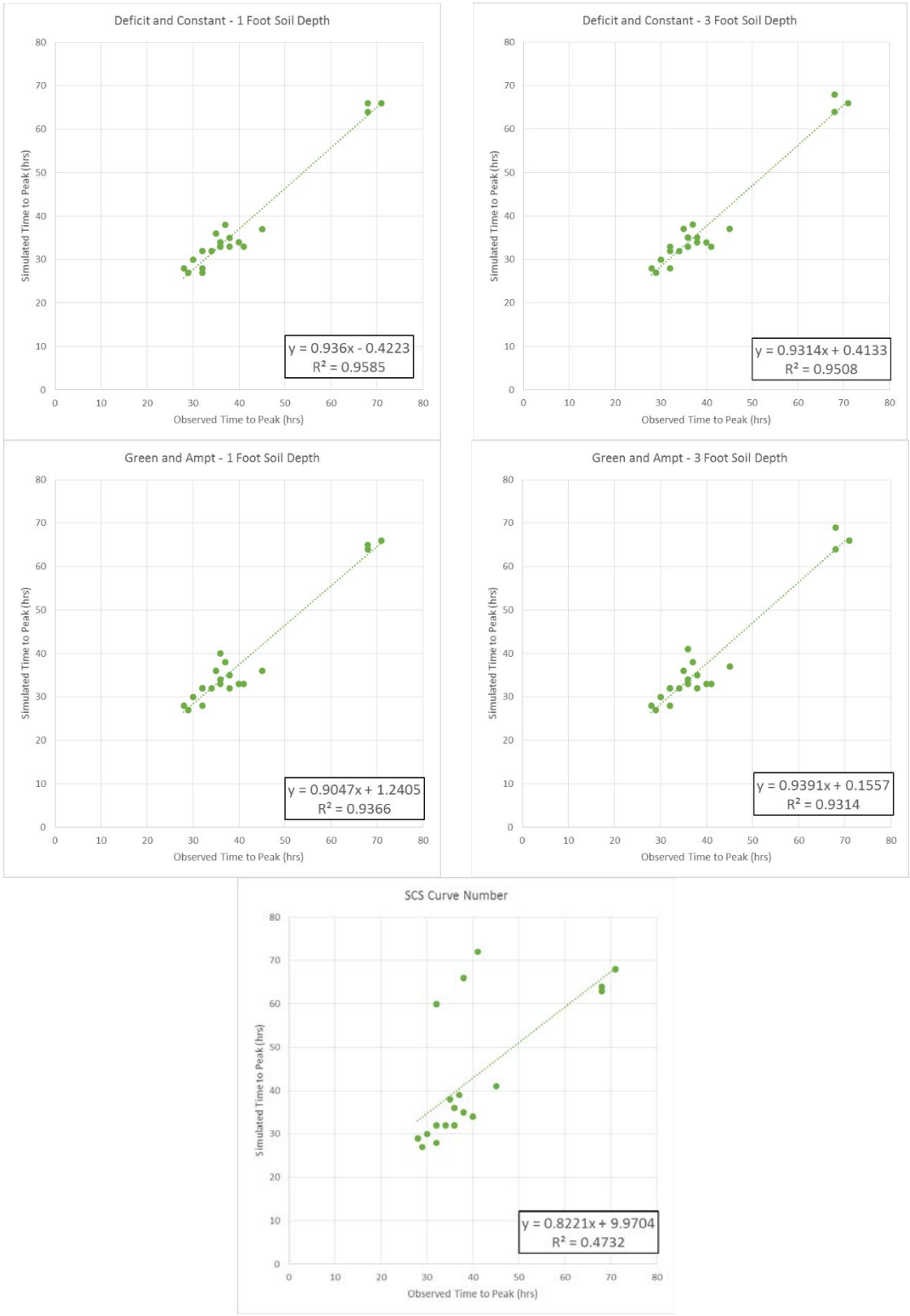

Figure 4 - 18. Time to Peak Regression Analyses – Distributed Parameterization – Optimized Initial Conditions

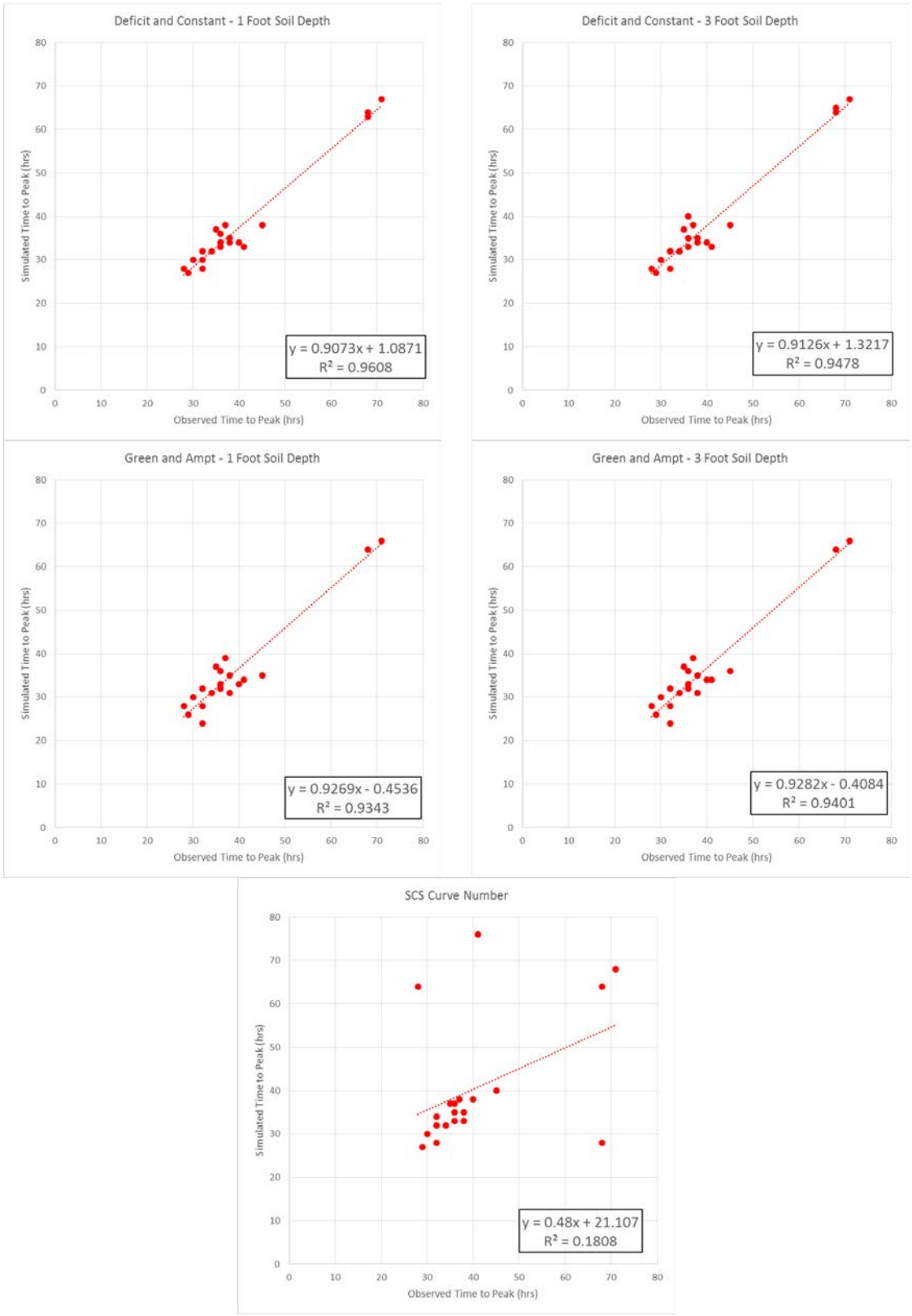

Figure 4 - 19. Runoff Volume Regression Analyses – Lumped Parameterization – Optimized Initial Conditions

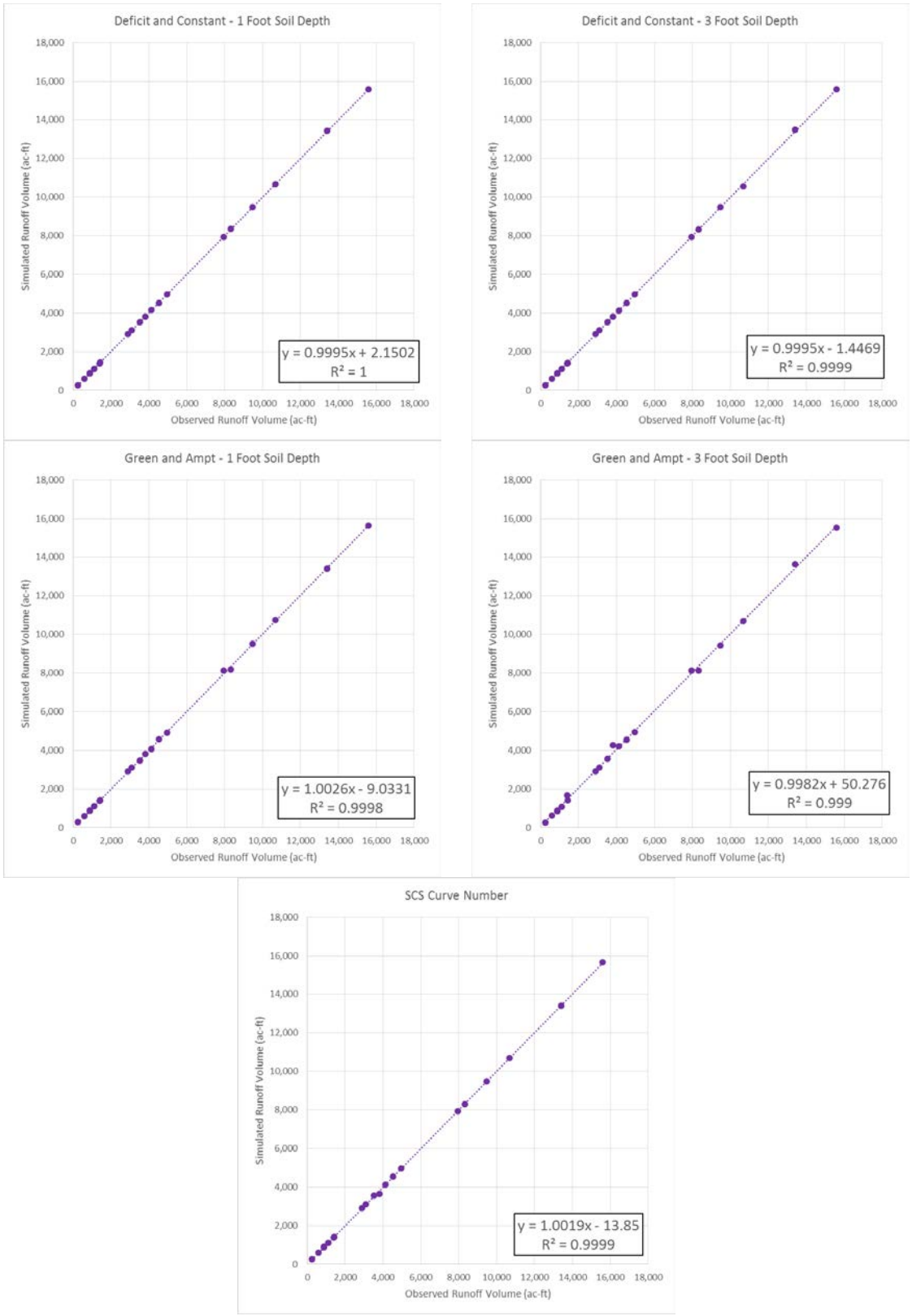

Figure 4 - 20. Runoff Volume Regression Analyses – Distributed Parameterization – Optimized Initial Conditions

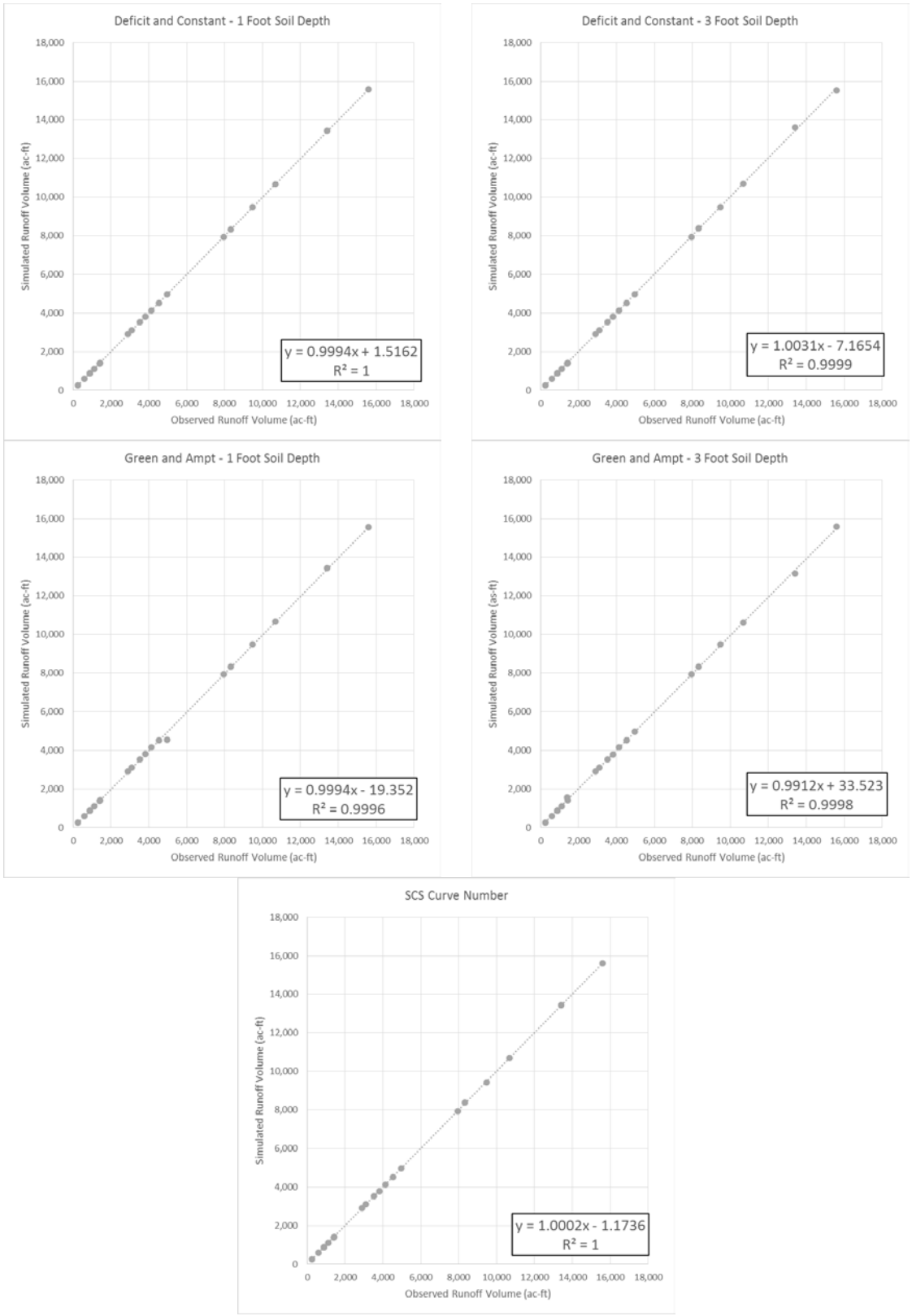

Figure 4 - 21. Peak Flow Regression Analyses – Lumped Parameterization – Non-Optimized Initial Conditions

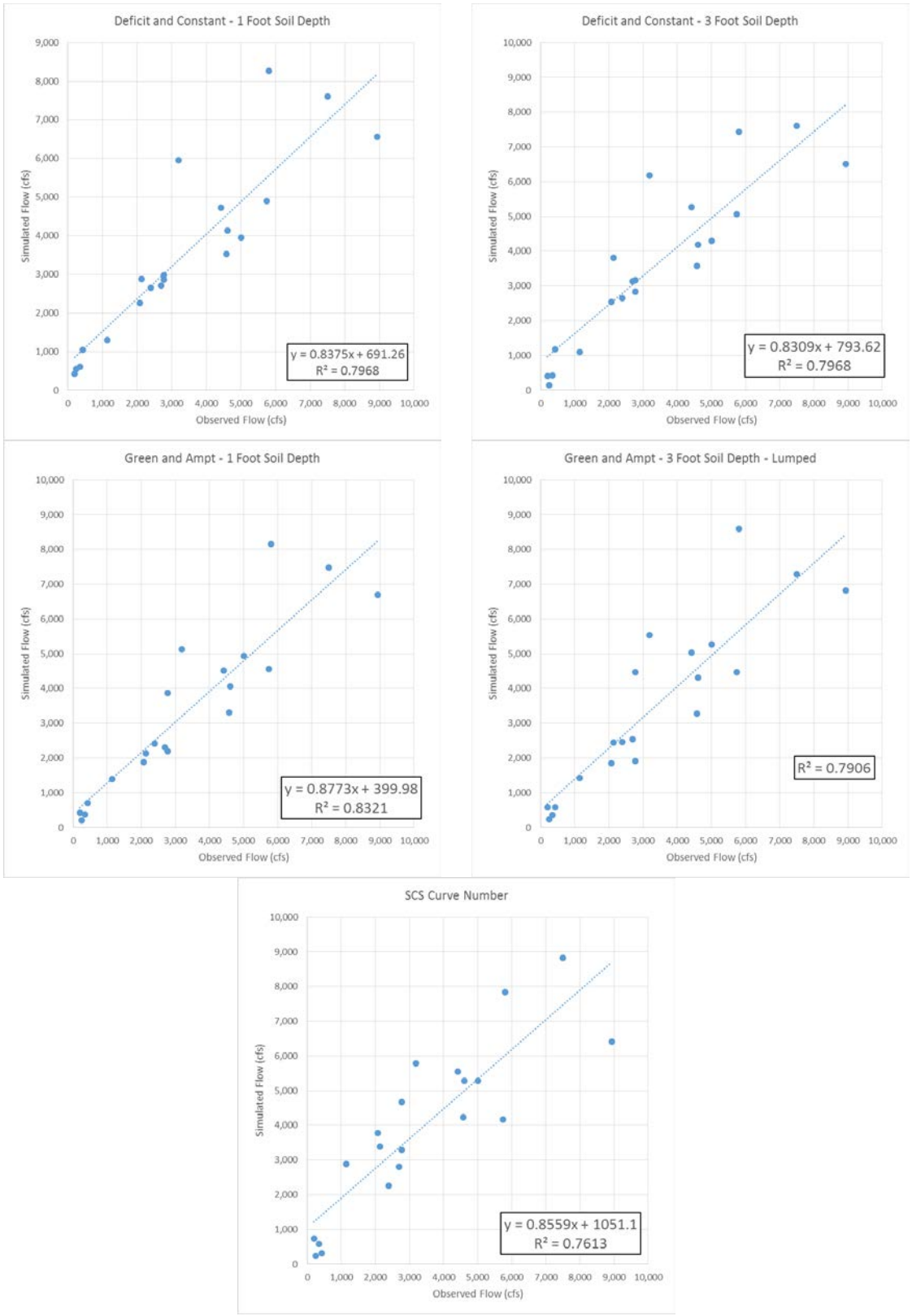

Figure 4 - 22. Peak Flow Regression Analyses – Distributed Parameterization – Non-Optimized Initial Conditions

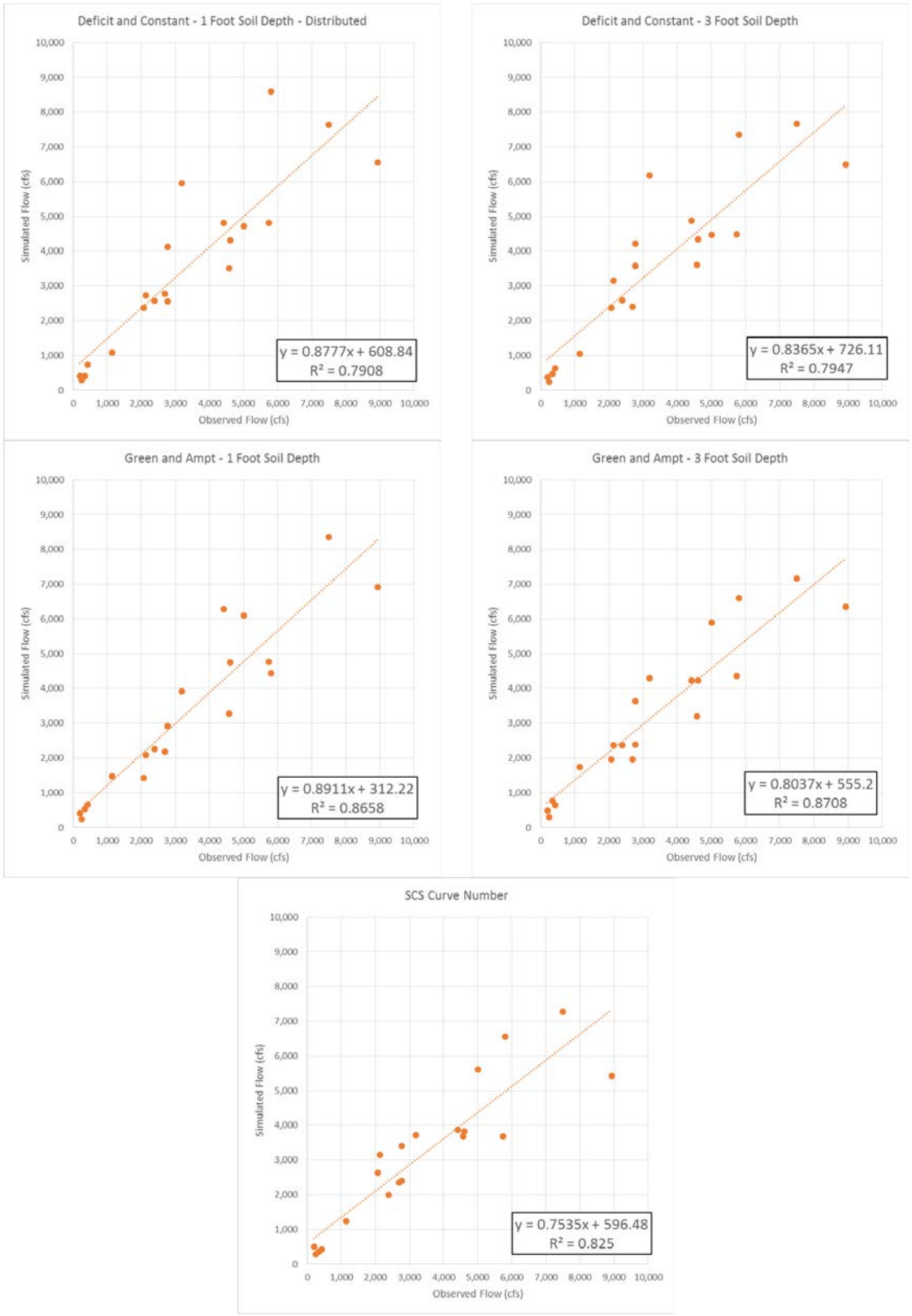

Figure 4 - 23. Time to Peak Regression Analyses – Lumped Parameterization – Non-Optimized Initial Conditions

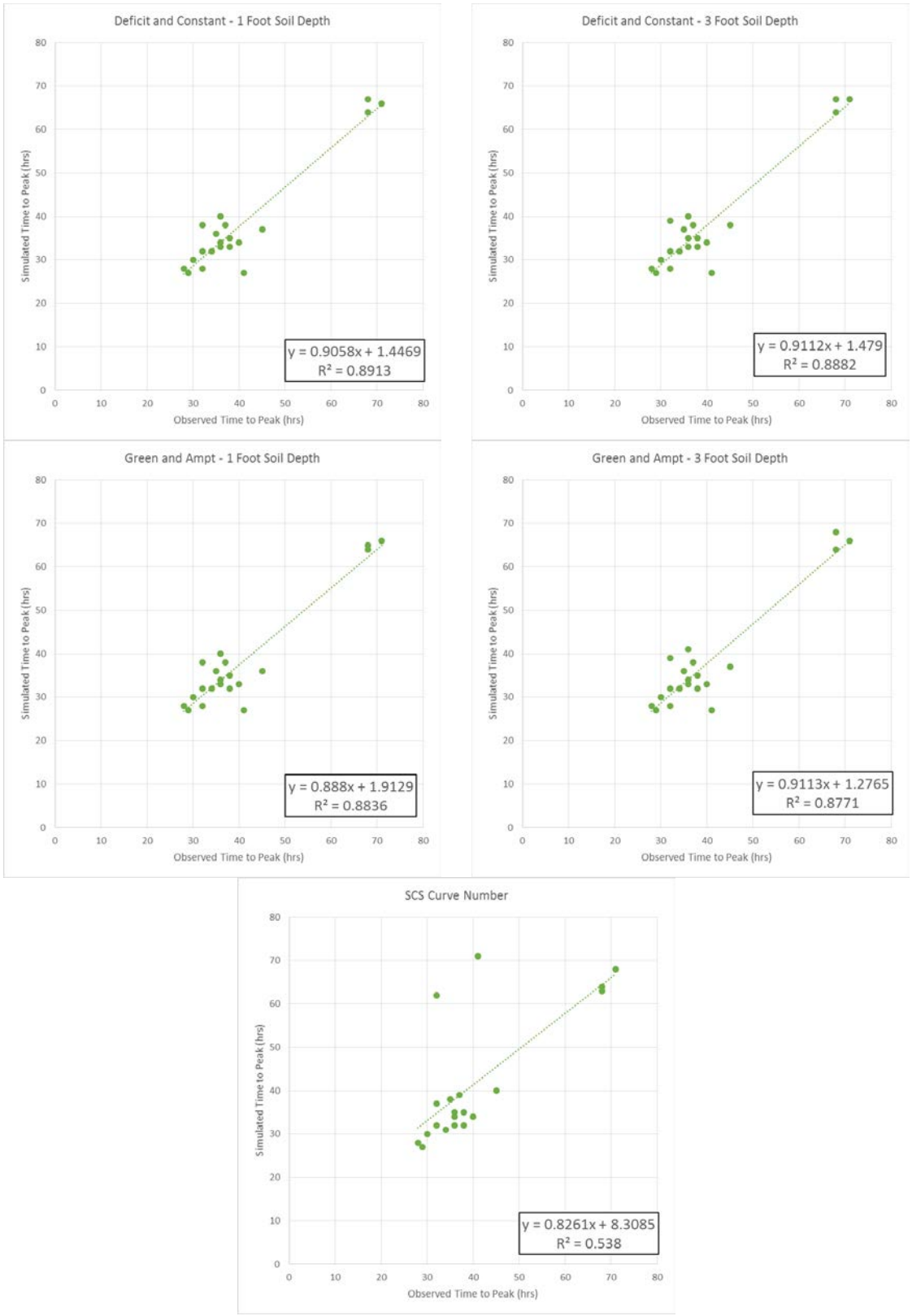

Figure 4 - 24. Time to Peak Regression Analyses – Distributed Parameterization – Non-Optimized Initial Conditions

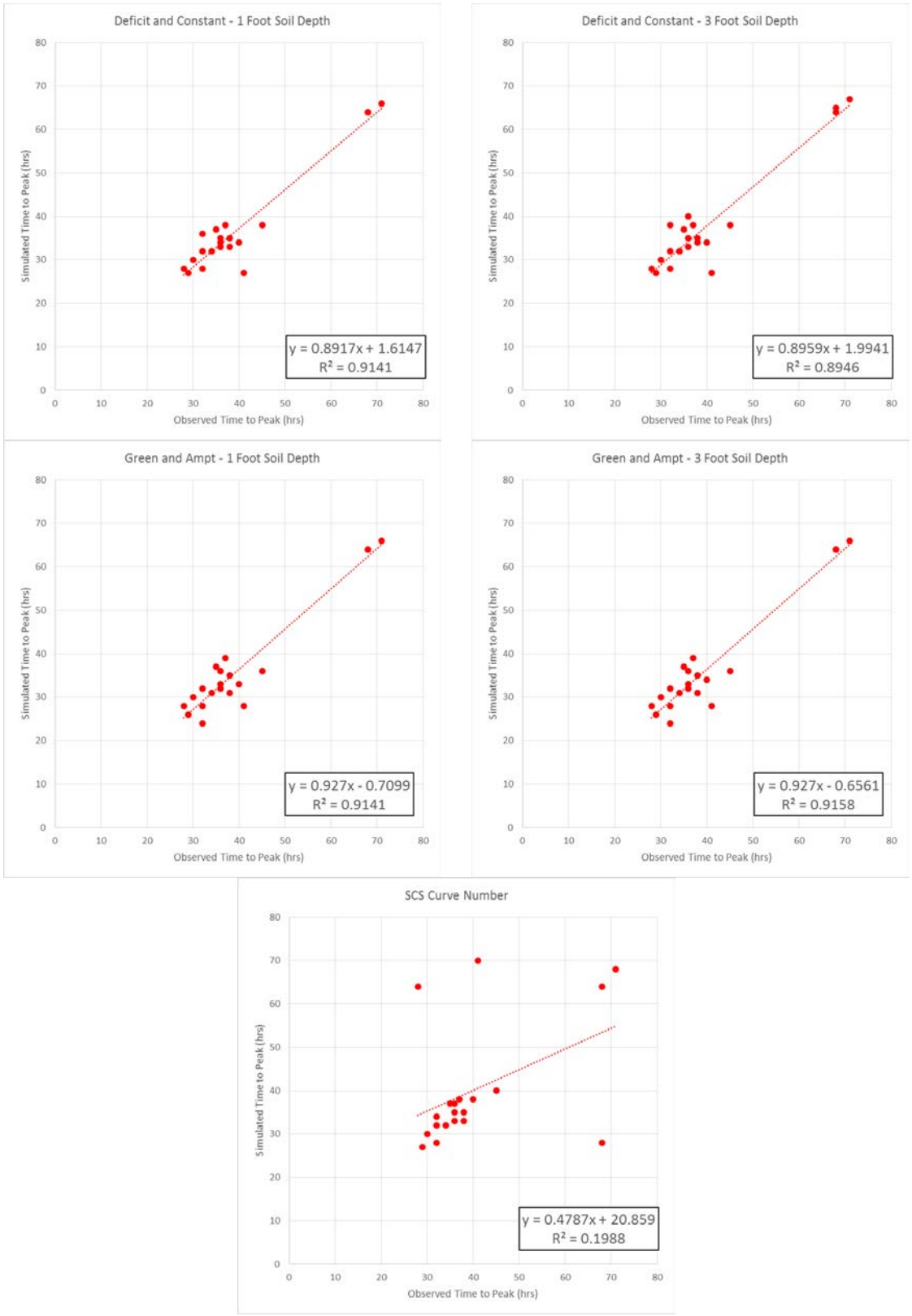

Figure 4 - 25. Runoff Volume Regression Analyses – Lumped Parameterization – Non-Optimized Initial Conditions

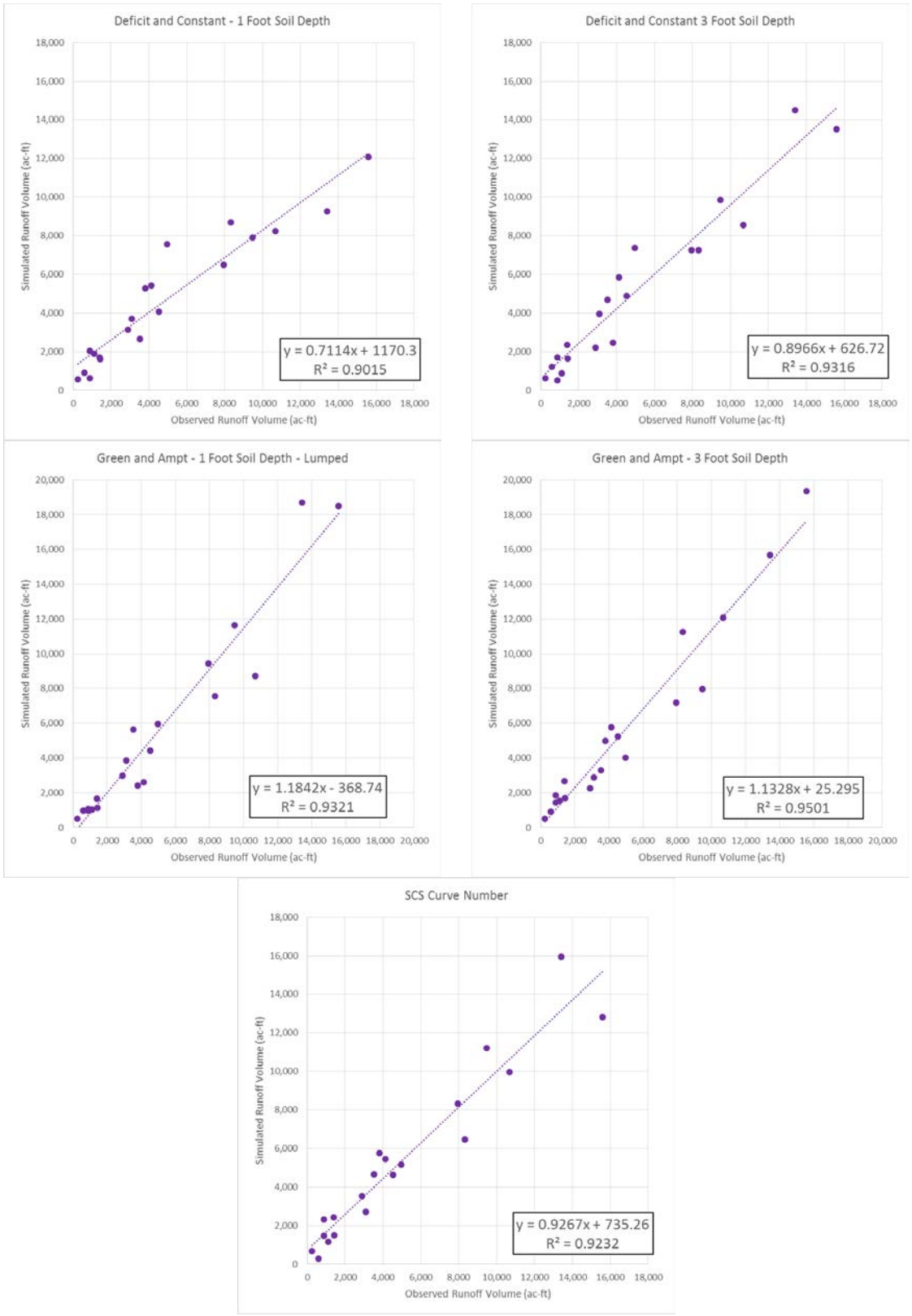

Figure 4 - 26. Runoff Volume Regression Analyses – Distributed Parameterization – Non-Optimized Initial Conditions

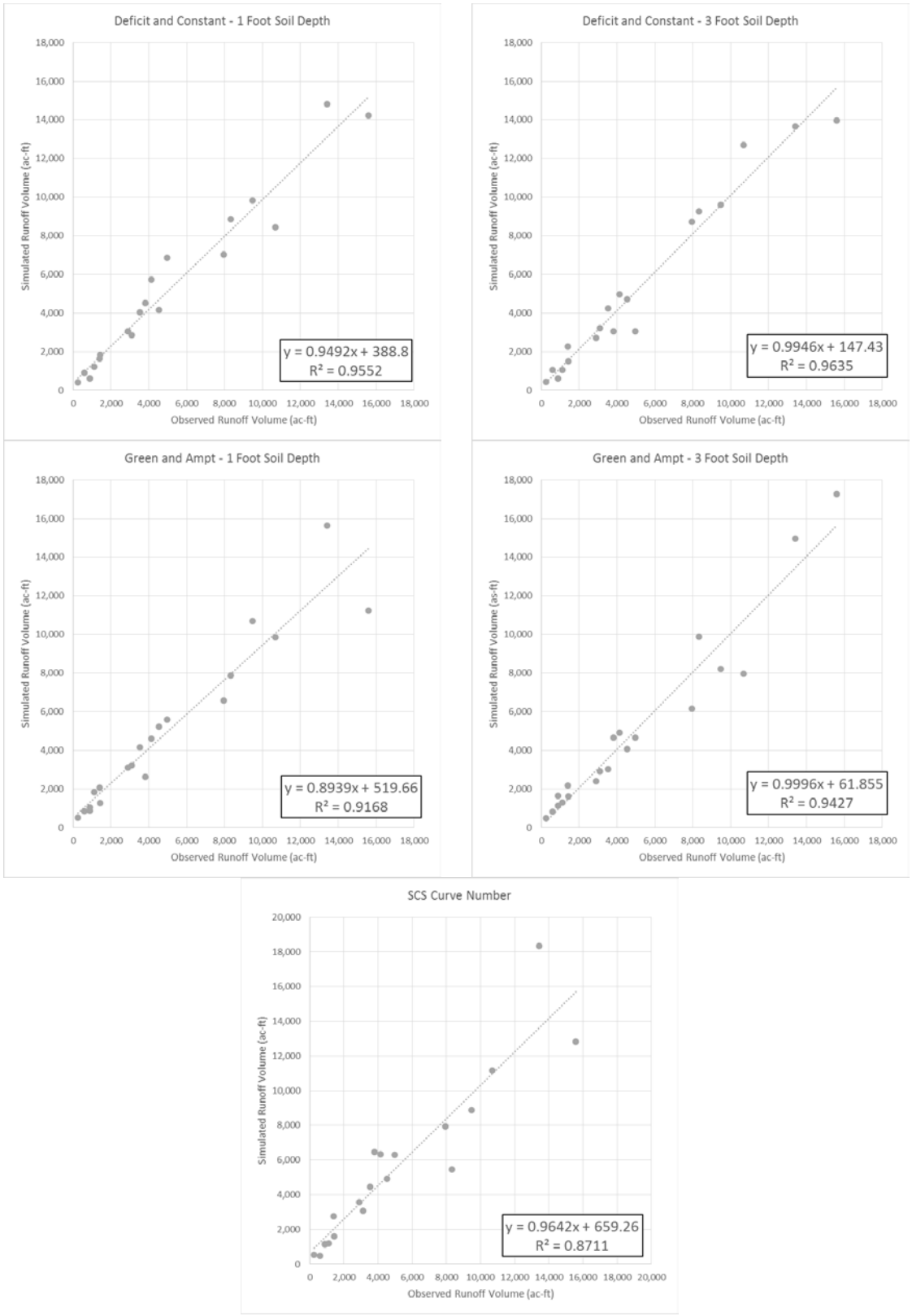

Table 4 - 1. Coefficients of Determination for Peak Flow Rate - Optimized Initial Conditions

	Loss Method	Soil Depth	Coefficient of Determination (R^2)
Lumped	Deficit and Constant	1 Foot	0.8146
		3 Foot	0.7909
	Green and Ampt	1 Foot	0.8643
		3 Foot	0.8511
	SCS Curve Number		0.6193
Distributed	Deficit and Constant	1 Foot	0.8420
		3 Foot	0.8316
	Green and Ampt	1 Foot	**0.9165**
		3 Foot	0.8950
	SCS Curve Number		0.7597

Table 4 - 2. Coefficients of Determination for Time to Peak - Optimized Initial Conditions

	Loss Method	Soil Depth	Coefficient of Determination (R2)
Lumped	Deficit and Constant	1 Foot	0.9585
		3 Foot	0.9508
	Green and Ampt	1 Foot	0.9366
		3 Foot	0.9314
	SCS Curve Number		0.4732
Distributed	Deficit and Constant	1 Foot	**0.9608**
		3 Foot	0.9478
	Green and Ampt	1 Foot	0.9343
		3 Foot	0.9401
	SCS Curve Number		0.1808

Table 4 - 3. Coefficients of Determination for Runoff Volume - Optimized Initial Conditions

	Loss Method	Soil Depth	Coefficient of Determination (R2)
Lumped	Deficit and Constant	1 Foot	**1**
		3 Foot	0.9999
	Green and Ampt	1 Foot	0.9998
		3 Foot	0.9990
	SCS Curve Number		0.9999
Distributed	Deficit and Constant	1 Foot	**1**
		3 Foot	0.9999
	Green and Ampt	1 Foot	0.9996
		3 Foot	0.9998
	SCS Curve Number		**1**

Table 4 - 4. Coefficients of Determination for Peak Flow Rate - Non-Optimized Initial Conditions

	Loss Method	Soil Depth	Coefficient of Determination (R^2)
Lumped	Deficit and Constant	1 foot	0.7968
		3 Foot	0.7968
	Green and Ampt	1 foot	0.8321
		3 Foot	0.7906
	SCS Curve Number		0.7613
Distributed	Deficit and Constant	1 foot	0.7908
		3 Foot	0.7947
	Green and Ampt	1 foot	0.8658
		3 Foot	**0.8708**
	SCS Curve Number		0.8250

Table 4 - 5. Coefficients of Determination for Time to Peak - Non-Optimized Initial Conditions

	Loss Method	Soil Depth	Coefficient of Determination (R2)
Lumped	Deficit and Constant	1 foot	0.8913
		3 Foot	0.8882
	Green and Ampt	1 foot	0.8836
		3 Foot	0.8771
	SCS Curve Number		0.5380
Distributed	Deficit and Constant	1 foot	0.9141
		3 Foot	0.8946
	Green and Ampt	1 foot	0.9141
		3 Foot	**0.9158**
	SCS Curve Number		0.1988

Table 4 - 6. Coefficients of Determination for Runoff Volume - Non-Optimized Initial Conditions

	Loss Method	Soil Depth	Coefficient of Determination (R^2)
Lumped	Deficit and Constant	1 foot	0.9015
		3 Foot	0.9316
	Green and Ampt	1 foot	0.9321
		3 Foot	0.9501
	SCS Curve Number		0.9232
Distributed	Deficit and Constant	1 foot	0.9552
		3 Foot	**0.9635**
	Green and Ampt	1 foot	0.9168
		3 Foot	0.9427
	SCS Curve Number		0.8711

One more analysis was done based on the regression analyses. In order to determine which loss method performed the "best" under each initial condition approach, the coefficients of determination for all three regression analyses were multiplied together to generate a "Composite R^2" value. These values were then ranked from highest to lowest, establishing a ranking of runoff methods accuracy. This process is shown in Table 4 - 7 through Table 4 - 10.

Table 4 - 7. Composite R^2 Value Calculation – Optimized Initial Conditions

	Method	Soil Depth	R-squared Values			
			Peak Flow	Time to Peak	Volume	Composite R^2
Lumped	Deficit and Constant	1 Foot	0.8146	0.9585	**1**	0.7808
		3 Foot	0.7909	0.9508	0.9999	0.7519
	Green and Ampt	1 Foot	0.8643	0.9366	0.9998	0.8093
		3 Foot	0.8511	0.9314	0.9990	0.7919
	SCS Curve Number		0.6193	0.4732	0.9999	0.2930
Distributed	Deficit and Constant	1 Foot	0.8420	**0.9608**	**1**	0.8090
		3 Foot	0.8316	0.9478	0.9999	0.7881
	Green and Ampt	1 Foot	**0.9165**	0.9343	0.9996	**0.8559**
		3 Foot	0.8950	0.9401	0.9998	0.8412
	SCS Curve Number		0.7597	0.1808	**1**	0.1374

Table 4 - 8. Ranking of Composite R^2 Value Calculation – Optimized Initial Conditions

	Method	Soil Depth	R-squared Values			
			Peak Flow	Time to Peak	Volume	Composite R^2
D	Green and Ampt	1 Foot	**0.9165**	0.9343	0.9996	**0.8559**
D	Green and Ampt	3 Foot	0.8950	0.9401	0.9998	0.8412
L	Green and Ampt	1 Foot	0.8643	0.9366	0.9998	0.8093
D	Deficit and Constant	1 Foot	0.8420	**0.9608**	**1**	0.8090
L	Green and Ampt	3 Foot	0.8511	0.9314	0.9990	0.7919
D	Deficit and Constant	3 Foot	0.8316	0.9478	0.9999	0.7881
L	Deficit and Constant	1 Foot	0.8146	0.9585	**1**	0.7808
L	Deficit and Constant	3 Foot	0.7909	0.9508	0.9999	0.7519
L	SCS Curve Number		0.6193	0.4732	0.9915	0.2906
D	SCS Curve Number		0.7597	0.1808	**1**	0.1374

Table 4 - 9. Composite R^2 Value Calculation – Non-Optimized Initial Conditions

	Method	Soil Depth	Coefficients of Determination			
			Peak Flow	Time to Peak	Volume	Composite R^2
Lumped	Deficit and Constant	1 Foot	0.7968	0.8913	0.9015	0.6402
		3 Foot	0.7968	0.8882	0.9316	0.6593
	Green and Ampt	1 Foot	0.8321	0.8836	0.9321	0.6853
		3 Foot	0.7906	0.8771	0.9501	0.6588
	SCS Curve Number		0.7613	0.5380	0.9232	0.3781
Distributed	Deficit and Constant	1 Foot	0.7908	0.9141	0.9552	0.6905
		3 Foot	0.7947	0.8946	**0.9635**	0.6850
	Green and Ampt	1 Foot	0.8658	0.9141	0.9168	0.7256
		3 Foot	**0.8708**	**0.9158**	0.9427	**0.7518**
	SCS Curve Number		0.8250	0.1988	0.8711	0.1429

Table 4 - 10. Ranking of Composite R^2 Value Calculation – Non-Optimized Initial Conditions

	Method	Soil Depth	R-squared Values			
			Peak Flow	Time to Peak	Volume	Composite R^2
D	Green and Ampt	3 Foot	**0.8708**	**0.9158**	0.9427	**0.7518**
D	Green and Ampt	1 Foot	0.8658	0.9141	0.9168	0.7256
D	Deficit and Constant	1 Foot	0.7908	0.9141	0.9552	0.6905
L	Green and Ampt	1 Foot	0.8321	0.8836	0.9321	0.6853
D	Deficit and Constant	3 Foot	0.7947	0.8946	**0.9635**	0.6850
L	Deficit and Constant	3 Foot	0.7968	0.8882	0.9316	0.6593
L	Green and Ampt	3 Foot	0.7906	0.8771	0.9501	0.6588
L	Deficit and Constant	1 Foot	0.7968	0.8913	0.9015	0.6402
L	SCS Curve Number		0.7613	0.5380	0.9232	0.3781
D	SCS Curve Number		0.8250	0.1988	0.8711	0.1429

The results of the regression analysis provide several insights into the quality of the runoff methods. Generally speaking for both initial condition approaches, the distributed versions of each loss method had higher coefficients of determination than their lumped counterparts. This indicates that for whatever runoff method was used in the hydrologic simulation, the distributed modeling framework provided more accurate results than the

lumped. Also of note is the trend regarding soil depth. For most methods that included soil depth, the 1-foot soil depth outperformed the 3-foot soil depth. The exception occurred during the non-optimized initial condition analysis where two methods performed better with the deeper soil profile. These differences, however, were only marginal. Finally, of the three runoff methods chosen for this analysis, Green and Ampt is the most "physically-based" method while the Curve Number method is the least. The results show that the more physically based a loss method is, the better it performed according to this performance metric.

For the time to peak analysis, the coefficients of determination were very similar for all methods excluding the Curve Number method. All Deficit and Constant and Green and Ampt methods had coefficients of determination better than 0.88, indicating excellent model performance. The Curve Number methods did not perform well in predicting correct times to peak. This is most likely due to a limitation within the curve number method itself. When discussion the limitation of application for the SCS Curve Number Method, Woodward et al (1999) noted that the method is only intended to estimate runoff for a single storm and that any discontinuous periods of rainfall should warrant and adjustment of the curve number. For this study, this limitation led to the method greatly over-predicting the runoff from secondary storms that occurred after the main event and skewed the results for time of peak. An example of this secondary peak over-estimation can be seen in Figure 4 - 27.

For the runoff volume analysis, the coefficients of determination were very high for all methods. The optimized initial conditions simulations were controlling for runoff volume which resulted values very close to one (>0.99). For the non-optimized conditions, the values were all better than 0.87. This indicates that all methods performed well from this perspective and that the chosen initial conditions were not far away from their optimized values. Also, there are no discernable trends with regards to method, soil depth, or lumped/distributed application.

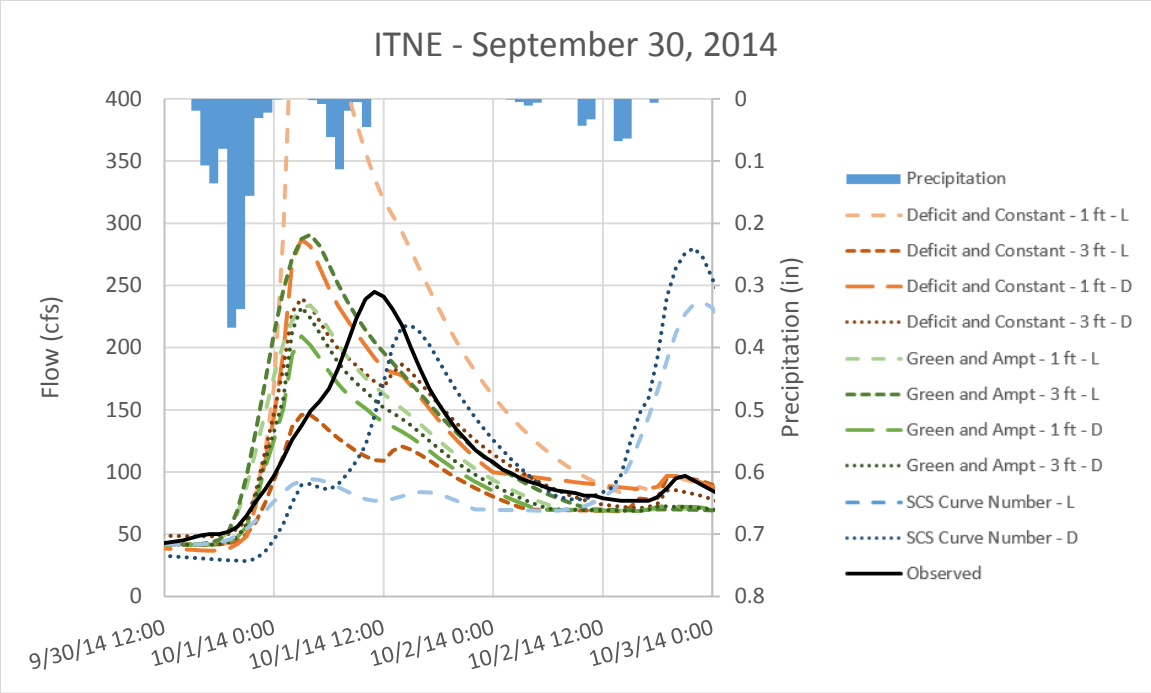

Figure 4 - 27. Runoff Hydrographs for SC04 - Salt Creek Dam Site 04 - Bluestem Lake for September 30, 2014 Event Non-Optimized Initial Conditions

The ranking of the composite R^2 values provides a few insights into the effectiveness of each loss method. First of all, several of the trends noticed during peak flow are seen again. The most physically based method of Green and Ampt was the top performer, followed by Deficit and Constant and then Curve Number. For the optimized initial conditions, the 1-foot soil depth version of each loss method marginally outperformed the 3-foot soil depth version. However, for non-optimized initial conditions, that trend was more varied with the Green and Ampt method with 3-foot soil depth scoring the highest. Finally, for both methods the top of the ranking list was once again dominated by distributed loss methods. However, the lumped Green and Ampt methods were shown to perform marginally better than the distributed Deficit and Constant methods.

One important note about the curve number method is that while it does not rank well for reasons already discussed related to time of peak, the coefficients of determination for peak flow and runoff volume are still very good, (>0.76 and >0.87, respectively). This indicates that for

single precipitation events, the issue related to time to peak would be eliminated and this method would likely score very well.

Finally, the approach for determining initial conditions did not have a significant impact on the rankings of the runoff methods. All coefficients of determination did go down from the optimized to the non-optimized initial conditions, but the trends remained largely unchanged. One noticeable change was the performance of the SCS Curve Number method. By altering the curve number according to antecedent moisture condition instead of adjusting the initial abstraction, the method showed improvements in all three metrics. However, the still poor performance in predicting time of peak kept the method at the bottom of the rankings.

4.4.2 Normalized Root Mean Squared Error

The Normalized Root Mean Square Error (NRMSE) was calculated for the peak flow, time to peak, and total runoff volume. The NRMSE is a variation of the Root Mean Square Error (RMSE), which is used to measure the difference between values predicted by a model and the observed data. The RMSE is calculated using Equation 4-2.

$$RMSE = \sqrt{\frac{\sum(X_{obs} - X_{sim})^2}{n}} \tag{4-2}$$

where X_{obs} is the observed value, X_{sim} is the simulated value, and n is the number of total data comparisons. The benefit of RMSE is its ability to express model error in the same measured units of the comparing values. In other words, the RMSE for peak flow rate is expressed in terms of cfs. However, with regard to this study, the problem with applying the RMSE to this study is one of scale. The flowrates observed at Bluestem Lake are often between 500 and 1,000 cfs while those at the Wahoo Creek at Ithaca gauge can exceed 20,000 cfs. As a result, an error of 1,000 cfs have significantly different meaning depending on where the error occurs.

To handle this issue, the RMSE was normalized into the NRMSE by dividing the RMSE by the full range of observed values as shown in Equation 4-3.

$$NRMSE = \frac{RMSE}{X_{obs,max} - X_{obs,min}} \quad (4\text{-}3)$$

NRMSE is unitless and generally has a value between 0 and 1. This structure allows for the comparison of NRMSE for different types of data. Since NRMSE is quantifying the error of the simulation performance, a perfect value is zero. These calculations were performed for each of the three parameters and the results are shown in Table 4 - 11. As with the coefficients of determination in the R^2 regression analysis, a composite NRMSE value was generated by multiplying the Peak Flow and Time to Peak NRMSE values together. The composite NRMSE was then used to rank the loss methods. For the optimized initial conditions, the runoff volume NRMSE was excluded from this calculation due to many of the values being equal to zero. The results from this procedure are shown in Table 4 - 6.

Table 4 - 11. Normalized Root Mean Square Error Values – Optimized Initial Conditions

	Loss Method	Soil Depth	NRMSE Values		
			Peak Flow	Time to Peak	Volume
Lumped	Deficit and Constant	1 Foot	0.12	0.09	0.00
		3 Foot	0.13	0.08	0.00
	Green and Ampt	1 Foot	0.10	0.09	0.00
		3 Foot	0.10	0.09	0.01
	SCS Curve Number		0.17	0.26	0.01
Distributed	Deficit and Constant	1 Foot	0.11	0.08	**0.00**
		3 Foot	0.11	**0.08**	0.00
	Green and Ampt	1 Foot	**0.08**	0.11	0.01
		3 Foot	0.09	0.10	0.00
	SCS Curve Number		0.14	0.33	0.00

Table 4 - 12. Ranking of Normalized Root Mean Square Error Values – Optimized Initial Conditions

	Method	Soil Depth	NRMSE Values		
			Peak Flow	Time to Peak	Composite
D	Green and Ampt	1 foot	**0.08**	0.11	**0.0087**
D	Deficit and Constant	1 foot	0.11	0.08	0.0091
D	Green and Ampt	3 foot	0.09	0.10	0.0091
D	Deficit and Constant	3 foot	0.11	**0.08**	0.0092
L	Green and Ampt	1 foot	0.10	0.09	0.0093
L	Green and Ampt	3 foot	0.10	0.09	0.0095
L	Deficit and Constant	3 foot	0.13	0.08	0.0105
L	Deficit and Constant	1 foot	0.12	0.09	0.0107
L	SCS Curve Number		0.17	0.26	0.0456
D	SCS Curve Number		0.14	0.33	0.0470

Table 4 - 13. Normalized Root Mean Square Error Values – Non-Optimized Initial Conditions

	Loss Method	Soil Depth	NRMSE Values		
			Peak Flow	Time to Peak	Volume
Lumped	Deficit and Constant	1 Foot	0.12	0.11	0.11
		3 Foot	0.12	0.11	0.07
	Green and Ampt	1 Foot	0.11	0.11	0.11
		3 Foot	0.13	0.11	0.09
	SCS Curve Number		0.15	0.23	0.07
Distributed	Deficit and Constant	1 Foot	0.13	**0.11**	0.06
		3 Foot	0.12	0.11	**0.05**
	Green and Ampt	1 Foot	**0.10**	0.12	0.08
		3 Foot	0.10	0.12	0.07
	SCS Curve Number		0.12	0.32	0.11

Table 4 - 14. Ranking of Normalized Root Mean Square Error Values – Non-Optimized Initial Conditions

	Loss Method	Soil Depth	NRMSE Values			
			Peak Flow	Time to Peak	Volume	**Composite**
D	Deficit and Constant	3 Foot	0.12	0.11	**0.05**	**0.0007**
D	Green and Ampt	3 Foot	0.10	0.12	0.07	0.0008
D	Deficit and Constant	1 Foot	0.13	**0.11**	0.06	0.0008
D	Green and Ampt	1 Foot	**0.10**	0.12	0.08	0.0009
L	Deficit and Constant	3 Foot	0.12	0.11	0.07	0.0010
L	Green and Ampt	3 Foot	0.13	0.11	0.09	0.0013
L	Green and Ampt	1 Foot	0.11	0.11	0.11	0.0014
L	Deficit and Constant	1 Foot	0.12	0.11	0.11	0.0014
L	SCS Curve Number		0.15	0.23	0.07	0.0024
D	SCS Curve Number		0.12	0.32	0.11	0.0040

The NRMSE values are useful to give a scope of the errors in the simulated results and to help determine their significance. For the peak flow analysis, all methods had a NRMSE of less than 0.2 indicating good model performance. As with the regression analysis, the distributed models out-performed their lumped counterparts, indicating that distributed modeling produced more accurate results. For the optimized initial conditions, the 1-foot soil depth produced better results than the 3-foot soil depth for the same loss method, and Green and Ampt was once again the best overall loss method followed by Deficit and Constant, and then Curve Number method. However, for the non-optimized initial conditions, all peak flow errors were very similar with no discernable trend relative to method or soil depth.

The time to peak analysis also showed similar results to that of the regression analysis with NRMSE value all falling between 0.08 and 0.11 for the Green and Ampt and Deficit and Constant methods, indicating excellent model performance. Once again, The Curve Number methods did not perform well in predicting correct times to peak.

The peak flow volumes were only analyzed for the non-optimized initial conditions. The trend with these data once again favored the use of distributed modeling techniques over the lumped counterparts. Interestingly, the Deficit and Constant method was the top performer followed by Green and Ampt and SCS Curve Number. Also, the 3-foot soil depth showed slightly better results than the 1-foot soil depth.

For the optimized initial conditions, the Composite NRMSE values followed similar trends to the regression analysis placing the Distributed Green and Ampt method for a 1-foot soil depth at the top of the ranking. However, the rest of the rankings changed. Now the top four rankings all belong to the distributed versions of the Green and Ampt and Deficit and Constant Loss methods, respectively. This is then followed by the lumped versions of those same methods with the two Curve Number methods once again rounding out the bottom two

spots. Also apparent in the table is that the 1-foot soil depth outperformed the 3-foot soil depth for rainfall runoff simulations.

For the non-optimized initial conditions, all rankings were changed. Once again, the list was dominated by the distributed modeling methods, but the favored soil depth was the deeper 3-foot. The Deficit and Constant and Green and Ampt methods were more mixed together in the rankings with neither clearly favored over the other. The Distributed Deficit and Constant with 3-foot soil depth is the top performer with the two Curve Number methods once again rounding out the bottom two spots.

Finally, there was a significant change in the rankings of runoff methods between the two approaches for initial conditions. While the optimized initial conditions still favored the Green and Ampt method, the non-optimized initial conditions changed the top performing method to the Deficit and Constant method. This change is due to the inclusion of the runoff volume. While the Deficit and Constant method had NRMSE values in the middle for peak flow and time to peak, the runoff volume was so low that it allowed the method to have the highest ranking with the smallest composite value.

Chapter 5 Summary and Conclusions

The goal of this research can be broken down into two main objectives:

1. The first objective was to develop a method for defining hydrologic loss parameter values for three different loss methods based on soil data contained within the SSURGO database. Such a method allows for derivation of parameter values in watershed where no observed data are available for model calibration. The three loss methods were:
    - Deficit and Constant Loss method
    - Green and Ampt method
    - SCS Curve Number method

    Each of the physically based loss methods were tested with two different soil depths, 1-foot and 3-foot, to determine the impact this parameter has on sensitivity and accuracy of results. The hypothesis is that a reasonably accurate set of hydrologic loss parameters can be developed for each of the selected loss methods for use in hydrologic modeling, and that the shallower soil depth (1-foot) parameters will provide a more accurate runoff hydrograph than those of the deep soil (3-foot).
2. The second objective was to create spatially variable datasets for each of the selected loss method parameters to compare the difference in simulated runoff between lumped and distributed modeling techniques. The hypothesis was that the spatial variability of soil properties will be more accurately represented in the distributed hydrologic model resulting in runoff hydrographs that more closely match observed results.

The Salt Creek Basin located in southeast Nebraska was used to test the study objectives. The physical soil data stored within the SSURGO database were used to calculate selected hydrologic loss methods' parameter values for each of the soil horizons. A series of

weighted averages was then applied to acquire average parameter values for each SSURGO map unit, first a depth-weighted average to find average component parameter values, then a percent-weighted average to determine average map unit parameter values. This information was used to create the loss parameter datasets to be applied in the hydrologic modeling.

5.1 Objective 1 Conclusions

To meet objective 1, the average map unit parameter values were used to generate average subbasin parameter values by way of an area-weighted average scheme. The generated loss parameter values were then applied to the Salt Creek Basin HEC-HMS model and used to simulate the runoff generated by three different precipitation events. Two approaches were utilized to set initial conditions. The first approach optimized initial conditions to control for total runoff volume, and the peak flow and time to peak results for each loss method were compared to the observed data. The second approach used a more traditional non-optimized approach based only on precipitation information prior to the beginning of rainfall event. A regression analysis was used to determine the correlation between the observed and simulated results for peak flow, time to peak, and runoff volume. The coefficients of determination for these tests were multiplied together to generate a ranking of the performance for each modeled loss method. Then, a Normalized Root Mean Square Error (NRMSE) was calculated for each loss method to determine the percent error over the full spectrum of observed flow values at the observation locations.

Table 4 - 1 through Table 4 - 6 show that the objective 1 hypothesis was partially true for physically based hydrologic loss methods. Table 4 - 1 and Table 4 - 4 show that all 10 methods achieved a coefficient of determination value of better than 0.6, indicating relatively good model performance. However, Table 4 - 2 and Table 4 - 5 show a clear distinction between the physically based loss methods, Deficit and Constant and Green and Ampt, and the least

physically based, SCS Curve Number. Generally speaking, the data trends from these two tables as well as the ranking schemes shown in Tables 4 - 7, 4 - 9, 4 - 12, and 4 - 14 show that the more physically based a loss model, the better the results. Based on these metrics, the Green and Ampt method performed the best followed by the Deficit and Constant method and the SCS Curve Number method, respectively.

Tables 4 - 7, 4 - 9, 4 - 12, and 4 - 14 also show a trend in terms of depth of soil analysis. The overall trend showed that the 1-foot soil depth version of the runoff methods was able to produce slightly better results than the 3-foot soil depth. The exceptions to this trend occurred with the non-optimized initial conditions. This conclusion suggests that this part of the hypothesis was correct. This result was expected, as the shallow soil depth would more accurately represent the soil column's response to single-event drive hydrologic modeling. The deeper soil depth information would be more appropriately applied to long-term hydrologic simulations and soil-moisture accounting methods.

5.2 Objective 2 Conclusions

To meet objective 2, the average map unit parameter values were applied to the map unit raster dataset provided in the SSURGO database. The raster was then reclassified to produce distributed hydrologic parameter grids for each of the loss methods. These loss parameter grids were then applied to the Salt Creek Basin HEC-HMS model and used to simulate the runoff generated by three different precipitation events. Again, two approaches were utilized to set initial conditions. The first approach optimized initial conditions to control for total runoff volume, while the second approach used more traditional non-optimized values based only on precipitation information prior to the beginning of rainfall event. A regression analysis was used to determine the correlation between the observed and simulated results for peak flow, time to peak, and runoff volume. The coefficients of determination for these tests

were then multiplied together to generate a ranking of the performance for each modeled loss method. Then, a Normalized Root Mean Square Error (NRMSE) was calculated for each loss method to determine the percent error over the full spectrum of observed flow values at the observation locations.

Every analysis metric used in this study showed that for all but one loss method, the distributed loss parameters produce a more accurate runoff hydrograph. The Distributed Green and Ampt method most metrics in this study, able to produce coefficients of determination greater than 0.86 for all regression analyses and having the smallest NRMSE value of 0.1. Tables 4 - 7, 4 - 9, 4 - 12, and 4 - 14 show that a side-by-side comparison for lumped versus distributed modeling techniques for each loss method indicates overall better model performance for the distributed loss methods.

The one exception to this trend was for the SCS Curve Number method. For both initial condition approaches, the regression analyses for peak flow rate and runoff volume initially showed that the distributed SCS Curve Number method performed better than the lumped version. The coefficients of determination for optimized and non-optimized initial conditions had peak flow coefficients of determination of 0.7597 and 0.8250, respectively, compared to the lumped parameter values of 0.6193 and 0.7613, respectively. However, the time to peak analysis for the distributed SCS Curve Number method was so poor ($R^2 = 0.1808$) that it lowered its composite R^2 value to rank last in terms of model performance. Also, while the distributed method performed the most poorly, the lumped model did not perform well either, falling below the $R^2 = 0.5$ with a coefficient of determination value of 0.4732. This outcome is a result of the SCS Curve Number method not being designed to simulate multiple precipitation events. The method should only be used to simulate single storms, and the curve numbers should be adjusted to simulate any subsequent precipitation events (Woodward, 1999).

5.3 General Conclusions

Hydrologic modeling requires the use of reliable input data and modeling parameters and techniques to produce an accurate representation of rainfall runoff. This research sought to generate reliable hydrologic loss parameters based on physical soil data and to not rely on calibration techniques. Three different runoff methods were analyzed at two different soil depths using both lumped and distributed modeling techniques. The results show that the more physically based techniques that rely on more physical soil property information were able to accurately predict runoff hydrographs when compared to the observed data.

The influence of soil depth on the analysis was also considered. For the physically based loss methods of Deficit and Constant and Green and Ampt, the role of soil depth showed a trend indicating a more accurate runoff hydrograph result produced from the shallower 1-foot soil depth parameters than the deeper 3-foot soil depth parameters. This is due to the influence of deeper soil textures altering the parameter values for each method when in reality these deeper soils do not impact the runoff generated within a watershed. While this trend is slight, it is also unanimous for the methods in this study.

The impact of distributed modeling parameters was also shown through this study. The distributed modeling parameters were able to produce more accurate results than the lumped counterpart for all methods except one. The only method of underperformance by the distributed modeling techniques was for the time of peak calculation for the SCS Curve Number method. This result suggests that the ability of distributed modeling to account for spatial variability in soil properties and loss methods will significantly improve the results generated through hydrologic modeling.

5.4 Future Research Opportunities

Several opportunities to the analysis procedure were identified during the course of this study. The first is the scope of the study area. This analysis produced promising results for the Salt Creek Basin, but this basin in southeast Nebraska has very similar soil texture (Silty Loams) throughout the basin and has a very shallow and uniform slope. Further analysis is needed to determine the effectiveness of the process described in this study when applied to different terrains, different soil groupings and different climates.

All of the modeled hydrologic processes affect the simulated runoff hydrograph in different ways. For this study, the ModClark method was used for the hydrograph transform method. While the methods used to determine the times of concentration (t_c) and the storage coefficient (R) were done carefully, there will always be discrepancy between computed and observed values that can only be rectified through calibration. Although these values were the same for all modeled simulations, they may also be inaccurate for all simulations and are being compensated for by altering of the initial condition. An example of this shortcoming can be seen in Figure 4 - 2 with the ascending limb of every simulated hydrograph lagging behind the observed hydrograph by a few hours. While the runoff volumes for these simulations match the observed data, the overall shape could be improved by obtaining calibrated t_c and R values.

Only a 2,000 meter grid cell scheme was used generate distributed runoff hydrographs and compare to that of the traditional lumped approach. Further research could be done to test the impact of more discretization moving to a 100 meter or even a 10 meter grid cell size. There are potential computational issues in moving to a smaller grid resolution, namely computation time, but there may be an even better quality result if the grid-based framework is further divided.

The influence of the initial condition showed significant influence on the quality and accuracy. The Green and Ampt method showed the most significant sensitivity with significant difference in peak flow and runoff volume occurring with only a single percentage point adjustment in the initial water content. A potential solution to this issue as well as similar issues dealing with the Deficit and Constant method is to begin the simulations several weeks before the precipitation event of interest. Doing so will require more data and other modeling techniques to account for other hydrologic processes such as evapotranspiration and groundwater interaction, but doing so should result in a more consistent and fair outcome with regard to initial condition influence. Also, the initial abstraction adjustments made to the SCS Curve Number method during the optimized initial condition simulations resulted in incorrect hydrograph shape with significant dampening on the first hydrograph peak in order to match runoff volumes. Another analysis should be done that isolates the precipitation event of interest and stops the simulation before a secondary precipitation event begins. Doing so would result in a more accurate time to peak calculation for this runoff method.

References

Anderson, R. M., Koren, V. I., & Reed, S. M. (2006). Using SSURGO data to improve Sacramento Model a priori parameter estimates. *Journal of Hydrology*, *320*(1), 103-116.

Andreassian, V., Hall, A., Chahinian, N., & Schaake, J. (2006). Large sample basin experiments for hydrological model parameterization: results of the Model Parameter Experiment (MOPEX). *Large sample basin experiments for hydrological model parameterization: results of the Model Parameter Experiment (MOPEX).*

Ao, T., Ishidaira, H., Takeuchi, K., Kiem, A. S., Yoshitari, J., Fukami, K., & Magome, J. (2006). Relating BTOPMC model parameters to physical features of MOPEX basins. *Journal of Hydrology*, *320*(1), 84-102.

Bárdossy, A. (2007). Calibration of hydrological model parameters for ungauged catchments. *Hydrology and Earth System Sciences Discussions*, *11*(2), 703-710.

Baumann, C. A., & Halaseh, A. A. (2011). Utilizing Interfacing Tools for GIS, HEC-GeoHMS, HEC-GeoRAS, and ArcHydro. In *World Environmental and Water Resources Congress 2011: Bearing Knowledge for Sustainability* (pp. 1953-1962).

Beven, K. (1993). Prophecy, reality and uncertainty in distributed hydrological modelling. *Advances in water resources*, *16*(1), 41-51.

Beven, K. J., Freer, J., Hankin, B., & Schulz, K. (2000). The use of generalised likelihood measures for uncertainty estimation in high order models of environmental systems. *Nonlinear and nonstationary signal processing*, 115-151.

Bradley, C. M. (2003). Effects of soil data resolution on modeling results using physically based rainfall-runoff model. Master's Thesis, University of Arizona

Brodnicki, E. C. (1983). *An Assessment of Cultural Resources in the Salt Creek Basin, Butler, Cass, Lancaster, Saunders, and Seward Counties, Nebraska*. CORPS OF ENGINEERS OMAHA NE.

Burgess, J. L., & Worthen, E. L. (1908). *Soil survey of Lancaster County, Nebraska*. US Government Printing Office.

Butts, M. B., Payne, J. T., Kristensen, M., & Madsen, H. (2004). An evaluation of the impact of model structure on hydrological modelling uncertainty for streamflow simulation. *Journal of Hydrology*, *298*(1), 242-266.

Chow, V. T. (1959). *Open channel hydraulics*. McGraw-Hill Book Company, Inc; New York.

Chow, V. T., Maidment, D. R., & Mays, L. W. (1988). Applied hydrology, 572 pp. *Editions McGraw-Hill, New York*.

Clark, C. O. (1945). Storage and the unit hydrograph. In *Proceedings of the American Society of Civil Engineers* (Vol. 69, No. 9, pp. 1333-1360). ASCE

Cronshey, R. (1986). *Urban hydrology for small watersheds*. US Dept. of Agriculture, Soil Conservation Service, Engineering Division.

Du, F., Zhu, A. X., Band, L., & Liu, J. (2015). Soil property variation mapping through data mining of soil category maps. *Hydrological Processes*, *29*(11), 2491-2503.

Duan, Q., Schaake, J., Andreassian, V., Franks, S., Goteti, G., Gupta, H. V., ... & Hogue, T. (2006). Model Parameter Estimation Experiment (MOPEX): An overview of science strategy and major results from the second and third workshops. *Journal of Hydrology*, *320*(1), 3-17.

ESRI 2011. ArcGIS Desktop: Release 10. Redlands, CA: Environmental Systems Research Institute.

Ficklin, D. L., & Zhang, M. (2012). A comparison of the curve number and green-ampt models in an agricultural watershed. *Transactions of the ASABE*, *56*(1), 61-69

Ficklin, D. L., Luo, Y., Zhang, M., & Gatzke, S. E. (2014). The use of soil taxonomy as a soil type identifier for the Shasta Lake Watershed using SWAT. *Transactions of the ASABE*, *57*(3), 71

Freyberg, D. L., Reeder, J. W., Franzini, J. B., & Remson, I. (1980). Application of the Green-Ampt Model to infiltration under time-dependent surface water depths. *Water Resources Research*, *16*(3), 517-528.

Gan, T. Y., & Burges, S. J. (2006). Assessment of soil-based and calibrated parameters of the Sacramento model and parameter transferability. *Journal of Hydrology*, *320*(1), 117-131

Gatzke, S. E., Beaudette, D. E., Ficklin, D. L., Luo, Y., & O'Geen, A. T. (2011). Aggregation strategies for SSURGO data: effects on SWAT soil inputs and hydrologic outputs. *Soil Science Society of America Journal*, *75*(5), 1908-1921.

Green, W. H., & Ampt, G. A. (1911). Studies on Soil Physics. *The Journal of Agricultural Science*, *4*(01), 1-24.

Gupta, H. V., Perrin, C., Blöschl, G., Montanari, A., Kumar, R., Clark, M., & Andréassian, V. (2014). Large-sample hydrology: a need to balance depth with breadth. *Hydrology and Earth System Sciences*, *18*(2), 463.

Hjelmfelt Jr, A. T. (1991). Investigation of curve number procedure. *Journal of Hydraulic Engineering*, *117*(6), 725-737.

Homer, C.G., Dewitz, J.A., Yang, L., Jin, S., Danielson, P., Xian, G., Coulston, J., Herold, N.D., Wickham, J.D., and Megown, K., (2015), Completion of the 2011 National Land Cover Database for the conterminous United States-Representing a decade of land cover change information. *Photogrammetric Engineering and Remote Sensing*, v. 81, no. 5, p. 345-354. Received from https://www.mrlc.gov/nlcd11_data.php

Hydrologic Engineering Center. (2000). *Hydrologic Modeling System HEC-GMS Technical Reference Manual.* Davis, CA: U.S. Army Corps of Engineers.

Hydrologic Engineering Center. (2010). *Hydrologic Modeling System HEC-HMS Release Notes Version 3.5.* Davis, CA: U.S. Army Corps of Engineers.

Hydrologic Engineering Center. (2013). *HEC-GeoHMS Geospatial Hydrologic Modeling Extension User's Manual version 10.1*. Davis, CA: U.S. Army Corps of Engineers.

Hydrologic Engineering Center. (2016). *Hydrologic Modeling System HEC-HMS User's Manual Version 4.2.* Davis, CA: U.S. Army Corps of Engineers.

Jones, J. A. A. (2014). *Global hydrology: processes, resources and environmental management*. Routledge.

Kling, H., & Gupta, H. (2009). On the development of regionalization relationships for lumped watershed models: The impact of ignoring sub-basin scale variability. *Journal of Hydrology*, *373*(3), 337-351.

Koren, V. I., Smith, M., Wang, D., & Zhang, Z. (2000). 2.16 USE OF SOIL PROPERTY DATA IN THE DERIVATION OF CONCEPTUAL RAINFALL-RUNOFF MODEL PARAMETERS

Li, H., Zhang, Y., & Zhou, X. (2015). Predicting surface runoff from catchment to large region. *Advances in Meteorology*, *2015*.

Li, R., Zhu, A. X., Song, X., Li, B., Pei, T., & Qin, C. (2012). Effects of spatial aggregation of soil spatial information on watershed hydrological modelling. *Hydrological Processes*, *26*(9), 1390-1404.

Livneh, B., Kumar, R., & Samaniego, L. (2015). Influence of soil textural properties on hydrologic fluxes in the Mississippi river basin. *Hydrological Processes*, *29*(21), 4638-4655.

Luo, Y., Ficklin, D. L., & Zhang, M. (2012). Approaches of soil data aggregation for hydrologic simulations. *Journal of hydrology*, *464*, 467-476.

Ma, Y., Feng, S., Su, D., Gao, G., & Huo, Z. (2010). Modeling water infiltration in a large layered soil column with a modified Green–Ampt model and HYDRUS-1D. *Computers and Electronics in Agriculture*, *71*, S40-S47.

Madsen, H. (2003). Parameter estimation in distributed hydrological catchment modelling using automatic calibration with multiple objectives. *Advances in water resources*, *26*(2), 205-216.

Maidment, D. R. (1993). *Handbook of hydrology* (Vol. 1). New York: McGraw-Hill.

Maidment, D. R. (2002). *Arc Hydro: GIS for water resources* (Vol. 1). ESRI, Inc.

Malone, R. W., Yagow, G., Baffaut, C., Gitau, M. W., Qi, Z., Amatya, D. M., ... & Green, T. R. (2015). Parameterization guidelines and considerations for hydrologic models. *Trans. ASABE*, *58*(6), 1681-1703.

Manning, R., Griffith, J. P., Pigot, T. F., & Vernon-Harcourt, L. F. (1890). *On the flow of water in open channels and pipes*.

McCarthy, G. T. (1938). The Unit Hydrograph and Flood Routing, Unpublished Manuscript, presented at a conference of the North Atlantic Division, U.S. Army Corps of Engineers, June 24, 1938

Merwade, V. (2012). Downloading SSURGO Soil Data from Internet. *Purdue University*.

Merz, R., & Blöschl, G. (2004). Regionalisation of catchment model parameters. *Journal of hydrology*, *287*(1), 95-123.

Mishra, S. K., & Singh, V. (2013). *Soil conservation service curve number (SCS-CN) methodology* (Vol. 42). Springer Science & Business Media.

Moreda, F., Koren, V., Zhang, Z., Reed, S., & Smith, M. (2006). Parameterization of distributed hydrological models: learning from the experiences of lumped modeling. *Journal of Hydrology*, *320*(1), 218-237.

Mosley, M. P. (1981). Delimitation of New Zealand hydrologic regions. *Journal of Hydrology*, *49*(1-2), 173-192.

Muleta, M. K., Nicklow, J. W., & Bekele, E. G. (2007). Sensitivity of a distributed watershed simulation model to spatial scale. *Journal of Hydrologic Engineering*, *12*(2), 163-172.

Molnar, D. K., & Julien, P. Y. (2000). Grid-size effects on surface runoff modeling. *Journal of Hydrologic Engineering*, *5*(1), 8-16.

Nash, J. E. (1959). A note on the Muskingum flood routing method. *J. Geophys. Res*, *64*(8), 1053-1056.

National Weather Service. (2017). Precipitation Shapefile Download. Retrieved from http://www.srh.noaa.gov/ridge2/RFC_Precip/

Ogden, F. L., Garbrecht, J., DeBarry, P. A., & Johnson, L. E. (2001). GIS and distributed watershed models. II: Modules, interfaces, and models. *Journal of Hydrologic Engineering*, *6*(6), 515-523.

Paudel, M., Nelson, E. J., & Scharffenberg, W. (2009). Comparison of lumped and quasi-distributed Clark runoff models using the SCS curve number equation. *Journal of Hydrologic Engineering*, *14*(10), 1098-1106.

Paudel, M. (2010). An examination of distributed hydrologic modeling methods as compared with traditional lumped parameter approaches. A Dissertation, Brigham Young University.

Paudel, M., Nelson, E. J., Downer, C. W., & Hotchkiss, R. (2011). Comparing the capability of distributed and lumped hydrologic models for analyzing the effects of land use change. *Journal of Hydroinformatics*, *13*(3), 461-473.

Post, D. A., Jones, J. A., & Grant, G. E. (1998). An improved methodology for predicting the daily hydrologic response of ungauged catchments. *Environmental modelling & software*, *13*(3), 395-403

Rawls, W. J., Brakensiek, D. L., & Miller, N. (1983). Green-Ampt infiltration parameters from soils data. *Journal of hydraulic engineering*, *109*(1), 62-70.

Reed, S., Koren, V., Smith, M., Zhang, Z., Moreda, F., Seo, D. J., & Participants, D. M. I. P. (2004). Overall distributed model intercomparison project results. *Journal of Hydrology*, *298*(1), 27-60.

Reinartz, D. J. (2016, September). Parameterization of Green & Ampt Infiltration Parameters for Use in the GSSHA Distributed Rainfall Runoff Model. In *2016 10th International Drainage Symposium Conference, 6-9 September 2016, Minneapolis, Minnesota* (pp. 1-9). American Society of Agricultural and Biological Engineers.

Sabol, G. V. (1988). Clark unit hydrograph and R-parameter estimation. *Journal of Hydraulic Engineering*, *114*(1), 103-111.

Saxton, K. E., & Rawls, W. J. (2006). Soil water characteristic estimates by texture and organic matter for hydrologic solutions. *Soil science society of America Journal*, *70*(5), 1569-1578.

Soil Survey Staff, Natural Resources Conservation Service, United States Department of Agriculture. (2016). *Web Soil Survey.* Accessed 02/24/16. Retrieved from https://websoilsurvey.nrcs.usda.gov/.

Sui, D. Z., & Maggio, R. C. (1999). Integrating GIS with hydrological modeling: practices, problems, and prospects. *Computers, environment and urban systems*, *23*(1), 33-51.

Tung, Y. K. (1985). River flood routing by nonlinear Muskingum method. *Journal of hydraulic engineering*, *111*(12), 1447-1460.

U.S. Army Corps of Engineers. (1978). *Reservoir Regulation Manual, 10 Salt Creek Dams and Lakes, Salt Creek and Tributaries, Nebraska*. U.S. Army Corps of Engineers. Omaha, NE

U.S. Department of Agriculture. (2017) *National soil survey handbook, title 430-VI*. U.S. Department of Agriculture, Natural Resources Conservation Service. Retrieved from http://www.nrcs.usda.gov/wps/portal/nrcs/detail/soils/ref/?cid=nrcs142p2_054242

USGS. (2016). United States Geological Survey National Elevation Dataset. *The National Map.* Retrieved from http://nationalmap.gov/elevation.html

Van Mullem, J. A. (1991). Runoff and peak discharges using Green-Ampt infiltration model. *Journal of Hydraulic Engineering*, *117*(3), 354-370.

Vandewiele, G. L., & Elias, A. (1995). Monthly water balance of ungauged catchments obtained by geographical regionalization. *Journal of hydrology*, *170*(1-4), 277-291.

Vieux, B. E. (2001). *Distributed Hydrologic Modeling Using GIS.* Springer Netherlands.

Wagener, T., & Wheater, H. S. (2006). Parameter estimation and regionalization for continuous rainfall-runoff models including uncertainty. *Journal of hydrology*, *320*(1), 132-154.

Wang, X., & Melesse, A. M. (2006). Effects of STATSGO and SSURGO as inputs on SWAT model's snowmelt simulation1. *Journal of the American Water Resources Association*, *42*(5), 1217.

Woodward, D. E., Hawkins, R. H., Hjelmmfelt Jr, A. T., VanMullen, J. E., & Quan, Q. D. (1999). Curve Number Method; Origins, applications and limitations (en línea): United States Department of Agriculture (USDA).

Woodward, D. E., Hawkins, R. H., Jiang, R., Hjelmfelt, Jr, A. T., Van Mullem, J. A., & Quan, Q. D. (2003). Runoff curve number method: examination of the initial abstraction ratio. In *World Water & Environmental Resources Congress 2003* (pp. 1-10).

Wurbs, R. A., & James, W. P. (2002). *Water resources engineering*. Prentice Hall.

Xian, G., Homer, C., Dewitz, J., Fry, J., Hossain, N., and Wickham, J., (2011). The change of impervious surface area between 2001 and 2006 in the conterminous United States. *Photogrammetric Engineering and Remote Sensing*, Vol. 77(8): 758-762. Retrieved from https://www.mrlc.gov/nlcd11_data.php

Zema, D. A., Labate, A., Martino, D., & Zimbone, S. M. (2017). Comparing Different Infiltration Methods of the HEC-HMS Model: The Case Study of the Mésima Torrent (Southern Italy). *Land Degradation & Development*, *28*(1), 294-308.

Zhang, Z., Koren, V., Reed, S., Smith, M., & Moreda, F. (2006). Comparison of simulation results using SSURGO-based and STATSGO-based parameters in a distributed hydrologic model. In *3rd Federal Interagency Hydrologic Modeling Conference, Reno, NV*.

Zhang, Z., Koren, V., Reed, S., Smith, M., Zhang, Y., Moreda, F., & Cosgrove, B. (2012). SAC-SMA a priori parameter differences and their impact on distributed hydrologic model simulations. *Journal of hydrology*, *420*, 216-227.

Appendix A – Model Development Tables and Figures

Terrain Pre-Processing Raster Datasets

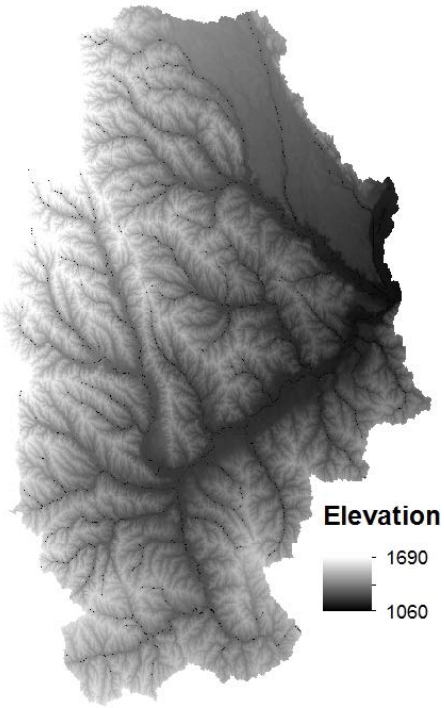

Figure A - 1. Raw DEM for Salt Creek Basin

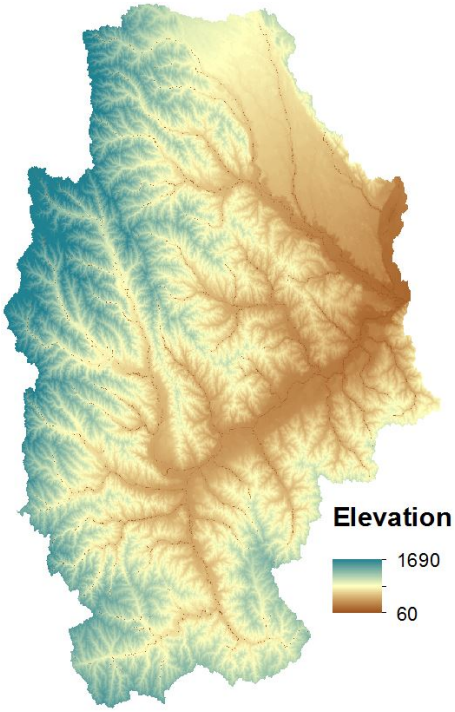

Figure A - 2. Burn Streams Grid

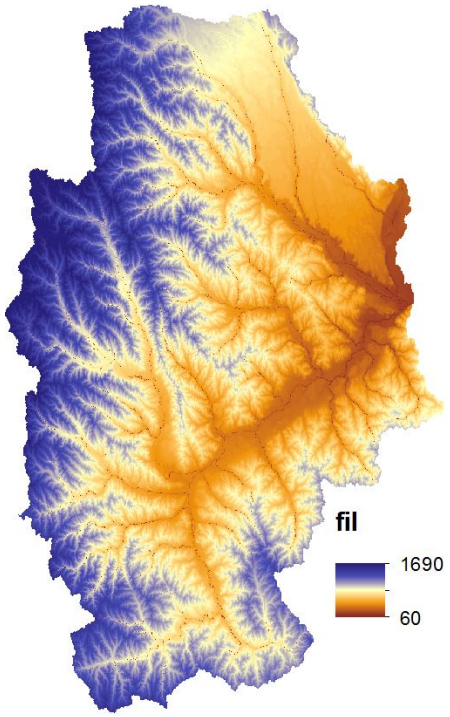

Figure A - 3. "Fil" - Fill Sinks Grid

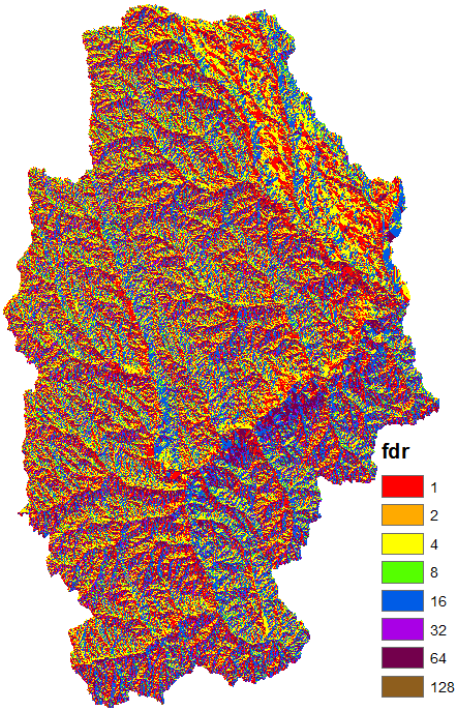

Figure A - 4. "Fdr" - Flow Direction Grid

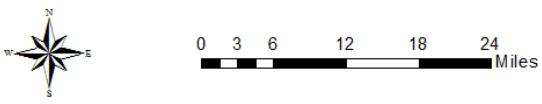

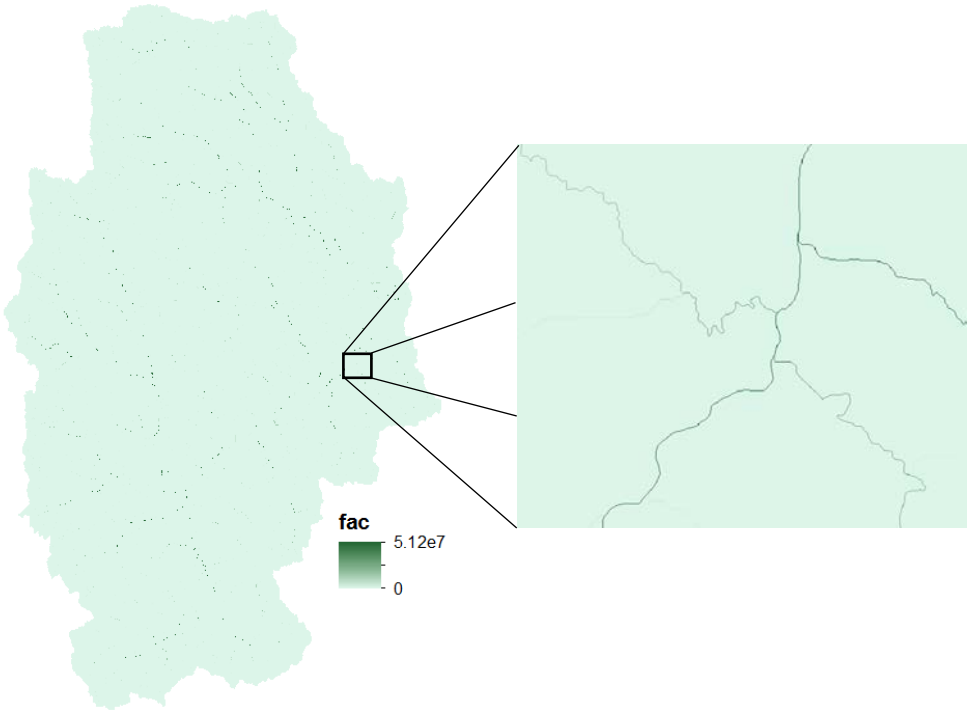

Figure A - 5. "Fac" - Flow Accumulation Grid

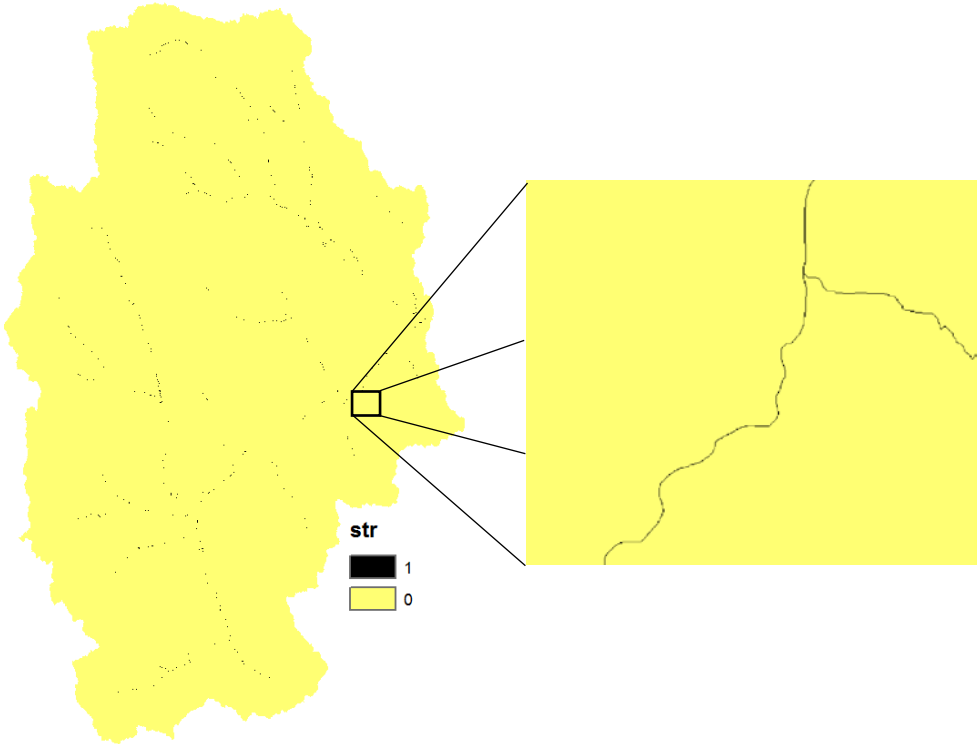

Figure A - 6. "Str" - Stream Definition Grid

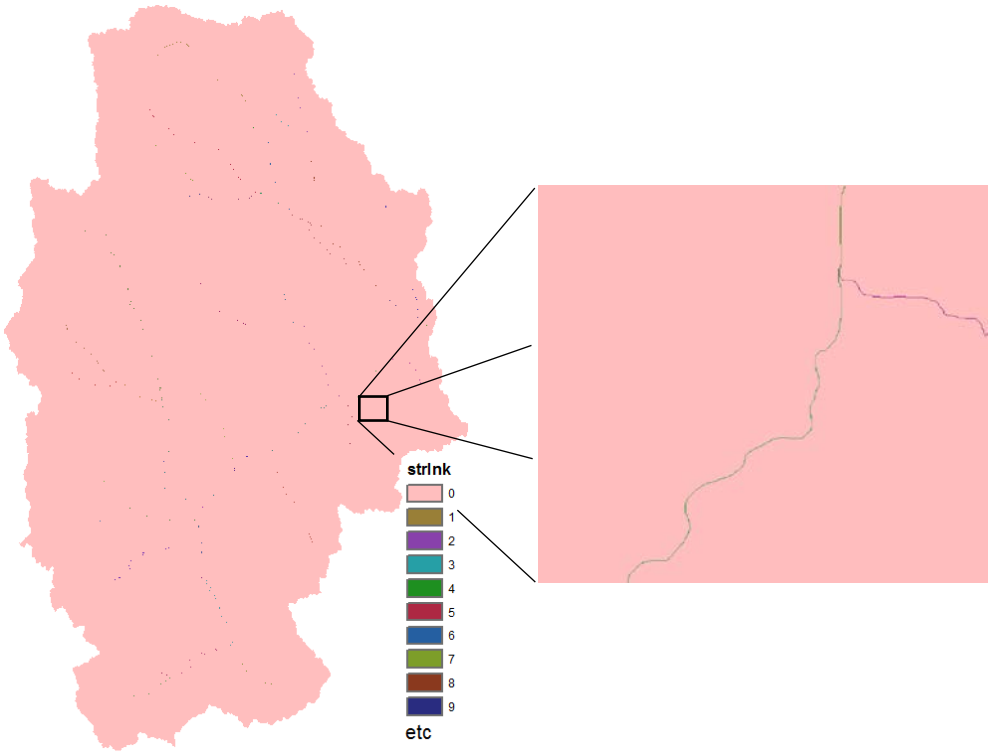

Figure A - 7. "StrLnk" - Stream Link Grid

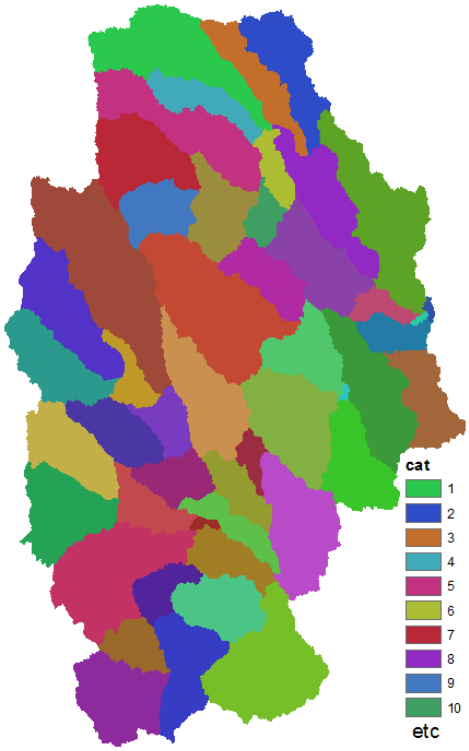

Figure A - 8. "Cat" - Catchment Grid

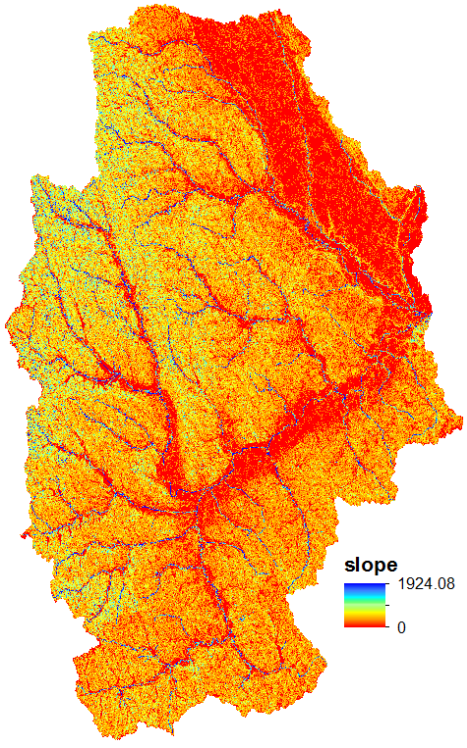

Figure A - 9. "Slope" - Slope Grid

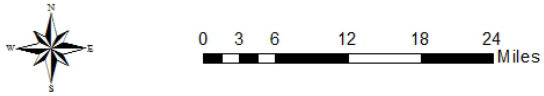

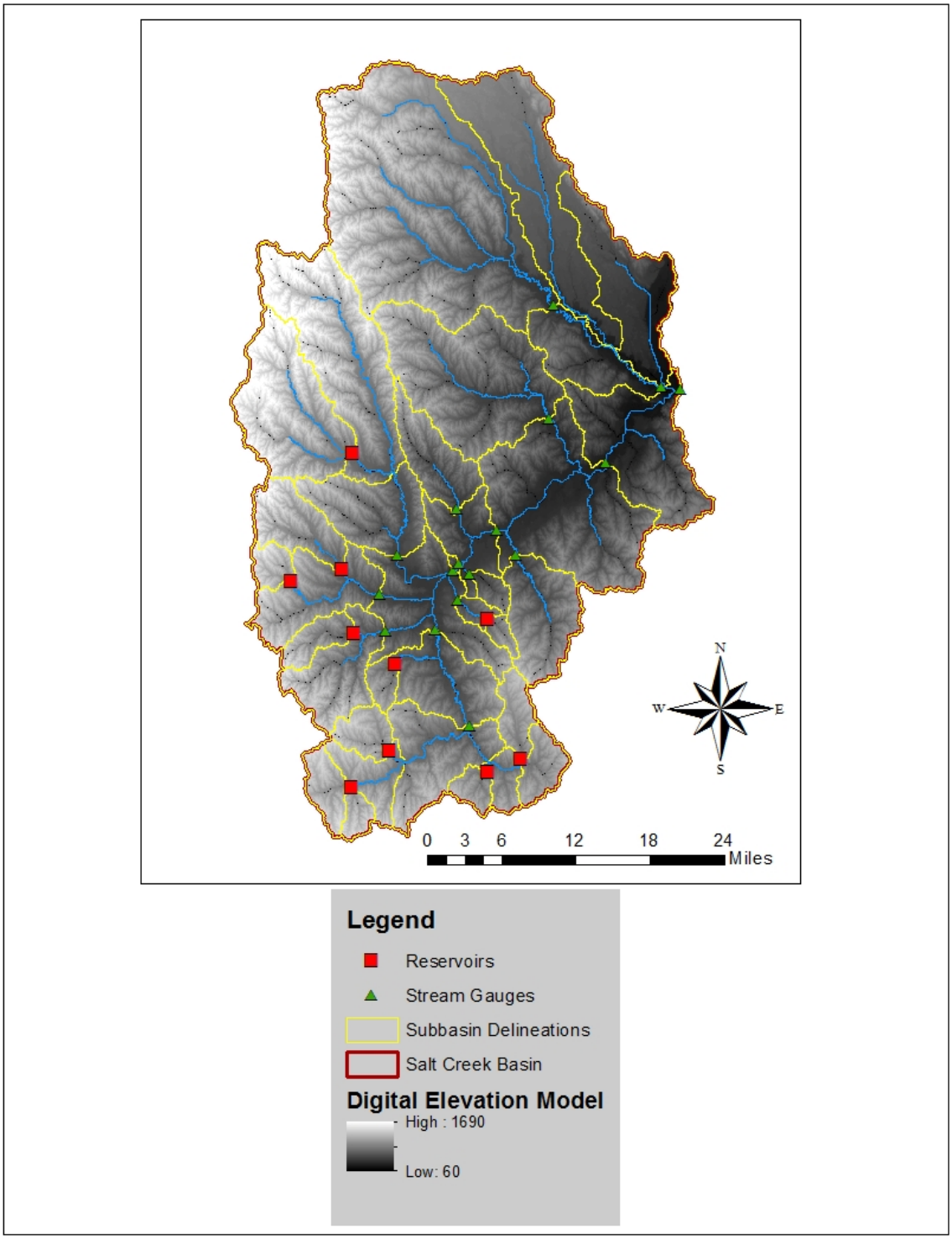

Figure A - 10. Final Subbasin Layout for Salt Creek Basin

Table A - 1. Subbasin Names and Parameters for Salt Creek Basin

Subbasin	Area		Basin Slope	Elevation			Longest Flow Path	
				Max	Min	Centroid	Length	Slope
	ac	mi^2	%	ft	ft	ft	ft	%
Antelope Cr abv ACNE	3,687	6	4.78	1348.1	124.6	1207.0	25,344	4.83
Clear Cr abv ASNE	41,349	65	2.45	1344.8	23.0	1161.1	129,450	1.02
Deadmans Run ab DRNE	4,485	7	5.38	1367.8	111.5	1197.2	28,953	4.34
Haines Br abv HBNE	26,811	42	8.25	1528.5	147.6	1275.9	89,316	1.55
Hickman Br abv SC08	10,720	17	5.42	1453.0	223.0	1295.6	35,200	3.49
Hickman Br abv SC09	7,324	11	5.69	1410.4	196.8	1269.4	33,174	3.66
Little Salt abv LSNE	21,543	34	7.81	1505.5	108.2	1200.5	84,135	1.66
Middle Cr abv MCNE	30,129	47	6.67	1466.2	131.2	1312.0	95,734	1.39
North Oak Creek	70,296	110	9.08	1685.9	160.7	1371.0	192,048	0.79
Oak Cr abv OCNE	31,555	49	6.51	1535.0	114.8	1246.4	89,769	1.58
Olive Br abv SC02	10,563	17	5.90	1492.4	1275.9	1348.1	40,803	0.53
Olive Br abv SC04	13,401	21	6.30	1495.7	223.0	1338.2	62,728	2.03
Rock Cr abv RCNE	76,560	120	7.03	1548.2	1089.0	1223.4	140,532	0.33
Salt Cr abv GWNE	83,921	131	4.83	1371.0	1043.0	1128.3	95,209	0.34
Salt Cr abv LCNE	602	1	6.29	1262.8	111.5	1167.7	8,843	13.02
Salt Creek abv ASNE	50,260	79	6.04	1341.5	23.0	1098.8	120,588	1.09
Salt Creek abv LFNE	40,016	63	5.07	1439.9	1095.5	1171.0	82,003	0.42
Salt Creek abv PBNE	28,720	45	5.29	1407.1	124.6	1177.5	96,678	1.33
Salt Creek abv RONE	33,117	52	5.93	1492.4	167.3	1321.8	104,857	1.26
Salt Creek abv SLNE	18,627	29	4.53	1364.5	72.2	1134.9	55,302	2.34
SC02 - Olive Creek	5,032	8	6.93	1508.8	1295.6	1420.2	26,399	0.81
SC04 - Bluestem	10,153	16	6.12	1482.6	265.7	1423.5	37,623	3.23
SC08 - Wagon Train	10,081	16	4.79	1456.3	255.8	1348.1	47,768	2.51
SC09 - Stagecoach	5,945	9	6.34	1436.6	226.3	1302.2	26,920	4.50
SC10 - Yankee Hill	5,486	9	6.47	1430.1	200.1	1351.4	26,297	4.68
SC12 - Conestoga	9,557	15	8.11	1528.5	193.5	1302.2	53,819	2.48
SC13 - Twin Lakes	6,653	10	7.89	1558.0	291.9	1459.6	31,231	4.05
SC14 - Pawnee	20,839	33	8.69	1594.1	1203.8	1377.6	76,481	0.51
SC17 - Holmes	3,344	5	6.90	1426.8	213.2	1321.8	25,271	4.80
SC18 - Branched Oak	52,600	82	9.16	1659.7	1236.6	1400.6	101,451	0.42
Silver Creek	67,391	105	1.82	1344.8	45.9	1230.0	185,011	0.70
Stevens Cr abv SCNE	30,301	47	5.75	1459.6	98.4	1282.5	92,944	1.46
Wahoo Cr abv ITNE	173,412	271	6.74	1633.4	82.0	1266.1	211,702	0.73
Wahoo Creek abv ASNE	25,267	39	4.51	1298.9	23.0	1161.1	114,565	1.11

Appendix B – Hydrologic Parameter Calculations

Table B - 1. TR-55 Time of Concentration Calculations for Subbasins in Salt Creek Basin

Subbasin	Sheet Flow $T_t = \frac{0.007(nL)^{0.8}}{(P_2)^{0.5}s^{0.4}}$				Shallow Concentrated Flow For U: $V = 16.1345s^{0.5}$ For P: $V = 20.3282s^{0.5}$ $T_t = \frac{L}{3600V}$				Channel Flow $V = \frac{1.49}{n}R^{2/3}s^{1/2}$ $T_t = \frac{L}{3600V}$				Time of Concentration	
Haines Br abv HBNE	n	Manning's n		0.24		Surface Type	(P/U)	P	A	Cross-section Area	ft2	12	Sheet Flow Tt	0.15
	L	Flow Length	(ft)	100	L	Flow Length	(ft)	8932	P	Wetted Perimeter	(ft)	11		
	P2	2-Yr 24-hr Rain	(in)	2.75	s	Land Slope	(ft/ft)	0.08	R	Hydraulic Radius	(ft)	1.0909	Shallow Conc Flow Tt	0.42
	s	Land Slope	(ft/ft)	0.08	V	Flow Velocity	(ft/s)	5.84	s	Channel Slope	(ft/ft)	0.0178		
									n	Manning's n		0.035	Channel Flow Tt	3.71
									V	Flow Velocity	(ft/s)	6.019		
									L	Flow Length	(ft)	80284		
	Sheet Flow Tt		**(hr)**	**0.15**	**Shallow Conc Flow Tt**		**(hr)**	**0.42**	**Channel Flow Tt**		**(hr)**	**3.71**	**4.28 hrs**	
Hickman Br abv SC08	n	Manning's n		0.24		Surface Type	(P/U)	P	A	Cross-section Area	ft2	6	Sheet Flow Tt	0.17
	L	Flow Length	(ft)	100	L	Flow Length	(ft)	2464	P	Wetted Perimeter	(ft)	5		
	P2	2-Yr 24-hr Rain	(in)	2.75	s	Land Slope	(ft/ft)	0.05	R	Hydraulic Radius	(ft)	1.2	Shallow Conc Flow Tt	0.14
	s	Land Slope	(ft/ft)	0.05	V	Flow Velocity	(ft/s)	4.73	s	Channel Slope	(ft/ft)	0.0138		
									n	Manning's n		0.04	Channel Flow Tt	1.83
									V	Flow Velocity	(ft/s)	4.941		
									L	Flow Length	(ft)	32636		
	Sheet Flow Tt		**(hr)**	**0.17**	**Shallow Conc Flow Tt**		**(hr)**	**0.14**	**Channel Flow Tt**		**(hr)**	**1.83**	**2.15 hrs**	
Hickman Br abv SC09	n	Manning's n		0.24		Surface Type	(P/U)	P	A	Cross-section Area	ft2	8	Sheet Flow Tt	0.17
	L	Flow Length	(ft)	100	L	Flow Length	(ft)	4313	P	Wetted Perimeter	(ft)	9		
	P2	2-Yr 24-hr Rain	(in)	2.75	s	Land Slope	(ft/ft)	0.06	R	Hydraulic Radius	(ft)	0.8889	Shallow Conc Flow Tt	0.25
	s	Land Slope	(ft/ft)	0.06	V	Flow Velocity	(ft/s)	4.85	s	Channel Slope	(ft/ft)	0.0138		
									n	Manning's n		0.04	Channel Flow Tt	1.97
									V	Flow Velocity	(ft/s)	4.045		
									L	Flow Length	(ft)	28762		
	Sheet Flow Tt		**(hr)**	**0.17**	**Shallow Conc Flow Tt**		**(hr)**	**0.25**	**Channel Flow Tt**		**(hr)**	**1.97**	**2.39 hrs**	

Subbasin	Sheet Flow $T_t = \frac{0.007(nL)^{0.8}}{(P_2)^{0.5}s^{0.4}}$				Shallow Concentrated Flow For U: $V = 16.1345s^{0.5}$ For P: $V = 20.3282s^{0.5}$ $T_t = \frac{L}{3600V}$				Channel Flow $V = \frac{1.49}{n}R^{2/3}s^{1/2}$ $T_t = \frac{L}{3600V}$				Time of Concentration	
Little Salt abv LSNE	n	Manning's n		0.24		Surface Type	(P/U)	P	A	Cross-section Area	ft2	16	Sheet Flow Tt	0.15
	L	Flow Length	(ft)	100	L	Flow Length	(ft)	8413	P	Wetted Perimeter	(ft)	15		
	P2	2-Yr 24-hr Rain	(in)	2.75	s	Land Slope	(ft/ft)	0.08	R	Hydraulic Radius	(ft)	1.0667	Shallow Conc Flow Tt	0.41
	s	Land Slope	(ft/ft)	0.08	V	Flow Velocity	(ft/s)	5.68	s	Channel Slope	(ft/ft)	0.0195		
									n	Manning's n		0.035	Channel Flow Tt	3.38
									V	Flow Velocity	(ft/s)	6.206		
									L	Flow Length	(ft)	75621		
	Sheet Flow Tt		**(hr)**	**0.15**	**Shallow Conc Flow Tt**		**(hr)**	**0.41**	**Channel Flow Tt**		**(hr)**	**3.38**	**3.94 hrs**	
Middle Cr abv MCNE	n	Manning's n		0.24		Surface Type	(P/U)	P	A	Cross-section Area	ft2	14	Sheet Flow Tt	0.16
	L	Flow Length	(ft)	100	L	Flow Length	(ft)	8616	P	Wetted Perimeter	(ft)	15		
	P2	2-Yr 24-hr Rain	(in)	2.75	s	Land Slope	(ft/ft)	0.07	R	Hydraulic Radius	(ft)	0.9333	Shallow Conc Flow Tt	0.46
	s	Land Slope	(ft/ft)	0.07	V	Flow Velocity	(ft/s)	5.25	s	Channel Slope	(ft/ft)	0.0185		
									n	Manning's n		0.033	Channel Flow Tt	4.12
									V	Flow Velocity	(ft/s)	5.865		
									L	Flow Length	(ft)	87018		
	Sheet Flow Tt		**(hr)**	**0.16**	**Shallow Conc Flow Tt**		**(hr)**	**0.46**	**Channel Flow Tt**		**(hr)**	**4.12**	**4.74 hrs**	
North Oak Creek	n	Manning's n		0.24		Surface Type	(P/U)	P	A	Cross-section Area	ft2	7	Sheet Flow Tt	0.14
	L	Flow Length	(ft)	100	L	Flow Length	(ft)	38410	P	Wetted Perimeter	(ft)	5		
	P2	2-Yr 24-hr Rain	(in)	2.75	s	Land Slope	(ft/ft)	0.09	R	Hydraulic Radius	(ft)	1.4	Shallow Conc Flow Tt	1.74
	s	Land Slope	(ft/ft)	0.09	V	Flow Velocity	(ft/s)	6.12	s	Channel Slope	(ft/ft)	0.0138		
									n	Manning's n		0.033	Channel Flow Tt	6.43
									V	Flow Velocity	(ft/s)	6.638		
									L	Flow Length	(ft)	153538		
	Sheet Flow Tt		**(hr)**	**0.14**	**Shallow Conc Flow Tt**		**(hr)**	**1.74**	**Channel Flow Tt**		**(hr)**	**6.43**	**8.31 hrs**	

Subbasin	Sheet Flow $T_t = \frac{0.007(nL)^{0.8}}{(P_2)^{0.5}s^{0.4}}$				Shallow Concentrated Flow For U: $V = 16.1345s^{0.5}$ For P: $V = 20.3282s^{0.5}$ $T_t = \frac{L}{3600V}$				Channel Flow $V = \frac{1.49}{n}R^{2/3}s^{1/2}$ $T_t = \frac{L}{3600V}$				Time of Concentration	
Oak Cr abv OCNE	n	Manning's n		0.24		Surface Type	(P/U)	P	A	Cross-section Area	ft2	23	Sheet Flow Tt	0.16
	L	Flow Length	(ft)	100	L	Flow Length	(ft)	10772	P	Wetted Perimeter	(ft)	26		
	P2	2-Yr 24-hr Rain	(in)	2.75	s	Land Slope	(ft/ft)	0.07	R	Hydraulic Radius	(ft)	0.8846	Shallow Conc Flow Tt	0.58
	s	Land Slope	(ft/ft)	0.07	V	Flow Velocity	(ft/s)	5.19	s	Channel Slope	(ft/ft)	0.0195		
									n	Manning's n		0.035	Channel Flow Tt	4.00
									V	Flow Velocity	(ft/s)	5.478		
									L	Flow Length	(ft)	78897		
	Sheet Flow Tt		**(hr)**	**0.16**	**Shallow Conc Flow Tt**		**(hr)**	**0.58**	**Channel Flow Tt**		**(hr)**	**4.00**	**4.74 hrs**	
Olive Br abv SC02	n	Manning's n		0.24		Surface Type	(P/U)	P	A	Cross-section Area	ft2	14	Sheet Flow Tt	0.17
	L	Flow Length	(ft)	100	L	Flow Length	(ft)	5712	P	Wetted Perimeter	(ft)	15		
	P2	2-Yr 24-hr Rain	(in)	2.75	s	Land Slope	(ft/ft)	0.06	R	Hydraulic Radius	(ft)	0.9333	Shallow Conc Flow Tt	0.32
	s	Land Slope	(ft/ft)	0.06	V	Flow Velocity	(ft/s)	4.94	s	Channel Slope	(ft/ft)	0.0140		
									n	Manning's n		0.033	Channel Flow Tt	1.90
									V	Flow Velocity	(ft/s)	5.102		
									L	Flow Length	(ft)	34990		
	Sheet Flow Tt		**(hr)**	**0.17**	**Shallow Conc Flow Tt**		**(hr)**	**0.32**	**Channel Flow Tt**		**(hr)**	**1.90**	**2.39 hrs**	
Olive Br abv SC04	n	Manning's n		0.24		Surface Type	(P/U)	P	A	Cross-section Area	ft2	8	Sheet Flow Tt	0.16
	L	Flow Length	(ft)	100	L	Flow Length	(ft)	12546	P	Wetted Perimeter	(ft)	9		
	P2	2-Yr 24-hr Rain	(in)	2.75	s	Land Slope	(ft/ft)	0.06	R	Hydraulic Radius	(ft)	0.8889	Shallow Conc Flow Tt	0.68
	s	Land Slope	(ft/ft)	0.06	V	Flow Velocity	(ft/s)	5.10	s	Channel Slope	(ft/ft)	0.0190		
									n	Manning's n		0.033	Channel Flow Tt	2.42
									V	Flow Velocity	(ft/s)	5.754		
									L	Flow Length	(ft)	50082		
	Sheet Flow Tt		**(hr)**	**0.16**	**Shallow Conc Flow Tt**		**(hr)**	**0.68**	**Channel Flow Tt**		**(hr)**	**2.42**	**3.26 hrs**	

Subbasin	Sheet Flow $T_t = \frac{0.007(nL)^{0.8}}{(P_2)^{0.5}s^{0.4}}$				Shallow Concentrated Flow For U: $V = 16.1345s^{0.5}$ For P: $V = 20.3282s^{0.5}$ $T_t = \frac{L}{3600V}$				Channel Flow $V = \frac{1.49}{n}R^{2/3}s^{1/2}$ $T_t = \frac{L}{3600V}$				Time of Concentration	
Rock Cr abv RCNE	n	Manning's n		0.24		Surface Type	(P/U)	P	A	Cross-section Area	ft2	18	**Sheet Flow Tt**	**0.16**
	L	Flow Length	(ft)	100	L	Flow Length	(ft)	22485	P	Wetted Perimeter	(ft)	18		
	P2	2-Yr 24-hr Rain	(in)	2.75	s	Land Slope	(ft/ft)	0.07	R	Hydraulic Radius	(ft)	1	**Shallow Conc Flow Tt**	**1.16**
	s	Land Slope	(ft/ft)	0.07	V	Flow Velocity	(ft/s)	5.39	s	Channel Slope	(ft/ft)	0.0228		
									n	Manning's n		0.034	**Channel Flow Tt**	**4.95**
									V	Flow Velocity	(ft/s)	6.617		
									L	Flow Length	(ft)	117947		
	Sheet Flow Tt		**(hr)**	**0.16**	**Shallow Conc Flow Tt**		**(hr)**	**1.16**	**Channel Flow Tt**		**(hr)**	**4.95**	**6.27 hrs**	
Salt Cr abv GWNE	n	Manning's n		0.24		Surface Type	(P/U)	P	A	Cross-section Area	ft2	36	**Sheet Flow Tt**	**0.18**
	L	Flow Length	(ft)	100	L	Flow Length	(ft)	18090	P	Wetted Perimeter	(ft)	42		
	P2	2-Yr 24-hr Rain	(in)	2.75	s	Land Slope	(ft/ft)	0.05	R	Hydraulic Radius	(ft)	0.8571	**Shallow Conc Flow Tt**	**1.12**
	s	Land Slope	(ft/ft)	0.05	V	Flow Velocity	(ft/s)	4.47	s	Channel Slope	(ft/ft)	0.0167		
									n	Manning's n		0.035	**Channel Flow Tt**	**4.31**
									V	Flow Velocity	(ft/s)	4.964		
									L	Flow Length	(ft)	77020		
	Sheet Flow Tt		**(hr)**	**0.18**	**Shallow Conc Flow Tt**		**(hr)**	**1.12**	**Channel Flow Tt**		**(hr)**	**4.31**	**5.61 hrs**	
Salt Cr abv LCNE	n	Manning's n		0.10		Surface Type	(P/U)	P	A	Cross-section Area	ft2	8	**Sheet Flow Tt**	**0.08**
	L	Flow Length	(ft)	100	L	Flow Length	(ft)	1150	P	Wetted Perimeter	(ft)	9		
	P2	2-Yr 24-hr Rain	(in)	2.75	s	Land Slope	(ft/ft)	0.06	R	Hydraulic Radius	(ft)	0.8889	**Shallow Conc Flow Tt**	**0.06**
	s	Land Slope	(ft/ft)	0.06	V	Flow Velocity	(ft/s)	5.10	s	Channel Slope	(ft/ft)	0.0190		
									n	Manning's n		0.033	**Channel Flow Tt**	**0.37**
									V	Flow Velocity	(ft/s)	5.754		
									L	Flow Length	(ft)	7594		
	Sheet Flow Tt		**(hr)**	**0.08**	**Shallow Conc Flow Tt**		**(hr)**	**0.06**	**Channel Flow Tt**		**(hr)**	**0.37**	**0.51 hrs**	

Subbasin	Sheet Flow $T_t = \frac{0.007(nL)^{0.8}}{(P_2)^{0.5}s^{0.4}}$				Shallow Concentrated Flow For U: $V = 16.1345s^{0.5}$ For P: $V = 20.3282s^{0.5}$ $T_t = \frac{L}{3600V}$				Channel Flow $V = \frac{1.49}{n}R^{2/3}s^{1/2}$ $T_t = \frac{L}{3600V}$				Time of Concentration	
Salt Creek abv ASNE	n	Manning's n		0.24		Surface Type	(P/U)	P	A	Cross-section Area	ft2	42	Sheet Flow Tt	0.16
	L	Flow Length	(ft)	100	L	Flow Length	(ft)	18088	P	Wetted Perimeter	(ft)	50		
	P2	2-Yr 24-hr Rain	(in)	2.75	s	Land Slope	(ft/ft)	0.06	R	Hydraulic Radius	(ft)	0.84	Shallow Conc Flow Tt	1.01
	s	Land Slope	(ft/ft)	0.06	V	Flow Velocity	(ft/s)	5.00	s	Channel Slope	(ft/ft)	0.0194		
									n	Manning's n		0.032	Channel Flow Tt	4.93
									V	Flow Velocity	(ft/s)	5.774		
									L	Flow Length	(ft)	102400		
	Sheet Flow Tt		**(hr)**	**0.16**	**Shallow Conc Flow Tt**		**(hr)**	**1.01**	**Channel Flow Tt**		**(hr)**	**4.93**	**6.1 hrs**	
Salt Creek abv LFNE	n	Manning's n		0.13		Surface Type	(P/U)	P	A	Cross-section Area	ft2	30	Sheet Flow Tt	0.11
	L	Flow Length	(ft)	100	L	Flow Length	(ft)	16401	P	Wetted Perimeter	(ft)	38		
	P2	2-Yr 24-hr Rain	(in)	2.75	s	Land Slope	(ft/ft)	0.05	R	Hydraulic Radius	(ft)	0.7895	Shallow Conc Flow Tt	1.00
	s	Land Slope	(ft/ft)	0.05	V	Flow Velocity	(ft/s)	4.58	s	Channel Slope	(ft/ft)	0.0134		
									n	Manning's n		0.032	Channel Flow Tt	3.95
									V	Flow Velocity	(ft/s)	4.604		
									L	Flow Length	(ft)	65503		
	Sheet Flow Tt		**(hr)**	**0.11**	**Shallow Conc Flow Tt**		**(hr)**	**1.00**	**Channel Flow Tt**		**(hr)**	**3.95**	**5.06 hrs**	
Salt Creek abv PBNE	n	Manning's n		0.24		Surface Type	(P/U)	P	A	Cross-section Area	ft2	25	Sheet Flow Tt	0.17
	L	Flow Length	(ft)	100	L	Flow Length	(ft)	11601	P	Wetted Perimeter	(ft)	28		
	P2	2-Yr 24-hr Rain	(in)	2.75	s	Land Slope	(ft/ft)	0.05	R	Hydraulic Radius	(ft)	0.8929	Shallow Conc Flow Tt	0.69
	s	Land Slope	(ft/ft)	0.05	V	Flow Velocity	(ft/s)	4.68	s	Channel Slope	(ft/ft)	0.0190		
									n	Manning's n		0.033	Channel Flow Tt	4.09
									V	Flow Velocity	(ft/s)	5.771		
									L	Flow Length	(ft)	84977		
	Sheet Flow Tt		**(hr)**	**0.17**	**Shallow Conc Flow Tt**		**(hr)**	**0.69**	**Channel Flow Tt**		**(hr)**	**4.09**	**4.95 hrs**	

Subbasin	Sheet Flow $T_t = \frac{0.007(nL)^{0.8}}{(P_2)^{0.5}s^{0.4}}$				Shallow Concentrated Flow For U: $V = 16.1345s^{0.5}$ For P: $V = 20.3282s^{0.5}$ $T_t = \frac{L}{3600V}$				Channel Flow $V = \frac{1.49}{n}R^{2/3}s^{1/2}$ $T_t = \frac{L}{3600V}$				Time of Concentration	
Salt Creek abv RONE	n	Manning's n		0.24		Surface Type	(P/U)	P	A	Cross-section Area	ft2	46	Sheet Flow Tt	0.17
	L	Flow Length	(ft)	100	L	Flow Length	(ft)	10486	P	Wetted Perimeter	(ft)	52		
	P2	2-Yr 24-hr Rain	(in)	2.75	s	Land Slope	(ft/ft)	0.06	R	Hydraulic Radius	(ft)	0.8846	Shallow Conc Flow Tt	0.59
	s	Land Slope	(ft/ft)	0.06	V	Flow Velocity	(ft/s)	4.95	s	Channel Slope	(ft/ft)	0.0200		
									n	Manning's n		0.032	Channel Flow Tt	4.32
									V	Flow Velocity	(ft/s)	6.068		
									L	Flow Length	(ft)	94271		
	Sheet Flow Tt		**(hr)**	**0.17**	**Shallow Conc Flow Tt**		**(hr)**	**0.59**	**Channel Flow Tt**		**(hr)**	**4.32**	**5.07 hrs**	
Salt Creek abv SLNE	n	Manning's n		0.24		Surface Type	(P/U)	P	A	Cross-section Area	ft2	16	Sheet Flow Tt	0.19
	L	Flow Length	(ft)	100	L	Flow Length	(ft)	8848	P	Wetted Perimeter	(ft)	18		
	P2	2-Yr 24-hr Rain	(in)	2.75	s	Land Slope	(ft/ft)	0.05	R	Hydraulic Radius	(ft)	0.8889	Shallow Conc Flow Tt	0.57
	s	Land Slope	(ft/ft)	0.05	V	Flow Velocity	(ft/s)	4.32	s	Channel Slope	(ft/ft)	0.0182		
									n	Manning's n		0.035	Channel Flow Tt	2.43
									V	Flow Velocity	(ft/s)	5.309		
									L	Flow Length	(ft)	46353		
	Sheet Flow Tt		**(hr)**	**0.19**	**Shallow Conc Flow Tt**		**(hr)**	**0.57**	**Channel Flow Tt**		**(hr)**	**2.43**	**3.18 hrs**	
SC02 - Olive Creek	n	Manning's n		0.24		Surface Type	(P/U)	P	A	Cross-section Area	ft2	13	Sheet Flow Tt	0.16
	L	Flow Length	(ft)	100	L	Flow Length	(ft)	3168	P	Wetted Perimeter	(ft)	15		
	P2	2-Yr 24-hr Rain	(in)	2.75	s	Land Slope	(ft/ft)	0.07	R	Hydraulic Radius	(ft)	0.8667	Shallow Conc Flow Tt	0.16
	s	Land Slope	(ft/ft)	0.07	V	Flow Velocity	(ft/s)	5.35	s	Channel Slope	(ft/ft)	0.0160		
									n	Manning's n		0.035	Channel Flow Tt	1.31
									V	Flow Velocity	(ft/s)	4.895		
									L	Flow Length	(ft)	23131		
	Sheet Flow Tt		**(hr)**	**0.16**	**Shallow Conc Flow Tt**		**(hr)**	**0.16**	**Channel Flow Tt**		**(hr)**	**1.31**	**1.63 hrs**	

Subbasin	Sheet Flow $T_t = \frac{0.007(nL)^{0.8}}{(P_2)^{0.5}s^{0.4}}$				Shallow Concentrated Flow For U: $V = 16.1345s^{0.5}$ For P: $V = 20.3282s^{0.5}$ $T_t = \frac{L}{3600V}$				Channel Flow $V = \frac{1.49}{n}R^{2/3}s^{1/2}$ $T_t = \frac{L}{3600V}$				Time of Concentration	
SC04 - Bluestem	n	Manning's n		0.24		Surface Type	(P/U)	P	A	Cross-section Area	ft2	12	Sheet Flow Tt	0.16
	L	Flow Length	(ft)	100	L	Flow Length	(ft)	6020	P	Wetted Perimeter	(ft)	12		
	P2	2-Yr 24-hr Rain	(in)	2.75	s	Land Slope	(ft/ft)	0.06	R	Hydraulic Radius	(ft)	1	Shallow Conc Flow Tt	0.33
	s	Land Slope	(ft/ft)	0.06	V	Flow Velocity	(ft/s)	5.03	s	Channel Slope	(ft/ft)	0.0145		
									n	Manning's n		0.035	Channel Flow Tt	1.71
									V	Flow Velocity	(ft/s)	5.126		
									L	Flow Length	(ft)	31503		
	Sheet Flow Tt		**(hr)**	**0.16**	**Shallow Conc Flow Tt**		**(hr)**	**0.33**	**Channel Flow Tt**		**(hr)**	**1.71**	**2.2 hrs**	
SC08 - Wagon Train	n	Manning's n		0.24		Surface Type	(P/U)	P	A	Cross-section Area	ft2	16	Sheet Flow Tt	0.18
	L	Flow Length	(ft)	100	L	Flow Length	(ft)	11464	P	Wetted Perimeter	(ft)	20		
	P2	2-Yr 24-hr Rain	(in)	2.75	s	Land Slope	(ft/ft)	0.05	R	Hydraulic Radius	(ft)	0.8	Shallow Conc Flow Tt	0.72
	s	Land Slope	(ft/ft)	0.05	V	Flow Velocity	(ft/s)	4.45	s	Channel Slope	(ft/ft)	0.0180		
									n	Manning's n		0.036	Channel Flow Tt	2.10
									V	Flow Velocity	(ft/s)	4.785		
									L	Flow Length	(ft)	36203		
	Sheet Flow Tt		**(hr)**	**0.18**	**Shallow Conc Flow Tt**		**(hr)**	**0.72**	**Channel Flow Tt**		**(hr)**	**2.10**	**3 hrs**	
SC09 - Stagecoach	n	Manning's n		0.24		Surface Type	(P/U)	P	A	Cross-section Area	ft2	13	Sheet Flow Tt	0.16
	L	Flow Length	(ft)	100	L	Flow Length	(ft)	4846	P	Wetted Perimeter	(ft)	15		
	P2	2-Yr 24-hr Rain	(in)	2.75	s	Land Slope	(ft/ft)	0.06	R	Hydraulic Radius	(ft)	0.8667	Shallow Conc Flow Tt	0.26
	s	Land Slope	(ft/ft)	0.06	V	Flow Velocity	(ft/s)	5.12	s	Channel Slope	(ft/ft)	0.0152		
									n	Manning's n		0.035	Channel Flow Tt	1.28
									V	Flow Velocity	(ft/s)	4.771		
									L	Flow Length	(ft)	21974		
	Sheet Flow Tt		**(hr)**	**0.16**	**Shallow Conc Flow Tt**		**(hr)**	**0.26**	**Channel Flow Tt**		**(hr)**	**1.28**	**1.7 hrs**	

Subbasin	Sheet Flow $T_t = \frac{0.007(nL)^{0.8}}{(P_2)^{0.5}s^{0.4}}$				Shallow Concentrated Flow For U: $V = 16.1345s^{0.5}$ For P: $V = 20.3282s^{0.5}$ $T_t = \frac{L}{3600V}$				Channel Flow $V = \frac{1.49}{n}R^{2/3}s^{1/2}$ $T_t = \frac{L}{3600V}$				Time of Concentration	
SC10 - Yankee Hill	n	Manning's n		0.24		Surface Type	(P/U)	P	A	Cross-section Area	ft2	15	Sheet Flow Tt	0.16
	L	Flow Length	(ft)	100	L	Flow Length	(ft)	7363	P	Wetted Perimeter	(ft)	16	Shallow Conc Flow Tt	0.40
	P2	2-Yr 24-hr Rain	(in)	2.75	s	Land Slope	(ft/ft)	0.06	R	Hydraulic Radius	(ft)	0.9375		
	s	Land Slope	(ft/ft)	0.06	V	Flow Velocity	(ft/s)	5.17	s	Channel Slope	(ft/ft)	0.0168		
									n	Manning's n		0.035	Channel Flow Tt	0.99
									V	Flow Velocity	(ft/s)	5.286		
									L	Flow Length	(ft)	18834		
	Sheet Flow Tt		**(hr)**	**0.16**	**Shallow Conc Flow Tt**		**(hr)**	**0.40**	**Channel Flow Tt**		**(hr)**	**0.99**	**1.55 hrs**	
SC12 - Conestoga	n	Manning's n		0.24		Surface Type	(P/U)	P	A	Cross-section Area	ft2	19	Sheet Flow Tt	0.15
	L	Flow Length	(ft)	100	L	Flow Length	(ft)	16146	P	Wetted Perimeter	(ft)	21		
	P2	2-Yr 24-hr Rain	(in)	2.75	s	Land Slope	(ft/ft)	0.08	R	Hydraulic Radius	(ft)	0.9048	Shallow Conc Flow Tt	0.77
	s	Land Slope	(ft/ft)	0.08	V	Flow Velocity	(ft/s)	5.79	s	Channel Slope	(ft/ft)	0.0179		
									n	Manning's n		0.035	Channel Flow Tt	1.96
									V	Flow Velocity	(ft/s)	5.328		
									L	Flow Length	(ft)	37573		
	Sheet Flow Tt		**(hr)**	**0.15**	**Shallow Conc Flow Tt**		**(hr)**	**0.77**	**Channel Flow Tt**		**(hr)**	**1.96**	**2.88 hrs**	
SC13 - Twin Lakes	n	Manning's n		0.24		Surface Type	(P/U)	P	A	Cross-section Area	ft2	15	Sheet Flow Tt	0.15
	L	Flow Length	(ft)	100	L	Flow Length	(ft)	7495	P	Wetted Perimeter	(ft)	18		
	P2	2-Yr 24-hr Rain	(in)	2.75	s	Land Slope	(ft/ft)	0.08	R	Hydraulic Radius	(ft)	0.8333	Shallow Conc Flow Tt	0.36
	s	Land Slope	(ft/ft)	0.08	V	Flow Velocity	(ft/s)	5.71	s	Channel Slope	(ft/ft)	0.0149		
									n	Manning's n		0.035	Channel Flow Tt	1.43
									V	Flow Velocity	(ft/s)	4.602		
									L	Flow Length	(ft)	23635		
	Sheet Flow Tt		**(hr)**	**0.15**	**Shallow Conc Flow Tt**		**(hr)**	**0.36**	**Channel Flow Tt**		**(hr)**	**1.43**	**1.94 hrs**	

Subbasin	Sheet Flow $T_t = \frac{0.007(nL)^{0.8}}{(P_2)^{0.5}s^{0.4}}$				Shallow Concentrated Flow For U: $V = 16.1345s^{0.5}$ For P: $V = 20.3282s^{0.5}$ $T_t = \frac{L}{3600V}$				Channel Flow $V = \frac{1.49}{n}R^{2/3}s^{1/2}$ $T_t = \frac{L}{3600V}$				Time of Concentration	
SC14 - Pawnee	n	Manning's n		0.24		Surface Type	(P/U)	P	A	Cross-section Area	ft2	22	Sheet Flow Tt	0.14
	L	Flow Length	(ft)	100	L	Flow Length	(ft)	10707	P	Wetted Perimeter	(ft)	24		
	P2	2-Yr 24-hr Rain	(in)	2.75	s	Land Slope	(ft/ft)	0.09	R	Hydraulic Radius	(ft)	0.9167	Shallow Conc Flow Tt	0.50
	s	Land Slope	(ft/ft)	0.09	V	Flow Velocity	(ft/s)	5.99	s	Channel Slope	(ft/ft)	0.0193		
									n	Manning's n		0.035	Channel Flow Tt	3.27
									V	Flow Velocity	(ft/s)	5.581		
									L	Flow Length	(ft)	65674		
	Sheet Flow Tt		**(hr)**	**0.14**	**Shallow Conc Flow Tt**		**(hr)**	**0.50**	**Channel Flow Tt**		**(hr)**	**3.27**	**3.91 hrs**	
SC17 - Holmes	n	Manning's n		0.24		Surface Type	(P/U)	P	A	Cross-section Area	ft2	17	Sheet Flow Tt	0.16
	L	Flow Length	(ft)	100	L	Flow Length	(ft)	7581	P	Wetted Perimeter	(ft)	18		
	P2	2-Yr 24-hr Rain	(in)	2.75	s	Land Slope	(ft/ft)	0.07	R	Hydraulic Radius	(ft)	0.9444	Shallow Conc Flow Tt	0.39
	s	Land Slope	(ft/ft)	0.07	V	Flow Velocity	(ft/s)	5.34	s	Channel Slope	(ft/ft)	0.0192		
									n	Manning's n		0.035	Channel Flow Tt	0.86
									V	Flow Velocity	(ft/s)	5.678		
									L	Flow Length	(ft)	17590		
	Sheet Flow Tt		**(hr)**	**0.16**	**Shallow Conc Flow Tt**		**(hr)**	**0.39**	**Channel Flow Tt**		**(hr)**	**0.86**	**1.41 hrs**	
SC18 - Branched Oak	n	Manning's n		0.24		Surface Type	(P/U)	P	A	Cross-section Area	ft2	22	Sheet Flow Tt	0.14
	L	Flow Length	(ft)	100	L	Flow Length	(ft)	15218	P	Wetted Perimeter	(ft)	27		
	P2	2-Yr 24-hr Rain	(in)	2.75	s	Land Slope	(ft/ft)	0.09	R	Hydraulic Radius	(ft)	0.8148	Shallow Conc Flow Tt	0.69
	s	Land Slope	(ft/ft)	0.09	V	Flow Velocity	(ft/s)	6.15	s	Channel Slope	(ft/ft)	0.0102		
									n	Manning's n		0.04	Channel Flow Tt	7.29
									V	Flow Velocity	(ft/s)	3.282		
									L	Flow Length	(ft)	86134		
	Sheet Flow Tt		**(hr)**	**0.14**	**Shallow Conc Flow Tt**		**(hr)**	**0.69**	**Channel Flow Tt**		**(hr)**	**7.29**	**8.12 hrs**	

Subbasin	Sheet Flow $T_t = \frac{0.007(nL)^{0.8}}{(P_2)^{0.5}s^{0.4}}$				Shallow Concentrated Flow For U: $V = 16.1345s^{0.5}$ For P: $V = 20.3282s^{0.5}$ $T_t = \frac{L}{3600V}$				Channel Flow $V = \frac{1.49}{n}R^{2/3}s^{1/2}$ $T_t = \frac{L}{3600V}$				Time of Concentration	
Silver Creek	n	Manning's n		0.24		Surface Type	(P/U)	P	A	Cross-section Area	ft2	23	Sheet Flow Tt	0.27
	L	Flow Length	(ft)	100	L	Flow Length	(ft)	11101	P	Wetted Perimeter	(ft)	26		
	P2	2-Yr 24-hr Rain	(in)	2.75	s	Land Slope	(ft/ft)	0.02	R	Hydraulic Radius	(ft)	0.8846	Shallow Conc Flow Tt	1.12
	s	Land Slope	(ft/ft)	0.02	V	Flow Velocity	(ft/s)	2.74	s	Channel Slope	(ft/ft)	0.0110		
									n	Manning's n		0.036	Channel Flow Tt	12.07
									V	Flow Velocity	(ft/s)	4.000		
									L	Flow Length	(ft)	173810		
	Sheet Flow Tt		**(hr)**	**0.27**	**Shallow Conc Flow Tt**		**(hr)**	**1.12**	**Channel Flow Tt**		**(hr)**	**12.07**	**13.46 hrs**	
Stevens Cr abv SCNE	n	Manning's n		0.24		Surface Type	(P/U)	P	A	Cross-section Area	ft2	17	Sheet Flow Tt	0.17
	L	Flow Length	(ft)	100	L	Flow Length	(ft)	9294	P	Wetted Perimeter	(ft)	18		
	P2	2-Yr 24-hr Rain	(in)	2.75	s	Land Slope	(ft/ft)	0.06	R	Hydraulic Radius	(ft)	0.9444	Shallow Conc Flow Tt	0.53
	s	Land Slope	(ft/ft)	0.06	V	Flow Velocity	(ft/s)	4.87	s	Channel Slope	(ft/ft)	0.0192		
									n	Manning's n		0.035	Channel Flow Tt	4.09
									V	Flow Velocity	(ft/s)	5.678		
									L	Flow Length	(ft)	83549		
	Sheet Flow Tt		**(hr)**	**0.17**	**Shallow Conc Flow Tt**		**(hr)**	**0.53**	**Channel Flow Tt**		**(hr)**	**4.09**	**4.78 hrs**	
Wahoo Cr abv ITNE	n	Manning's n		0.24		Surface Type	(P/U)	P	A	Cross-section Area	ft2	28	Sheet Flow Tt	0.16
	L	Flow Length	(ft)	100	L	Flow Length	(ft)	10585	P	Wetted Perimeter	(ft)	26		
	P2	2-Yr 24-hr Rain	(in)	2.75	s	Land Slope	(ft/ft)	0.07	R	Hydraulic Radius	(ft)	1.0769	Shallow Conc Flow Tt	0.56
	s	Land Slope	(ft/ft)	0.07	V	Flow Velocity	(ft/s)	5.28	s	Channel Slope	(ft/ft)	0.0214		
									n	Manning's n		0.035	Channel Flow Tt	8.53
									V	Flow Velocity	(ft/s)	6.543		
									L	Flow Length	(ft)	201017		
	Sheet Flow Tt		**(hr)**	**0.16**	**Shallow Conc Flow Tt**		**(hr)**	**0.56**	**Channel Flow Tt**		**(hr)**	**8.53**	**9.25 hrs**	

Subbasin	Sheet Flow $T_t = \frac{0.007(nL)^{0.8}}{(P_2)^{0.5} s^{0.4}}$				Shallow Concentrated Flow For U: $V = 16.1345 s^{0.5}$ For P: $V = 20.3282 s^{0.5}$ $T_t = \frac{L}{3600V}$				Channel Flow $V = \frac{1.49}{n} R^{2/3} S^{1/2}$ $T_t = \frac{L}{3600V}$				Time of Concentration	
Wahoo Creek abv ASNE	n	Manning's n		0.24		Surface Type	(P/U)	P	A	Cross-section Area	ft2	27	**Sheet Flow Tt**	**0.19**
	L	Flow Length	(ft)	100	L	Flow Length	(ft)	10311	P	Wetted Perimeter	(ft)	34		
	P2	2-Yr 24-hr Rain	(in)	2.75	s	Land Slope	(ft/ft)	0.05	R	Hydraulic Radius	(ft)	0.7941	**Shallow Conc Flow Tt**	**0.66**
	s	Land Slope	(ft/ft)	0.05	V	Flow Velocity	(ft/s)	4.32	s	Channel Slope	(ft/ft)	0.0111		
									n	Manning's n		0.04	**Channel Flow Tt**	**8.60**
									V	Flow Velocity	(ft/s)	3.365		
									L	Flow Length	(ft)	104154		
	Sheet Flow Tt		**(hr)**	**0.19**	**Shallow Conc Flow Tt**		**(hr)**	**0.66**	**Channel Flow Tt**		**(hr)**	**8.60**	**9.45 hrs**	

$$\frac{T_c}{R} = 1.46 - 0.0867\frac{L^2}{A}$$

Table B - 2. Clark Unit Hydrograph Storage Coefficient (R) Calculations for Salt Creek Basin

Subbasin	Longest Flow Path L	Basin Area A		Time of Concentration Tc	Storage Coefficient R
	(ft)	(ac)	ft^2	(hr)	**(hr)**
Antelope Cr abv ACNE	25,344	3,687	1.61E+08	1.81	**1.62**
Clear Cr abv ASNE	129,450	41,349	1.80E+09	9.34	**14.29**
Deadmans Run ab DRNE	28,953	4,485	1.95E+08	1.85	**1.70**
Haines Br abv HBNE	89,316	26,811	1.17E+09	4.28	**4.93**
Hickman Br abv SC08	35,200	10,720	4.67E+08	2.15	**1.75**
Hickman Br abv SC09	33,174	7,324	3.19E+08	2.39	**2.06**
Little Salt abv LSNE	84,135	21,543	9.38E+08	3.94	**4.89**
Middle Cr abv MCNE	95,734	30,129	1.31E+09	4.74	**5.54**
North Oak Creek	192,048	70,296	3.06E+09	8.31	**19.98**
Oak Cr abv OCNE	89,769	31,555	1.37E+09	4.74	**4.98**
Olive Br abv SC02	40,803	10,563	4.60E+08	2.39	**2.09**
Olive Br abv SC04	62,728	13,401	5.84E+08	3.26	**3.73**
Rock Cr abv RCNE	140,532	76,560	3.33E+09	6.27	**6.62**
Salt Cr abv GWNE	95,209	83,921	3.66E+09	5.61	**4.51**
Salt Cr abv LCNE	8,843	602	2.62E+07	0.51	**0.42**
Salt Creek abv ASNE	120,588	50,260	2.19E+09	6.10	**6.90**
Salt Creek abv LFNE	82,003	40,016	1.74E+09	5.06	**4.49**
Salt Creek abv PBNE	96,678	28,720	1.25E+09	4.95	**6.10**
Salt Creek abv RONE	104,857	33,117	1.44E+09	5.07	**6.34**
Salt Creek abv SLNE	55,302	18,627	8.11E+08	3.18	**2.80**
SC02 - Olive Creek	26,399	5,032	2.19E+08	1.63	**1.38**
SC04 - Bluestem	37,623	10,153	4.42E+08	2.20	**1.86**
SC08 - Wagon Train	47,768	10,081	4.39E+08	3.00	**2.97**
SC09 - Stagecoach	26,920	5,945	2.59E+08	1.70	**1.40**
SC10 - Yankee Hill	26,297	5,486	2.39E+08	1.55	**1.28**
SC12 - Conestoga	53,819	9,557	4.16E+08	2.88	**3.36**
SC13 - Twin Lakes	31,231	6,653	2.90E+08	1.94	**1.66**
SC14 - Pawnee	76,481	20,839	9.08E+08	3.91	**4.34**
SC17 - Holmes	25,271	3,344	1.46E+08	1.41	**1.31**
SC18 - Branched Oak	101,451	52,600	2.29E+09	8.12	**7.58**
Silver Creek	185,011	67,391	2.94E+09	13.46	**29.98**
Stevens Cr abv SCNE	92,944	30,301	1.32E+09	4.78	**5.36**
Wahoo Cr abv ITNE	211,702	173,412	7.55E+09	9.25	**9.78**
Wahoo Creek abv ASNE	114,565	25,267	1.10E+09	9.45	**22.17**

Table B - 3. Muskingum Routing Parameter Calculations for Salt Creek Basin

Reach	Length	Slope	n	R	K (hr)	x	subreaches
	(ft)	(ft/ft)		(ft)	(hr)		
R250	10039	0.00199	0.032	1.00	1.34	0.25	1
R320	17844	0.00091	0.040	1.50	3.37	0.25	1
R360	11867	0.00009	0.035	2.00	5.19	0.25	1
R1010	11392	0.00132	0.035	1.50	1.56	0.25	1
R470	19499	0.00092	0.035	2.25	2.45	0.25	1
R1280	6374	0.00126	0.040	1.50	1.02	0.25	1
R1260	9272	0.00108	0.050	1.00	2.62	0.25	1
R450	24425	0.00074	0.050	1.25	7.22	0.25	1
R1410	16330	0.00241	0.040	1.75	1.71	0.25	1
R420	9972	0.00150	0.050	1.50	1.83	0.25	1
R1820	8263	0.00934	0.035	2.25	0.32	0.25	1
R1660	22150	0.00858	0.035	2.50	0.85	0.25	1
R380	12676	0.00079	0.050	0.75	5.09	0.25	1
R1550	6501	0.00776	0.040	0.50	0.87	0.25	1
R1510	15471	0.00135	0.040	0.75	3.81	0.25	1
R2080	5359	0.00541	0.050	1.00	0.68	0.25	1
R2000	4811	0.00104	0.035	1.50	0.74	0.25	1
R2170	1275	0.00008	0.035	1.75	0.65	0.25	1
R2230	9009	0.01594	0.035	2.00	0.29	0.25	1
R290	8935	0.00330	0.050	2.50	0.79	0.25	1
R2250	10549	0.00523	0.040	0.75	1.32	0.25	1
R300	21413	0.00946	0.040	1.50	1.25	0.25	1
R2510	17047	0.00099	0.050	2.25	2.95	0.25	1
R2410	25247	0.00269	0.035	0.75	3.85	0.25	1
R190	17948	0.00140	0.035	1.50	2.39	0.25	1
R110	29152	0.00098	0.045	2.50	4.24	0.25	1
R2780	10758	0.00112	0.035	1.25	1.81	0.25	1
R150	2635	0.00007	0.050	1.00	2.87	0.25	1

Table B - 4. Hydrologic Loss Parameters for Salt Creek Basin – 1-Foot Soil Depth

Subbasin	Deficit and Constant Parameters		Green and Ampt Parameters			SCS Curve Number
	Infiltration Rate	Maximum Deficit	W.F. Suction	Infiltration Rate	Porosity / Saturated Content	Curve Number
	(in/hr)	(in)	(in)	(in/hr)	(%)	AMC II
Antelope Cr abv ACNE	0.093	3.68	19.12	0.093	0.418	82
Clear Cr abv ASNE	0.377	3.26	19.65	0.377	0.444	82
Deadmans Run ab DRNE	0.095	3.51	19.58	0.095	0.418	83
Haines Br abv HBNE	0.163	2.69	19.04	0.163	0.413	78
Hickman Br abv SC08	0.105	2.57	22.02	0.105	0.424	83
Hickman Br abv SC09	0.134	2.69	21.14	0.134	0.426	82
Little Salt abv LSNE	0.145	2.71	20.52	0.145	0.425	80
Middle Cr abv MCNE	0.144	2.72	20.68	0.144	0.424	80
North Oak Creek	0.166	2.80	19.39	0.166	0.426	78
Oak Cr abv OCNE	0.146	2.79	20.56	0.146	0.427	81
Olive Br abv SC02	0.126	2.61	20.14	0.126	0.416	82
Olive Br abv SC04	0.132	2.62	20.15	0.132	0.417	82
Rock Cr abv RCNE	0.163	2.86	20.83	0.163	0.439	80
Salt Cr abv GWNE	0.144	2.77	21.61	0.144	0.436	84
Salt Cr abv LCNE	0.137	3.01	18.53	0.137	0.413	86
Salt Creek abv ASNE	0.194	2.80	21.08	0.194	0.436	82
Salt Creek abv LFNE	0.129	3.01	20.03	0.129	0.419	83
Salt Creek abv PBNE	0.129	2.70	21.63	0.129	0.427	83
Salt Creek abv RONE	0.122	2.61	21.14	0.122	0.422	82
Salt Creek abv SLNE	0.137	2.97	20.36	0.137	0.424	84
SC02 - Olive Creek	0.139	2.57	18.69	0.139	0.405	81
SC04 - Bluestem	0.102	2.41	19.93	0.102	0.405	82
SC08 - Wagon Train	0.097	2.40	21.71	0.097	0.412	82
SC09 - Stagecoach	0.128	2.47	19.74	0.128	0.405	81
SC10 - Yankee Hill	0.097	2.41	20.57	0.097	0.408	83
SC12 - Conestoga	0.127	2.53	19.20	0.127	0.403	78
SC13 - Twin Lakes	0.132	2.50	19.23	0.132	0.401	77
SC14 - Pawnee	0.150	2.65	18.47	0.150	0.404	76
SC17 - Holmes	0.119	2.54	20.79	0.119	0.414	84
SC18 - Branched Oak	0.163	2.69	18.43	0.163	0.408	77
Silver Creek	0.285	3.24	20.38	0.285	0.448	84
Stevens Cr abv SCNE	0.137	2.68	21.39	0.137	0.431	81
Wahoo Cr abv ITNE	0.211	2.99	20.87	0.211	0.441	78
Wahoo Creek abv ASNE	0.216	2.96	20.84	0.216	0.441	81

Table B - 5. Hydrologic Loss Parameters for Salt Creek Basin – 3-Foot Soil Depth

Subbasin	Deficit and Constant Parameters		Green and Ampt Parameters			SCS Curve Number
	Infiltration Rate	Maximum Deficit	W.F. Suction	Infiltration Rate	Porosity / Saturated Content	Curve Number
	(in/hr)	(in)	(in)	(in/hr)	(%)	AMC II
Antelope Cr abv ACNE	0.084	12.16	19.44	0.084	0.416	82
Clear Cr abv ASNE	0.342	10.38	20.75	0.342	0.434	82
Deadmans Run ab DRNE	0.083	11.58	19.96	0.083	0.416	83
Haines Br abv HBNE	0.146	8.58	20.44	0.146	0.409	78
Hickman Br abv SC08	0.079	8.31	23.47	0.079	0.419	83
Hickman Br abv SC09	0.114	8.69	22.67	0.114	0.420	82
Little Salt abv LSNE	0.126	8.98	21.14	0.126	0.420	80
Middle Cr abv MCNE	0.131	8.95	21.36	0.131	0.421	80
North Oak Creek	0.146	9.44	19.81	0.146	0.424	78
Oak Cr abv OCNE	0.122	9.19	21.44	0.122	0.423	81
Olive Br abv SC02	0.095	8.18	21.98	0.095	0.409	82
Olive Br abv SC04	0.112	8.27	21.77	0.112	0.409	82
Rock Cr abv RCNE	0.150	9.81	21.21	0.150	0.435	80
Salt Cr abv GWNE	0.112	9.19	22.05	0.112	0.432	84
Salt Cr abv LCNE	0.130	9.97	19.01	0.130	0.408	86
Salt Creek abv ASNE	0.190	9.72	21.15	0.190	0.435	82
Salt Creek abv LFNE	0.109	9.82	20.86	0.109	0.415	83
Salt Creek abv PBNE	0.106	8.80	22.65	0.106	0.423	83
Salt Creek abv RONE	0.101	8.38	22.77	0.101	0.416	82
Salt Creek abv SLNE	0.106	9.61	20.64	0.106	0.419	84
SC02 - Olive Creek	0.106	8.09	20.66	0.106	0.400	81
SC04 - Bluestem	0.078	7.67	22.58	0.078	0.400	82
SC08 - Wagon Train	0.073	7.81	23.14	0.073	0.407	82
SC09 - Stagecoach	0.103	7.85	21.98	0.103	0.400	81
SC10 - Yankee Hill	0.075	7.82	22.71	0.075	0.405	83
SC12 - Conestoga	0.101	8.08	20.44	0.101	0.399	78
SC13 - Twin Lakes	0.105	8.12	20.29	0.105	0.399	77
SC14 - Pawnee	0.125	8.47	19.44	0.125	0.400	76
SC17 - Holmes	0.088	8.21	22.01	0.088	0.409	84
SC18 - Branched Oak	0.139	8.85	18.98	0.139	0.407	77
Silver Creek	0.189	9.90	22.28	0.189	0.433	84
Stevens Cr abv SCNE	0.105	8.63	22.64	0.105	0.425	81
Wahoo Cr abv ITNE	0.196	10.27	21.29	0.196	0.437	78
Wahoo Creek abv ASNE	0.199	10.09	21.38	0.199	0.438	81

Table B - 6. Average Subbasin Curve Numbers for all Antecedent Moisture Conditions for the Salt Creek Basin

Subbasin	SCS Curve Number		
	AMC I	AMC II	AMC III
Antelope Cr abv ACNE	67	82	91
Clear Cr abv ASNE	67	82	91
Deadmans Run ab DRNE	68	83	92
Haines Br abv HBNE	61	78	89
Hickman Br abv SC08	68	83	92
Hickman Br abv SC09	67	82	91
Little Salt abv LSNE	64	80	90
Middle Cr abv MCNE	64	80	90
North Oak Creek	61	78	89
Oak Cr abv OCNE	65	81	91
Olive Br abv SC02	67	82	91
Olive Br abv SC04	67	82	91
Rock Cr abv RCNE	64	80	90
Salt Cr abv GWNE	70	84	92
Salt Cr abv LCNE	73	86	94
Salt Creek abv ASNE	67	82	91
Salt Creek abv LFNE	68	83	92
Salt Creek abv PBNE	68	83	92
Salt Creek abv RONE	67	82	91
Salt Creek abv SLNE	70	84	92
SC02 - Olive Creek	65	81	91
SC04 - Bluestem	67	82	91
SC08 - Wagon Train	67	82	91
SC09 - Stagecoach	65	81	91
SC10 - Yankee Hill	68	83	92
SC12 - Conestoga	61	78	89
SC13 - Twin Lakes	59	77	89
SC14 - Pawnee	58	76	88
SC17 - Holmes	70	84	92
SC18 - Branched Oak	59	77	89
Silver Creek	70	84	92
Stevens Cr abv SCNE	65	81	91
Wahoo Cr abv ITNE	61	78	89
Wahoo Creek abv ASNE	65	81	91

Table B - 7. Green and Ampt Parameters According to Soil Texture Classes and Horizons

Soil texture class (1)	Horizon (2)	Sample size (3)	Total porosity, ϕ, in cubic centimeters per cubic centimeters (4)	Effective porosity, θ_e, in cubic centimeters per cubic centimeters (5)	Wetted front capillary pressure, ψ_f,[a] in centimeters (6)	Hydraulic conductivity, K,[b] in centimeters per hour (7)
Sand[c]		762	0.437 0.374–0.500[d]	0.417 (0.354–0.480)	4.95 (0.97–25.36)	11.78
	A	370	0.452 (0.396–0.508)	0.431 (0.375–0.487)	5.34 (1.24–23.06)	
	B	185	0.440 (0.385–0.495)	0.421 (0.365–0.477)	6.38 (1.31–31.06)	
	C	127	0.424 (0.385–0.463)	0.408 (0.365–0.451)	2.07 (0.32–13.26)	
Loamy sand		338	0.437 (0.363–0.506)	0.401 (0.329–0.473)	6.13 (1.35–27.94)	2.99
	A	110	0.457 (0.385–0.529)	0.424 (0.347–0.501)	6.01 (1.58–22.87)	
	B	49	0.447 (0.379–0.515)	0.412 (0.334–0.490)	4.21 (1.03–17.24)	
	C	36	0.424 (0.372–0.476)	0.385 (0.323–0.447)	5.16 (0.76–34.85)	
Sandy loam		666	0.453 (0.351–0.555)	0.412 (0.283–0.541)	11.01 (2.67–45.47)	1.09
	A	119	0.505 (0.399–0.611)	0.469 (0.330–0.608)	15.24 (5.56–41.76)	
	B	219	0.466 (0.352–0.580)	0.428 (0.271–0.585)	8.89 (2.02–39.06)	
	C	66	0.418 (0.352–0.484)	0.389 (0.310–0.468)	6.79 (1.16–39.65)	
Loam		383	0.463 (0.375–0.551)	0.434 (0.334–0.534)	8.89 (1.33–59.38)	0.34
	A	76	0.512 (0.427–0.597)	0.476 (0.376–0.576)	10.01 (2.14–46.81)	
	B	67	0.512 (0.408–0.616)	0.498 (0.382–0.614)	6.40 (1.01–40.49)	
	C	47	0.412 (0.350–0.474)	0.382 (0.305–0.459)	9.27 (0.87–99.29)	
Silt loam		1,206	0.501 (0.420–0.582)	0.486 (0.394–0.578)	16.68 (2.92–95.39)	0.65
	A	361	0.527 (0.444–0.610)	0.514 (0.425–0.603)	10.91 (1.89–63.05)	
	B	267	0.533 (0.430–0.636)	0.515 (0.387–0.643)	7.21 (0.86–60.82)	
	C	73	0.470 (0.409–0.531)	0.460 (0.396–0.524)	12.62 (3.94–40.45)	
Sandy clay loam		498	0.398 (0.332–0.464)	0.330 (0.235–0.425)	21.85 (4.42–108.0)	0.15
	A	—[e]	— —	— —	— —	
	B	198	0.393 (0.310–0.476)	0.330 (0.223–0.437)	26.10 (4.79–142.30)	
	C	32	0.407 (0.359–0.455)	0.332 (0.251–0.413)	23.90 (5.51–103.75)	
Clay loam		366	0.464 (0.409–0.519)	0.309 (0.279–0.501)	20.88 (4.79–91.10)	0.10
	A	28	0.497 (0.434–0.560)	0.430 (0.328–0.532)	27.00 (6.13–118.9)	
	B	99	0.451 (0.401–0.501)	0.397 (0.228–0.530)	18.52 (4.36–78.73)	
	C	55	0.452 (0.412–0.492)	0.400 (0.320–0.480)	15.21 (3.79–61.01)	
Silty clay loam		689	0.471 (0.418–0.524)	0.432 (0.347–0.517)	27.30 (5.67–131.50)	0.10
	A	65	0.509 (0.449–0.569)	0.477 (0.410–0.544)	13.97 (4.20–46.53)	
	B	191	0.469 (0.423–0.515)	0.441 (0.374–0.508)	18.56 (4.08–84.44)	
	C	39	0.475 (0.436–0.514)	0.451 (0.386–0.516)	21.54 (4.56–101.7)	
Sandy clay		45	0.430 (0.370–0.490)	0.321 (0.207–0.435)	23.90 (4.08–140.2)	0.06
	A	—	— —	— —	— —	
	B	23	0.435 (0.371–0.499)	0.335 (0.220–0.450)	36.74 (8.33–162.1)	
	C	—	— —	— —	— —	
Silty clay		127	0.479 (0.425–0.533)	0.423 (0.334–0.512)	29.22 (6.13–139.4)	0.05
	A	—	— —	— —	— —	
	B	38	0.476 (0.445–0.507)	0.424 (0.345–0.503)	30.66 (7.15–131.5)	
	C	21	0.464 (0.430–0.498)	0.416 (0.346–0.486)	45.65 (18.27–114.1)	
Clay		291	0.475 (0.427–0.523)	0.385 (0.269–0.501)	31.63 (6.39–156.5)	0.03
	A	—	— —	— —	— —	
	B	70	0.470 (0.426–0.514)	0.412 (0.309–0.515)	27.72 (6.21–123.7)	
	C	23	0.483 (0.441–0.525)	0.419 (0.294–0.544)	54.65 (10.59–282.0)	

[a]Antilog of the log mean and standard deviation.
[b]Values for Rawls, et al. (13).
[c]Values for the texture class.
[d]Numbers in ( ) ± one standard deviation.
[e]Insufficient sample to determine parameters.

Note: Retrieved from "Green-Ampt Infiltration Parameters from Soils Data" by Rawls et al, *Journal of Hydraulic Engineering, 109(1).* 1983 Copyright ASCE. Reprinted with Permission

Appendix C – Watershed Hydrographs for Optimized Initial Conditions

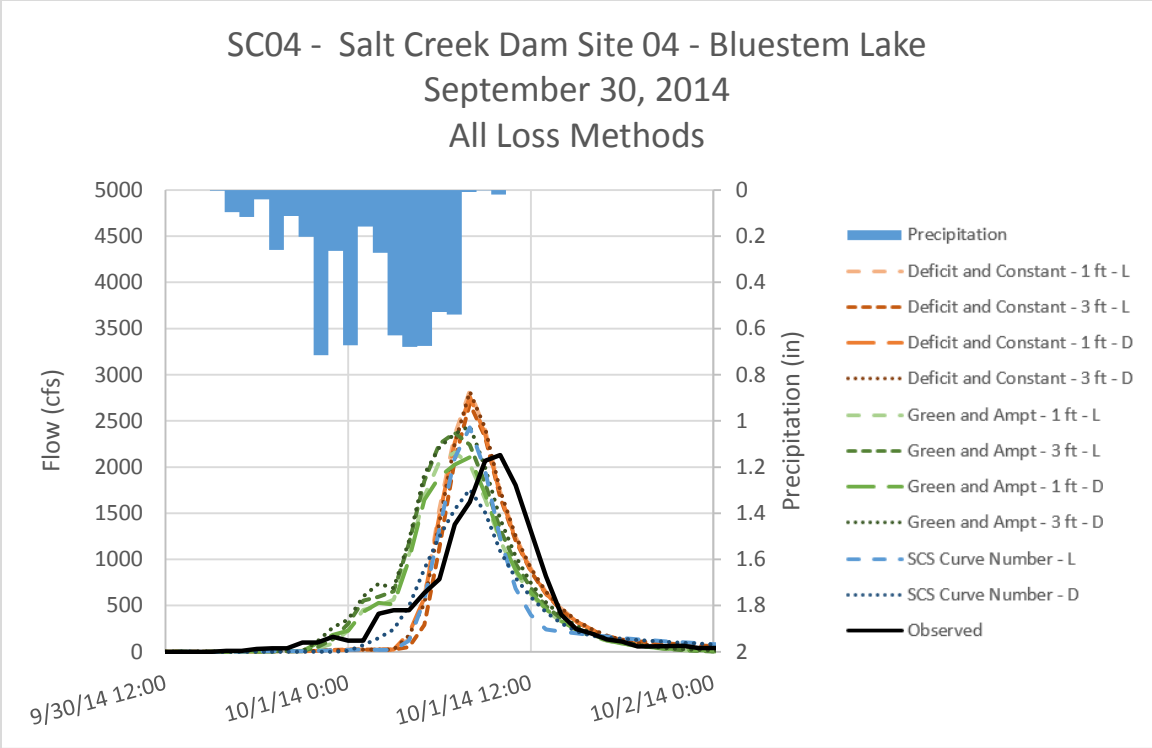

Figure C - 1. Runoff Hydrographs for SC04 - Salt Creek Dam Site 04 - Bluestem Lake for September 30, 2014 Event All Loss Method – Optimized Initial Conditions

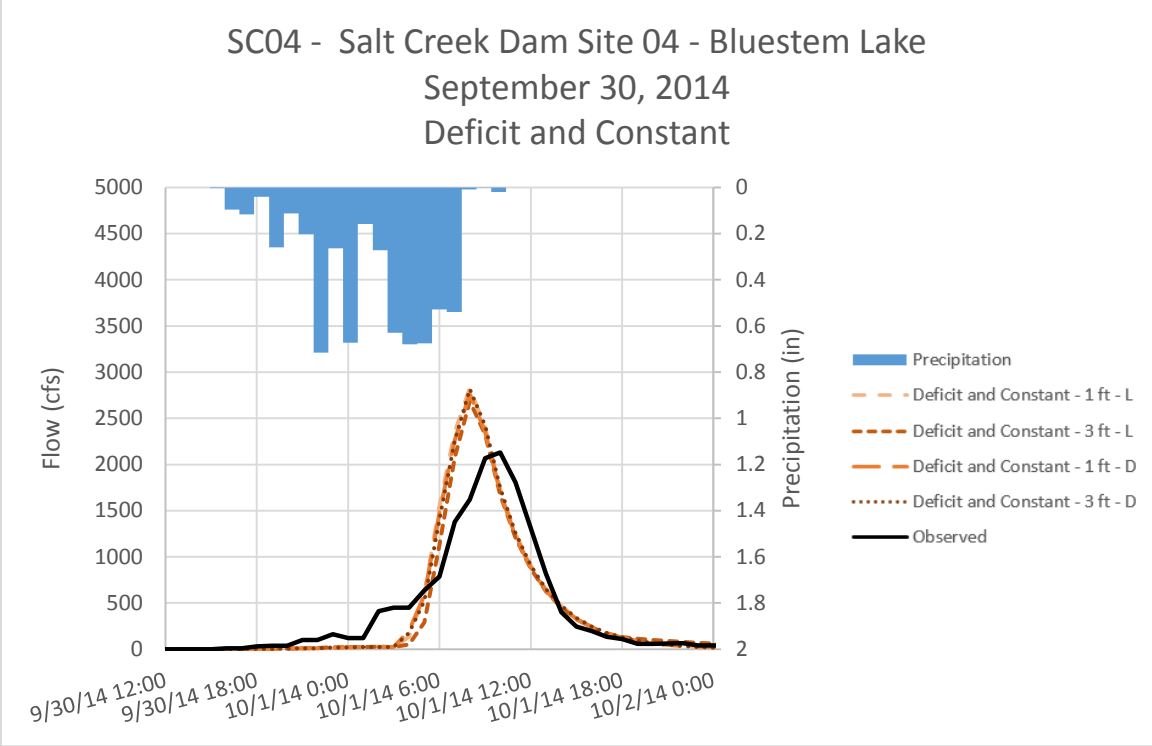

Figure C - 2. Runoff Hydrographs for SC04 - Salt Creek Dam Site 04 - Bluestem Lake for September 30, 2014 Event Deficit and Constant Method – Optimized Initial Conditions

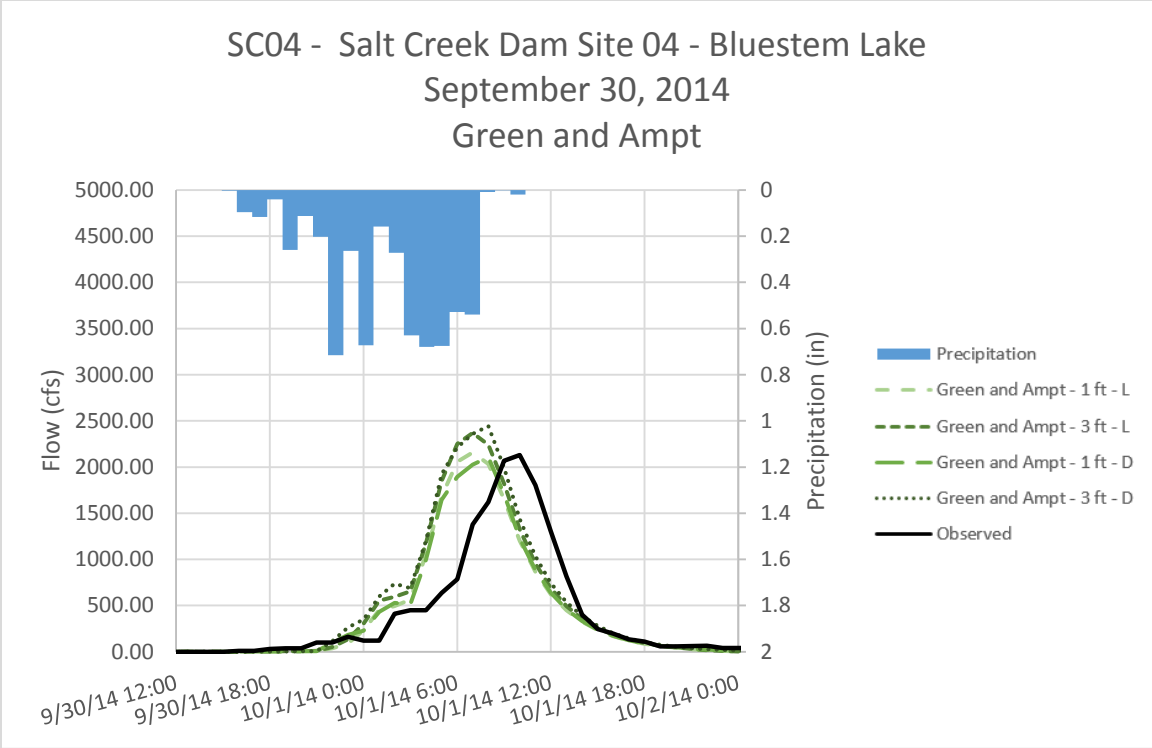

Figure C - 3. Runoff Hydrographs for SC04 - Salt Creek Dam Site 04 - Bluestem Lake for September 30, 2014 Event Green and Ampt Method – Optimized Initial Conditions

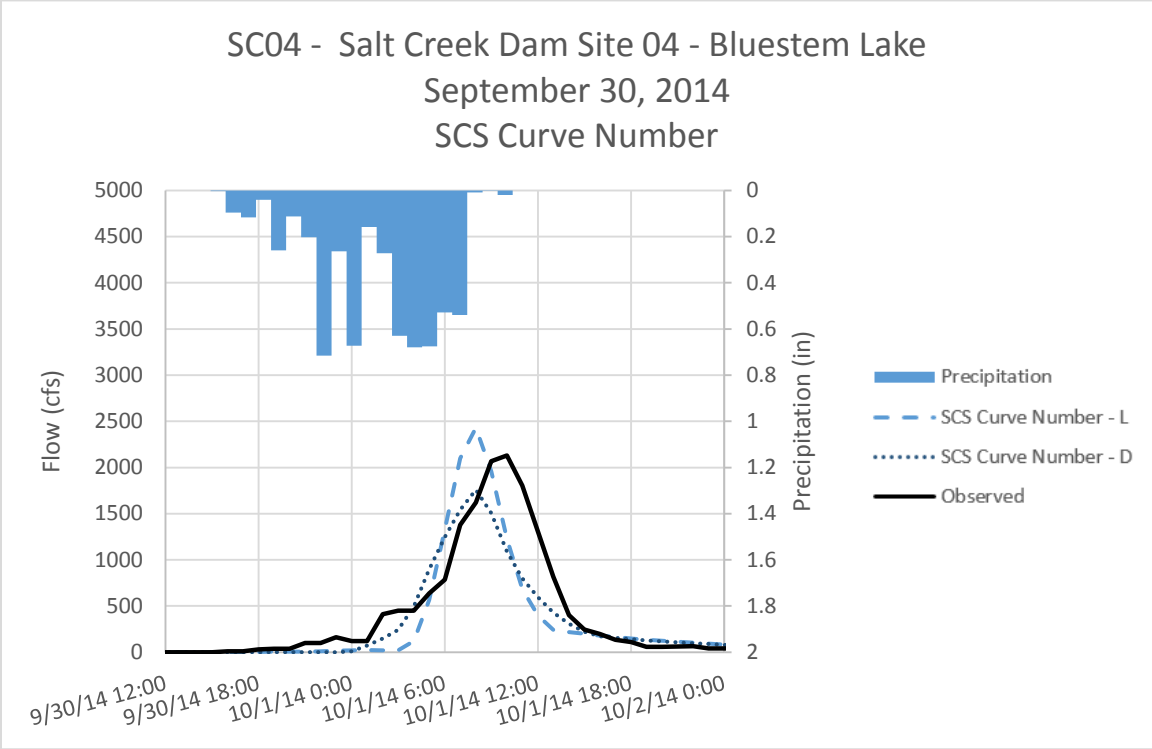

Figure C - 4. Runoff Hydrographs for SC04 - Salt Creek Dam Site 04 - Bluestem Lake for September 30, 2014 Event SCS Curve Number Method – Optimized Initial Conditions

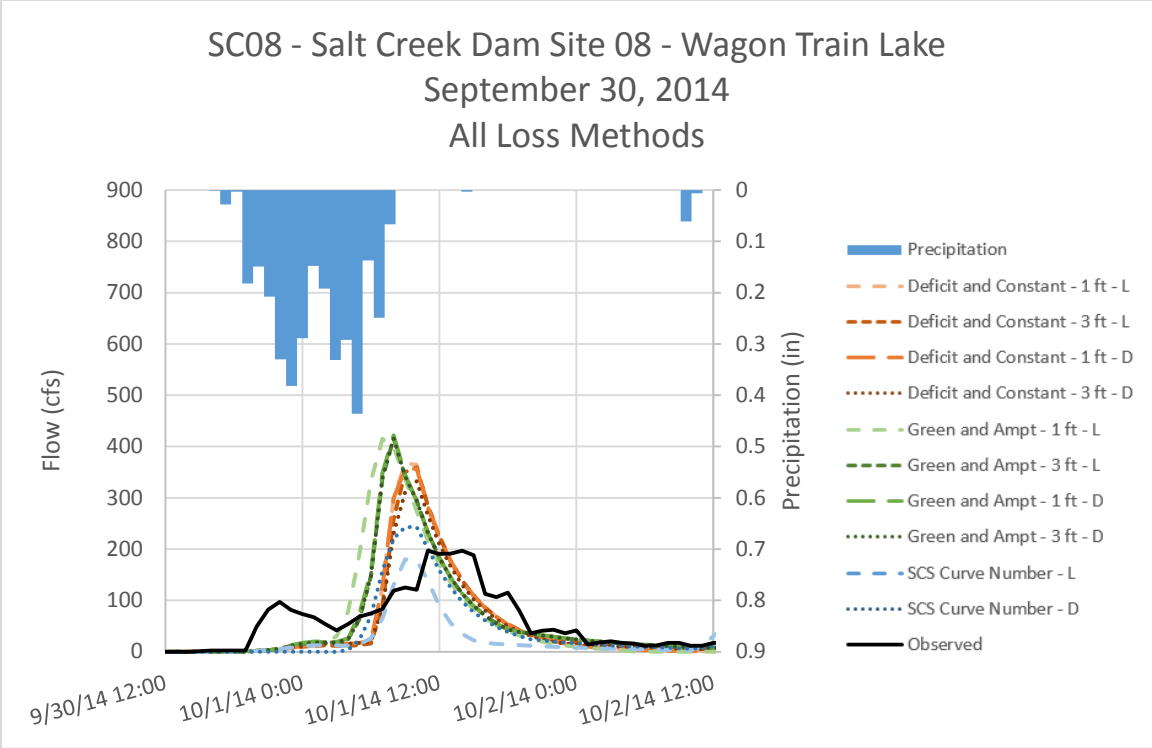

Figure C - 5. Runoff Hydrographs for SC08 - Salt Creek Dam Site 08 – Wagon Train Lake for September 30, 2014 Event All Loss Methods – Optimized Initial Conditions

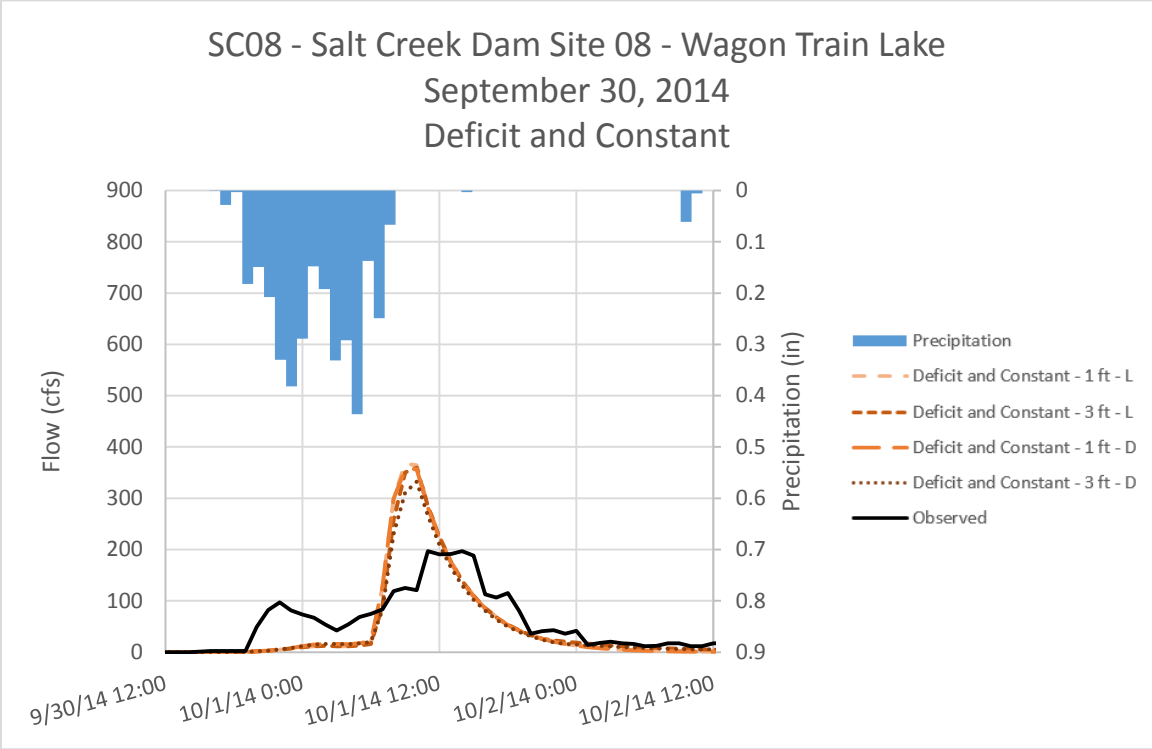

Figure C - 6. Runoff Hydrographs for SC08 - Salt Creek Dam Site 08 – Wagon Train Lake for September 30, 2014 Event Deficit and Constant Method – Optimized Initial Conditions

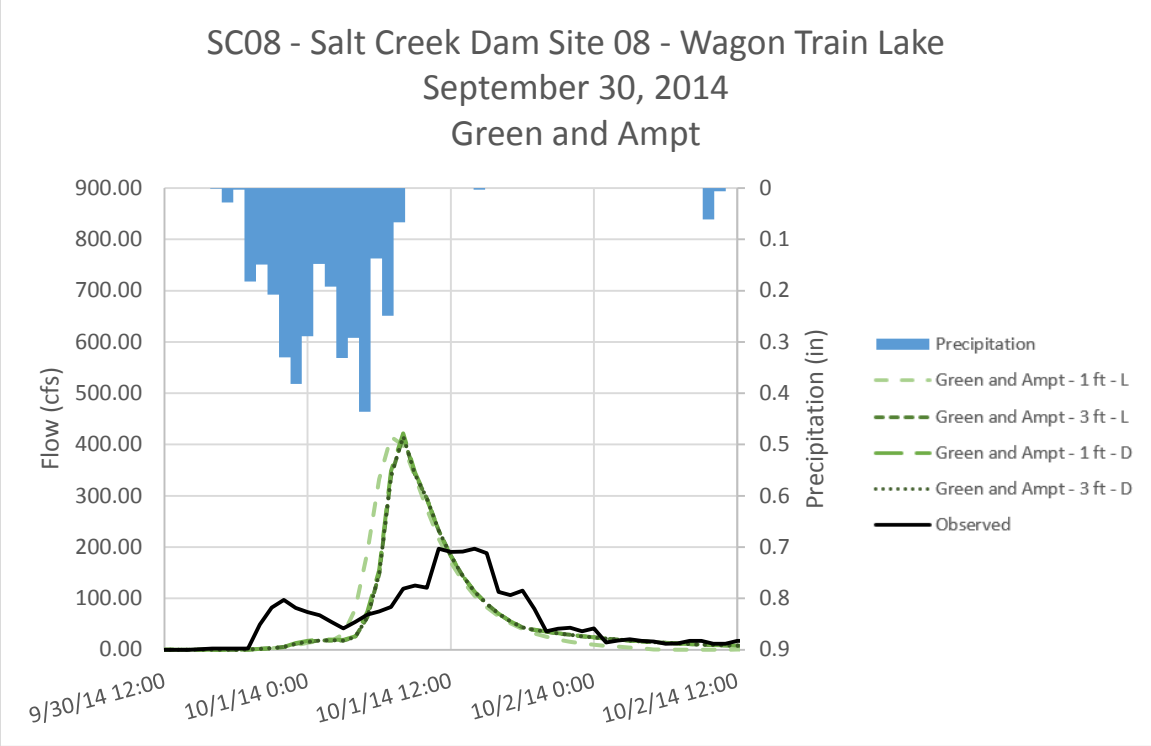

Figure C - 7. Runoff Hydrographs for SC08 - Salt Creek Dam Site 08 – Wagon Train Lake for September 30, 2014 Event Green and Ampt Method – Optimized Initial Conditions

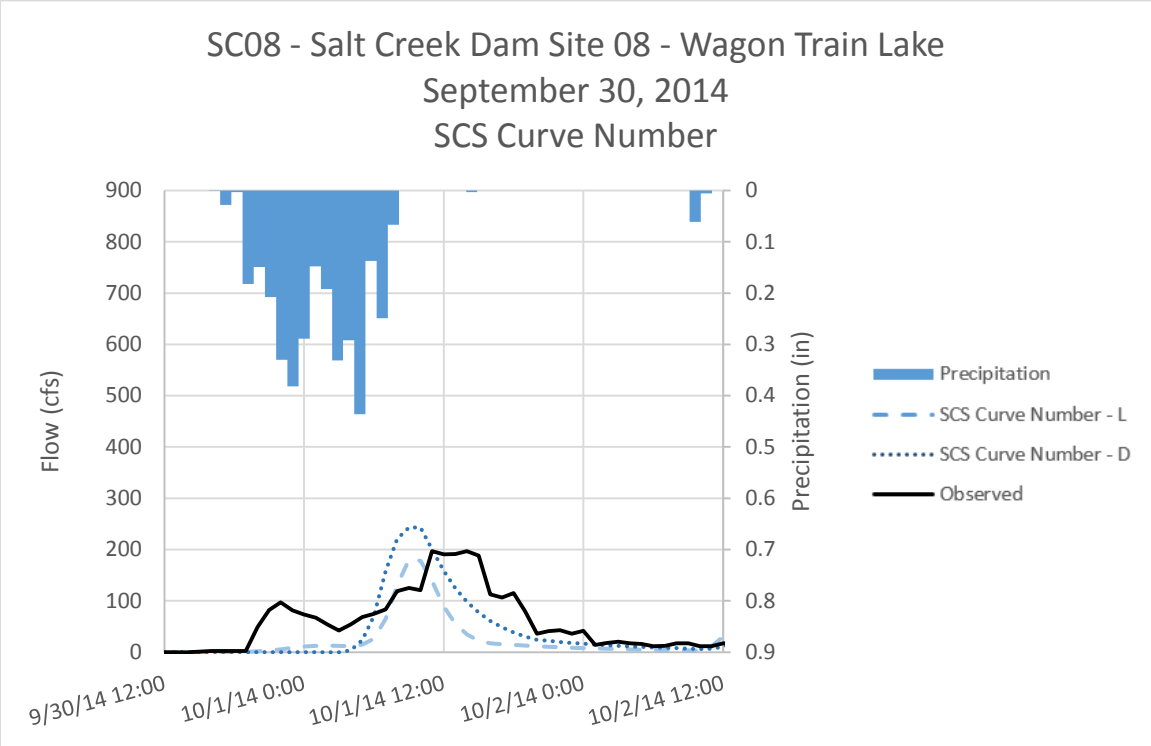

Figure C - 8. Runoff Hydrographs for SC08 - Salt Creek Dam Site 08 – Wagon Train Lake for September 30, 2014 Event SCS Curve Number Method – Optimized Initial Conditions

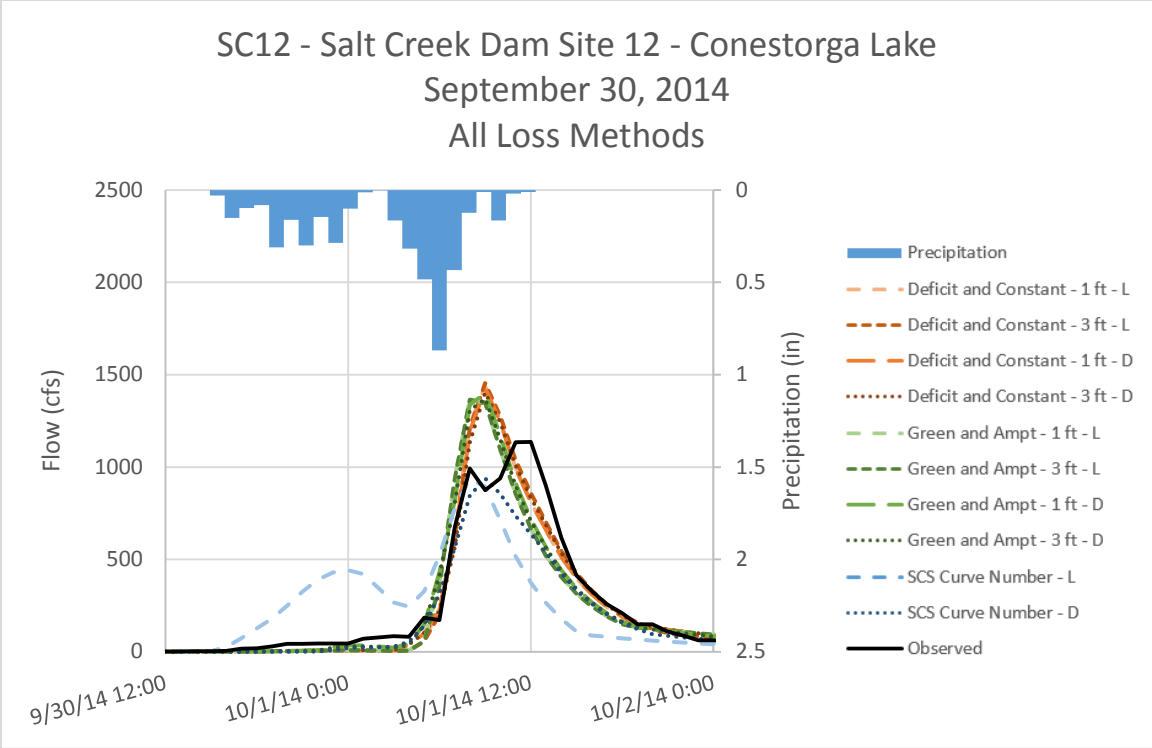

Figure C - 9. Runoff Hydrographs for SC12 - Salt Creek Dam Site 12 – Conestoga Lake for September 30, 2014 Event All Loss Methods – Optimized Initial Conditions

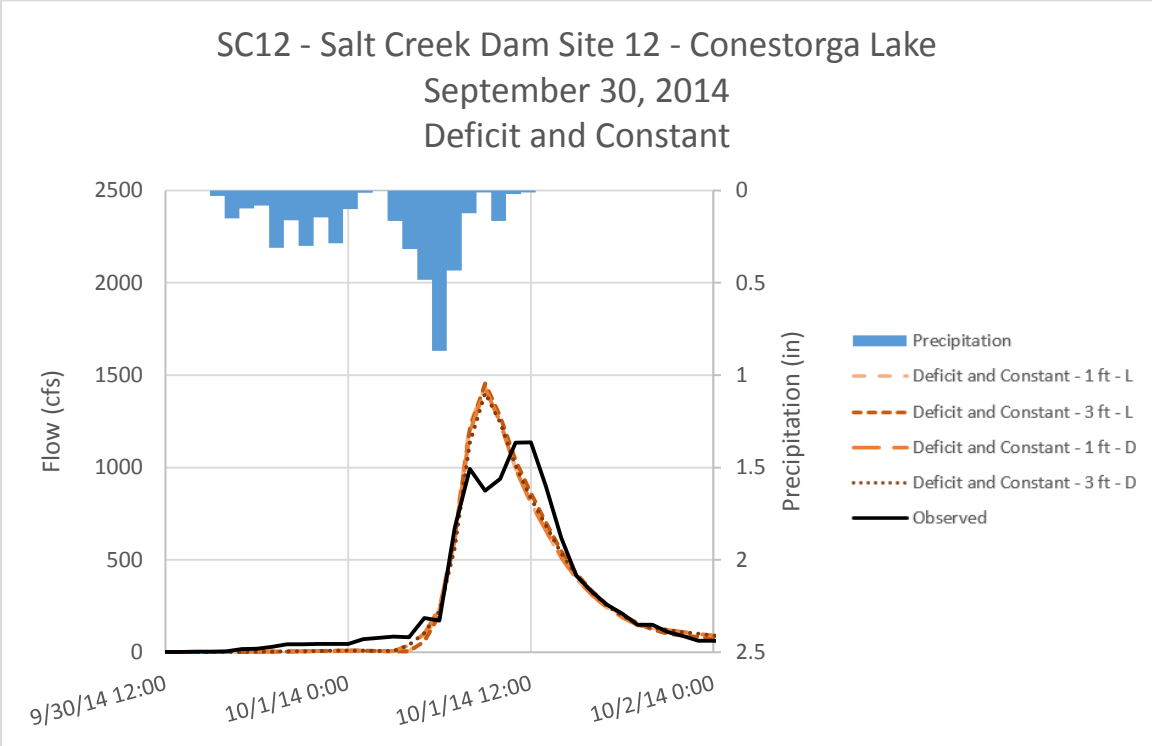

Figure C - 10. Runoff Hydrographs for SC12 - Salt Creek Dam Site 12 – Conestoga Lake for September 30, 2014 Event Deficit and Constant Method – Optimized Initial Conditions

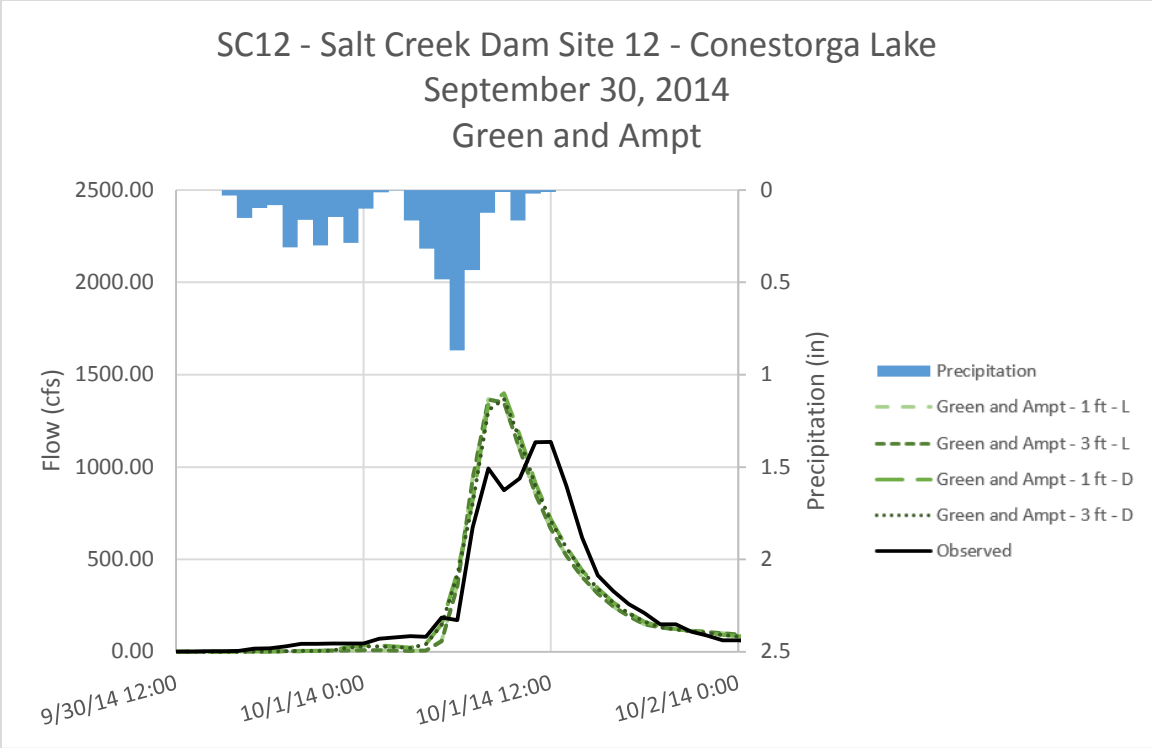

Figure C - 11. Runoff Hydrographs for SC12 - Salt Creek Dam Site 12 – Conestoga Lake for September 30, 2014 Event Green and Ampt Method – Optimized Initial Conditions

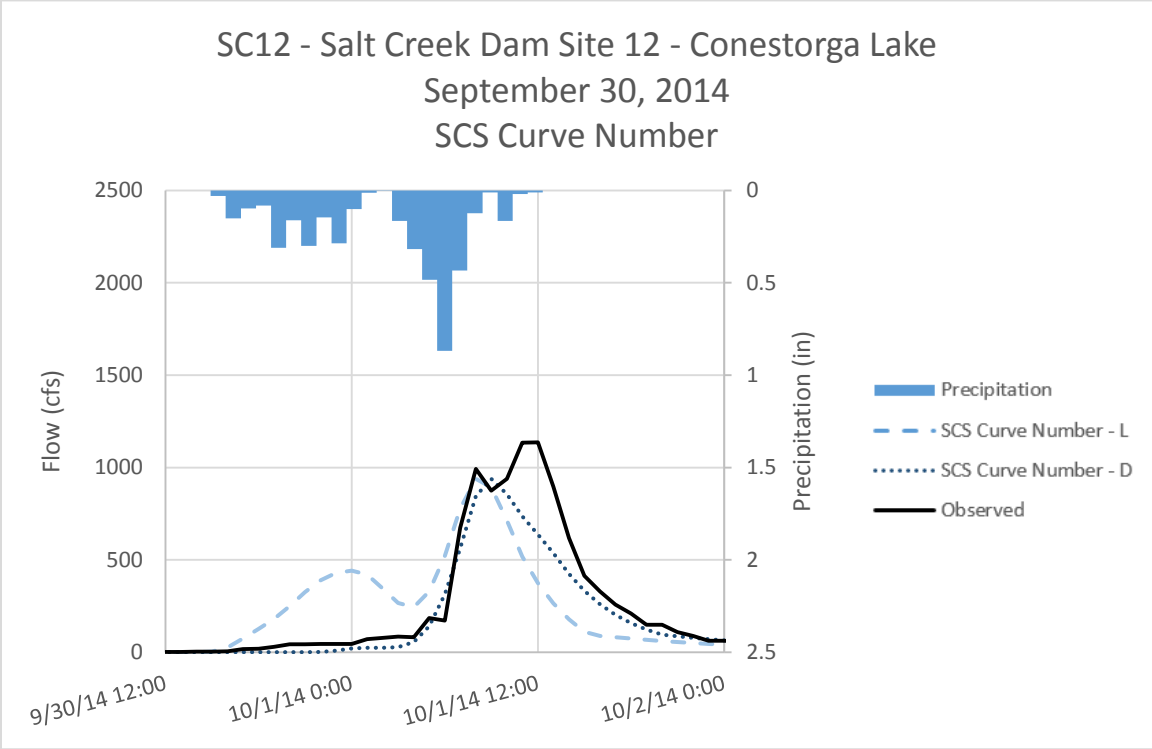

Figure C - 12. Runoff Hydrographs for SC12 - Salt Creek Dam Site 12 – Conestoga Lake for September 30, 2014 Event SCS Curve Number – Optimized Initial Conditions

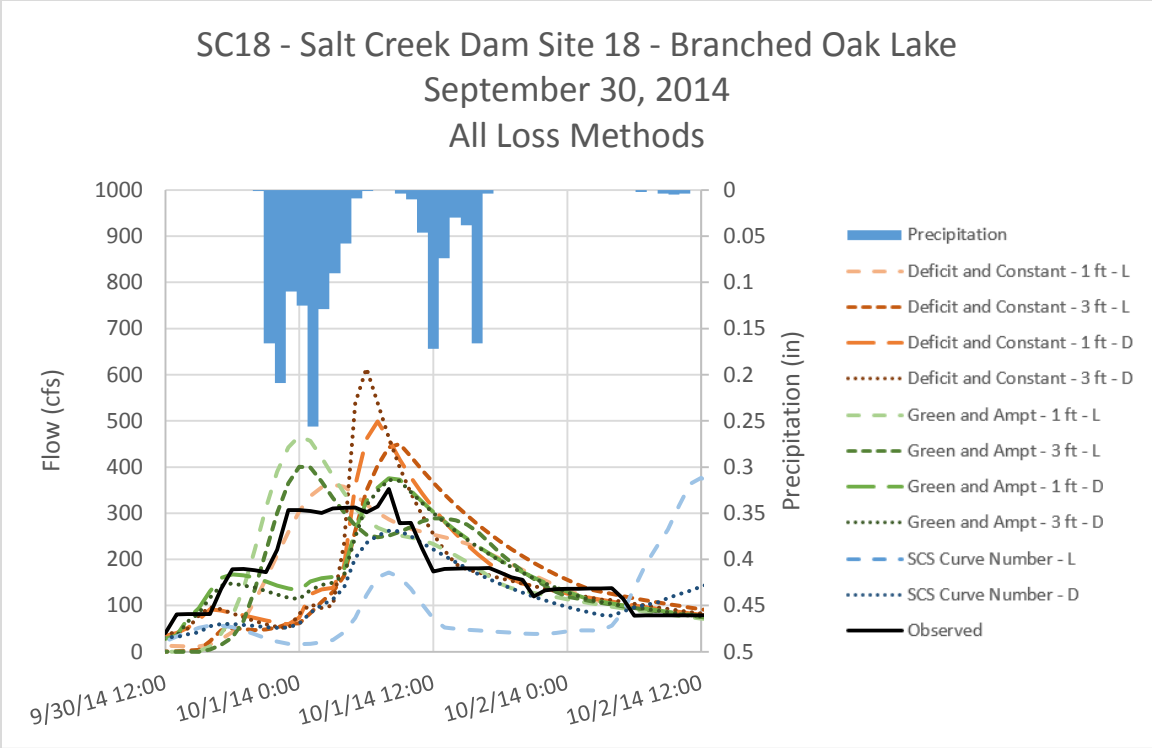

Figure C - 13. Runoff Hydrographs for SC18 - Salt Creek Dam Site 18 - Branched Oak Lake for September 30, 2014 Event All Loss Methods – Optimized Initial Conditions

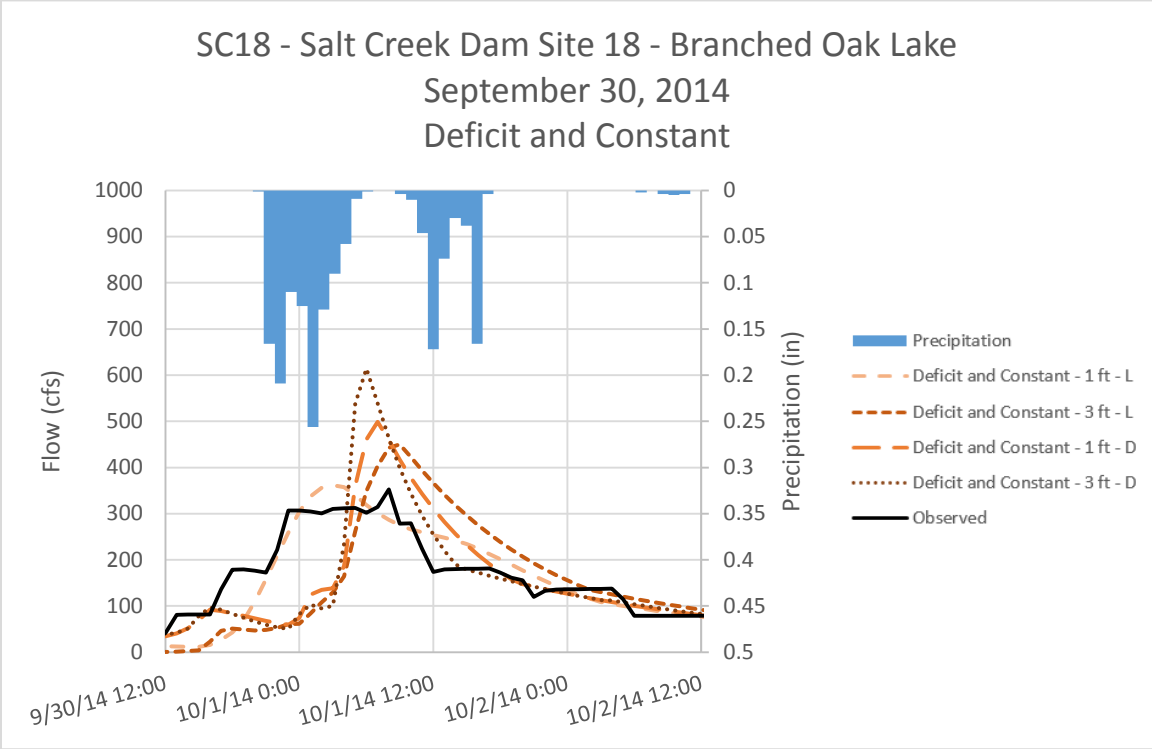

Figure C - 14. Runoff Hydrographs for SC18 - Salt Creek Dam Site 18 - Branched Oak Lake for September 30, 2014 Event Deficit and Constant Method – Optimized Initial Conditions

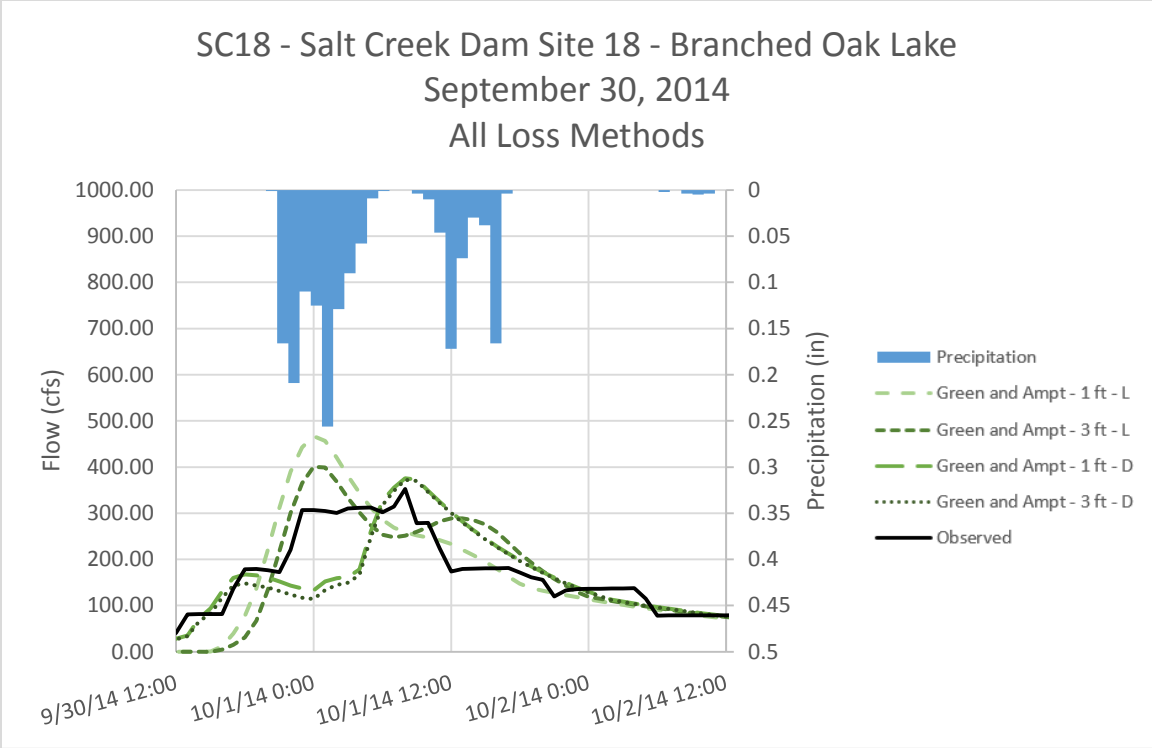

Figure C - 15. Runoff Hydrographs for SC18 - Salt Creek Dam Site 18 - Branched Oak Lake for September 30, 2014 Event Green and Ampt Method – Optimized Initial Conditions

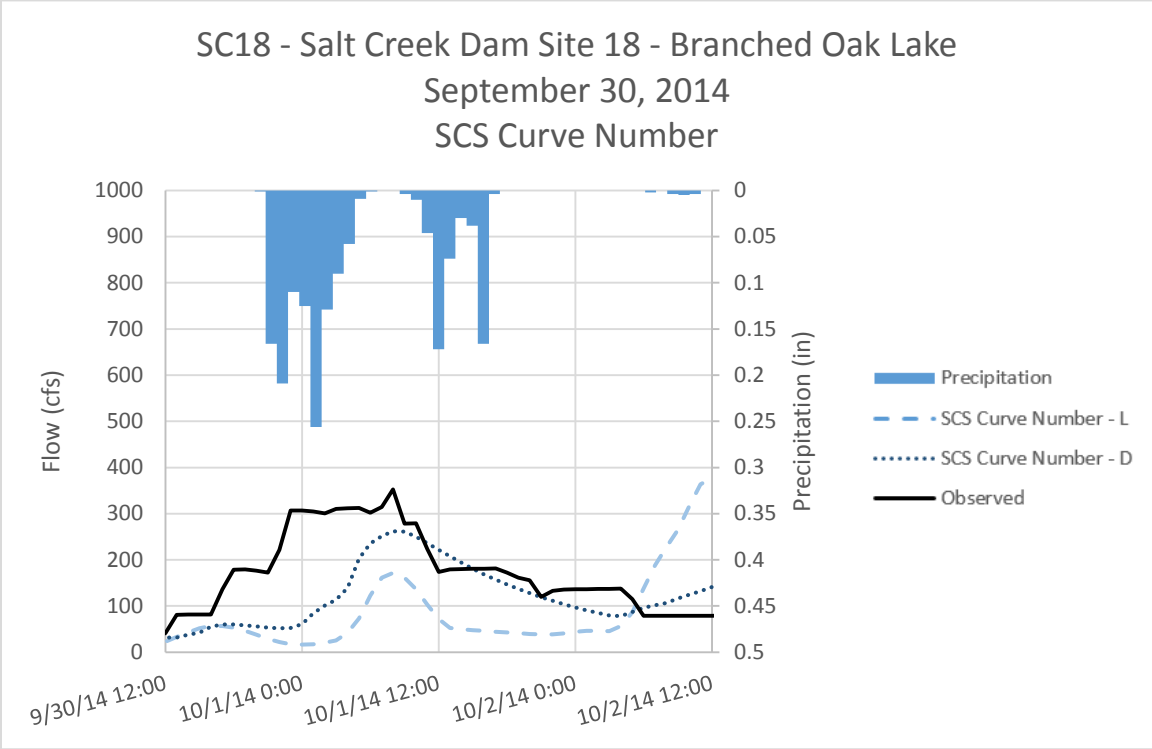

Figure C - 16. Runoff Hydrographs for SC18 - Salt Creek Dam Site 18 - Branched Oak Lake for September 30, 2014 Event SCS Curve Number Method – Optimized Initial Conditions

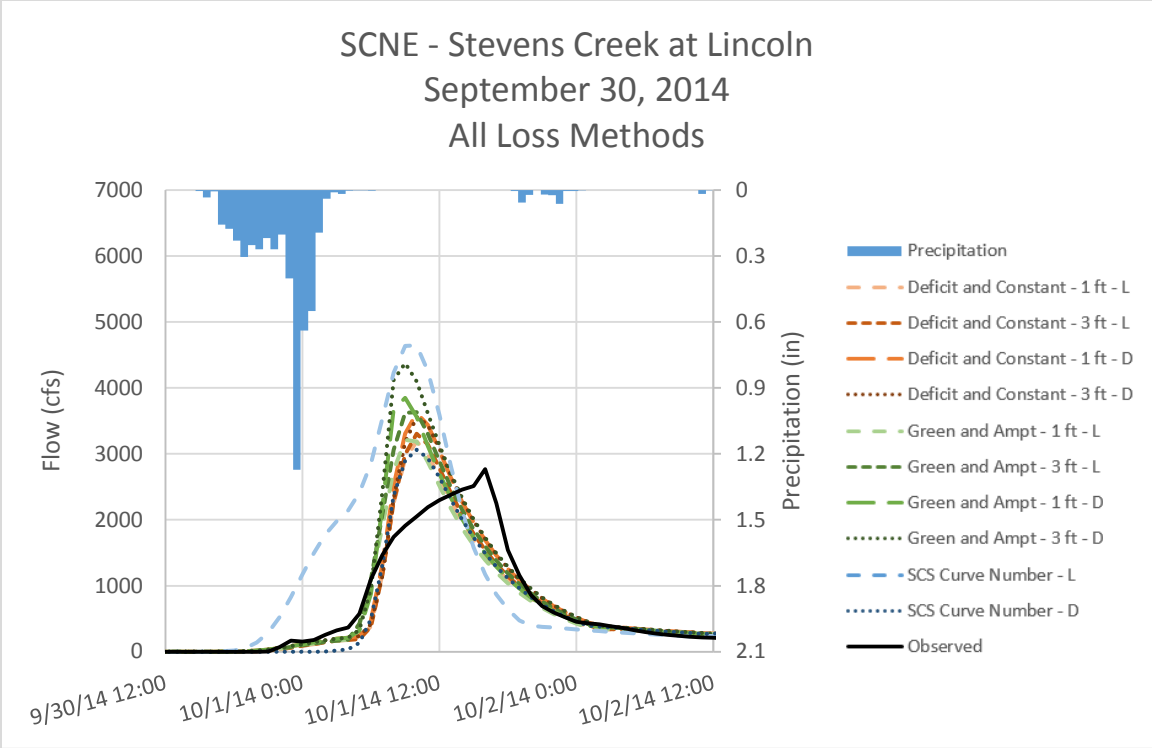

Figure C - 17. Runoff Hydrographs for SCNE – Stevens Creek at Lincoln for September 30, 2014 Event
All Loss Methods – Optimized Initial Conditions

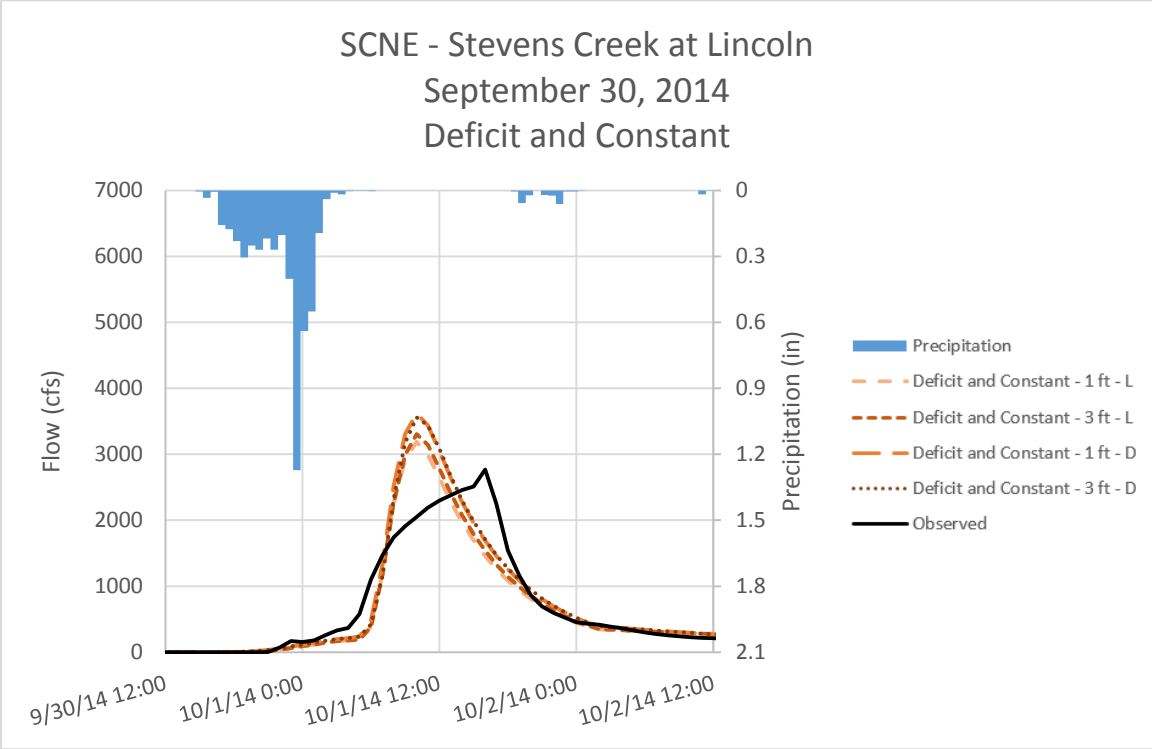

Figure C - 18. Runoff Hydrographs for SCNE – Stevens Creek at Lincoln for September 30, 2014 Event
Deficit and Constant Method – Optimized Initial Conditions

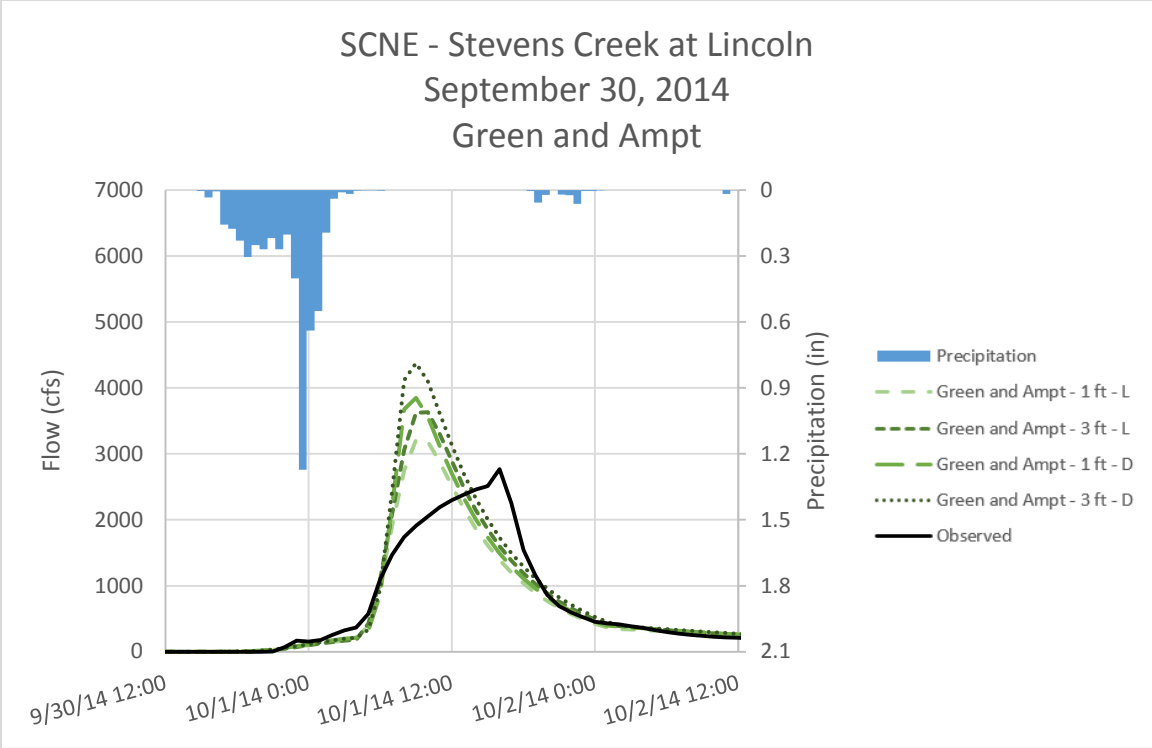

Figure C - 19. Runoff Hydrographs for SCNE – Stevens Creek at Lincoln for September 30, 2014 Event Green and Ampt Method – Optimized Initial Conditions

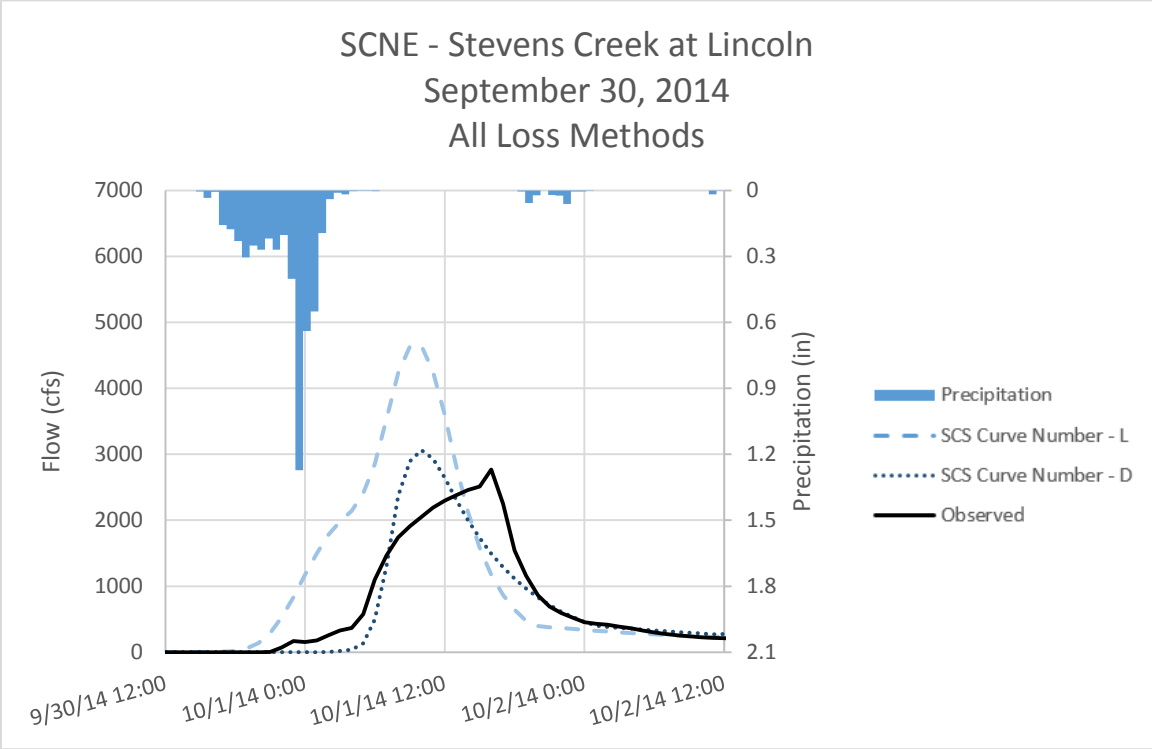

Figure C - 20. Runoff Hydrographs for SCNE – Stevens Creek at Lincoln for September 30, 2014 Event SCS Curve Number Method – Optimized Initial Conditions

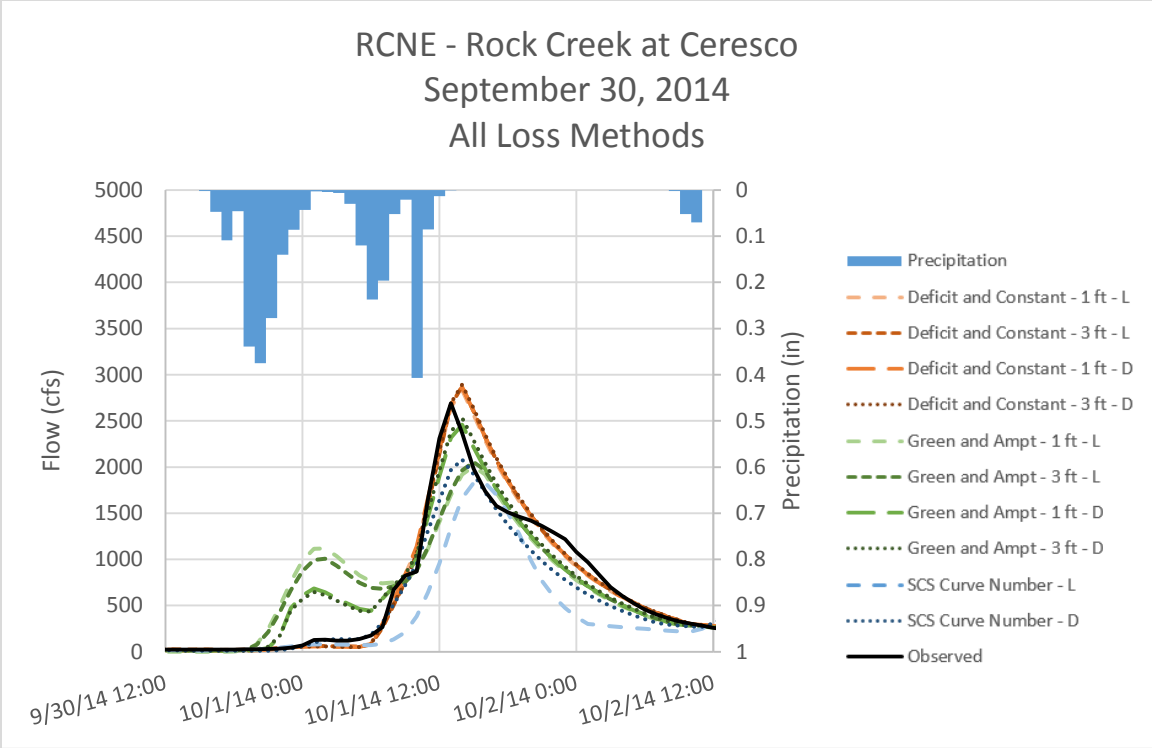

Figure C - 21. Runoff Hydrographs for RCNE – Rock Creek at Ceresco for September 30, 2014 Event
All Loss Methods – Optimized Initial Conditions

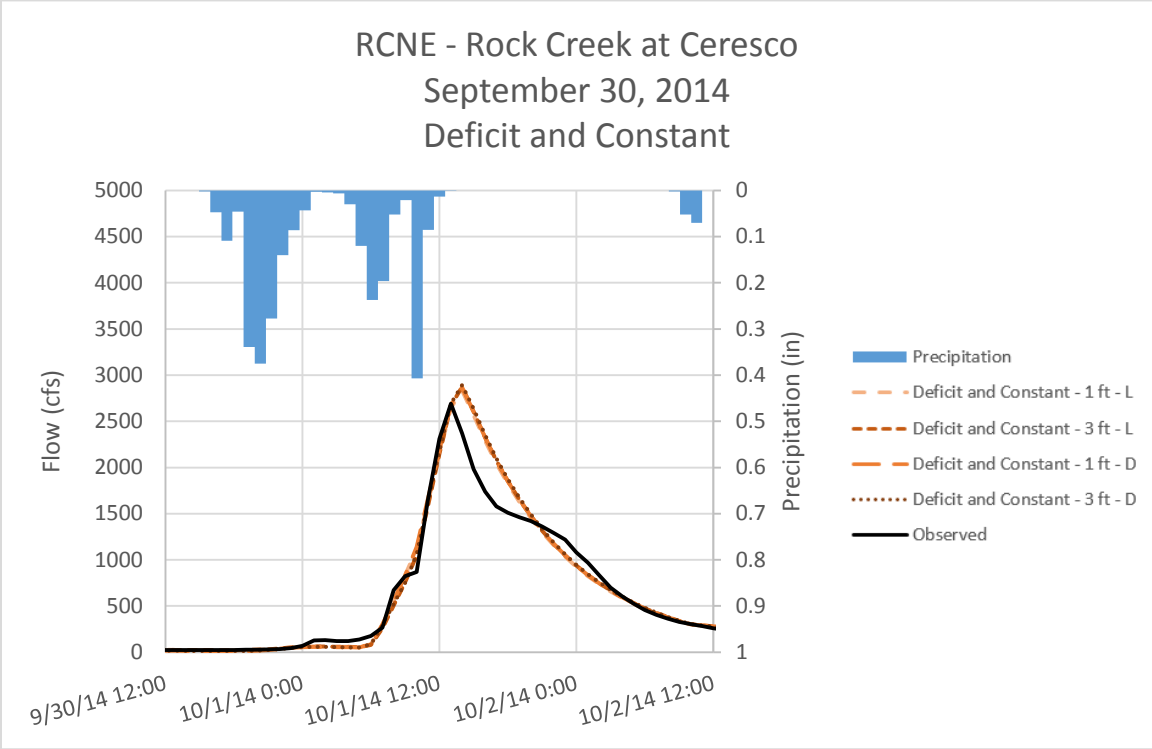

Figure C - 22. Runoff Hydrographs for RCNE – Rock Creek at Ceresco for September 30, 2014 Event
Deficit and Constant Method – Optimized Initial Conditions

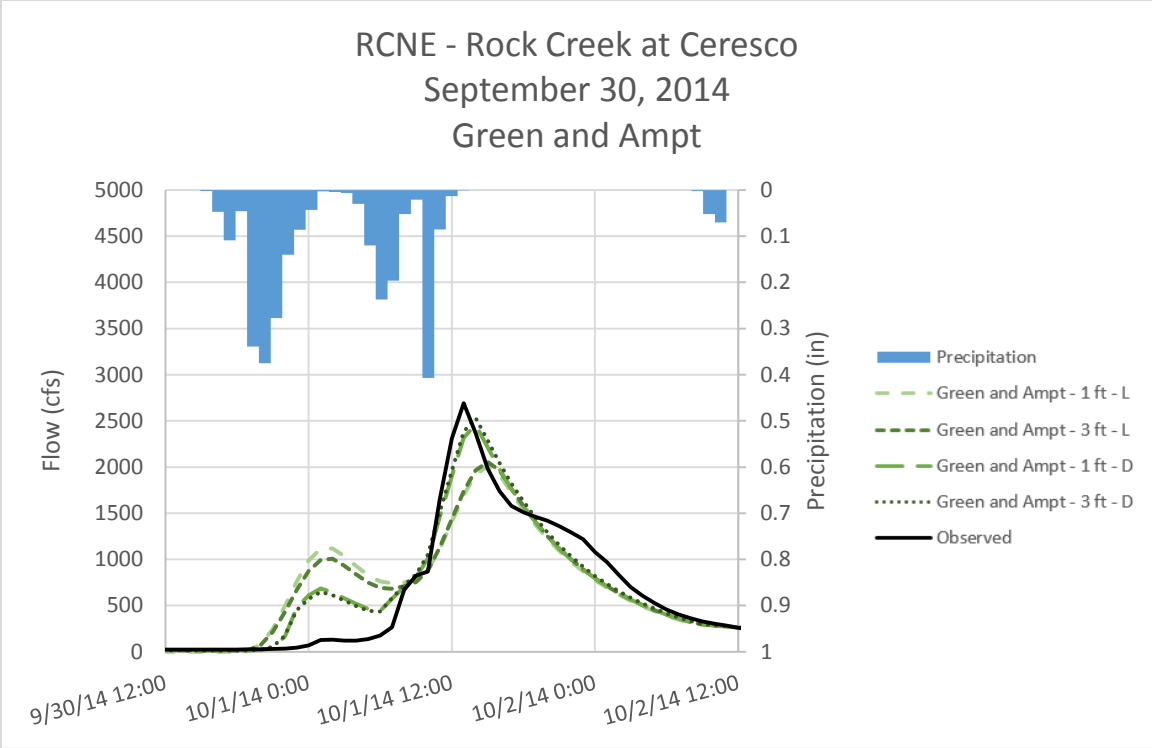

Figure C - 23. Runoff Hydrographs for RCNE – Rock Creek at Ceresco for September 30, 2014 Event
Green and Ampt Method – Optimized Initial Conditions

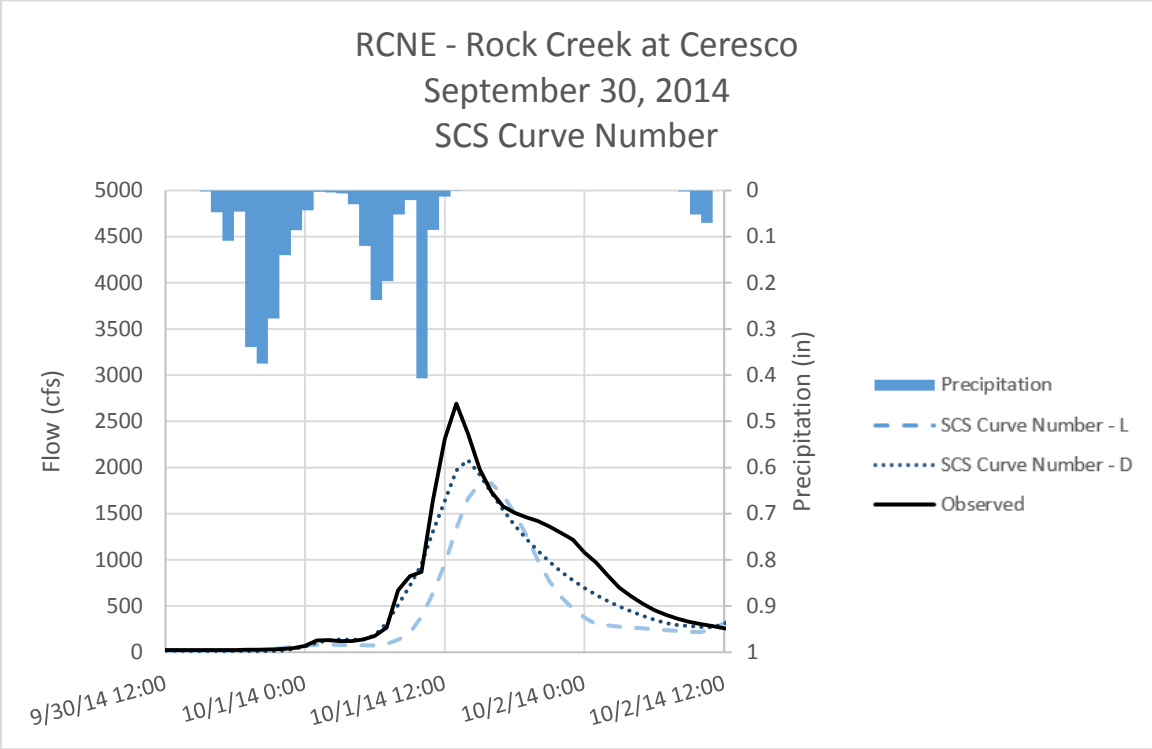

Figure C - 24. Runoff Hydrographs for RCNE – Rock Creek at Ceresco for September 30, 2014 Event
SCS Curve Number Method – Optimized Initial Conditions

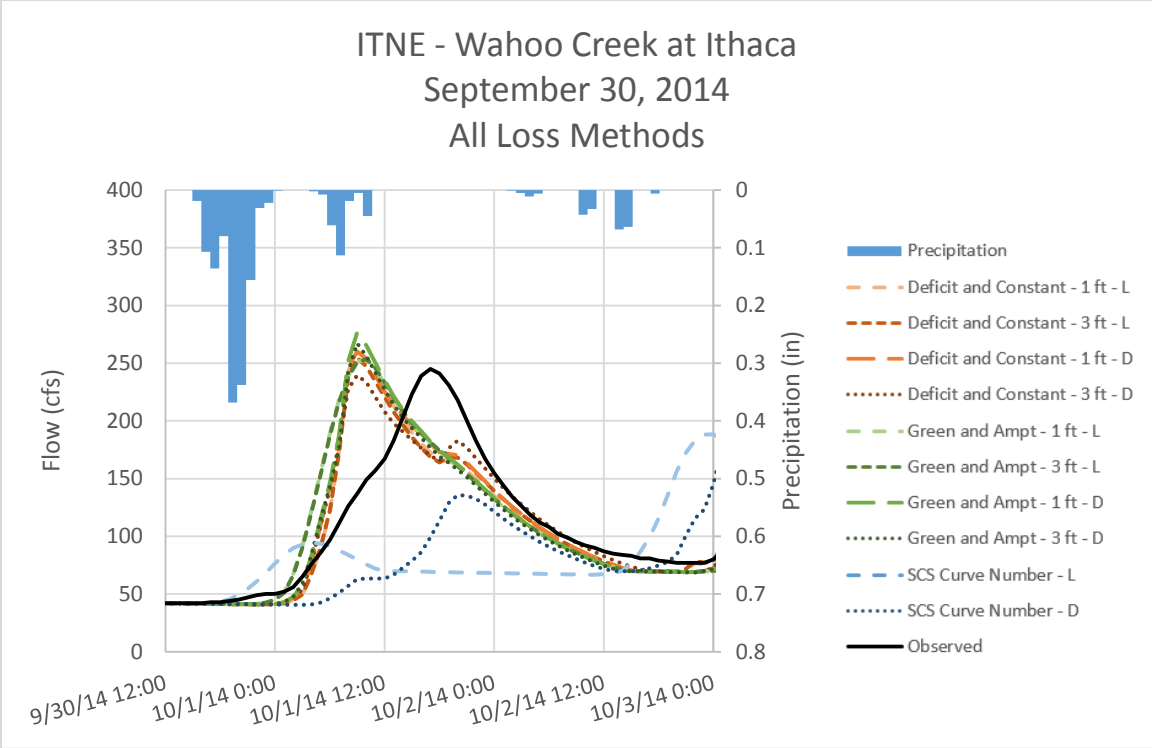

Figure C - 25. Runoff Hydrographs for ITNE – Wahoo Creek at Ithaca for September 30, 2014 Event
All Loss Methods – Optimized Initial Conditions

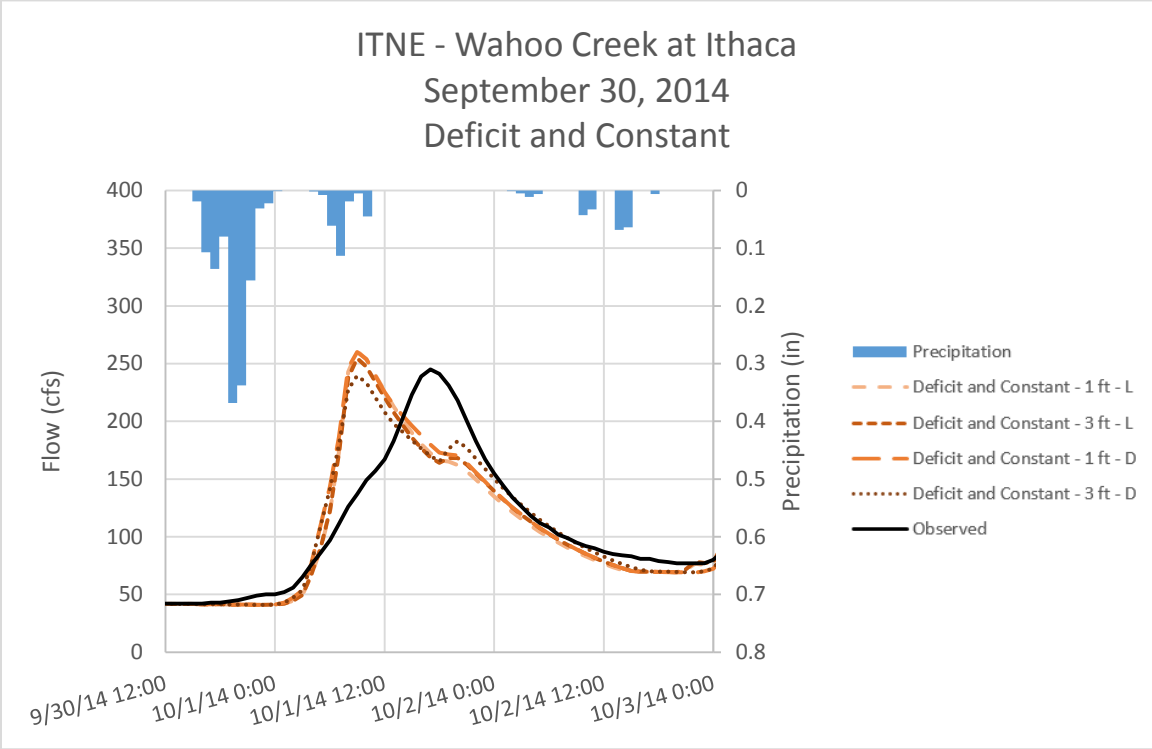

Figure C - 26. Runoff Hydrographs for ITNE – Wahoo Creek at Ithaca for September 30, 2014 Event
Deficit and Constant Method – Optimized Initial Conditions

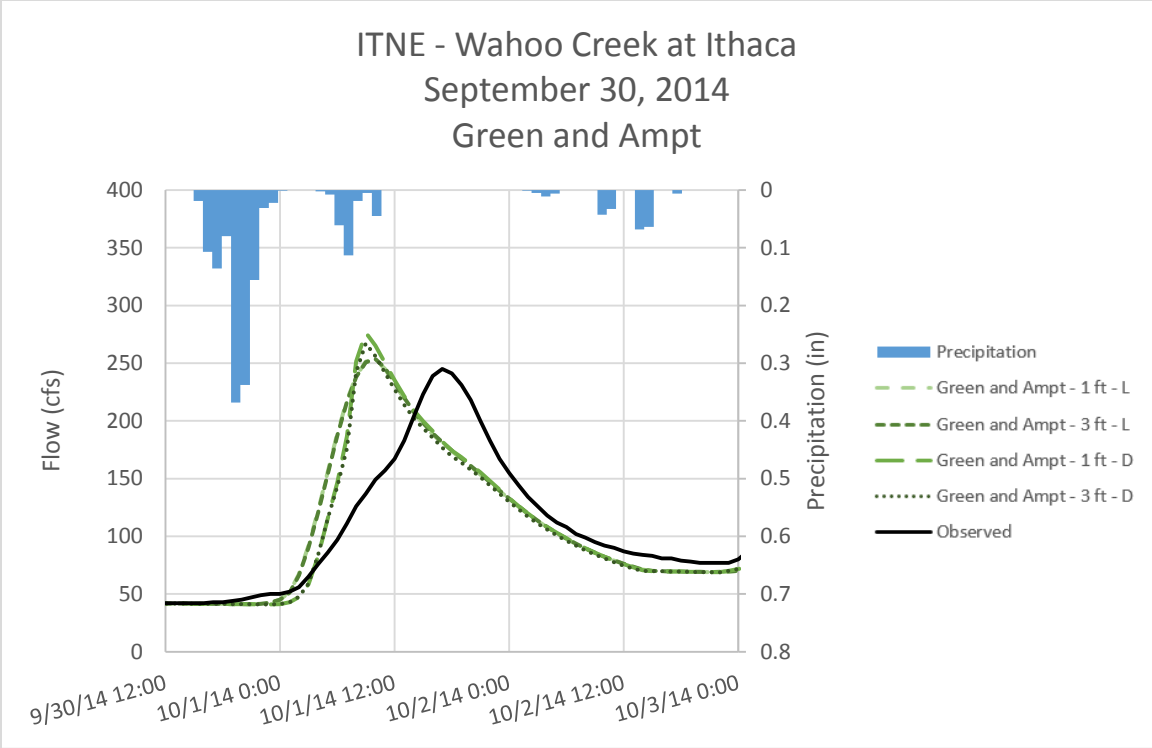

Figure C - 27. Runoff Hydrographs for ITNE – Wahoo Creek at Ithaca for September 30, 2014 Event Green and Ampt Method – Optimized Initial Conditions

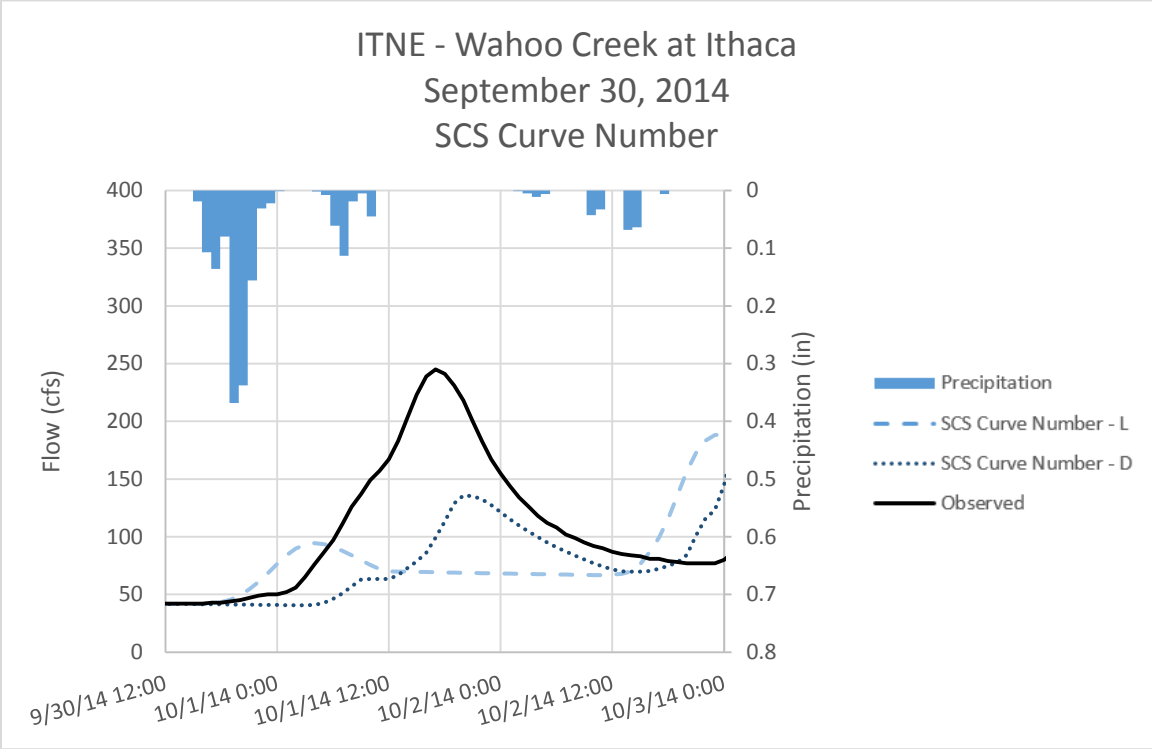

Figure C - 28. Runoff Hydrographs for ITNE – Wahoo Creek at Ithaca for September 30, 2014 Event SCS Curve Number Method – Optimized Initial Conditions

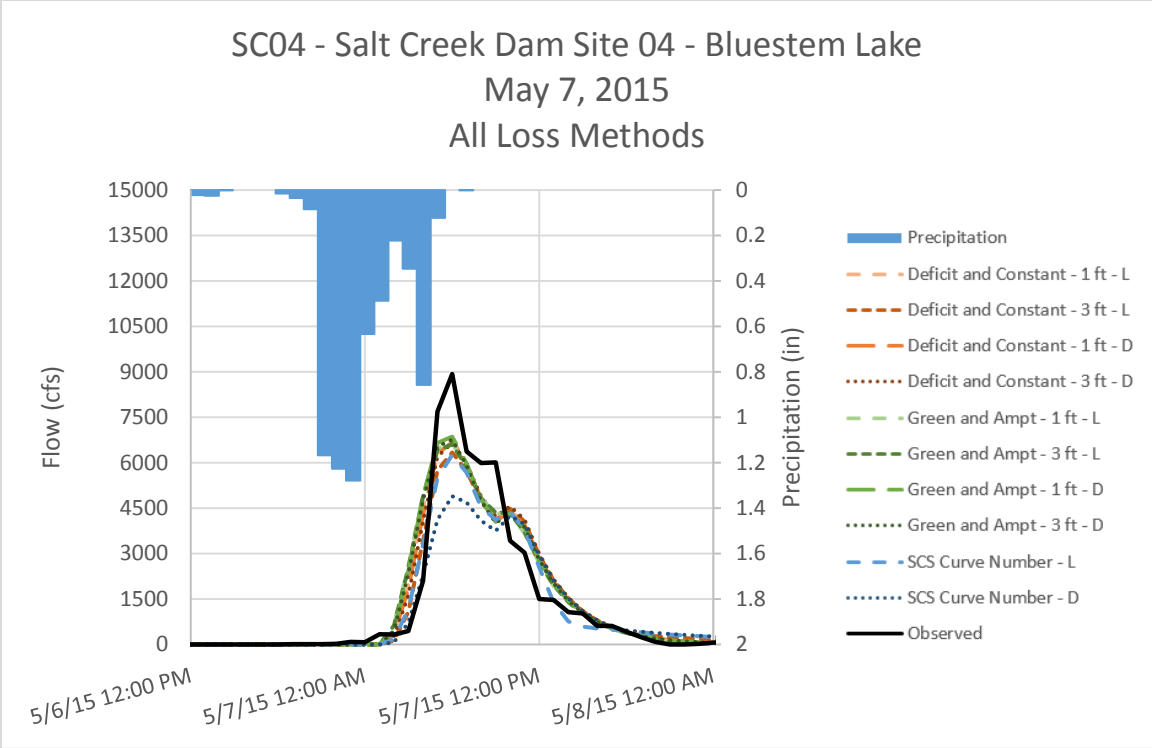

Figure C - 29. Runoff Hydrographs for SC04 - Salt Creek Dam Site 04 - Bluestem Lake for May 7, 2015 Event
All Loss Methods – Optimized Initial Conditions

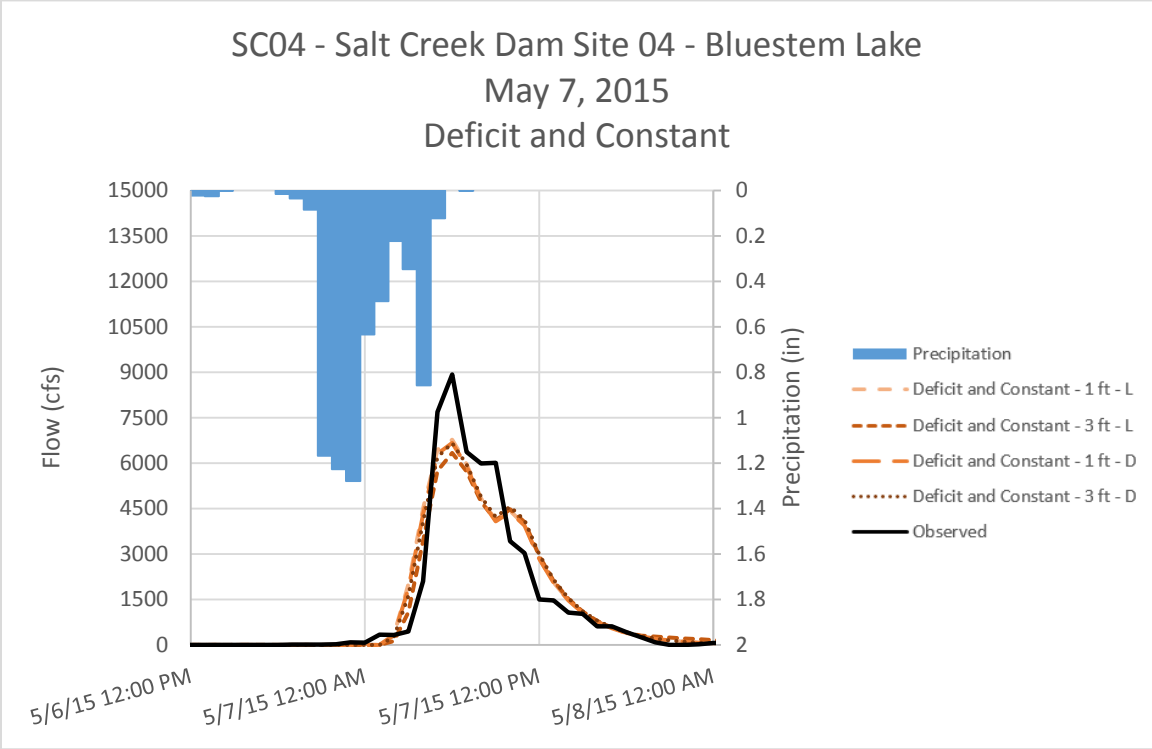

Figure C - 30. Runoff Hydrographs for SC04 - Salt Creek Dam Site 04 - Bluestem Lake for May 7, 2015 Event
Deficit and Constant Method – Optimized Initial Conditions

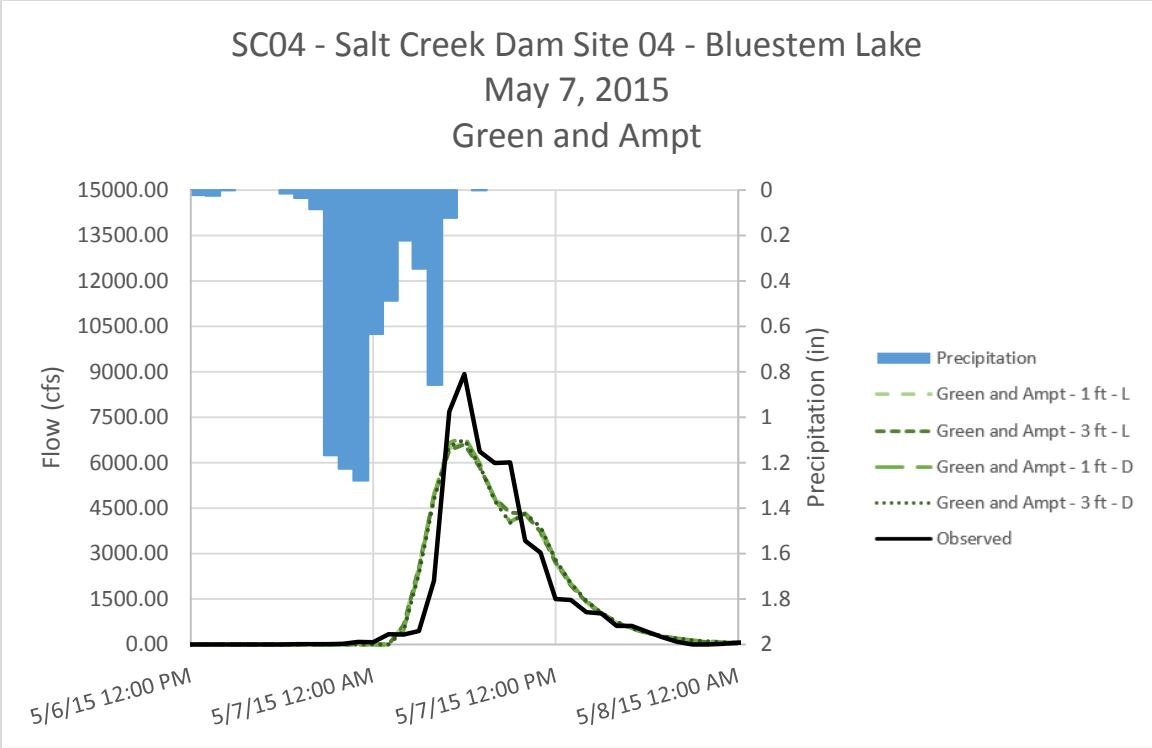

Figure C - 31. Runoff Hydrographs for SC04 - Salt Creek Dam Site 04 - Bluestem Lake for May 7, 2015 Event Green and Ampt Method – Optimized Initial Conditions

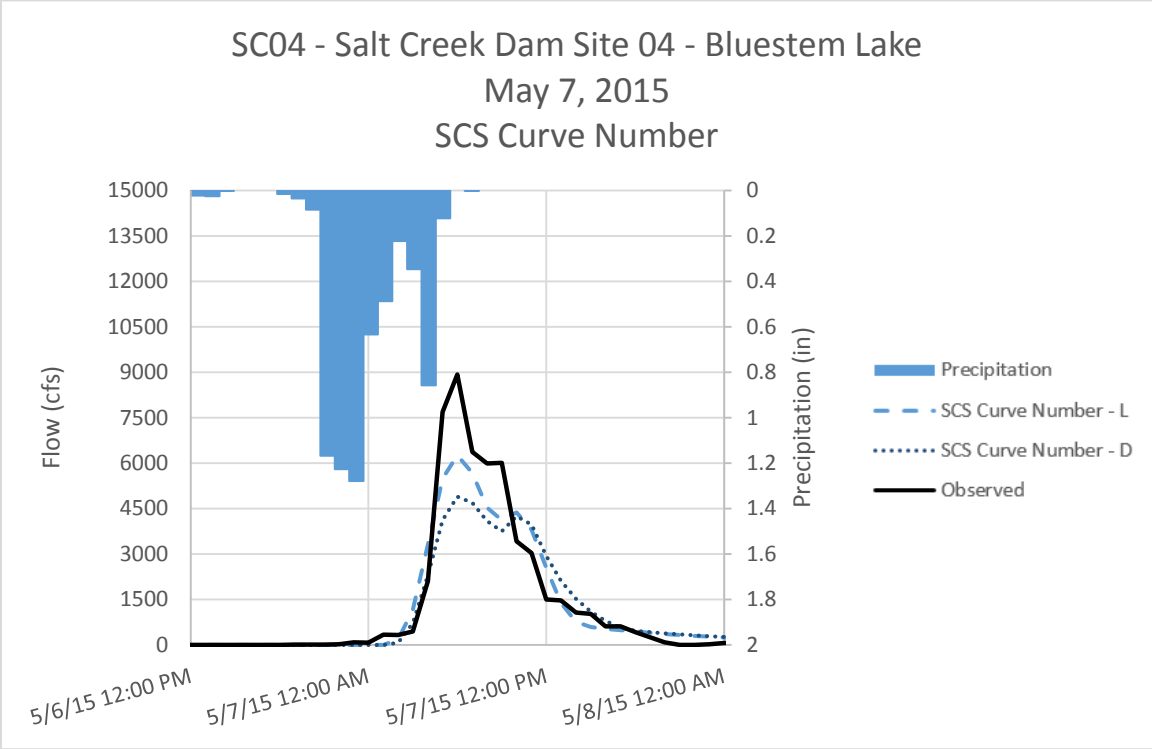

Figure C - 32. Runoff Hydrographs for SC04 - Salt Creek Dam Site 04 - Bluestem Lake for May 7, 2015 Event SCS Curve Number Method – Optimized Initial Conditions

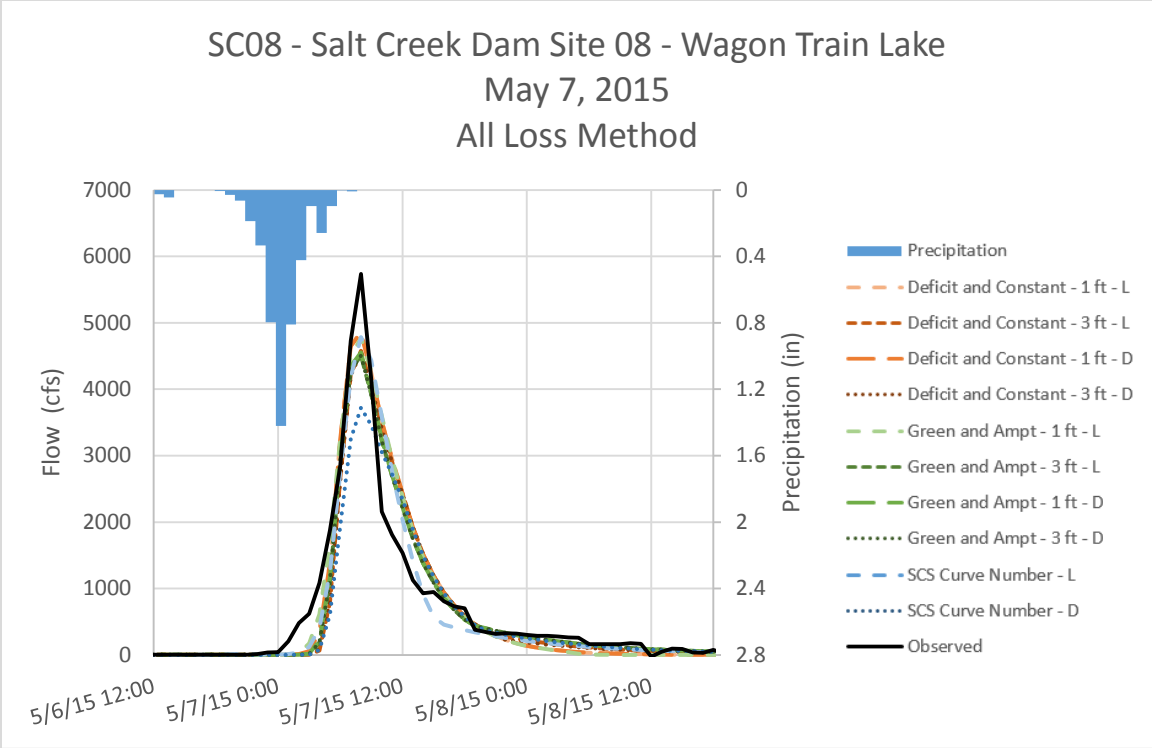

Figure C - 33. Runoff Hydrographs for SC08 - Salt Creek Dam Site 08 – Wagon Train Lake for May 7, 2015 Event All Loss Methods – Optimized Initial Conditions

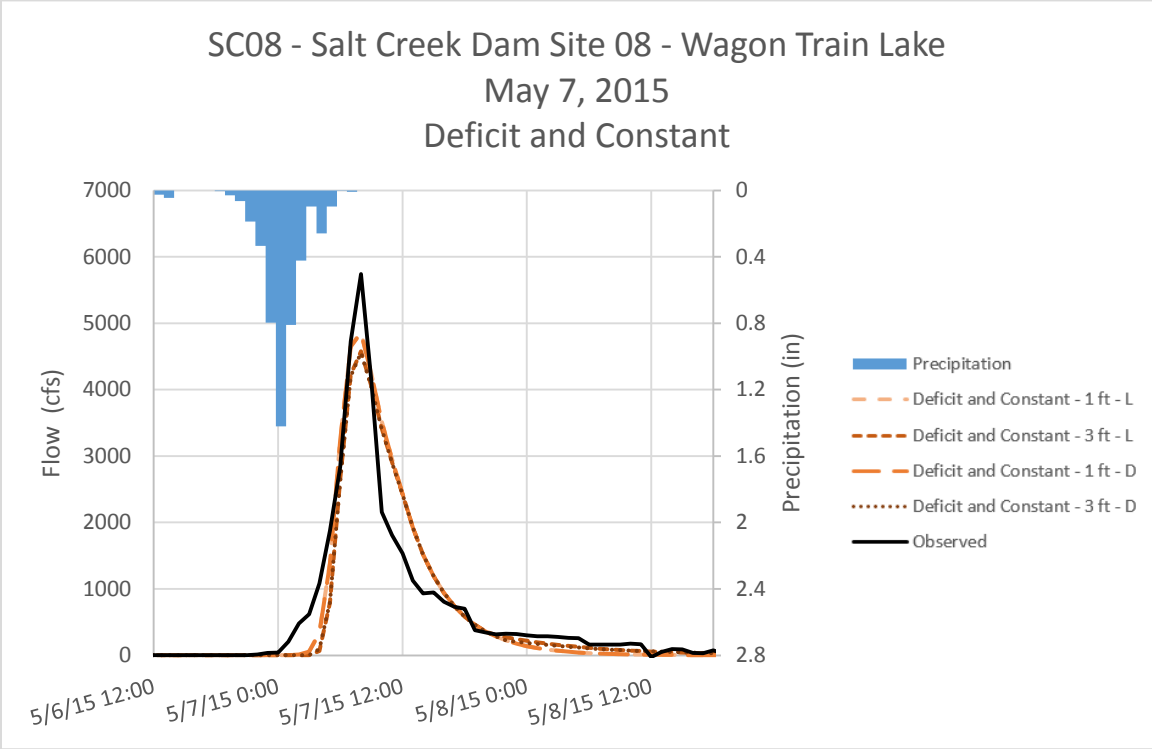

Figure C - 34. Runoff Hydrographs for SC08 - Salt Creek Dam Site 08 – Wagon Train Lake for May 7, 2015 Event Deficit and Constant Method – Optimized Initial Conditions

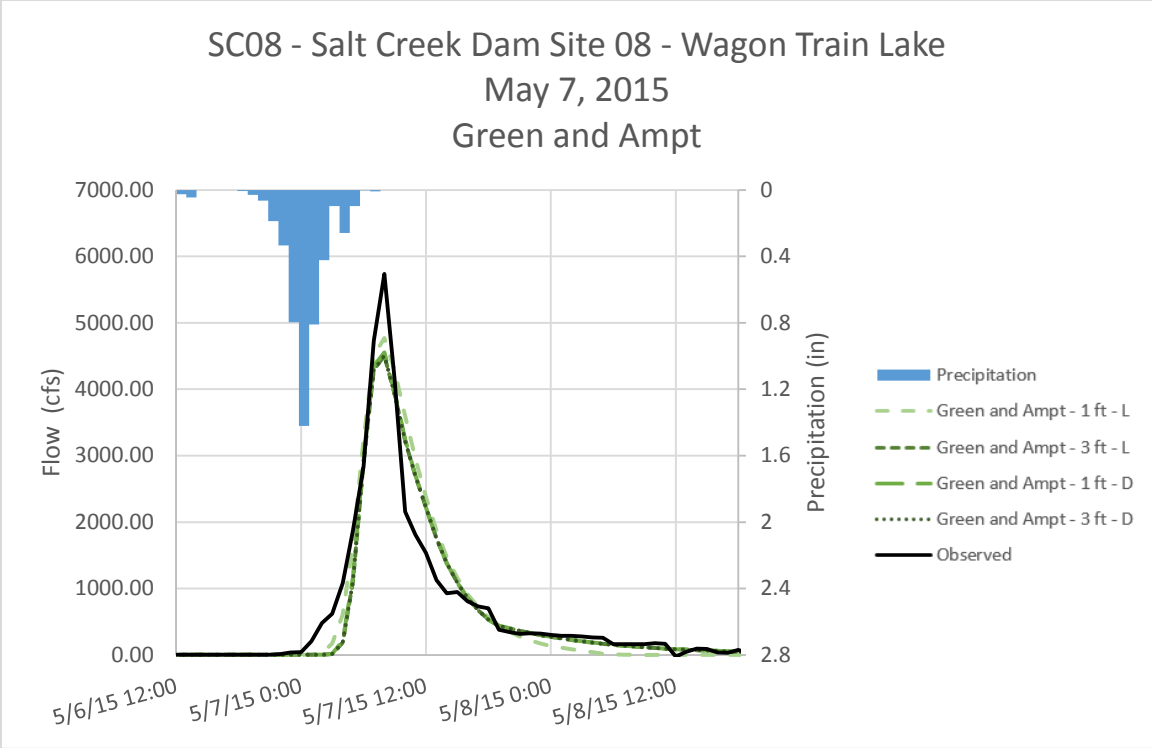

Figure C - 35. Runoff Hydrographs for SC08 - Salt Creek Dam Site 08 – Wagon Train Lake for May 7, 2015 Event Green and Ampt Method – Optimized Initial Conditions

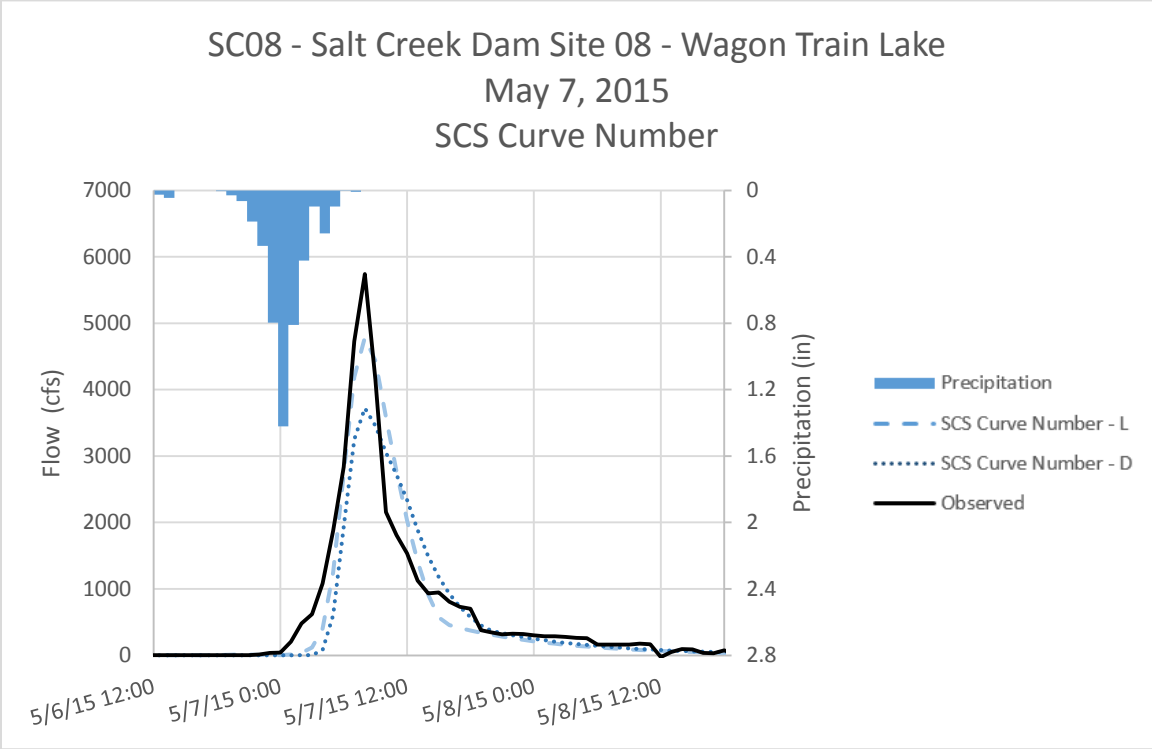

Figure C - 36. Runoff Hydrographs for SC08 - Salt Creek Dam Site 08 – Wagon Train Lake for May 7, 2015 Event SCS Curve Number Method – Optimized Initial Conditions

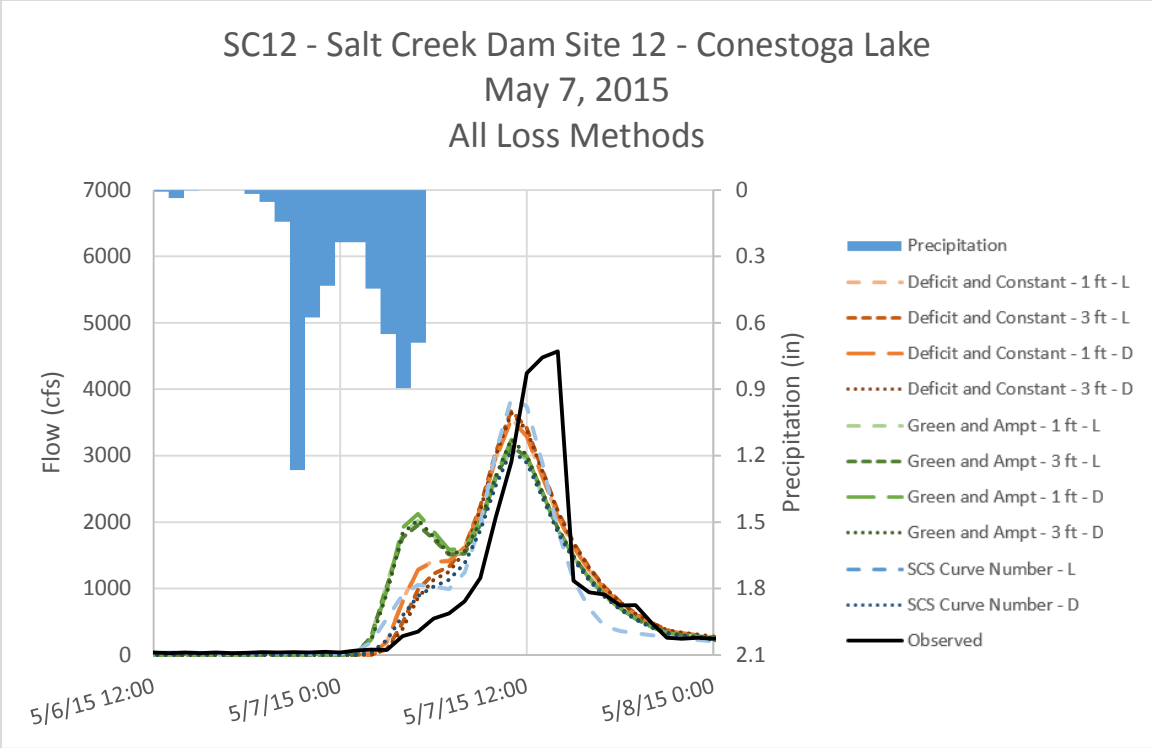

Figure C - 37. Runoff Hydrographs for SC12 - Salt Creek Dam Site 12 – Conestoga Lake for May 7, 2015 Event
All Loss Methods – Optimized Initial Conditions

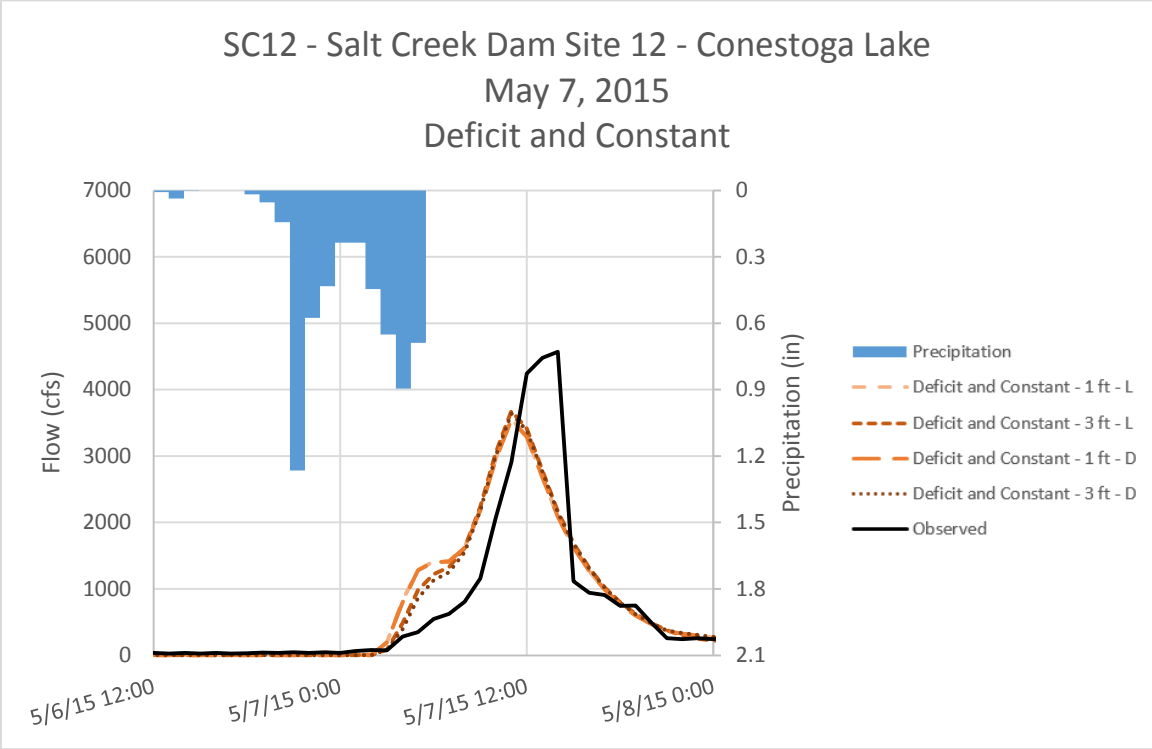

Figure C - 38. Runoff Hydrographs for SC12 - Salt Creek Dam Site 12 – Conestoga Lake for May 7, 2015 Event
Deficit and Constant Method – Optimized Initial Conditions

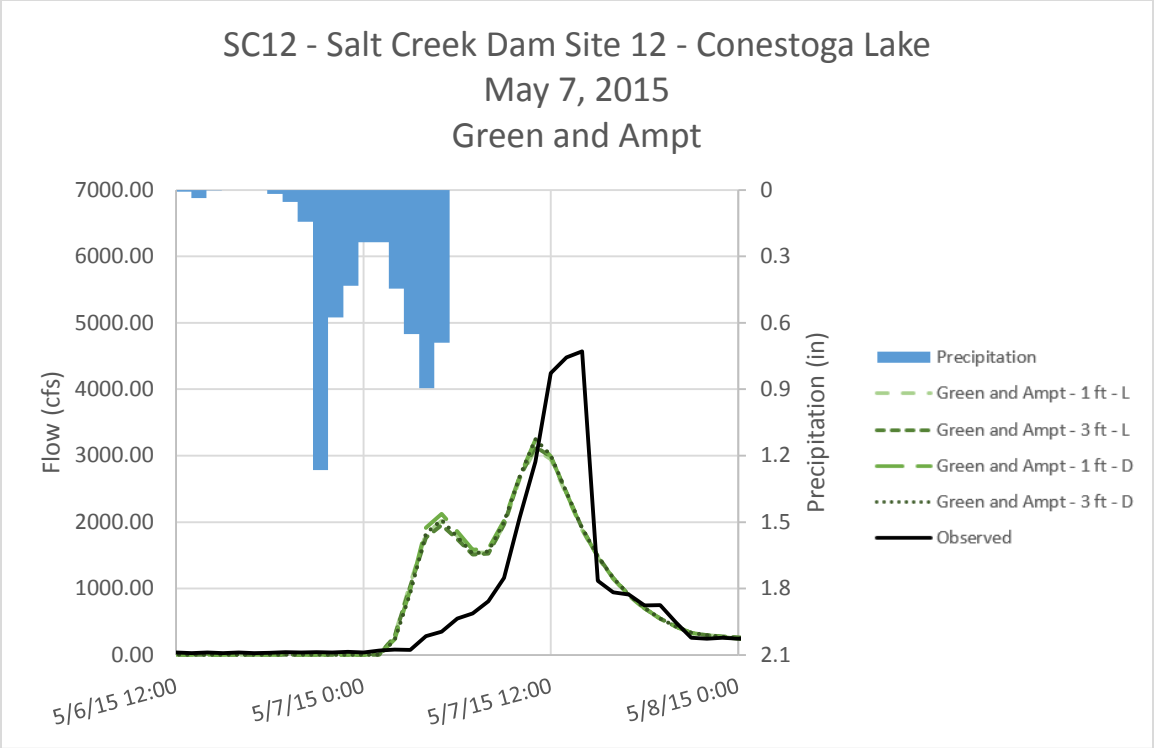

Figure C - 39. Runoff Hydrographs for SC12 - Salt Creek Dam Site 12 – Conestoga Lake for May 7, 2015 Event Green and Ampt Method – Optimized Initial Conditions

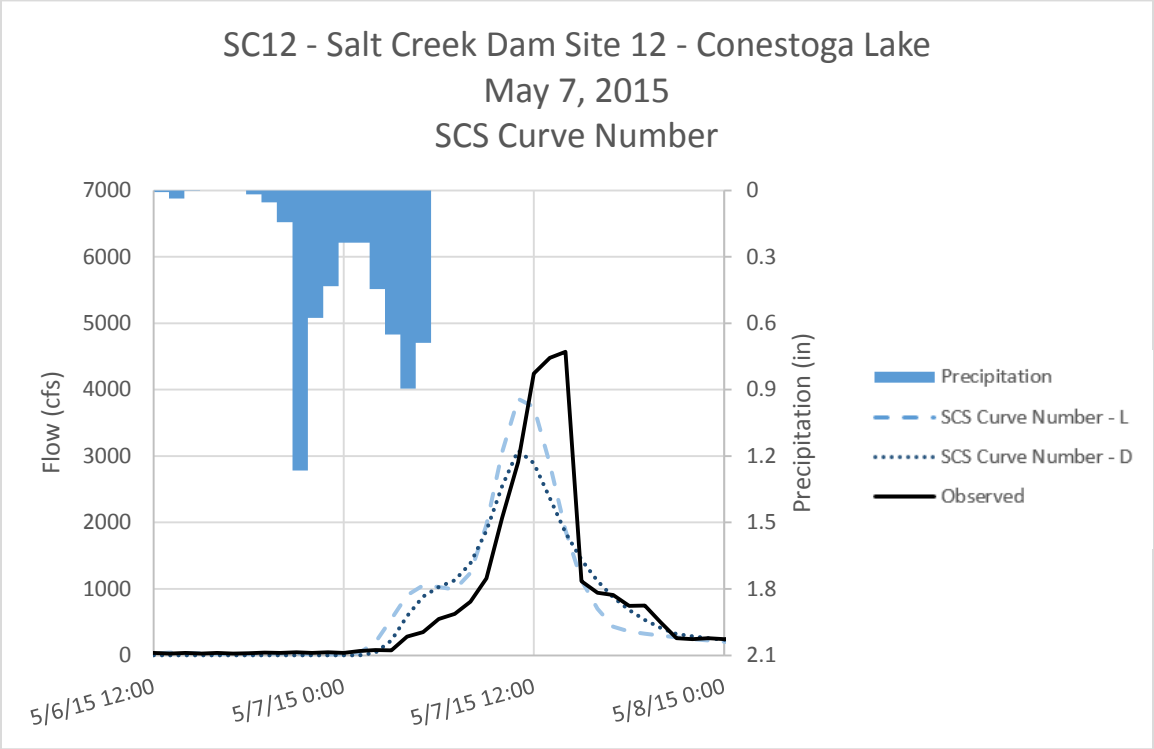

Figure C - 40. Runoff Hydrographs for SC12 - Salt Creek Dam Site 12 – Conestoga Lake for May 7, 2015 Event SCS Curve Number Method – Optimized Initial Conditions

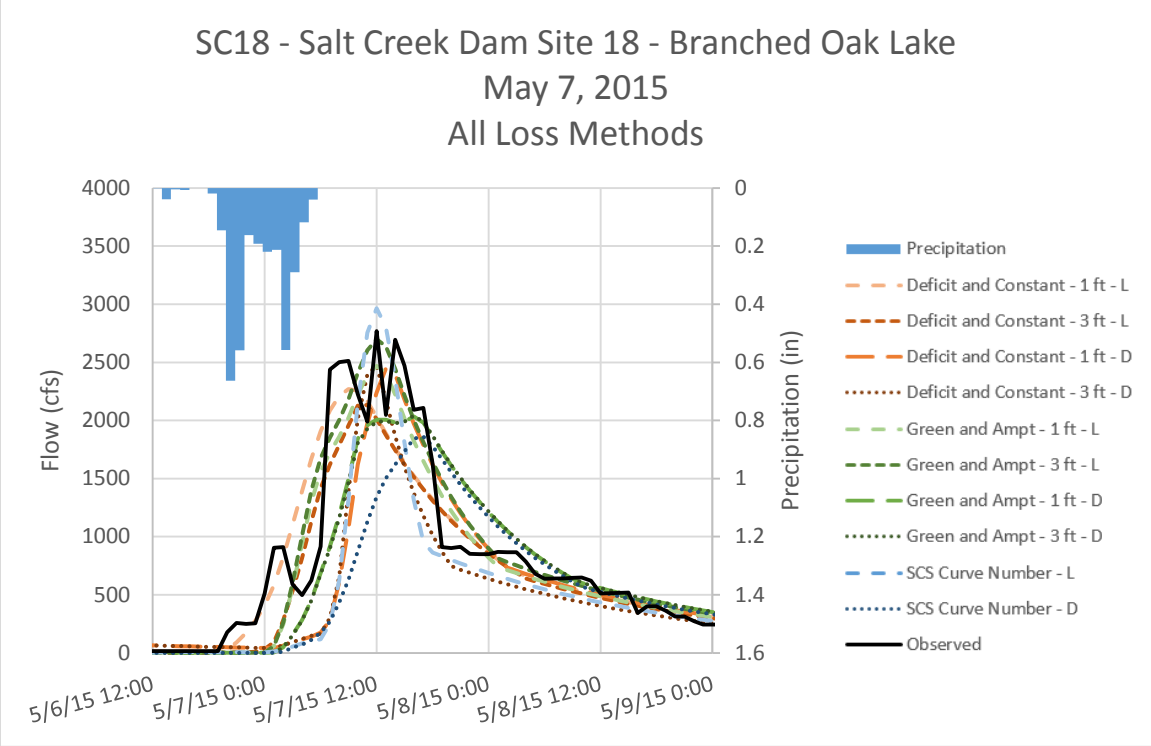

Figure C - 41. Runoff Hydrographs for SC18 - Salt Creek Dam Site 18 – Branched Oak Lake for May 7, 2015 Event All Loss Methods – Optimized Initial Conditions

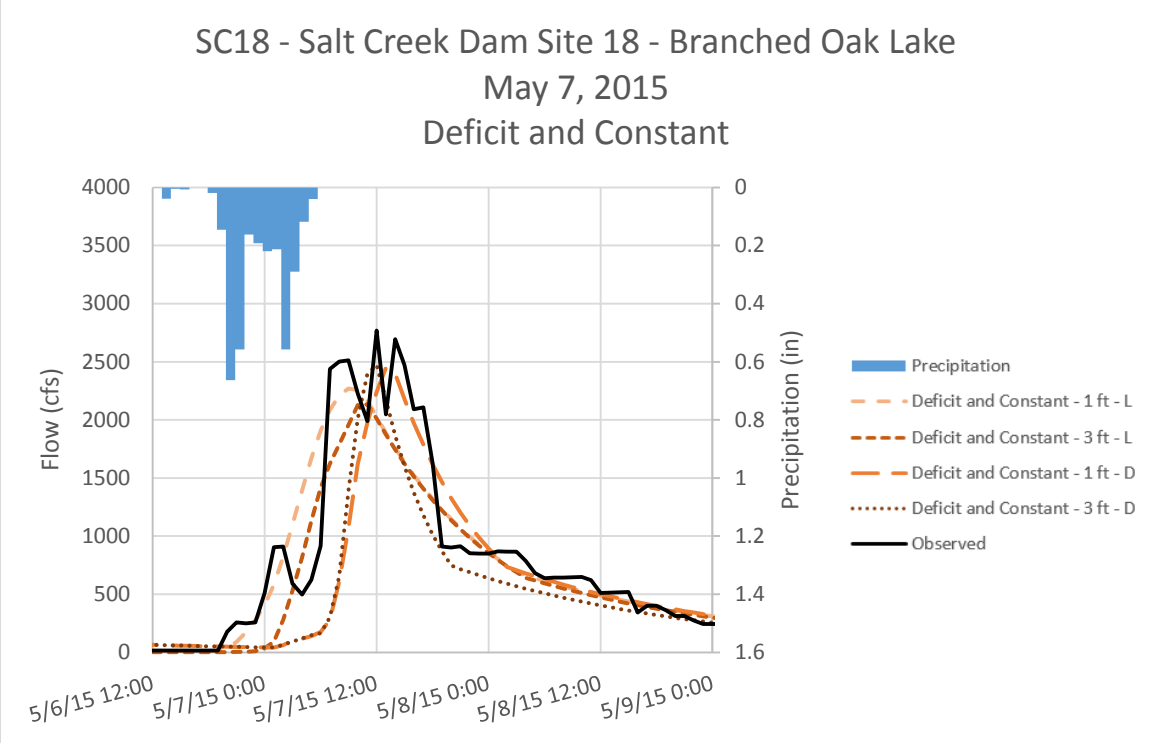

Figure C - 42. Runoff Hydrographs for SC18 - Salt Creek Dam Site 18 – Branched Oak Lake for May 7, 2015 Event Deficit and Constant Method – Optimized Initial Conditions

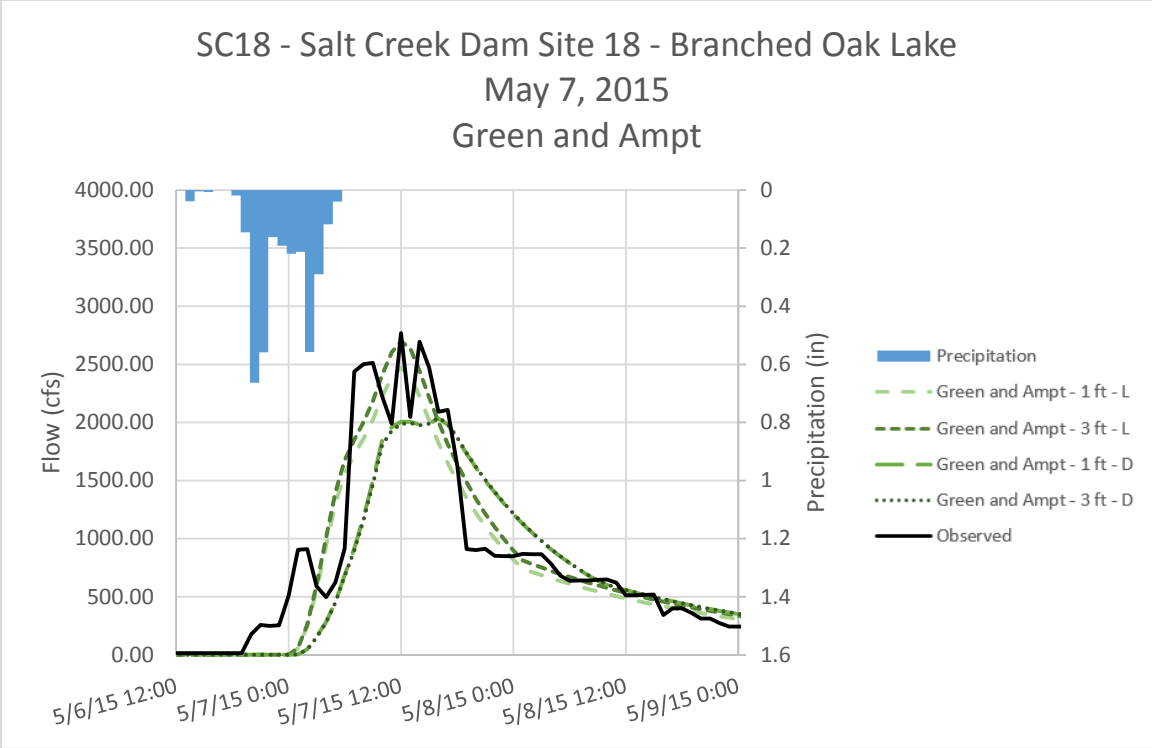

Figure C - 43. Runoff Hydrographs for SC18 - Salt Creek Dam Site 18 – Branched Oak Lake for May 7, 2015 Event Green and Ampt Method – Optimized Initial Conditions

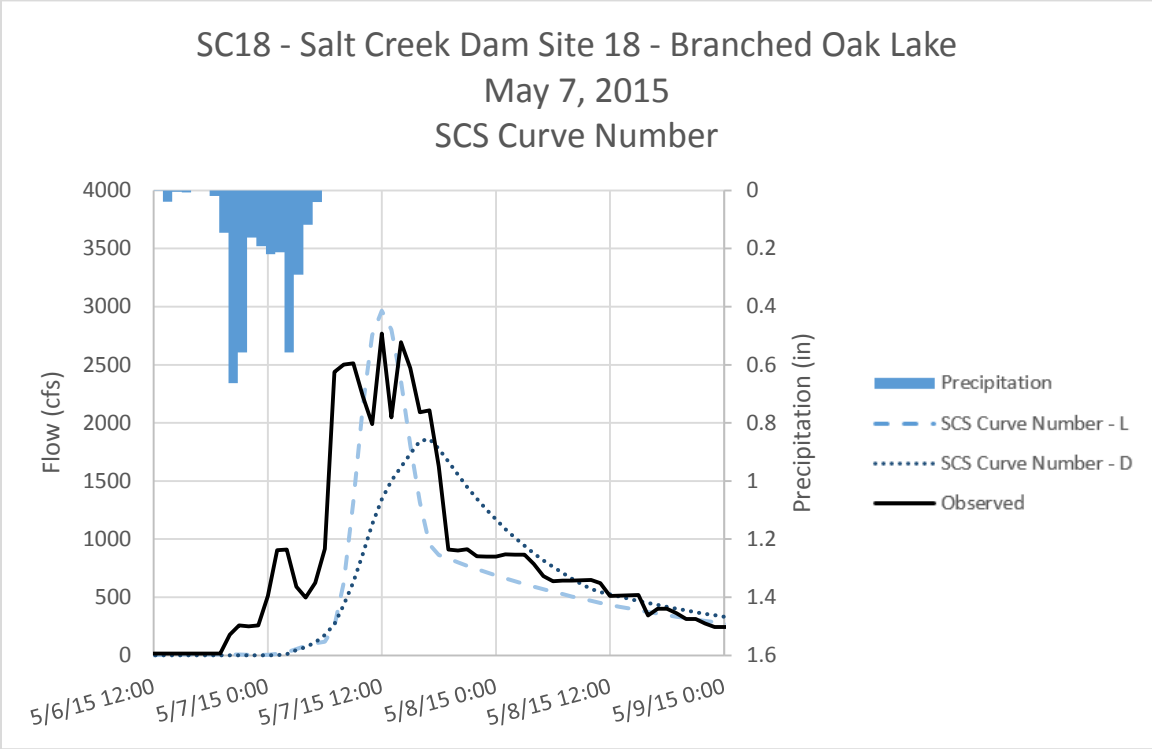

Figure C - 44. Runoff Hydrographs for SC18 - Salt Creek Dam Site 18 – Branched Oak Lake for May 7, 2015 Event SCS Curve Number Method – Optimized Initial Conditions

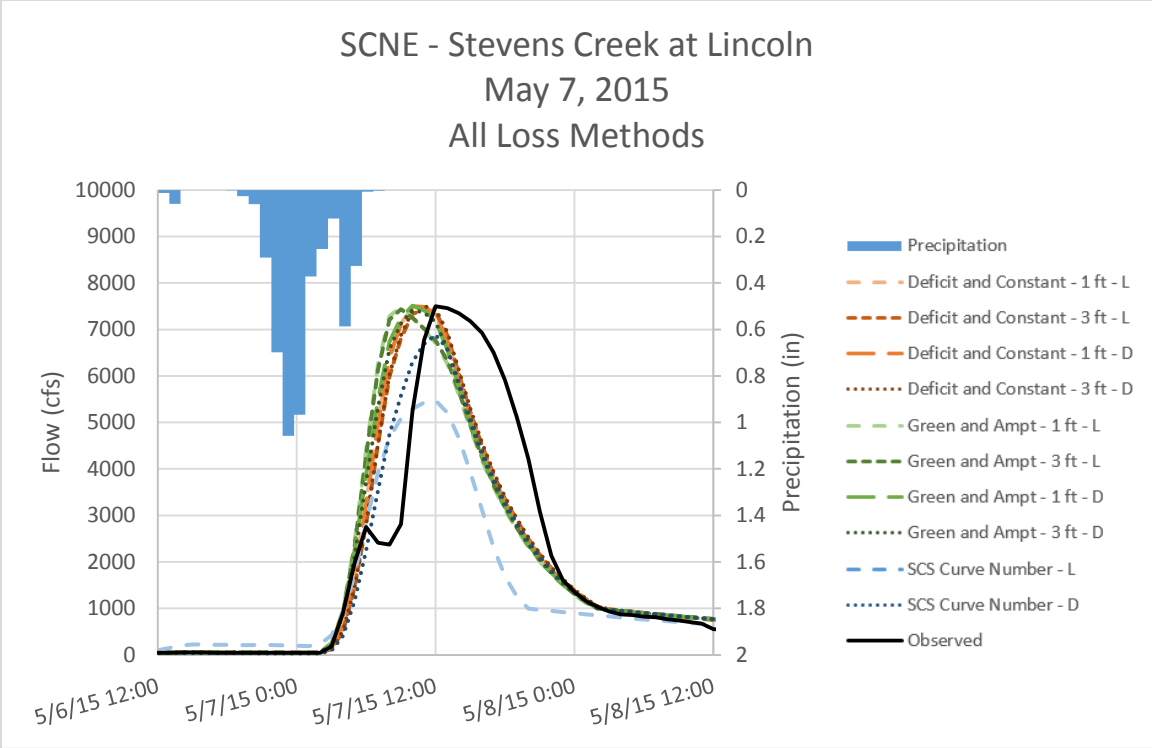

Figure C - 45. Runoff Hydrographs for SCNE – Stevens Creek at Lincoln for May 7, 2015 Event
All Loss Methods – Optimized Initial Conditions

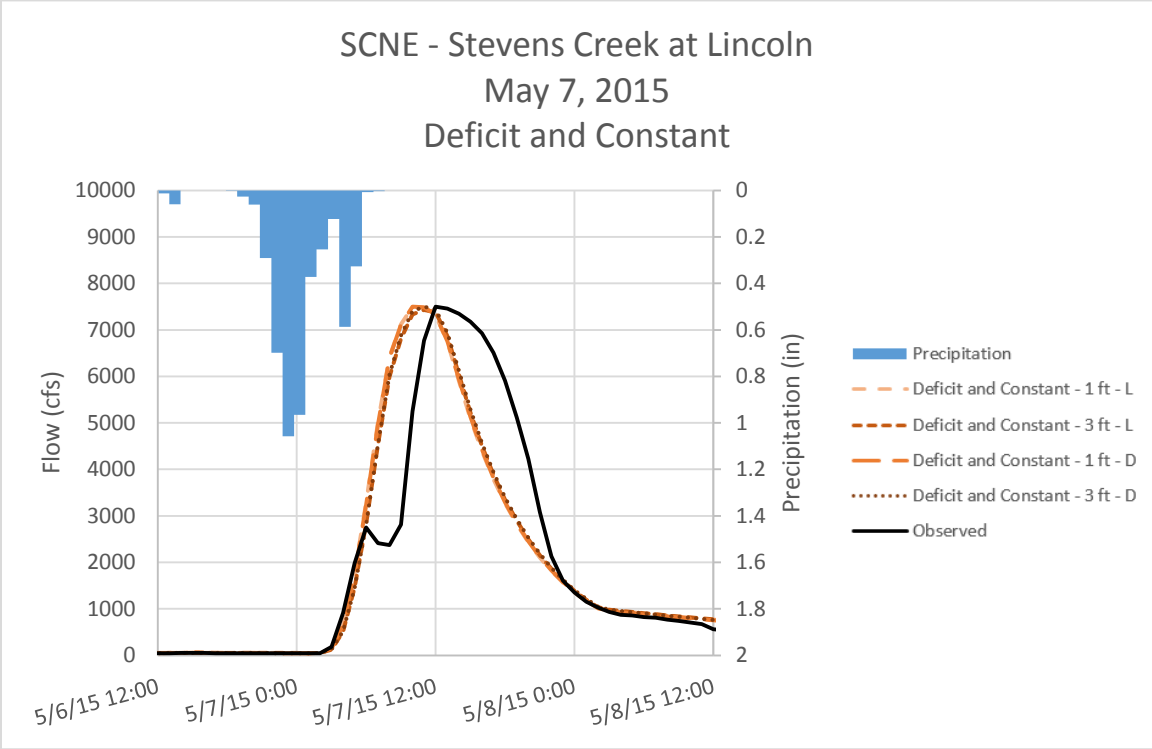

Figure C - 46. Runoff Hydrographs for SCNE – Stevens Creek at Lincoln for May 7, 2015 Event
Deficit and Constant Method – Optimized Initial Conditions

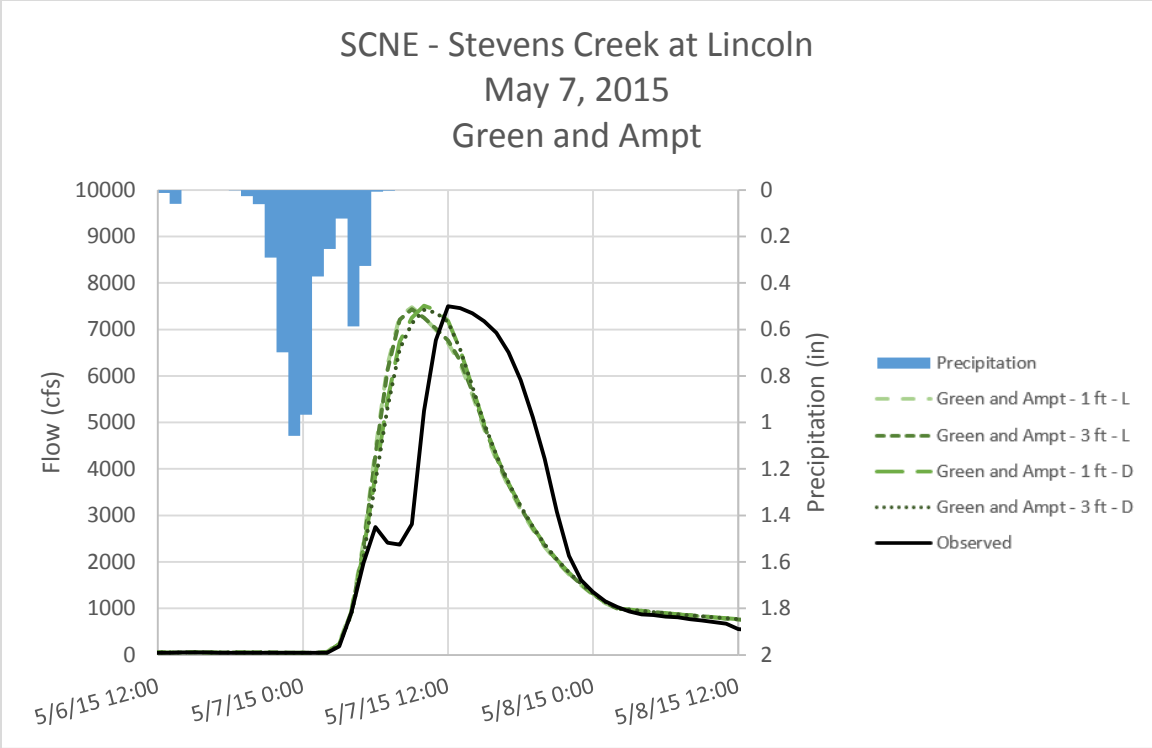

Figure C - 47. Runoff Hydrographs for SCNE – Stevens Creek at Lincoln for May 7, 2015 Event
Green and Ampt Method – Optimized Initial Conditions

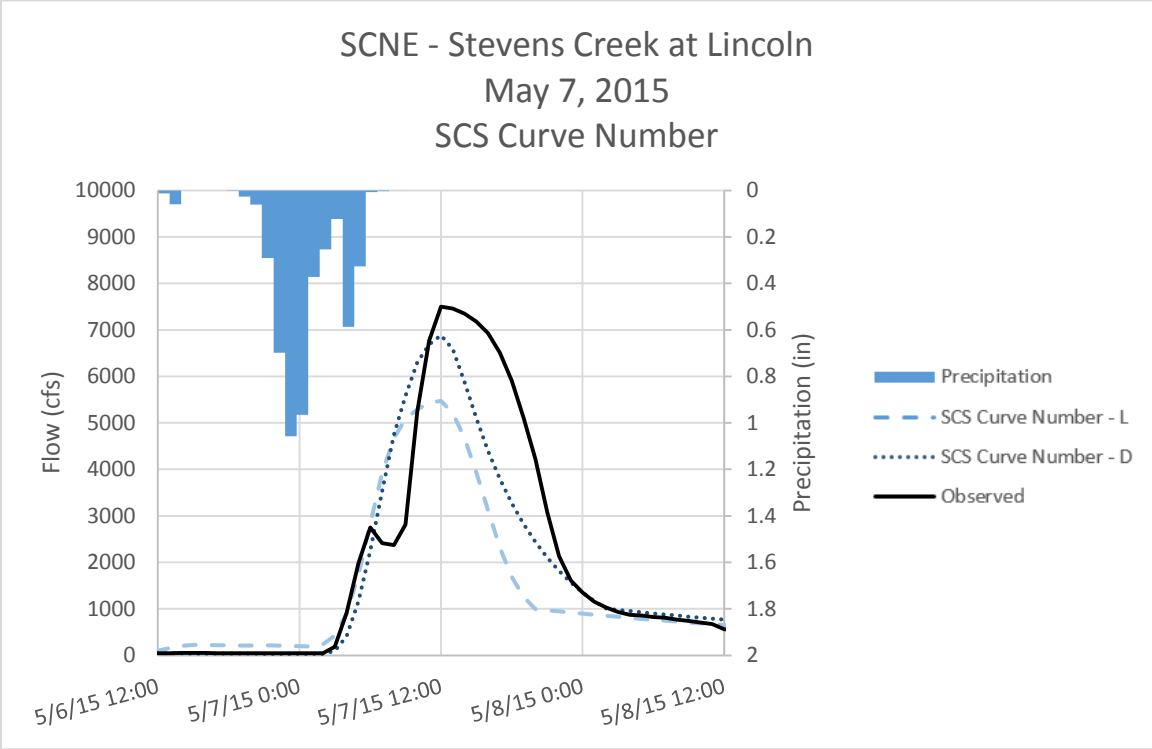

Figure C - 48. Runoff Hydrographs for SCNE – Stevens Creek at Lincoln for May 7, 2015 Event
SCS Curve Number Method – Optimized Initial Conditions

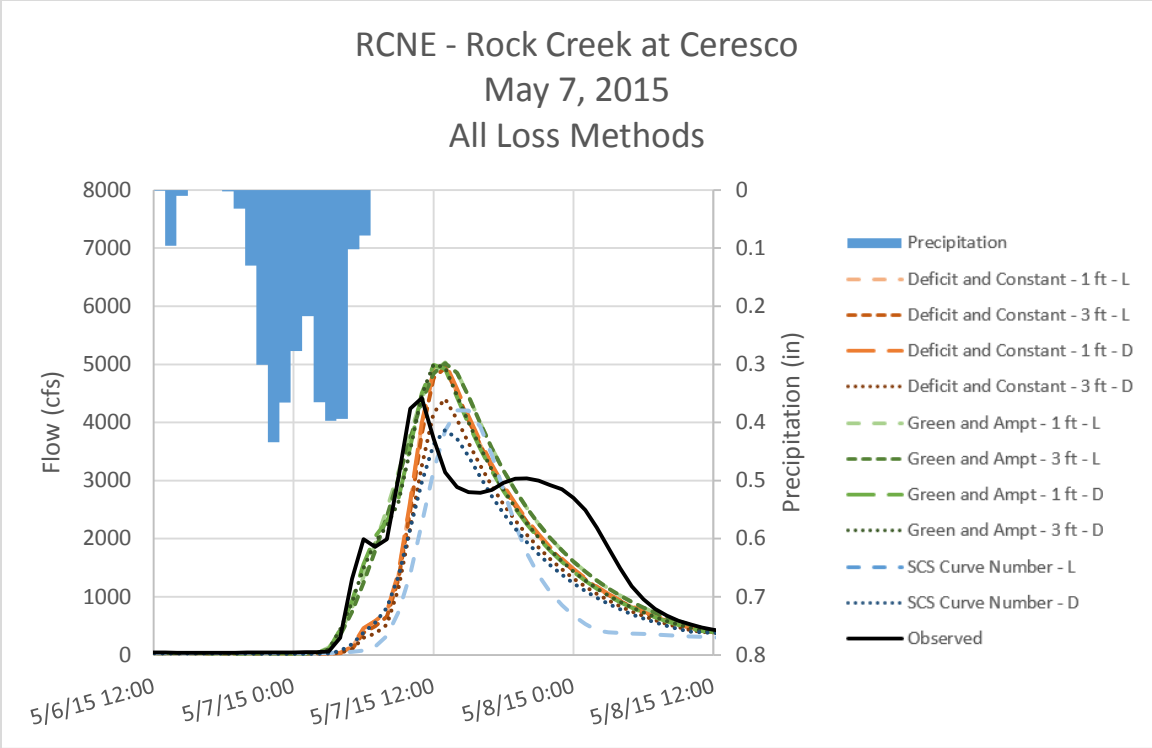

Figure C - 49. Runoff Hydrographs for RCNE – Rock Creek at Ceresco for May 7, 2015 Event
All Loss Methods – Optimized Initial Conditions

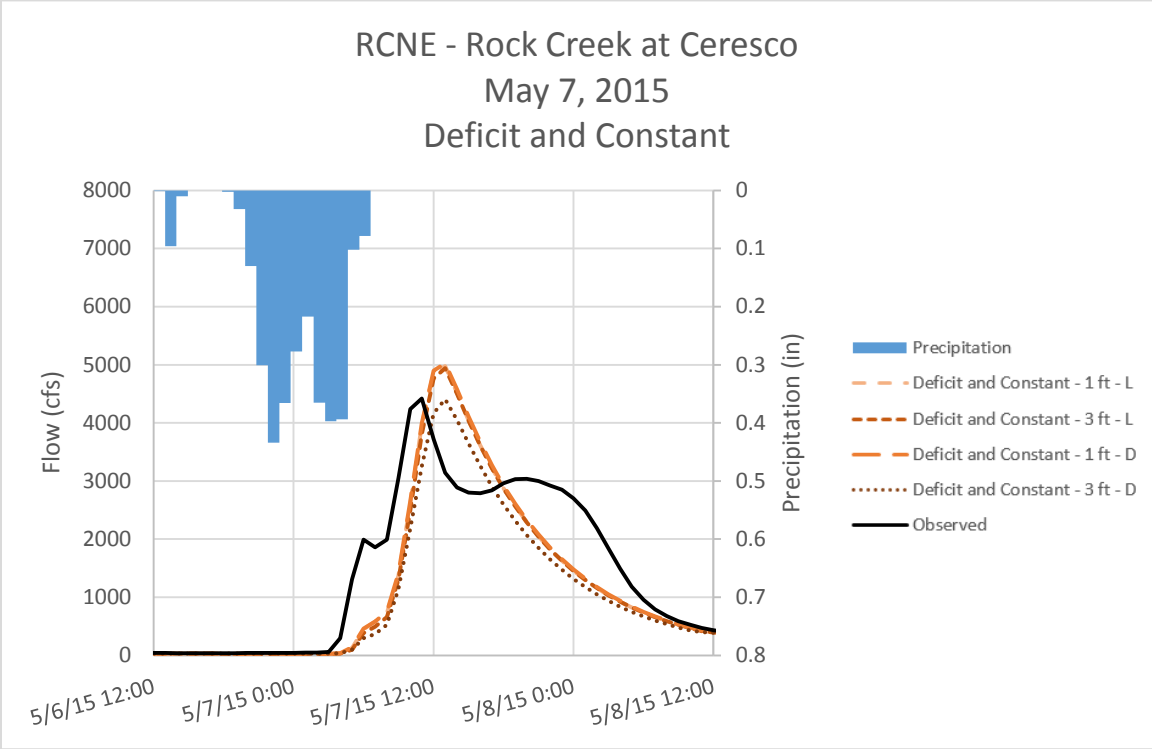

Figure C - 50. Runoff Hydrographs for RCNE – Rock Creek at Ceresco for May 7, 2015 Event
Deficit and Constant Method – Optimized Initial Conditions

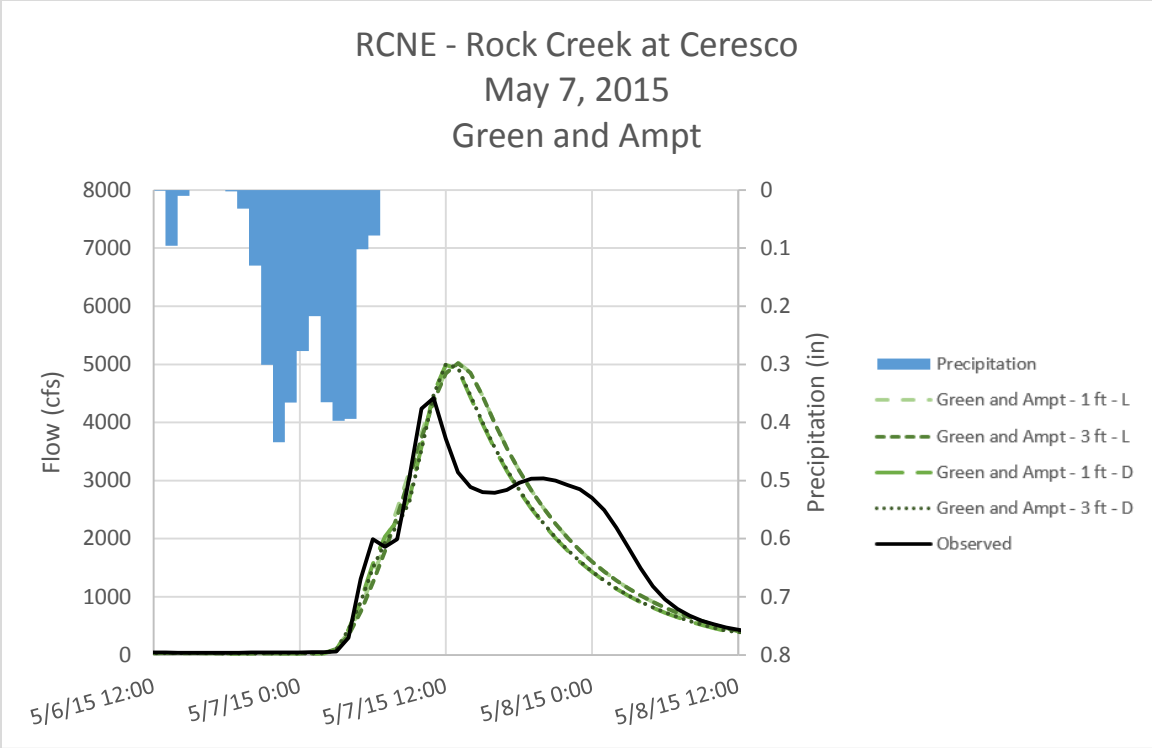

Figure C - 51. Runoff Hydrographs for RCNE – Rock Creek at Ceresco for May 7, 2015 Event
Green and Ampt Method – Optimized Initial Conditions

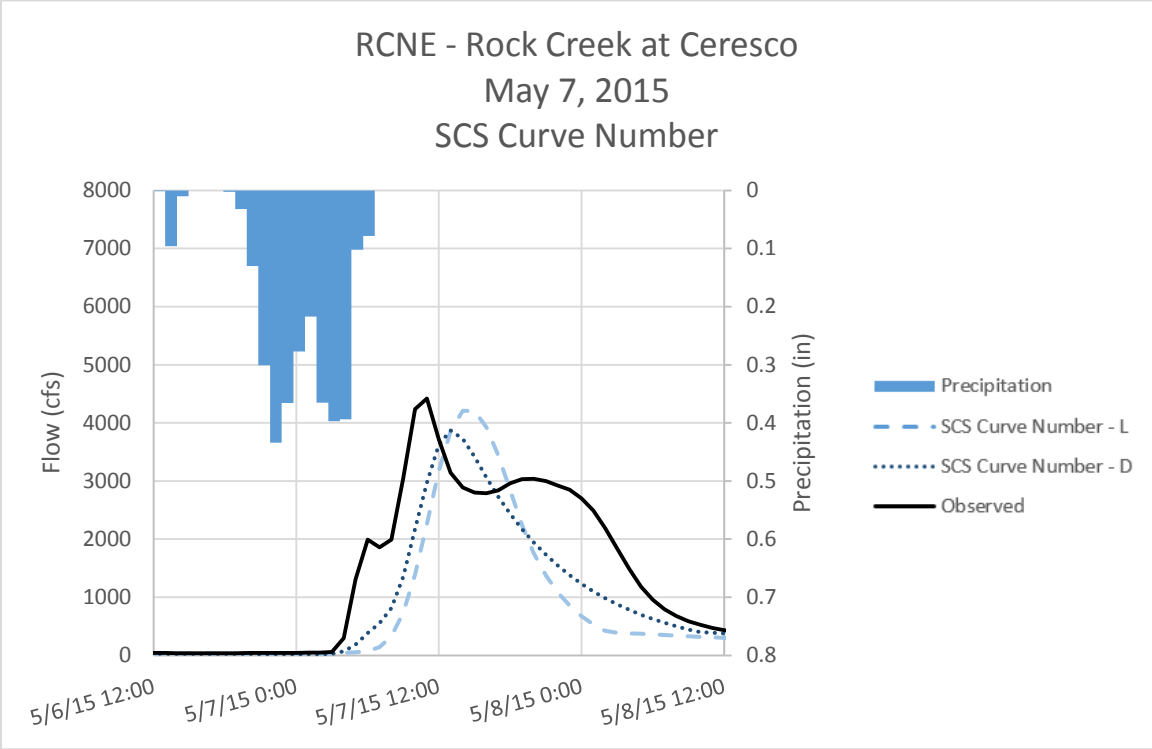

Figure C - 52. Runoff Hydrographs for RCNE – Rock Creek at Ceresco for May 7, 2015 Event
SCS Curve Number Method – Optimized Initial Conditions

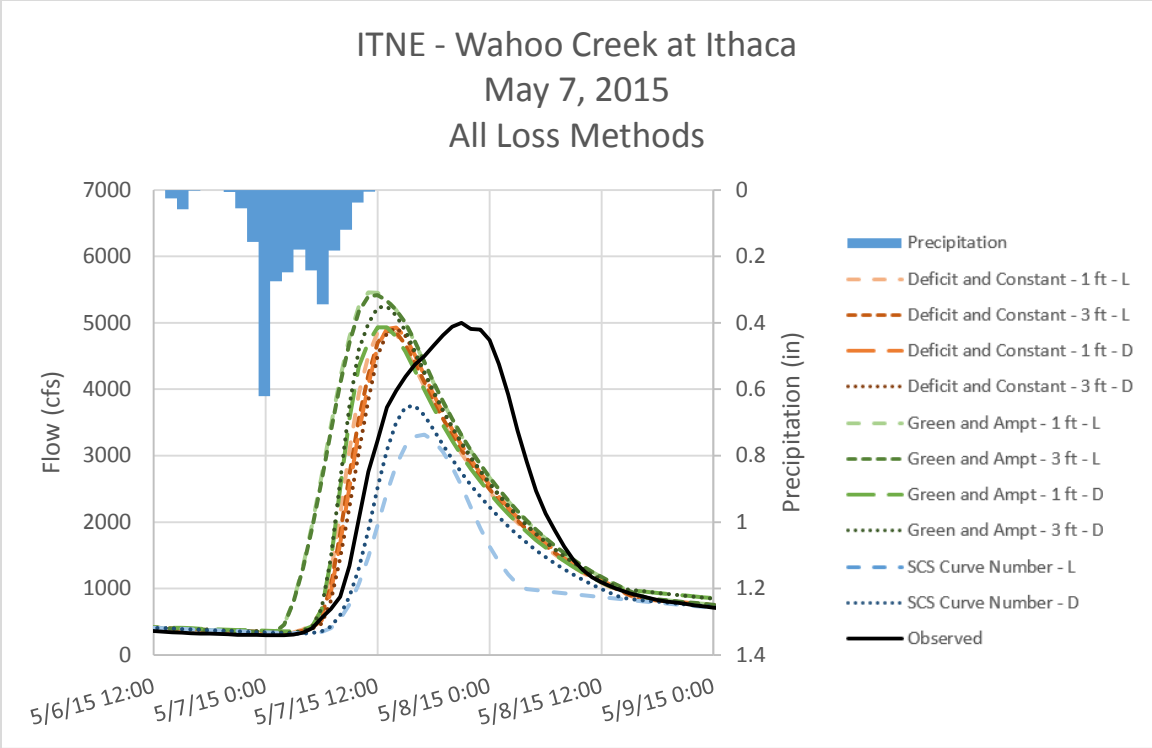

Figure C - 53. Runoff Hydrographs for ITNE – Wahoo Creek at Ithaca for May 7, 2015 Event
All Loss Methods – Optimized Initial Conditions

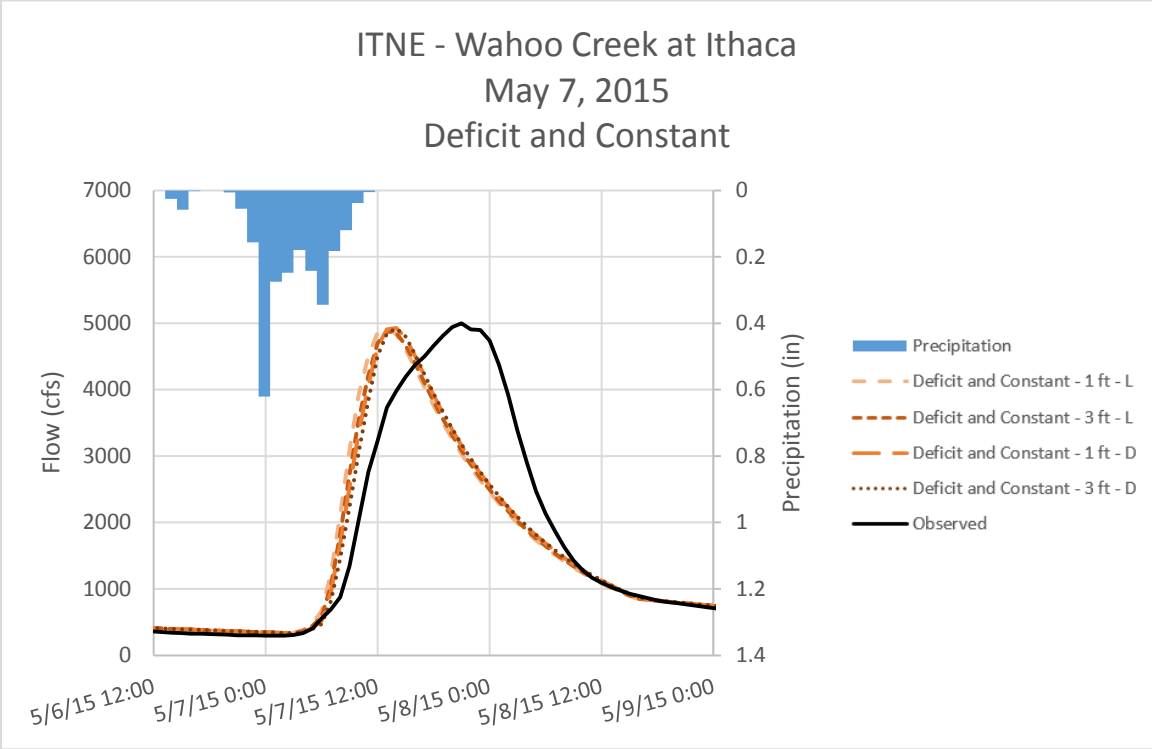

Figure C - 54. Runoff Hydrographs for ITNE – Wahoo Creek at Ithaca for May 7, 2015 Event
Deficit and Constant Method – Optimized Initial Conditions

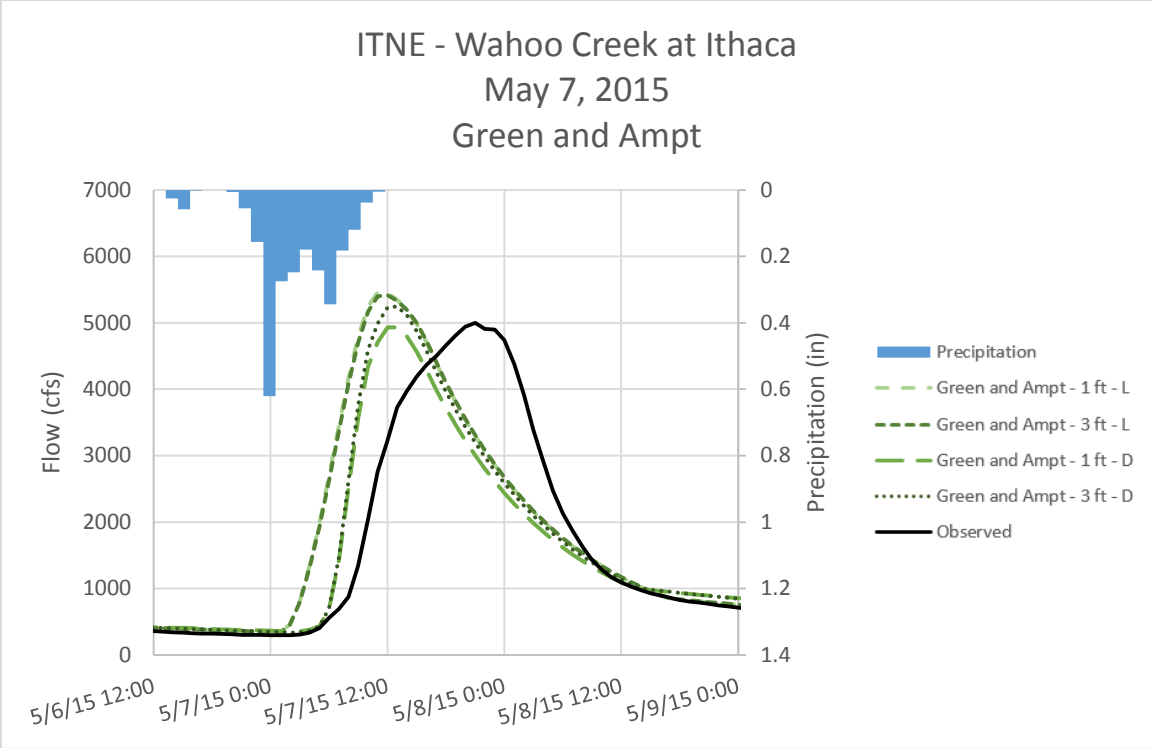

Figure C - 55. Runoff Hydrographs for ITNE – Wahoo Creek at Ithaca for May 7, 2015 Event
Green and Ampt Method – Optimized Initial Conditions

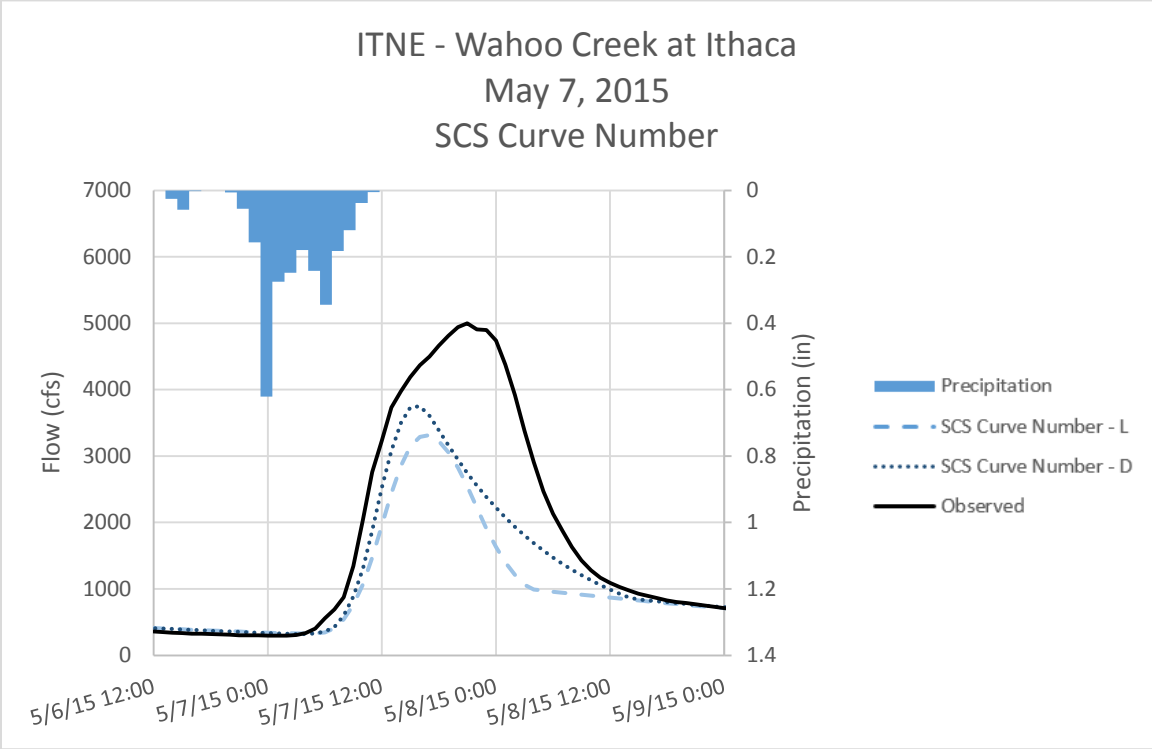

Figure C - 56. Runoff Hydrographs for ITNE – Wahoo Creek at Ithaca for May 7, 2015 Event
SCS Curve Number – Optimized Initial Conditions

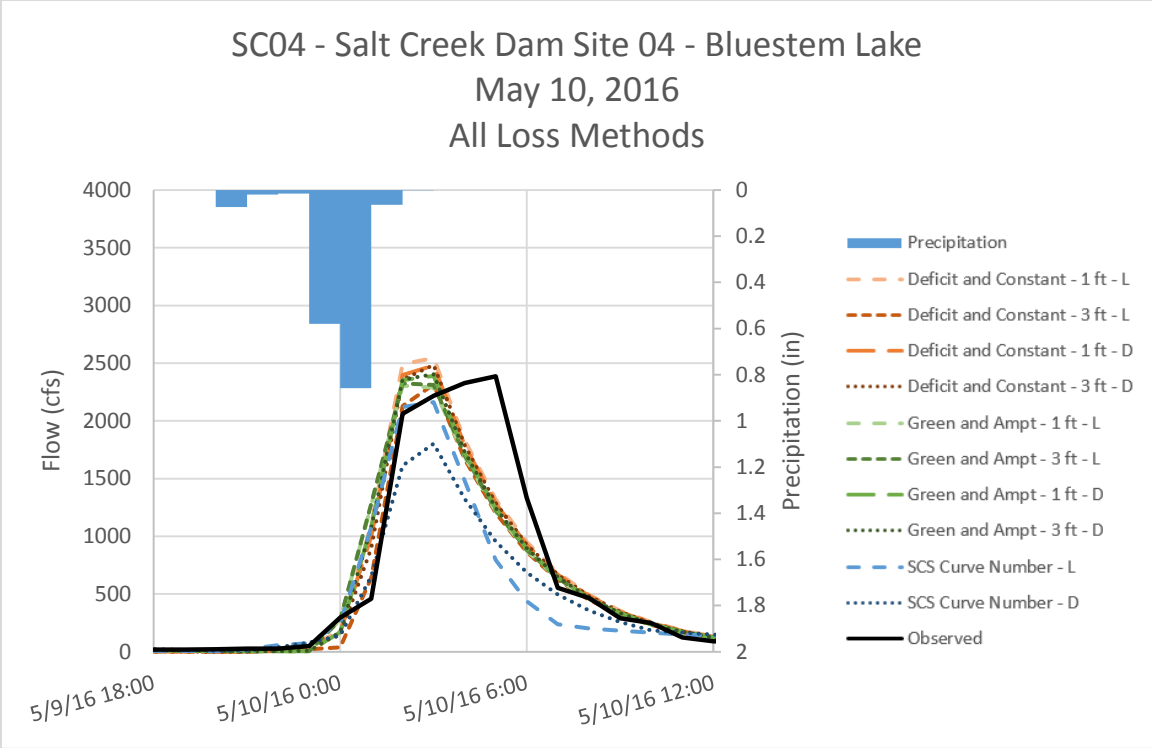

Figure C - 57. Runoff Hydrographs for SC04 - Salt Creek Dam Site 04 - Bluestem Lake for May 10, 2016 Event All Loss Methods – Optimized Initial Conditions

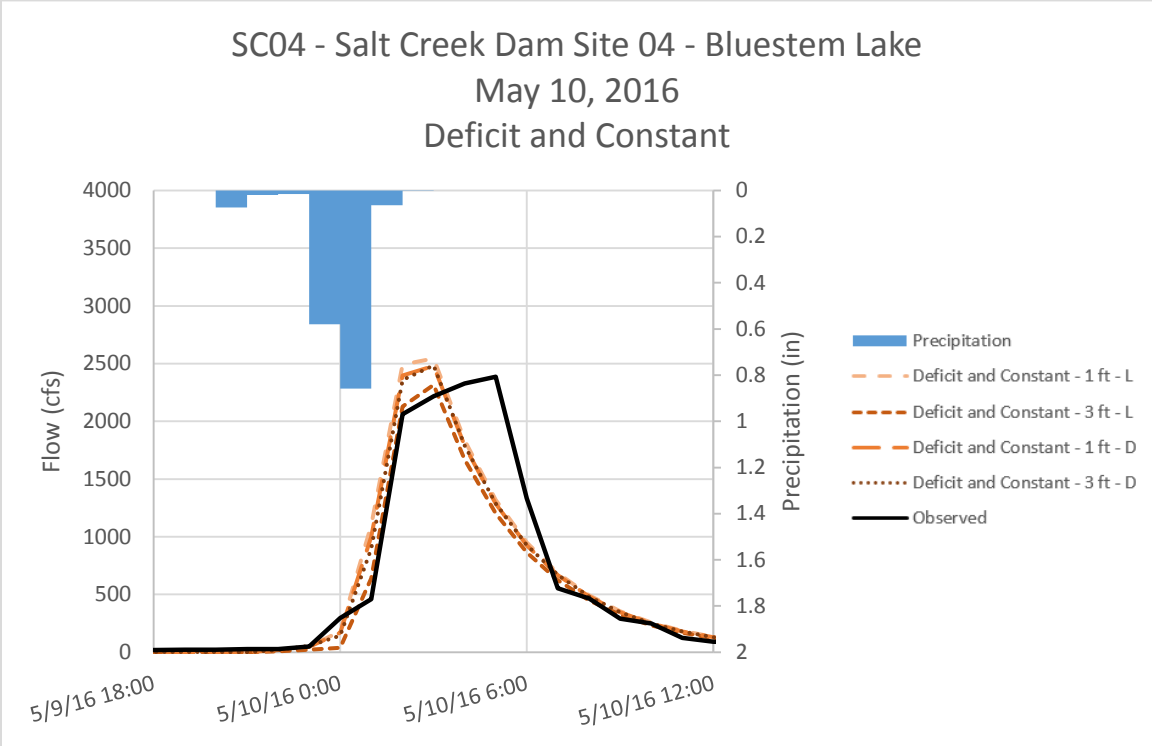

Figure C - 58. Runoff Hydrographs for SC04 - Salt Creek Dam Site 04 - Bluestem Lake for May 10, 2016 Event Deficit and Constant Method – Optimized Initial Conditions

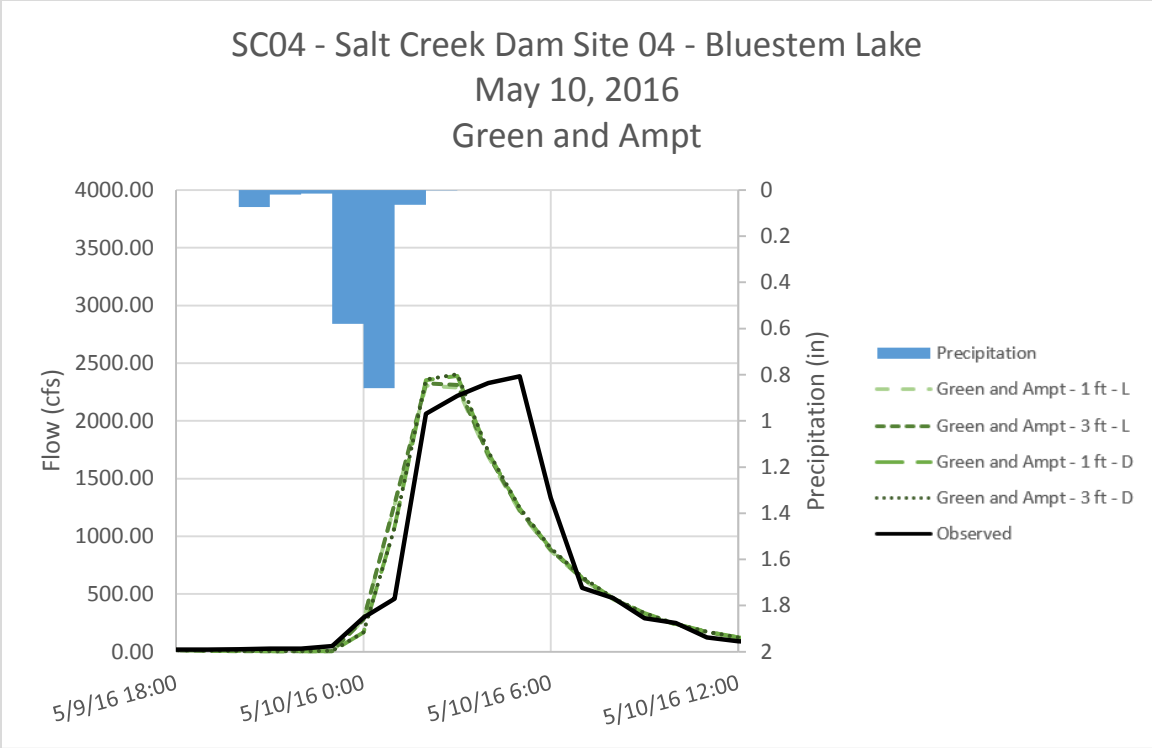

Figure C - 59. Runoff Hydrographs for SC04 - Salt Creek Dam Site 04 - Bluestem Lake for May 10, 2016 Event Green and Ampt Method – Optimized Initial Conditions

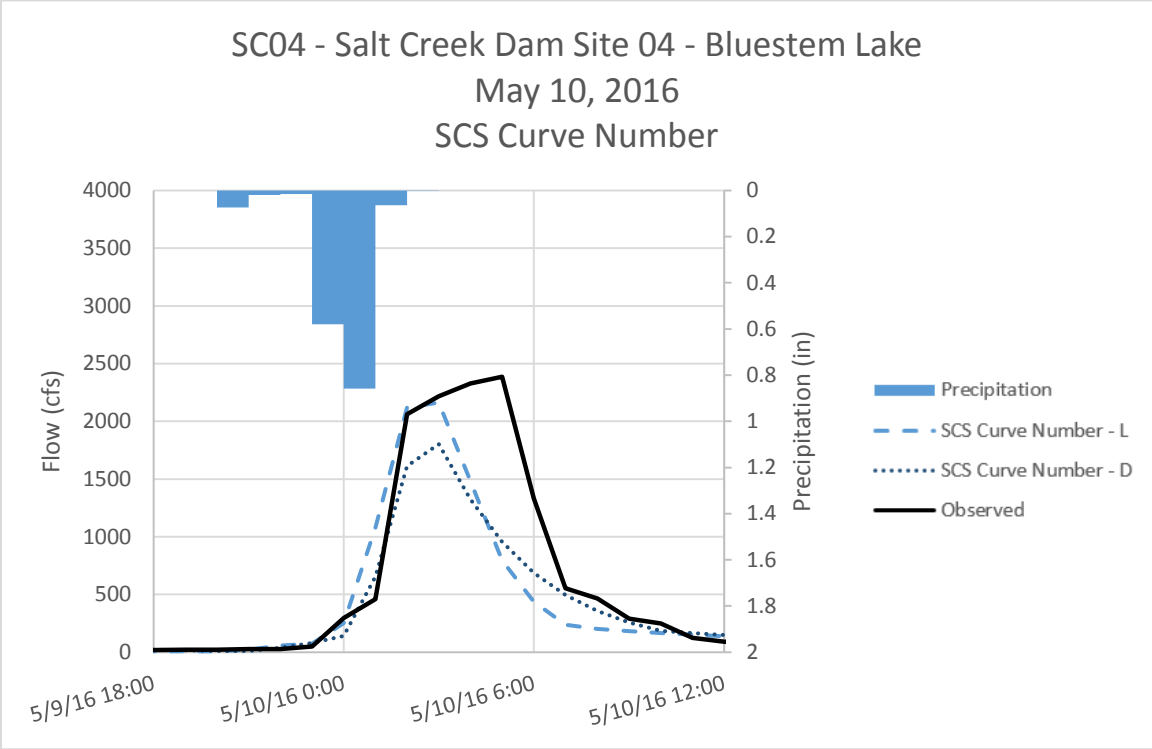

Figure C - 60. Runoff Hydrographs for SC04 - Salt Creek Dam Site 04 - Bluestem Lake for May 10, 2016 Event SCS Curve Number Method – Optimized Initial Conditions

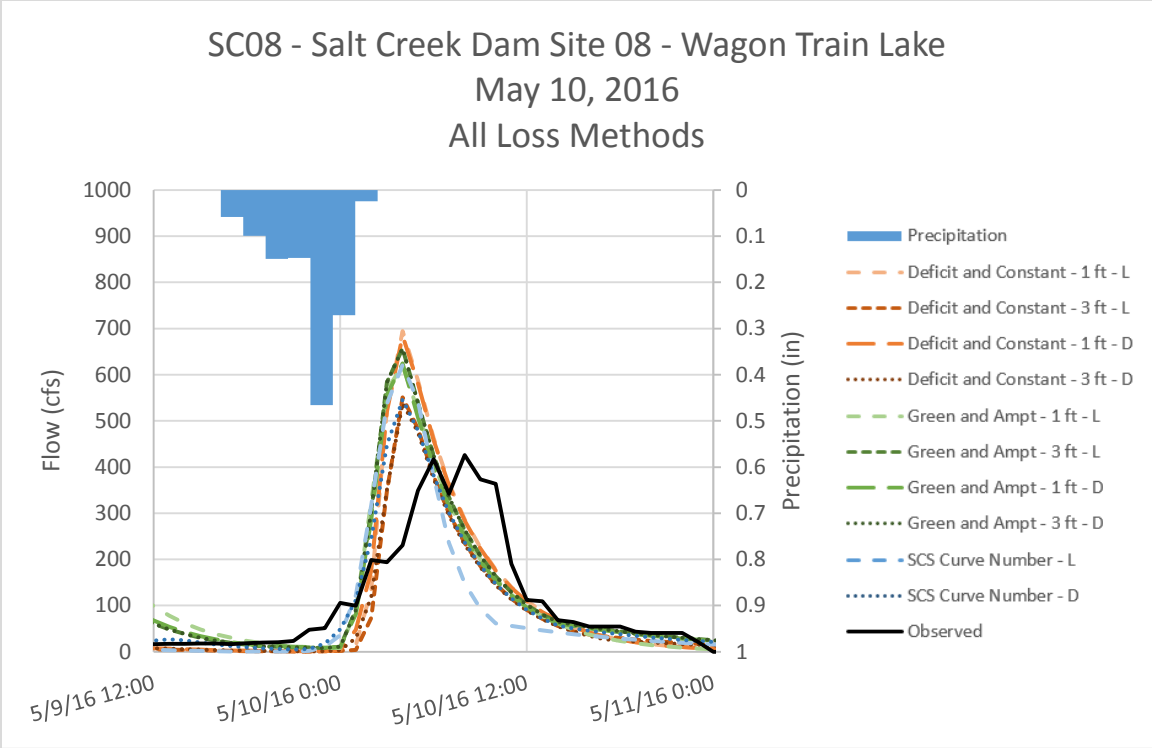

Figure C - 61. Runoff Hydrographs for SC08 - Salt Creek Dam Site 08 - Wagon Train Lake for May 10, 2016 Event All Loss Methods – Optimized Initial Conditions

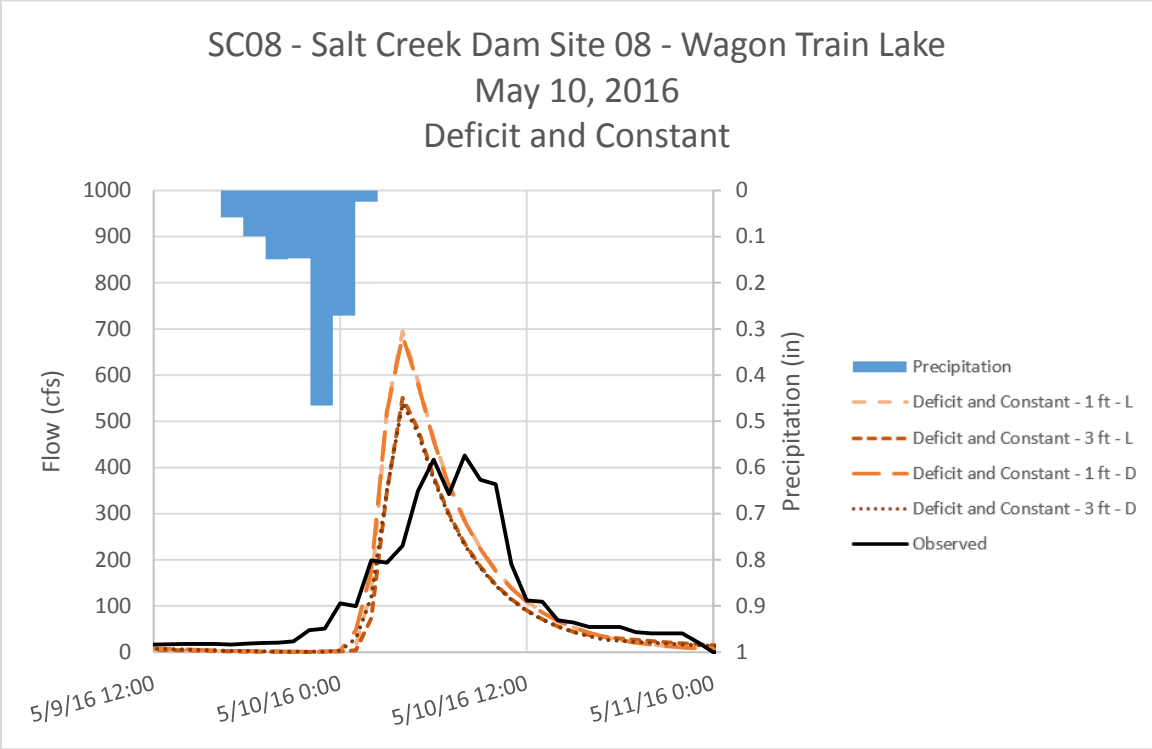

Figure C - 62. Runoff Hydrographs for SC08 - Salt Creek Dam Site 08 - Wagon Train Lake for May 10, 2016 Event Deficit and Constant Method – Optimized Initial Conditions

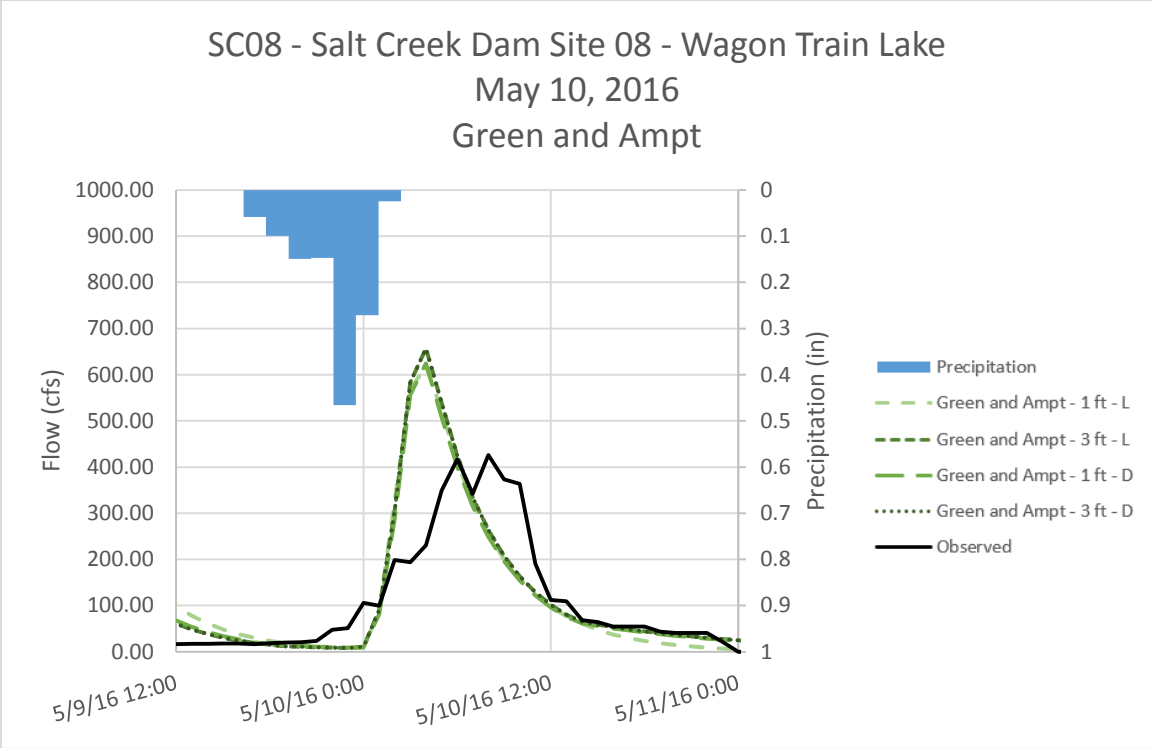

Figure C - 63. Runoff Hydrographs for SC08 - Salt Creek Dam Site 08 - Wagon Train Lake for May 10, 2016 Event Green and Ampt Method – Optimized Initial Conditions

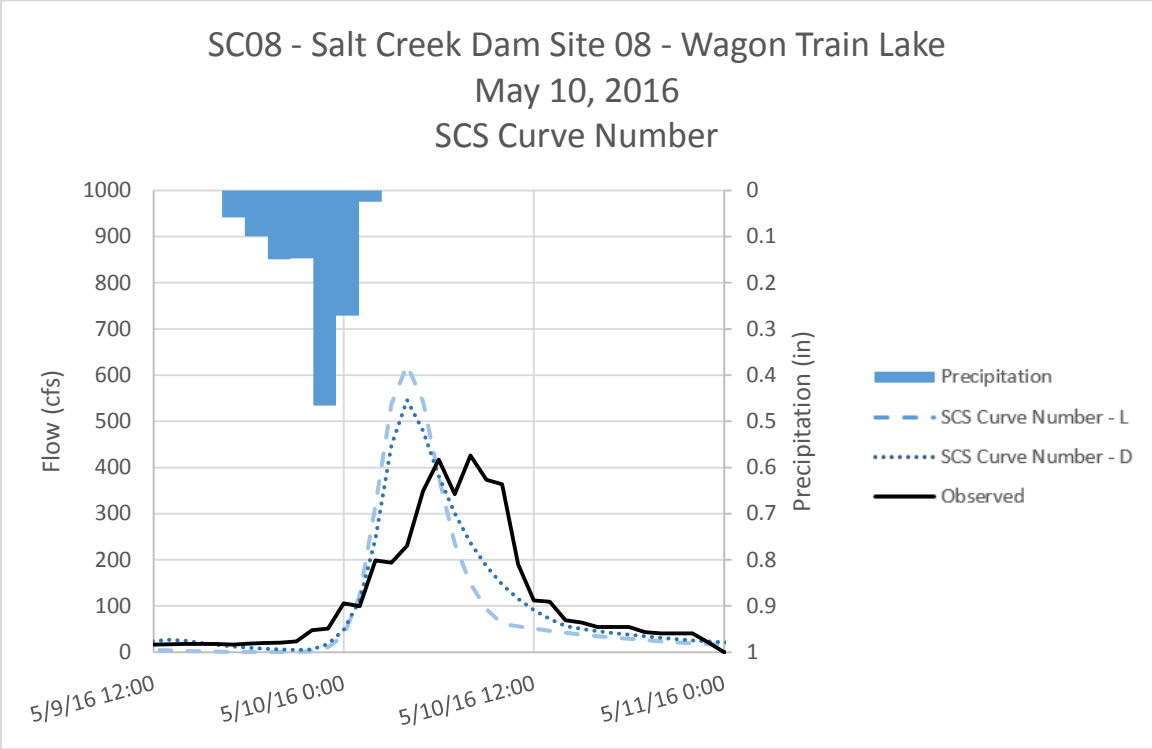

Figure C - 64. Runoff Hydrographs for SC08 - Salt Creek Dam Site 08 - Wagon Train Lake for May 10, 2016 Event SCS Curve Number Method – Optimized Initial Conditions

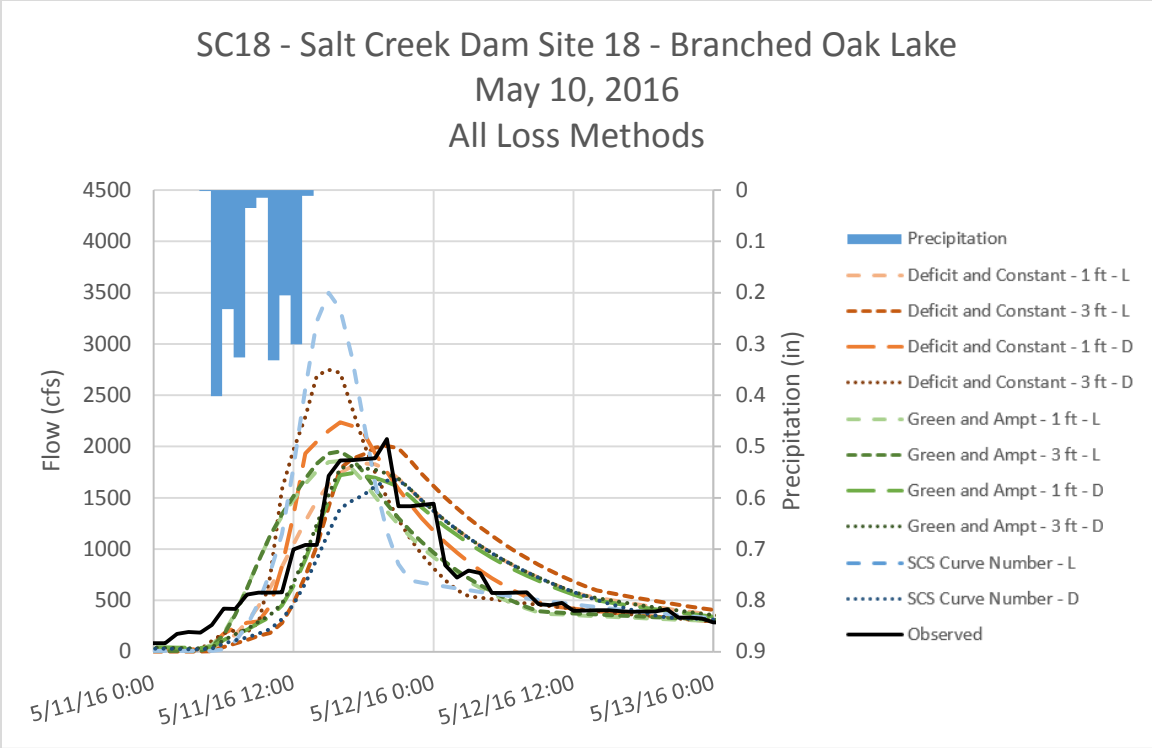

Figure C - 65. Runoff Hydrographs for SC18 - Salt Creek Dam Site 18 – Branched Oak Lake for May 10, 2016 Event All Loss Methods – Optimized Initial Conditions

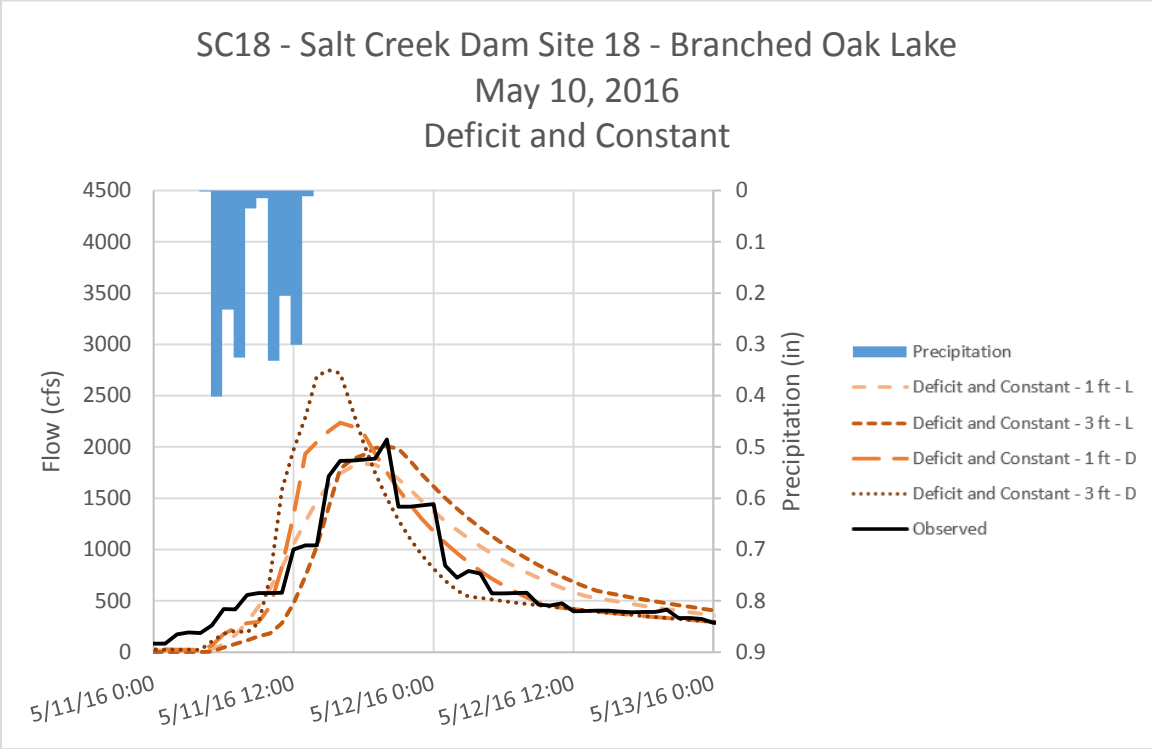

Figure C - 66. Runoff Hydrographs for SC18 - Salt Creek Dam Site 18 – Branched Oak Lake for May 10, 2016 Event Deficit and Constant Method – Optimized Initial Conditions

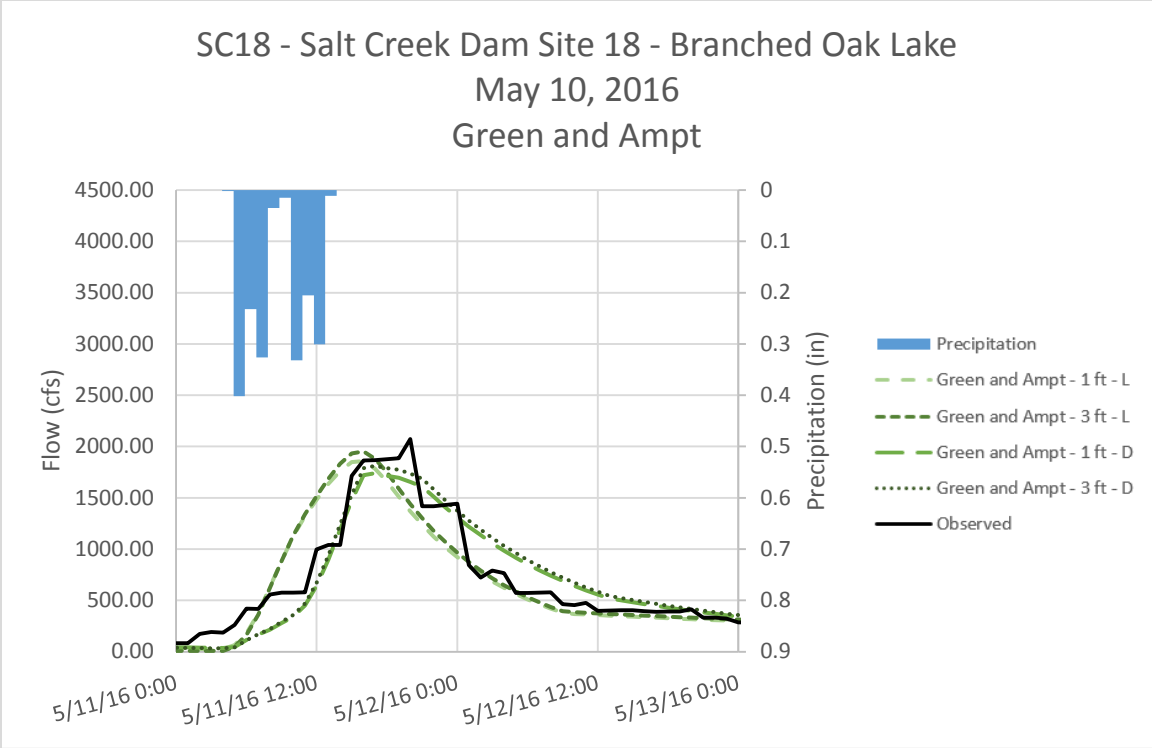

Figure C - 67. Runoff Hydrographs for SC18 - Salt Creek Dam Site 18 – Branched Oak Lake for May 10, 2016 Event Green and Ampt Method – Optimized Initial Conditions

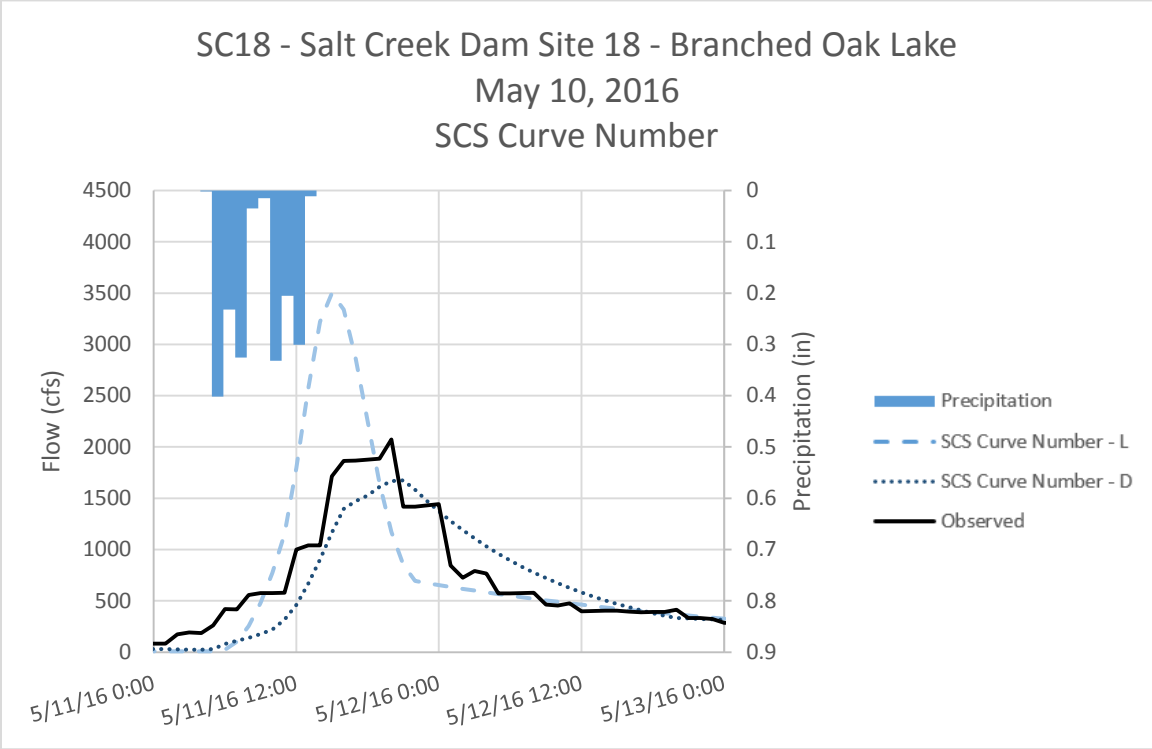

Figure C - 68. Runoff Hydrographs for SC18 - Salt Creek Dam Site 18 – Branched Oak Lake for May 10, 2016 Event SCS Curve Number Method – Optimized Initial Conditions

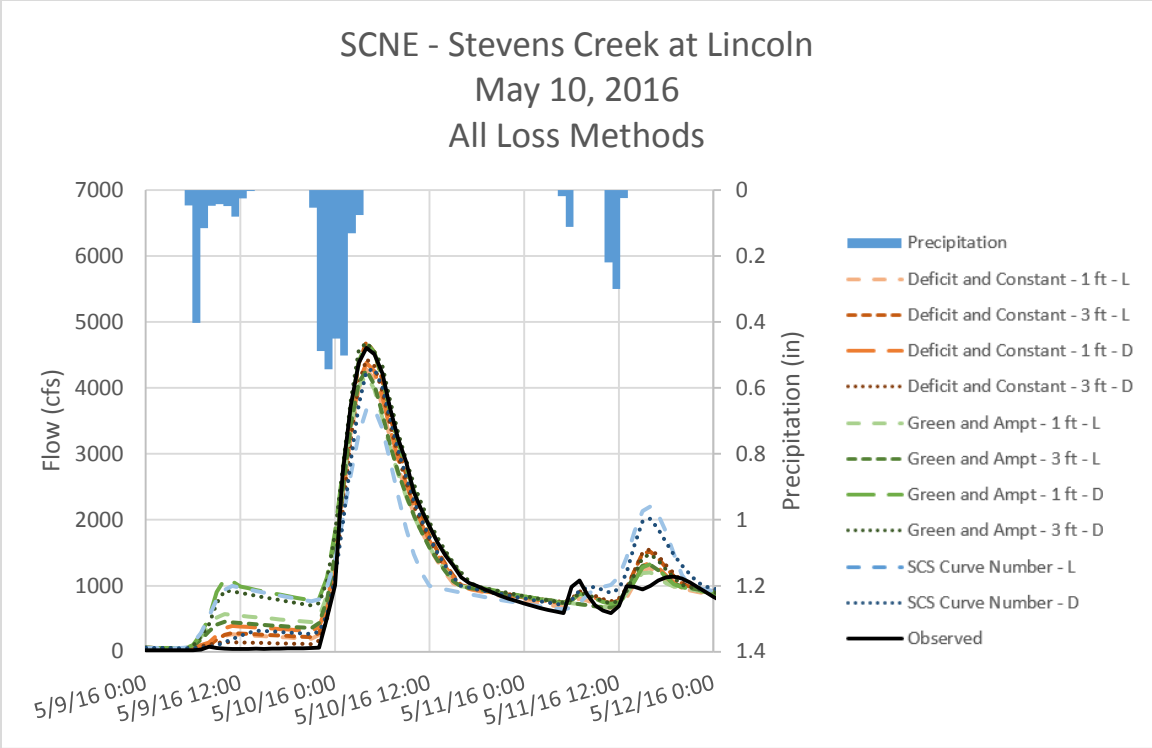

Figure C - 69. Runoff Hydrographs for SCNE – Stevens Creek at Lincoln for May 10, 2016 Event
All Loss Methods – Optimized Initial Conditions

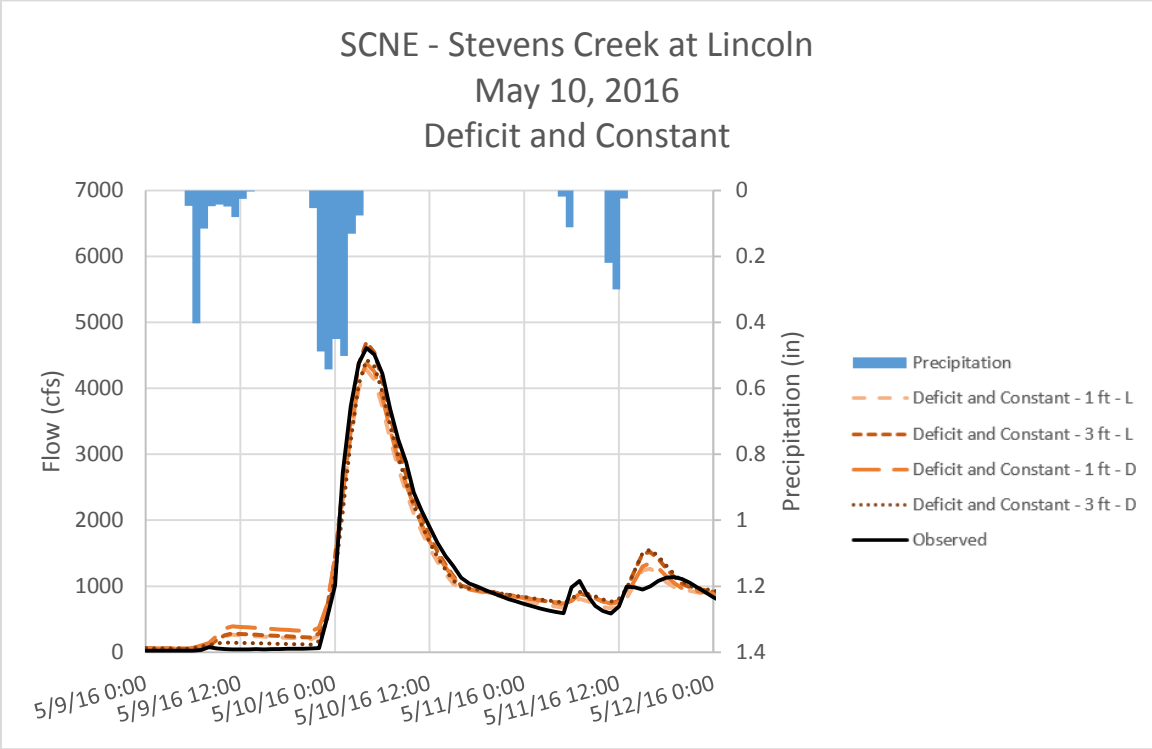

Figure C - 70. Runoff Hydrographs for SCNE – Stevens Creek at Lincoln for May 10, 2016 Event
Deficit and Constant Method – Optimized Initial Conditions

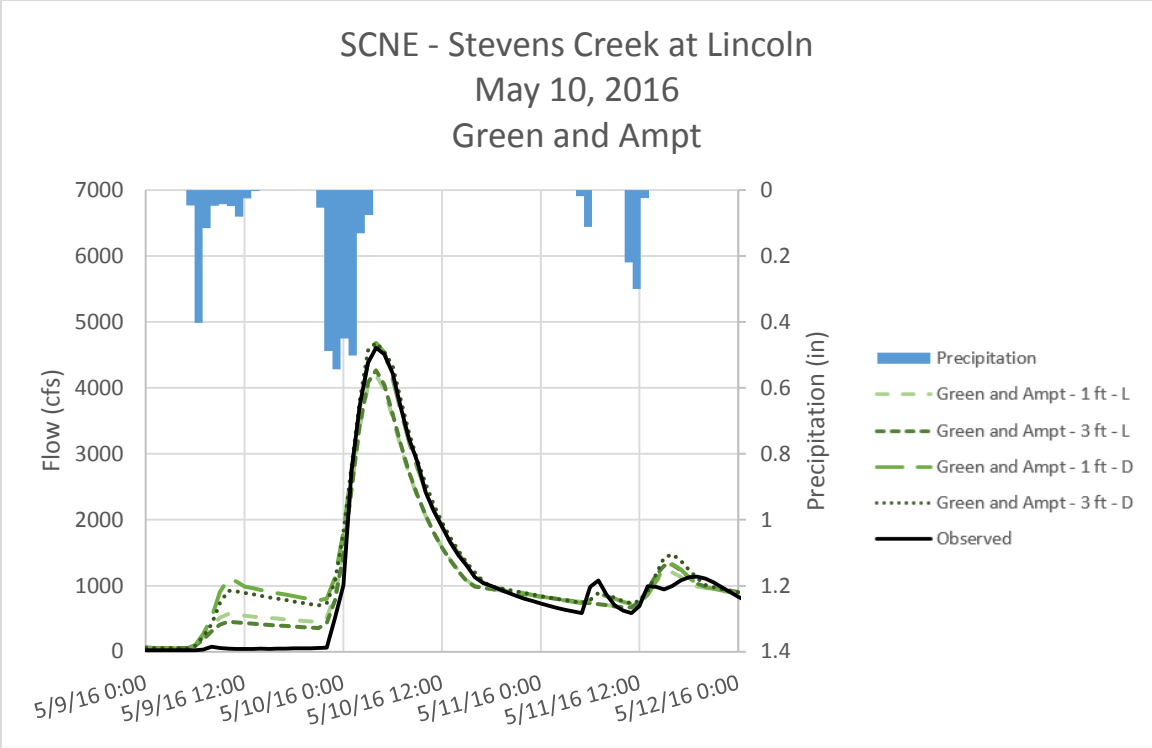

Figure C - 71. Runoff Hydrographs for SCNE – Stevens Creek at Lincoln for May 10, 2016 Event
Green and Ampt Method – Optimized Initial Conditions

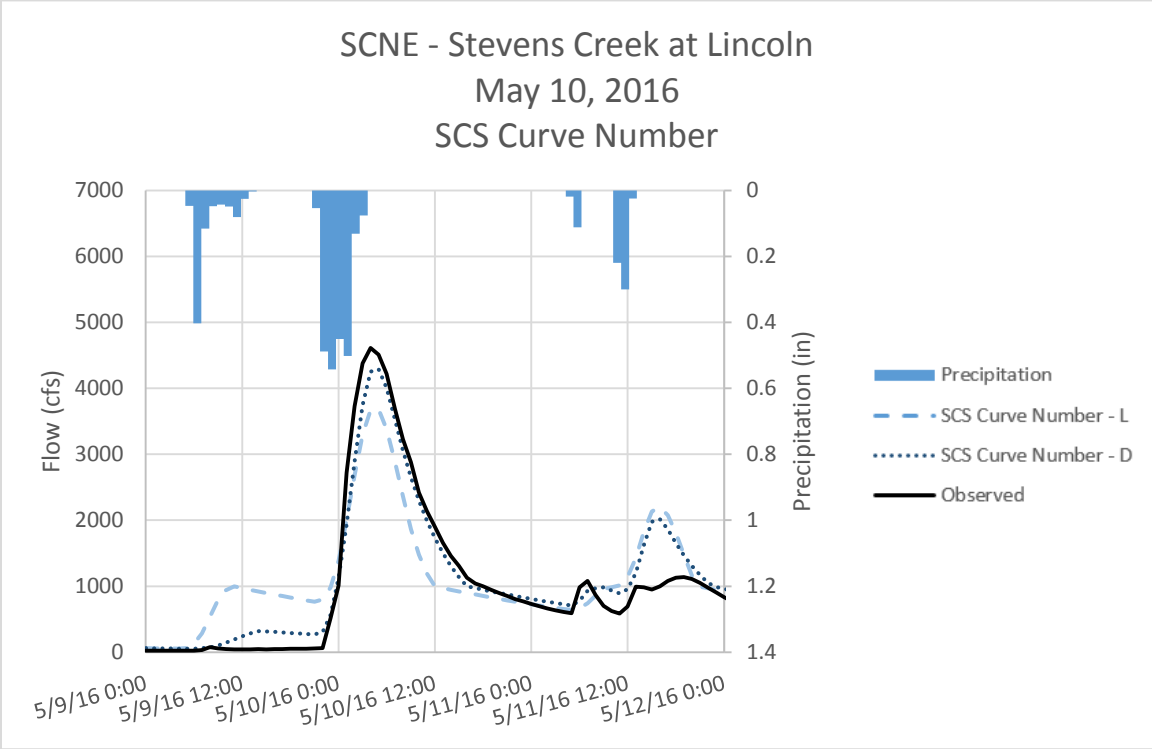

Figure C - 72. Runoff Hydrographs for SCNE – Stevens Creek at Lincoln for May 10, 2016 Event
SCS Curve Number Method – Optimized Initial Conditions

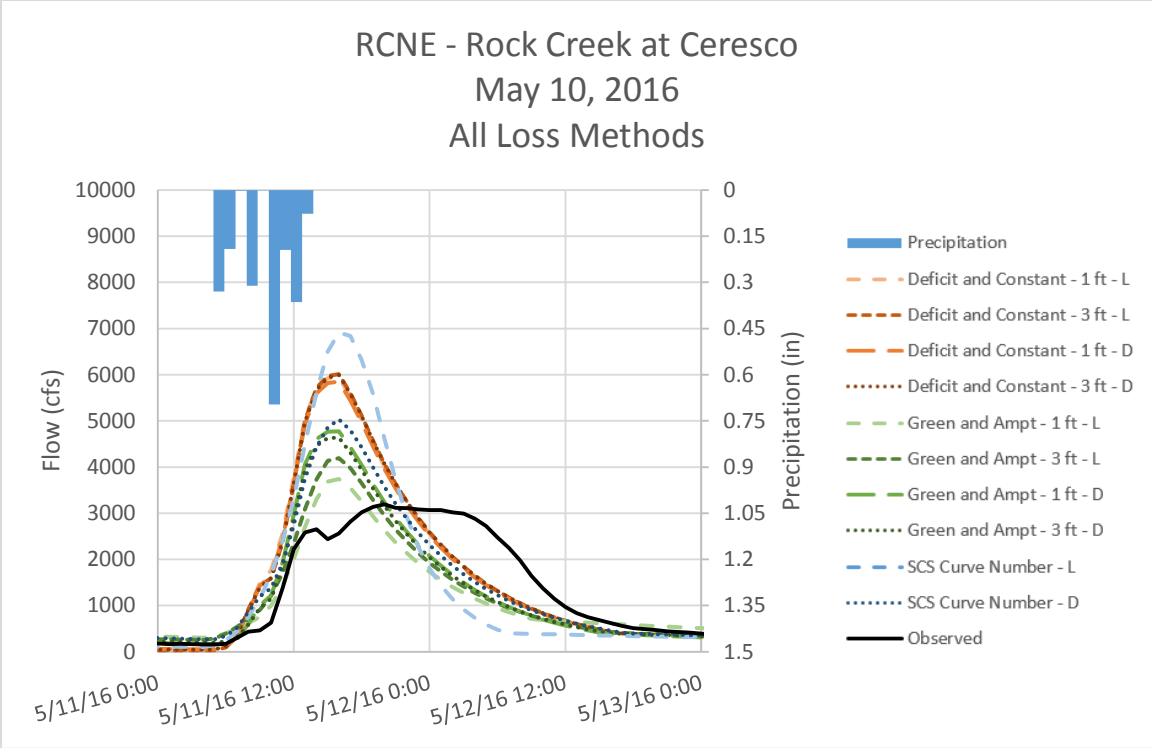

Figure C - 73. Runoff Hydrographs for RCNE – Rock Creek at Ceresco for May 10, 2016 Event
All Loss Methods – Optimized Initial Conditions

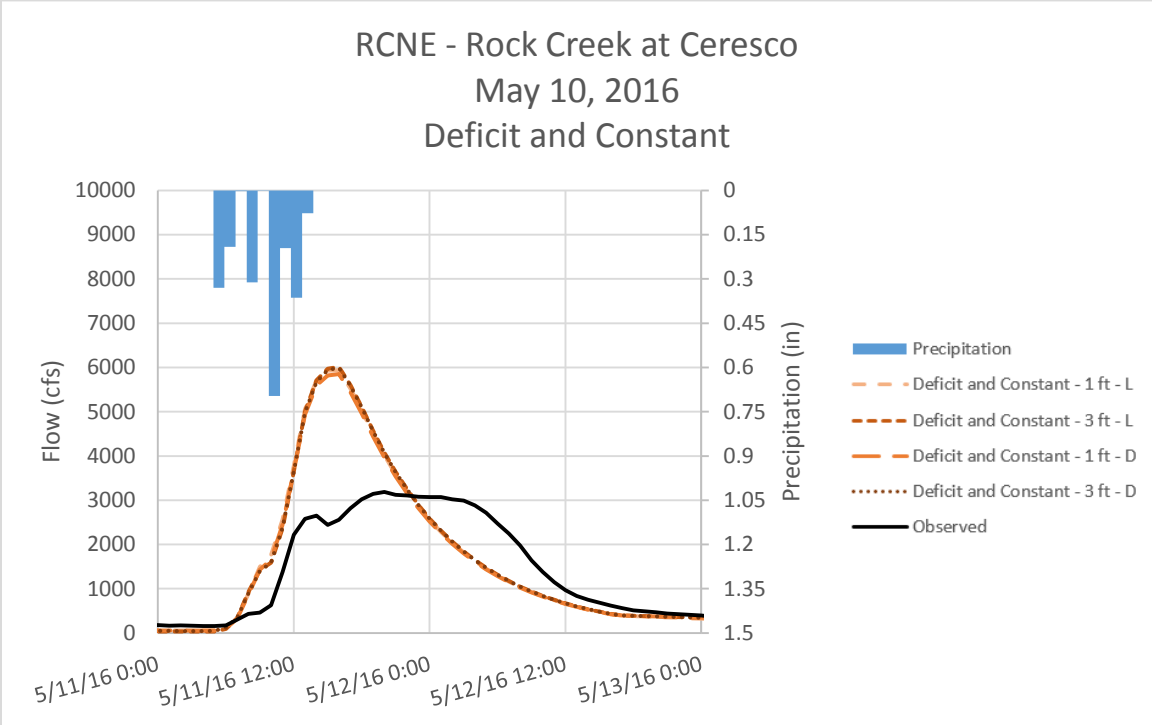

Figure C - 74. Runoff Hydrographs for RCNE – Rock Creek at Ceresco for May 10, 2016 Event
Deficit and Constant Method – Optimized Initial Conditions

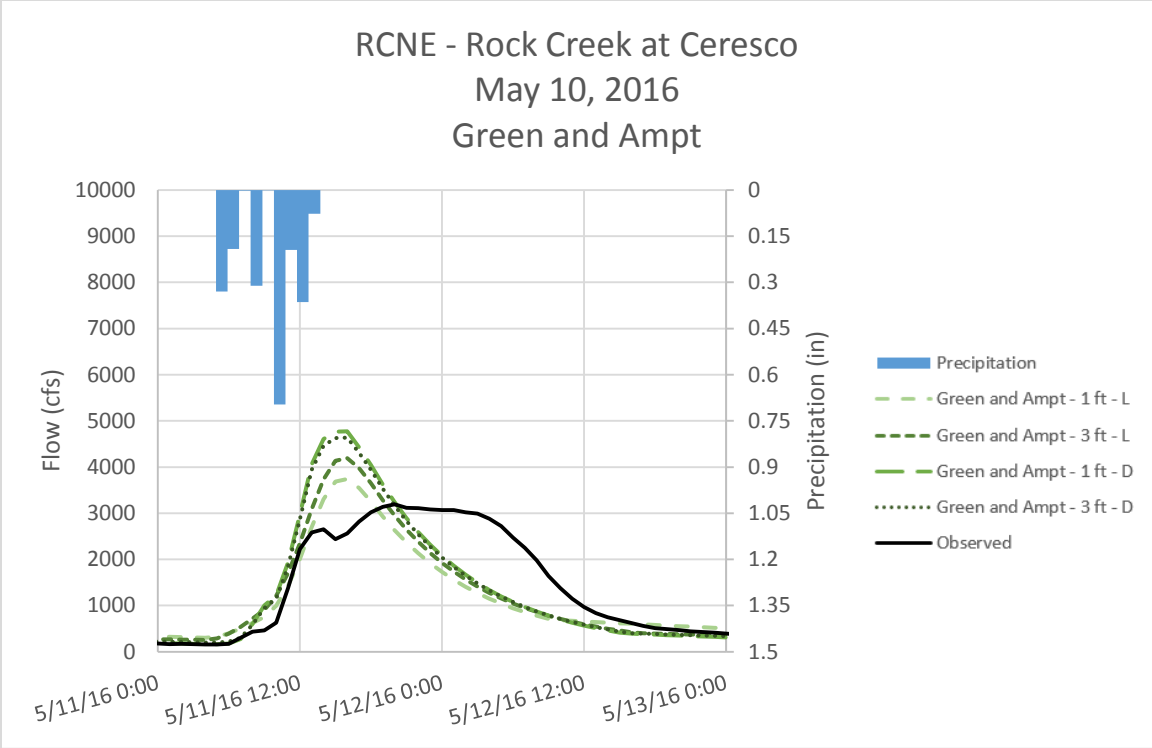

Figure C - 75. Runoff Hydrographs for RCNE – Rock Creek at Ceresco for May 10, 2016 Event
Green and Ampt Method – Optimized Initial Conditions

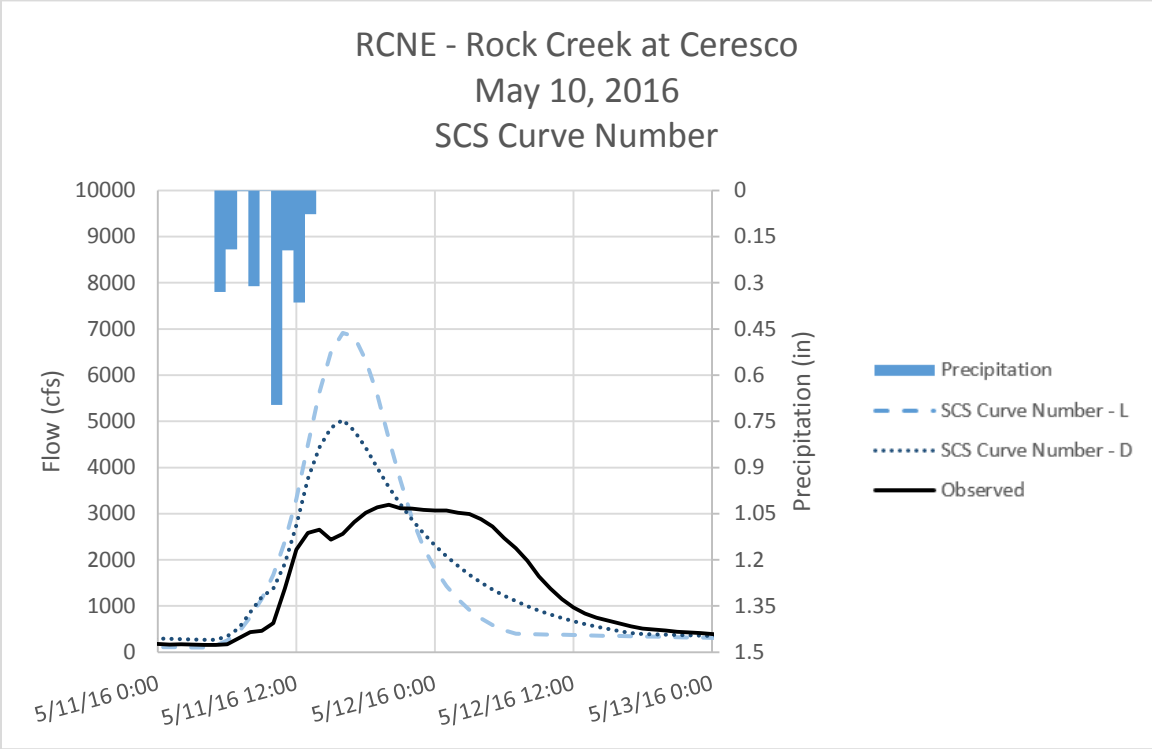

Figure C - 76. Runoff Hydrographs for RCNE – Rock Creek at Ceresco for May 10, 2016 Event
SCS Curve Number Method – Optimized Initial Conditions

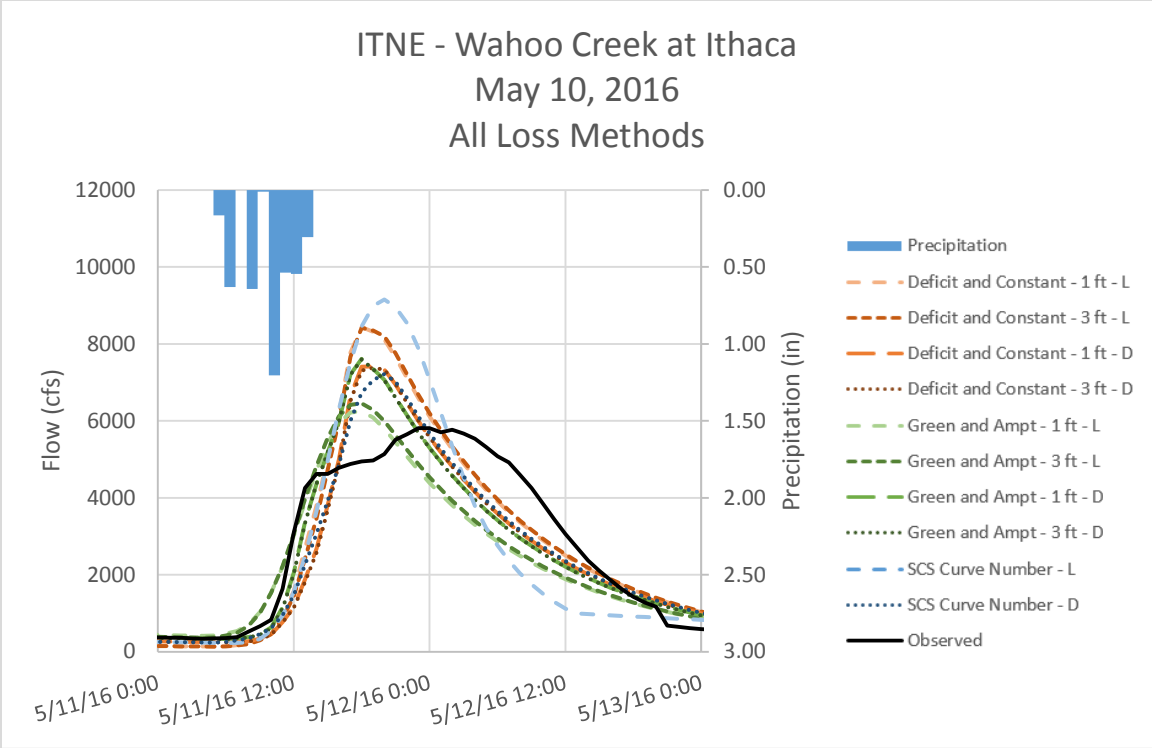

Figure C - 77. Runoff Hydrographs for ITNE – Wahoo Creek at Ithaca for May 10, 2016 Event
All Loss Methods – Optimized Initial Conditions

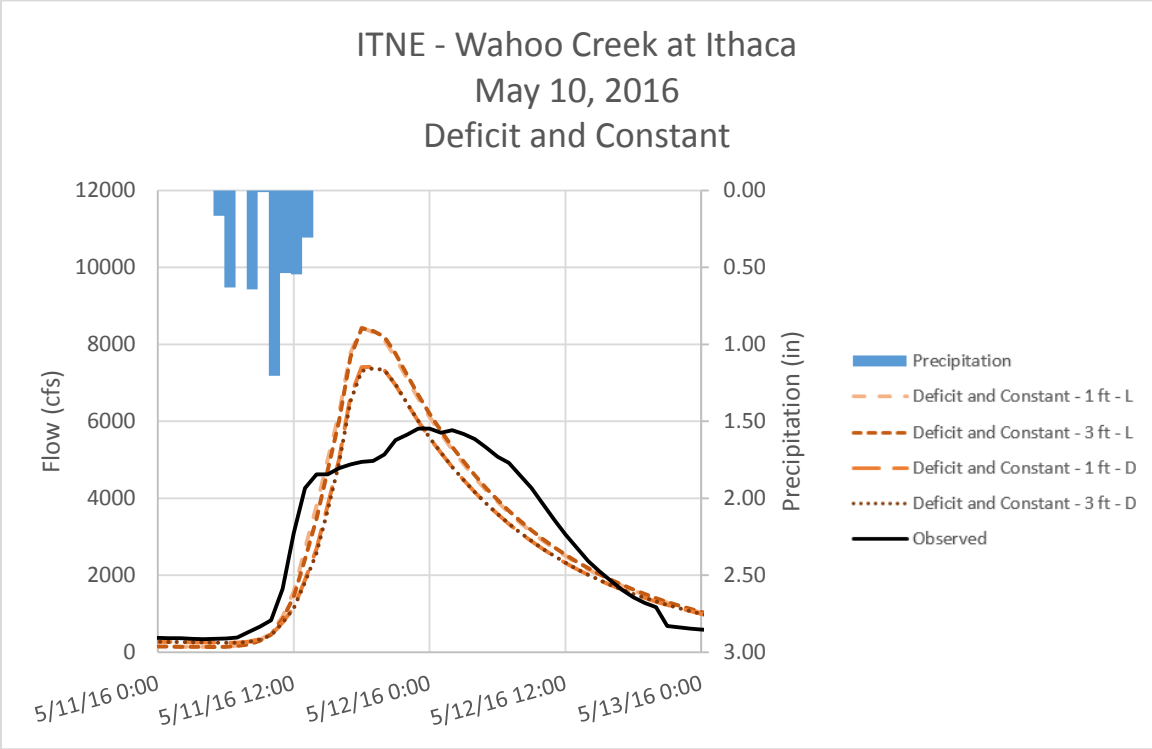

Figure C - 78. Runoff Hydrographs for ITNE – Wahoo Creek at Ithaca for May 10, 2016 Event
Deficit and Constant Method – Optimized Initial Conditions

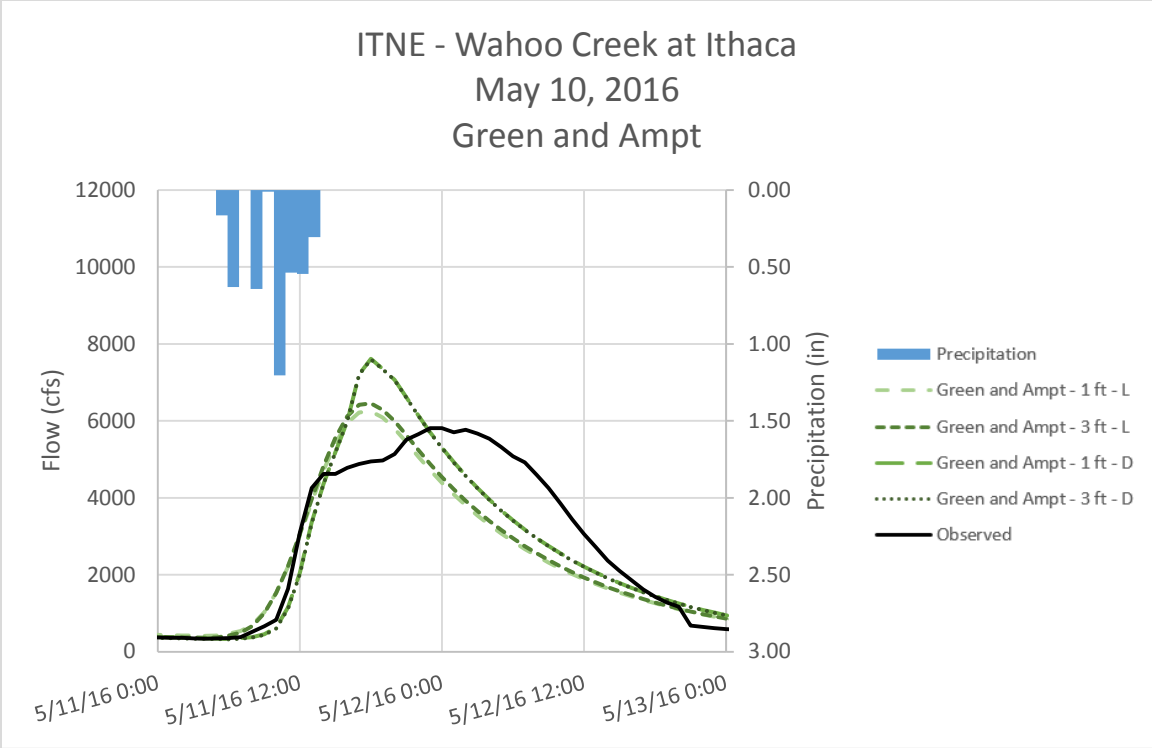

Figure C - 79. Runoff Hydrographs for ITNE – Wahoo Creek at Ithaca for May 10, 2016 Event
Green and Ampt Method – Optimized Initial Conditions

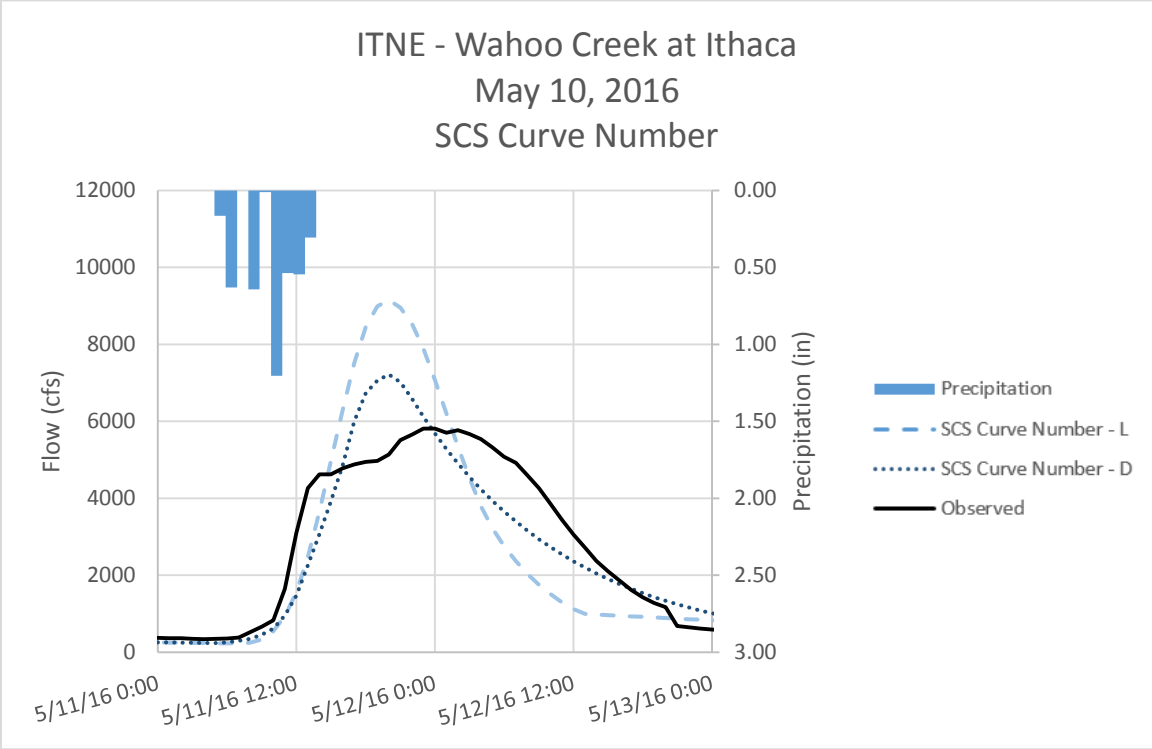

Figure C - 80. Runoff Hydrographs for ITNE – Wahoo Creek at Ithaca for May 10, 2016 Event
SCS Curve Number Method – Optimized Initial Conditions

Appendix D – Watershed Hydrographs for Non-Optimized Initial Conditions

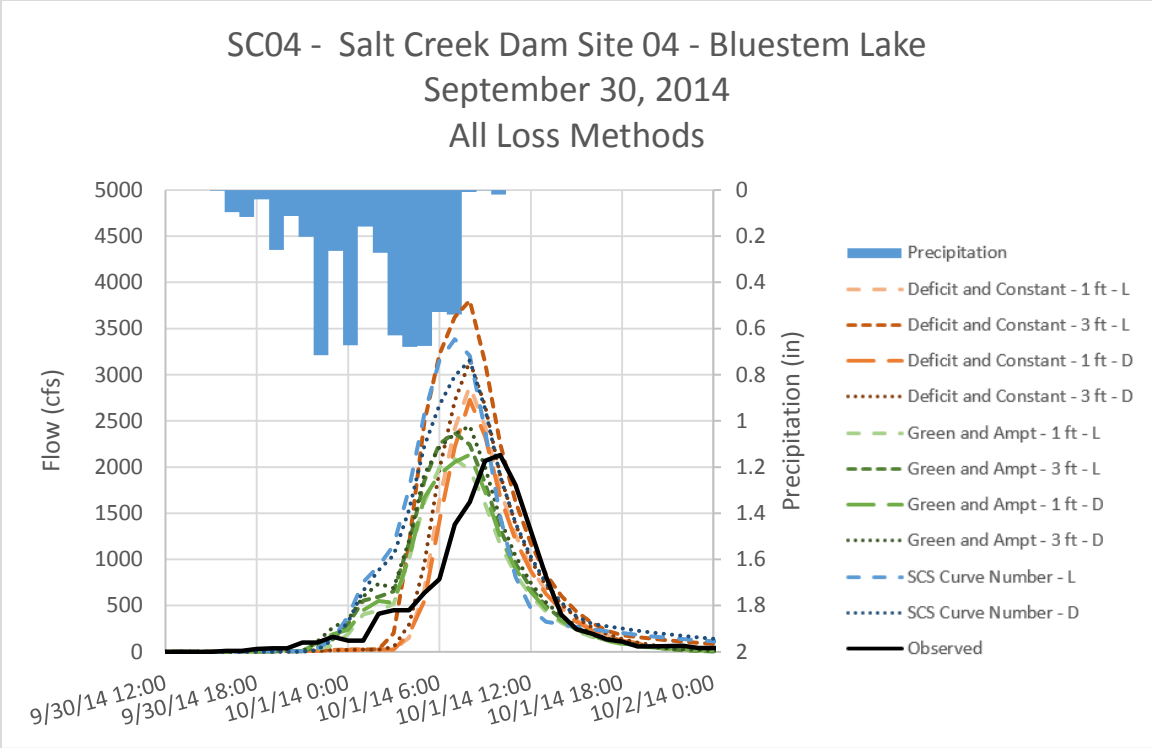

Figure D - 1. Runoff Hydrographs for SC04 - Salt Creek Dam Site 04 - Bluestem Lake for September 30, 2014 Event All Loss Methods – Non-Optimized Initial Conditions

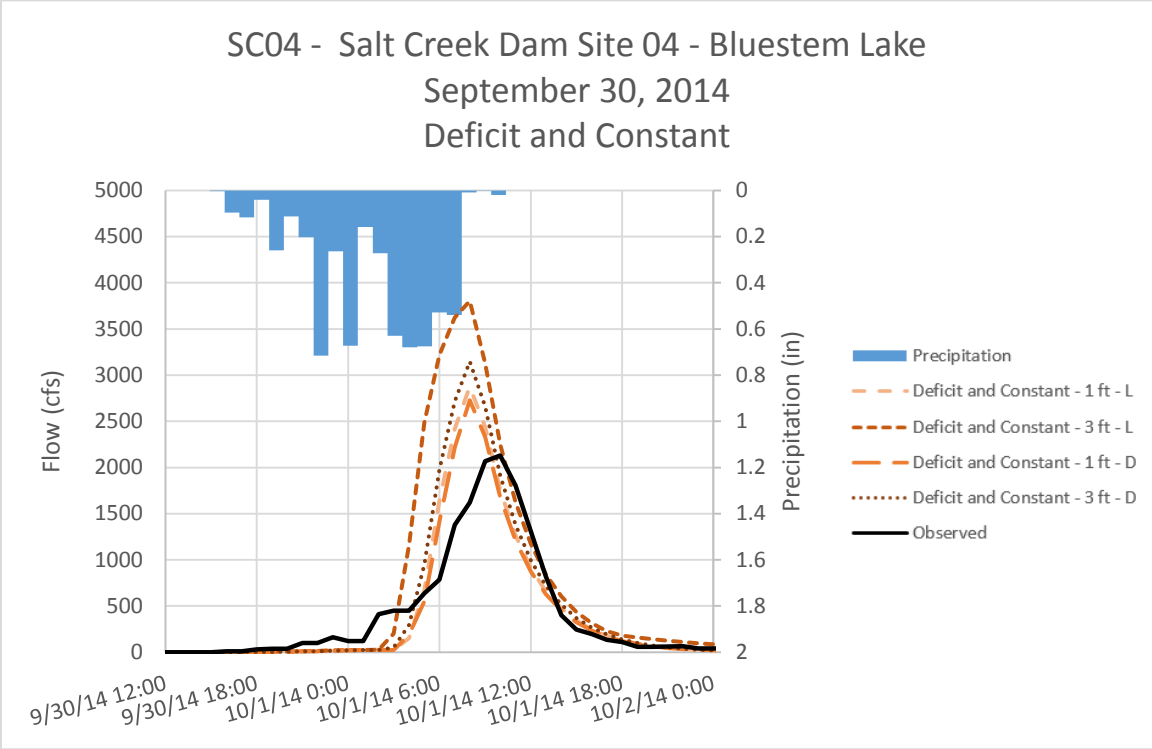

Figure D - 2. Runoff Hydrographs for SC04 - Salt Creek Dam Site 04 - Bluestem Lake for September 30, 2014 Event Deficit and Constant Method – Non-Optimized Initial Conditions

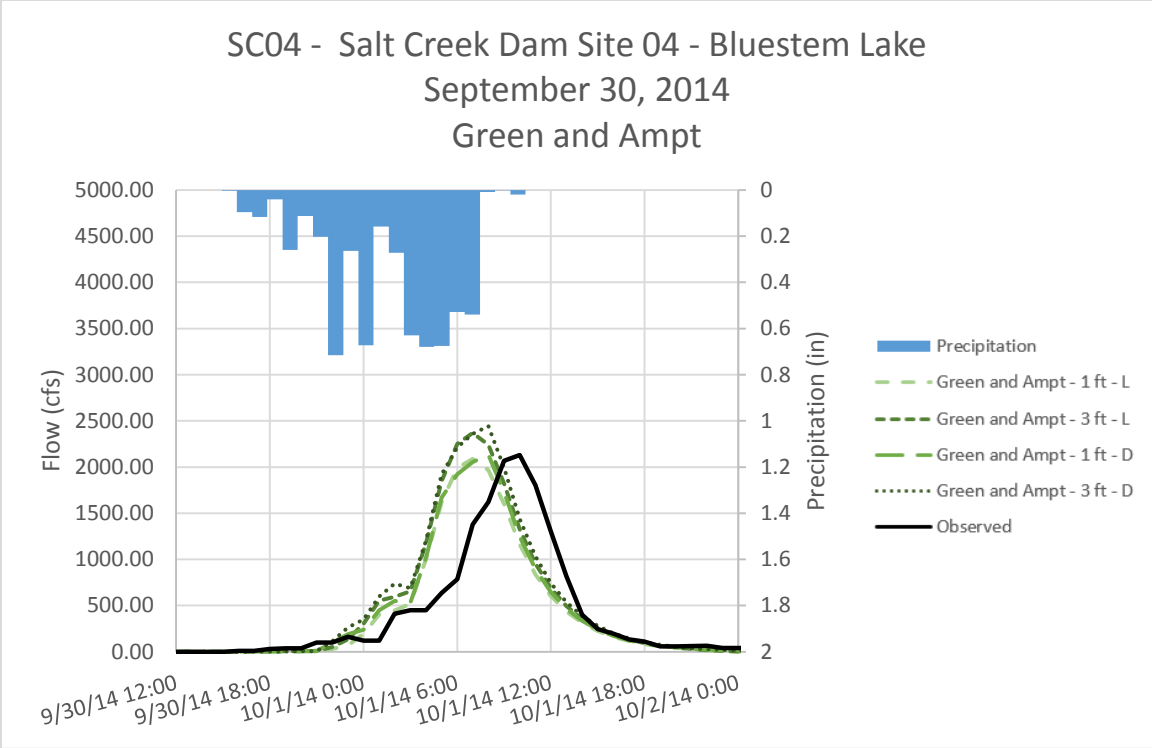

Figure D - 3. Runoff Hydrographs for SC04 - Salt Creek Dam Site 04 - Bluestem Lake for September 30, 2014 Event Green and Ampt Method – Non-Optimized Initial Conditions

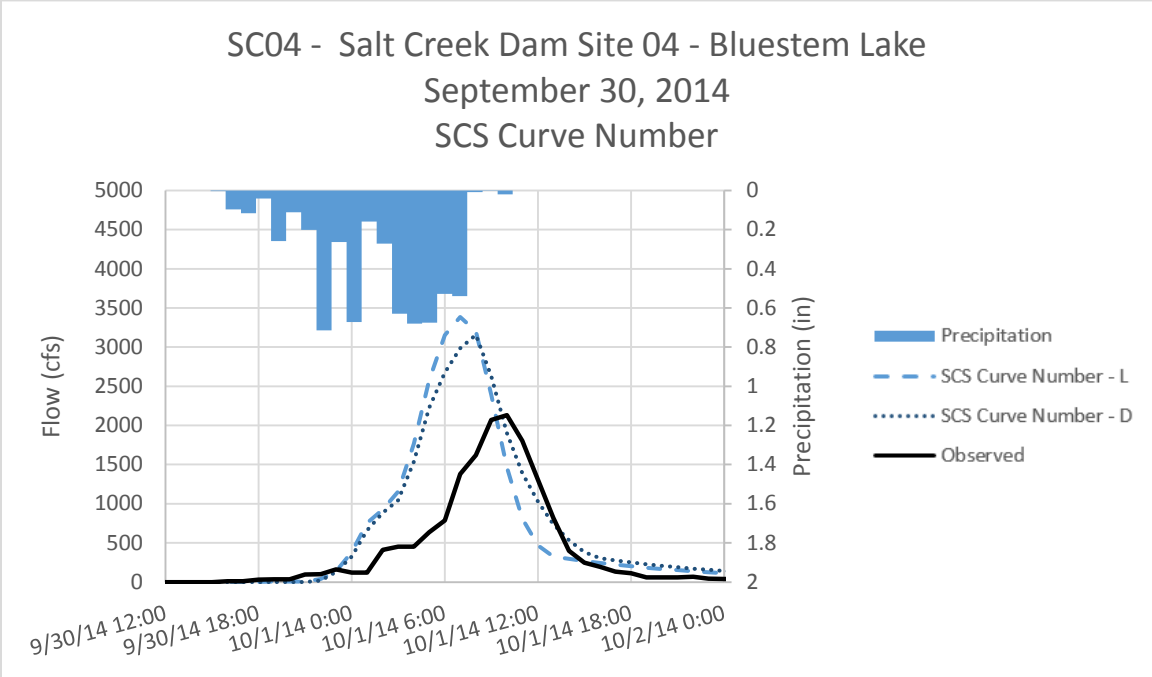

Figure D - 4. Runoff Hydrographs for SC04 - Salt Creek Dam Site 04 - Bluestem Lake for September 30, 2014 Event SCS Curve Number Method – Non-Optimized Initial Conditions

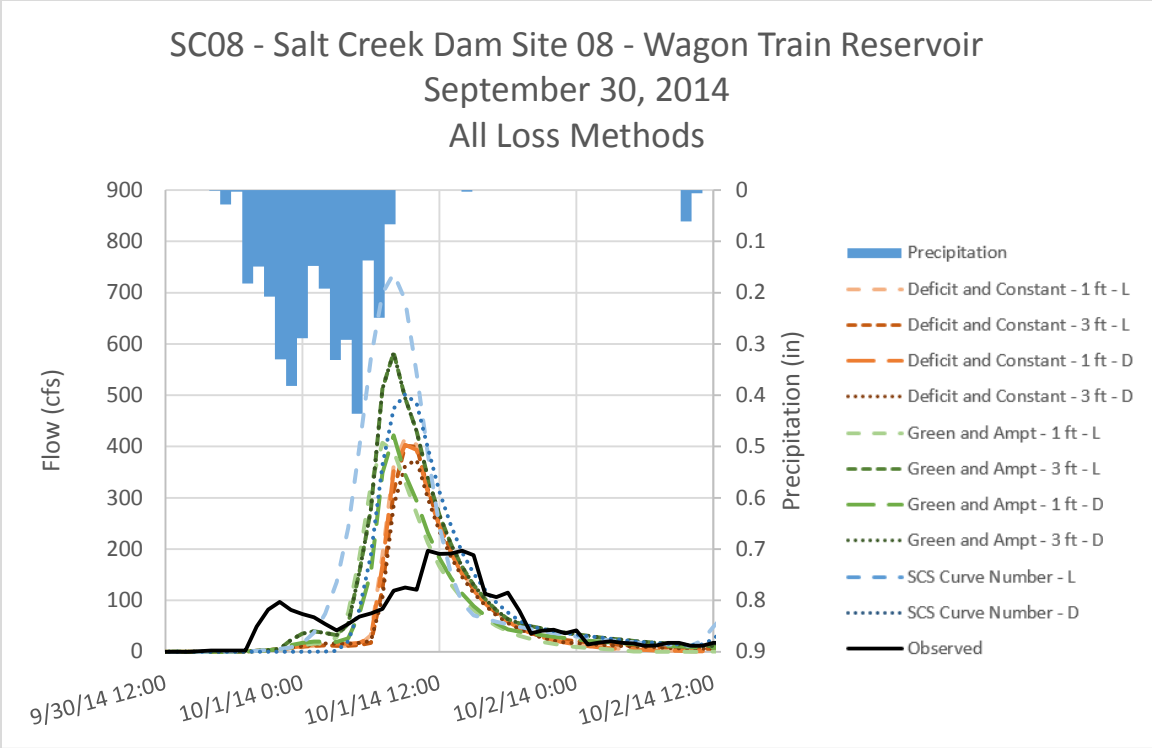

Figure D - 5. Runoff Hydrographs for SC08 - Salt Creek Dam Site 08 – Wagon Train Lake for September 30, 2014 Event All Loss Methods – Non-Optimized Initial Conditions

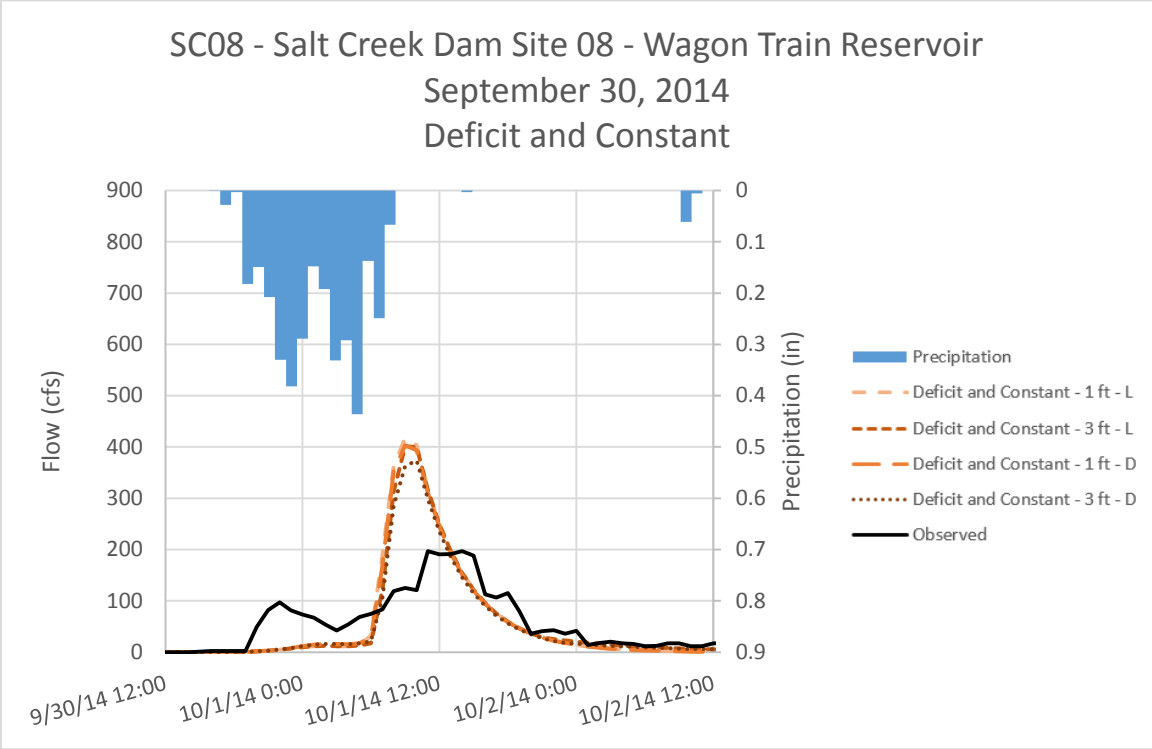

Figure D - 6. Runoff Hydrographs for SC08 - Salt Creek Dam Site 08 – Wagon Train Lake for September 30, 2014 Event Deficit and Constant Method – Non-Optimized Initial Conditions

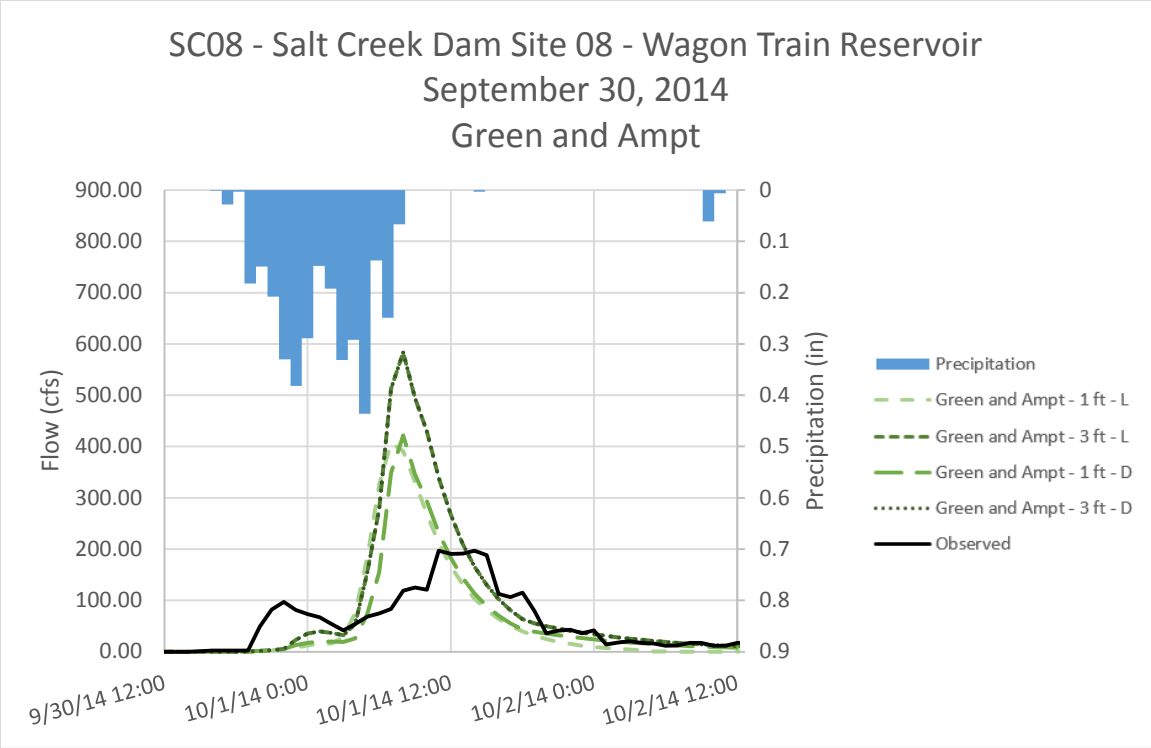

Figure D - 7. Runoff Hydrographs for SC08 - Salt Creek Dam Site 08 – Wagon Train Lake for September 30, 2014 Event Green and Ampt Method – Non-Optimized Initial Conditions

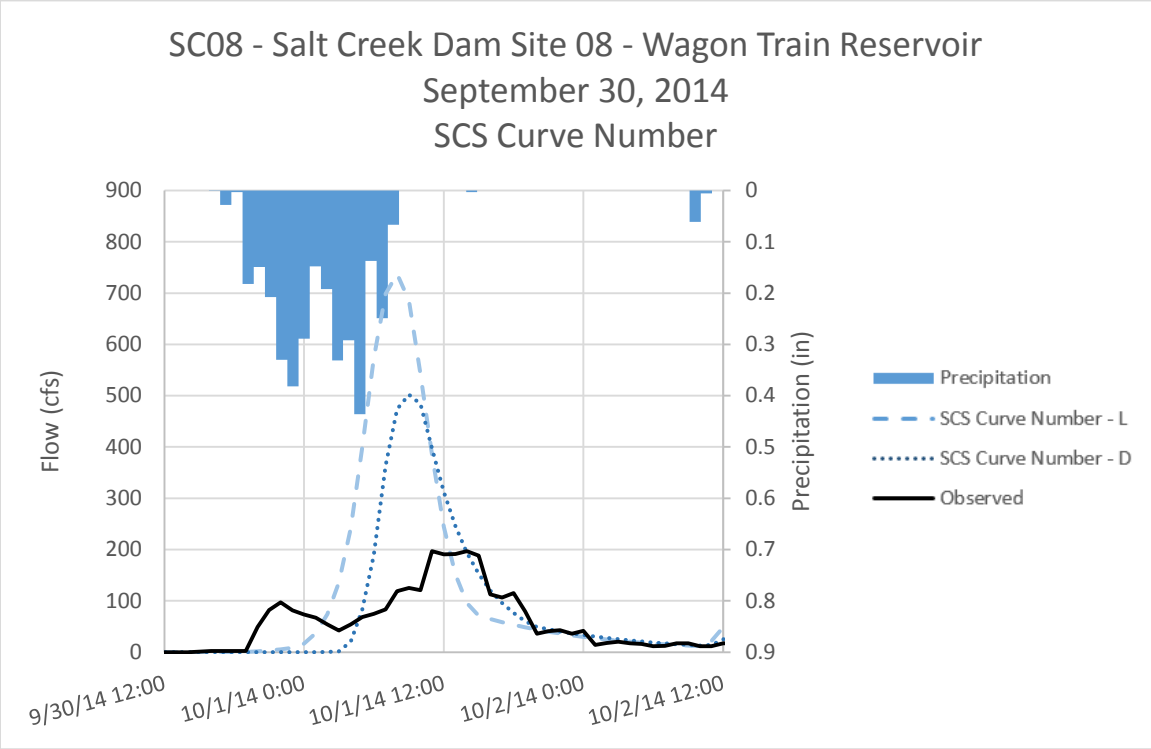

Figure D - 8. Runoff Hydrographs for SC08 - Salt Creek Dam Site 08 – Wagon Train Lake for September 30, 2014 Event SCS Curve Number Method – Non-Optimized Initial Conditions

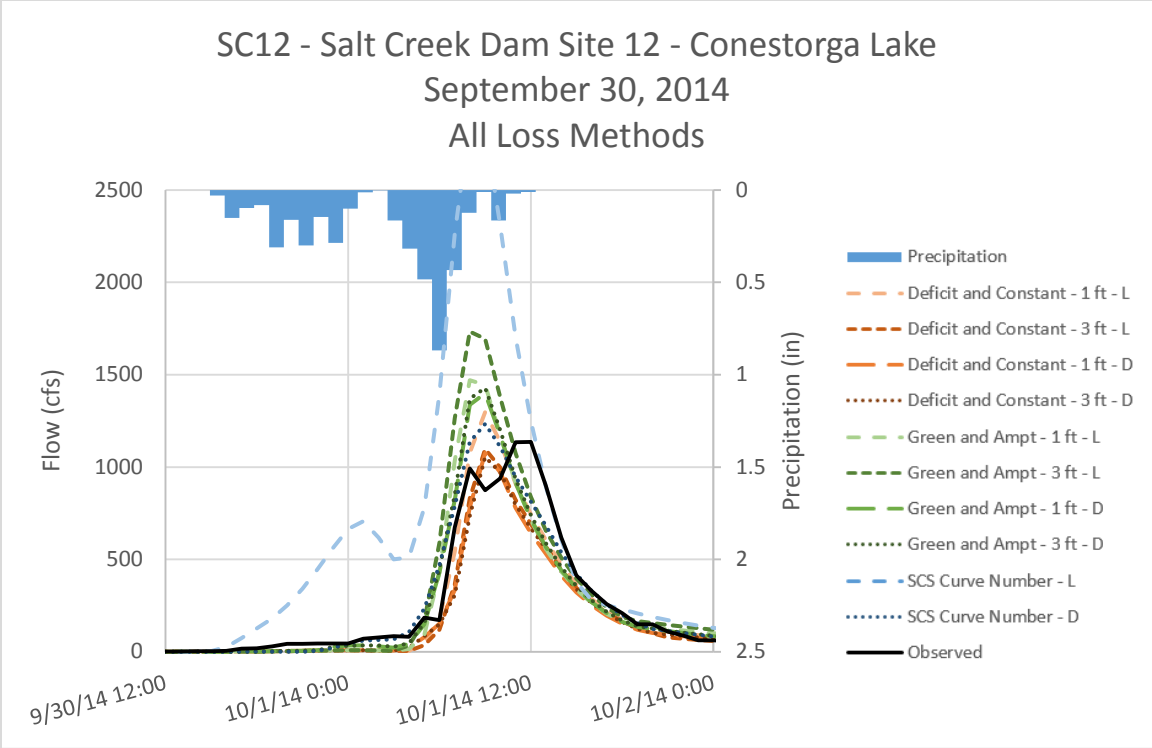

Figure D - 9. Runoff Hydrographs for SC12 - Salt Creek Dam Site 12 – Conestoga Lake for September 30, 2014 Event All Loss Methods – Non-Optimized Initial Conditions

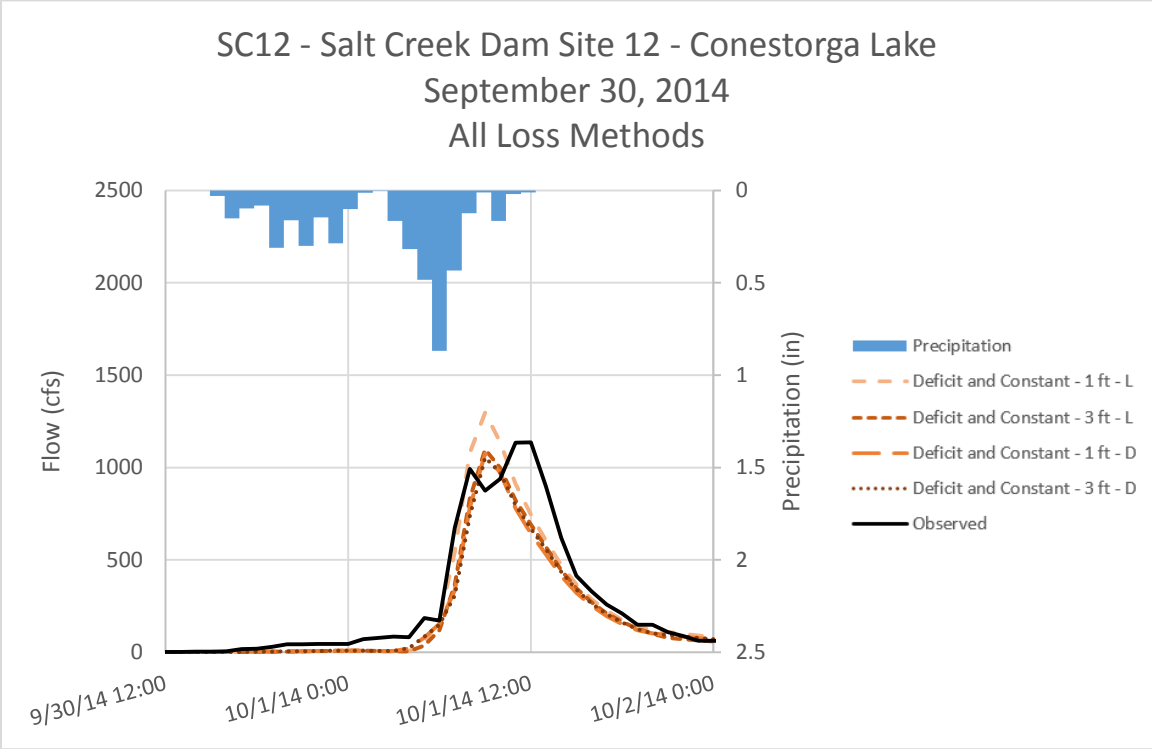

Figure D - 10. Runoff Hydrographs for SC12 - Salt Creek Dam Site 12 – Conestoga Lake for September 30, 2014 Event Deficit and Constant Method – Non-Optimized Initial Conditions

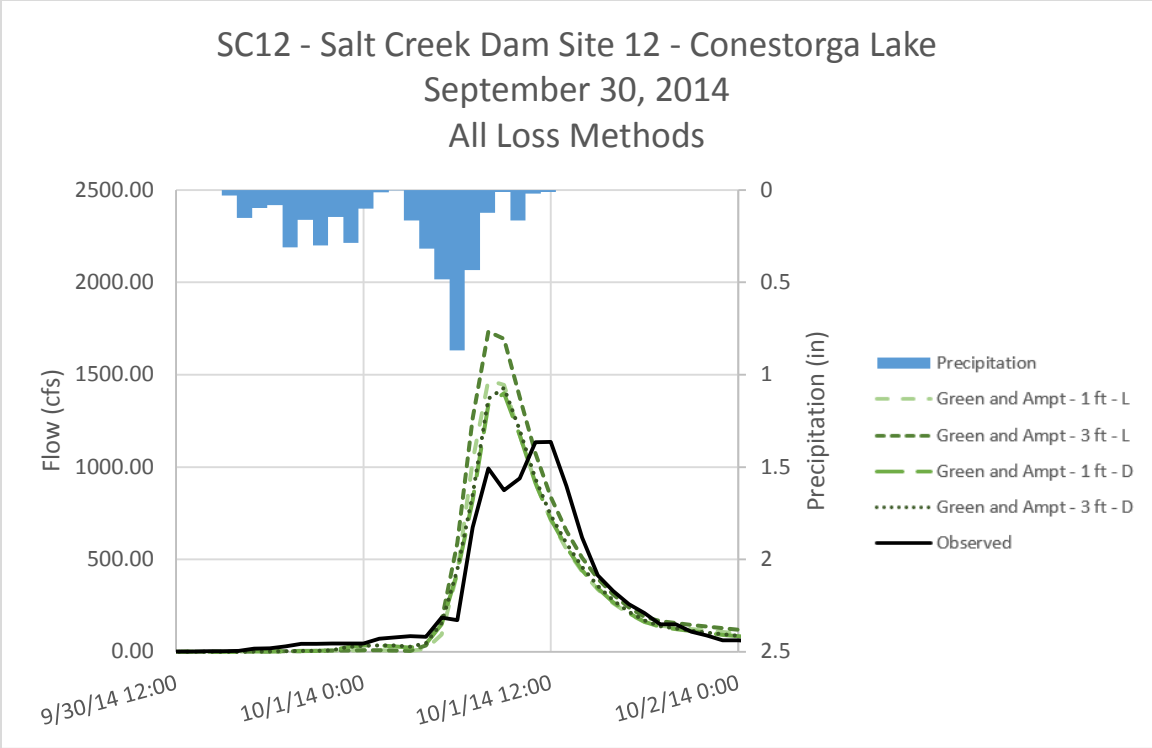

Figure D - 11. Runoff Hydrographs for SC12 - Salt Creek Dam Site 12 – Conestoga Lake for September 30, 2014 Event Green and Ampt Method – Non-Optimized Initial Conditions

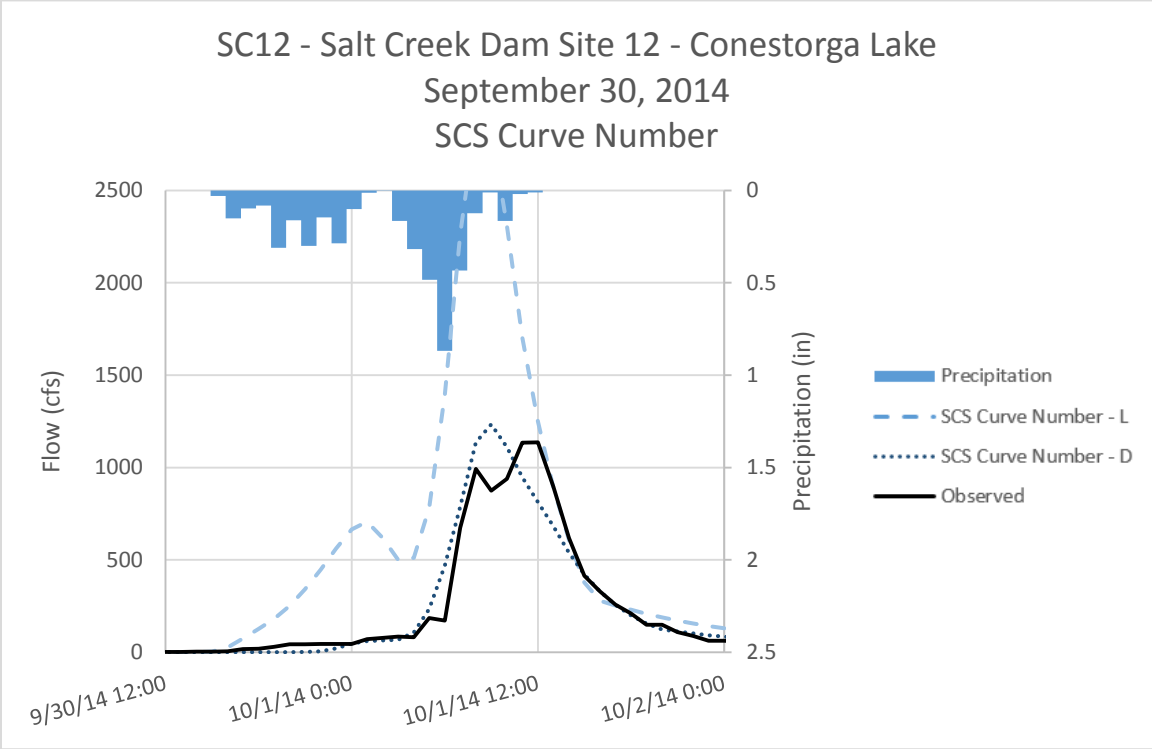

Figure D - 12. Runoff Hydrographs for SC12 - Salt Creek Dam Site 12 – Conestoga Lake for September 30, 2014 Event SCS Curve Number – Non-Optimized Initial Conditions

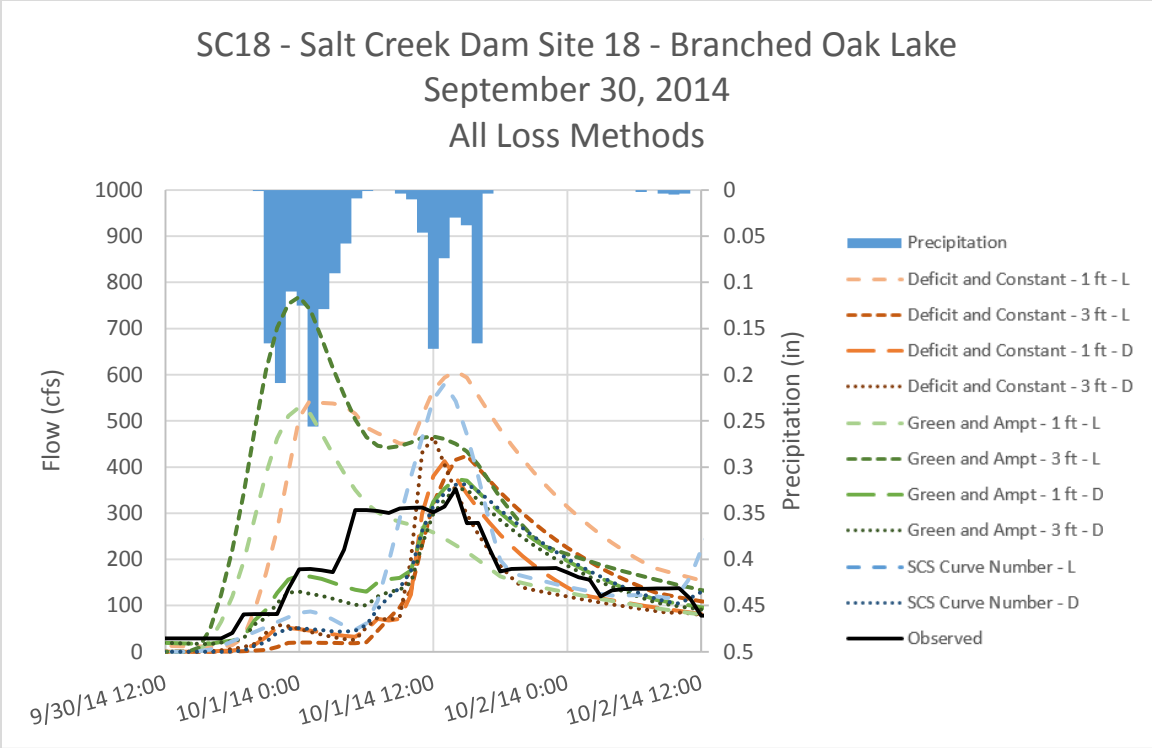

Figure D - 13. Runoff Hydrographs for SC18 - Salt Creek Dam Site 18 -Branched Oak Lake for September 30, 2014 Event All Loss Methods – Non-Optimized Initial Conditions

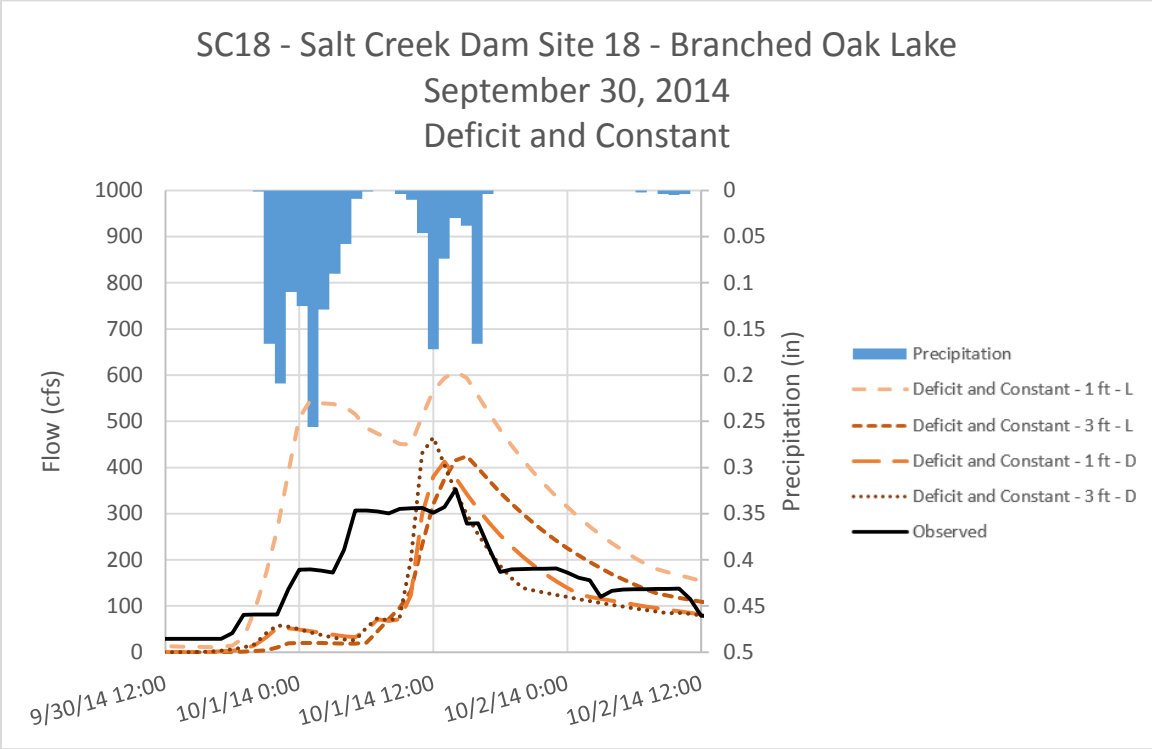

Figure D - 14. Runoff Hydrographs for SC18 - Salt Creek Dam Site 18 -Branched Oak Lake for September 30, 2014 Event Deficit and Constant Method – Non-Optimized Initial Conditions

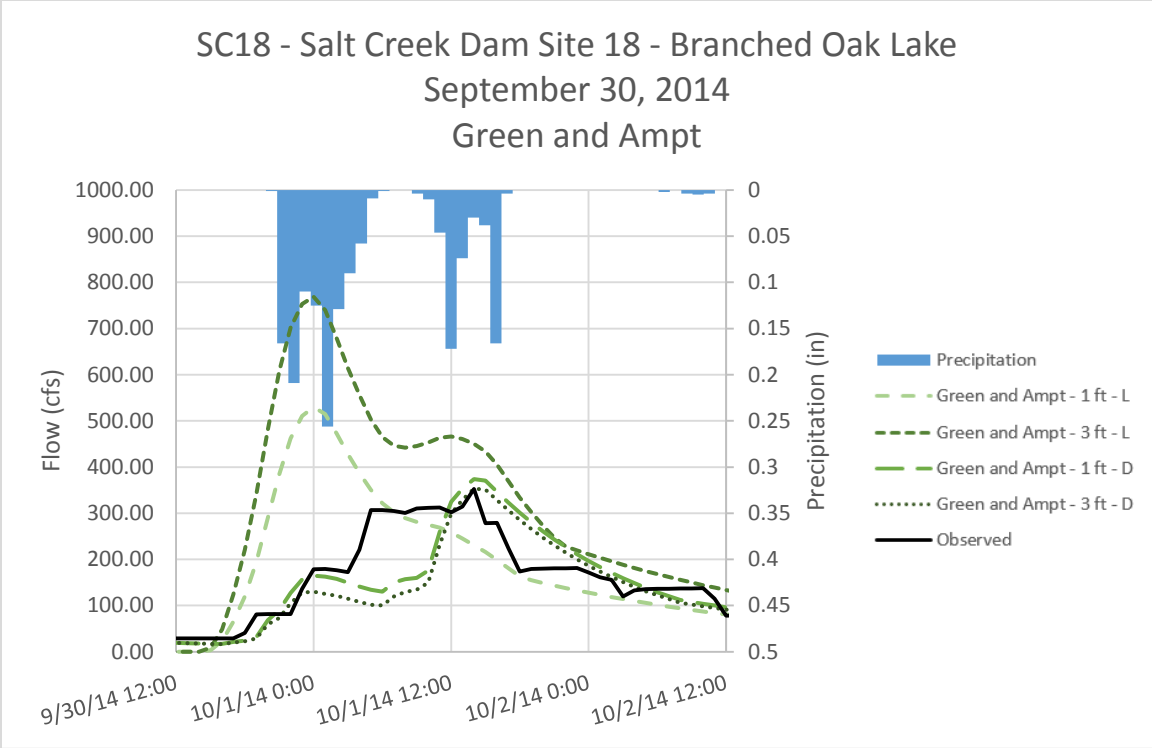

Figure D - 15. Runoff Hydrographs for SC18 - Salt Creek Dam Site 18 -Branched Oak Lake for September 30, 2014 Event Green and Ampt Method – Non-Optimized Initial Conditions

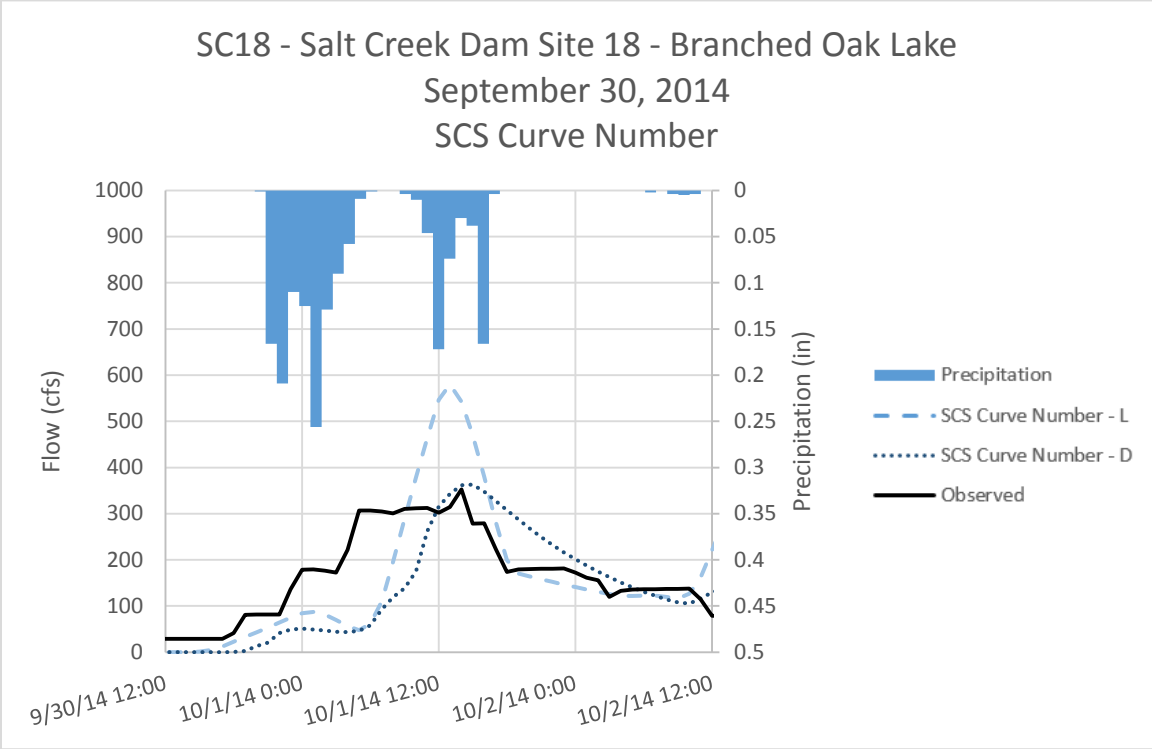

Figure D - 16. Runoff Hydrographs for SC18 - Salt Creek Dam Site 18 -Branched Oak Lake for September 30, 2014 Event SCS Curve Number Method – Non-Optimized Initial Conditions

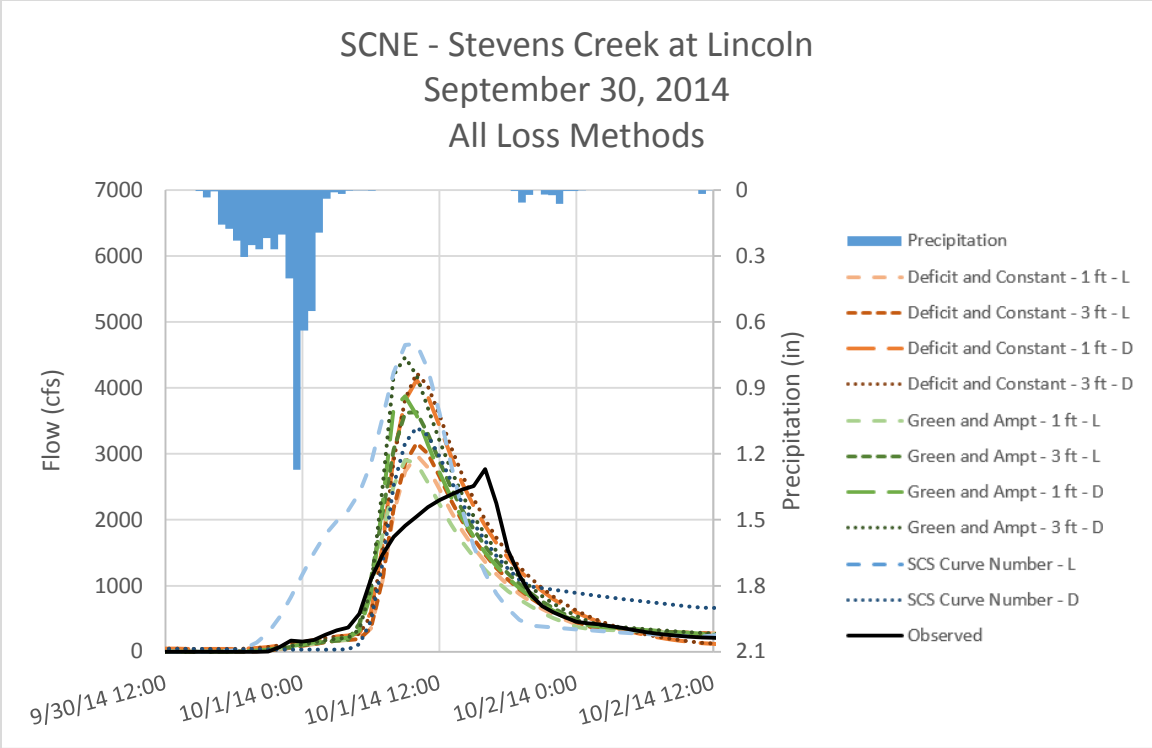

Figure D - 17. Runoff Hydrographs for SCNE – Stevens Creek at Lincoln for September 30, 2014 Event All Loss Methods – Non-Optimized Initial Conditions

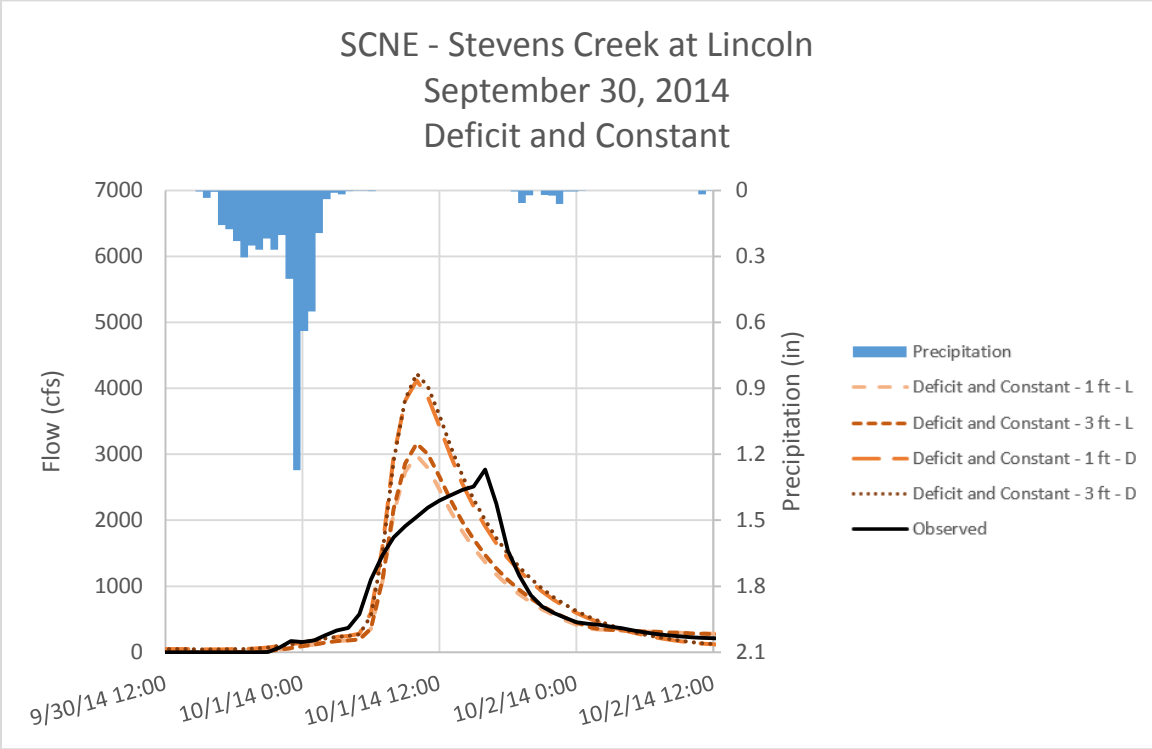

Figure D - 18. Runoff Hydrographs for SCNE – Stevens Creek at Lincoln for September 30, 2014 Event Deficit and Constant Method – Non-Optimized Initial Conditions

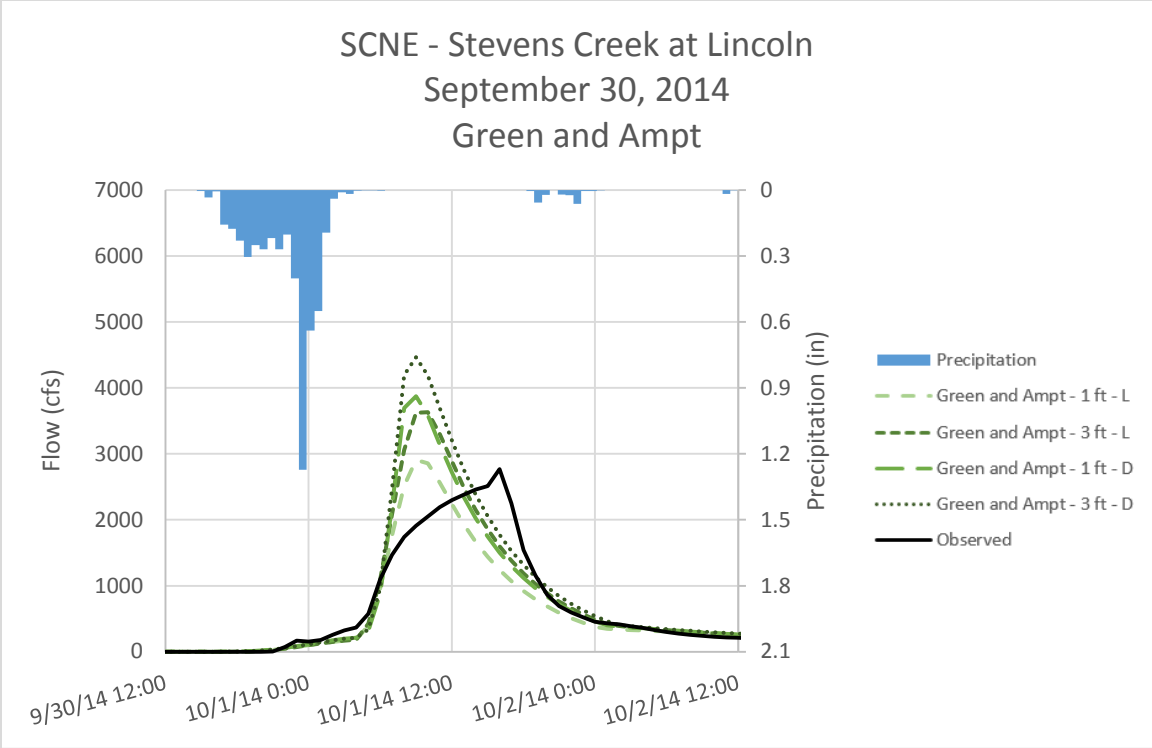

Figure D - 19. Runoff Hydrographs for SCNE – Stevens Creek at Lincoln for September 30, 2014 Event
Green and Ampt Method – Non-Optimized Initial Conditions

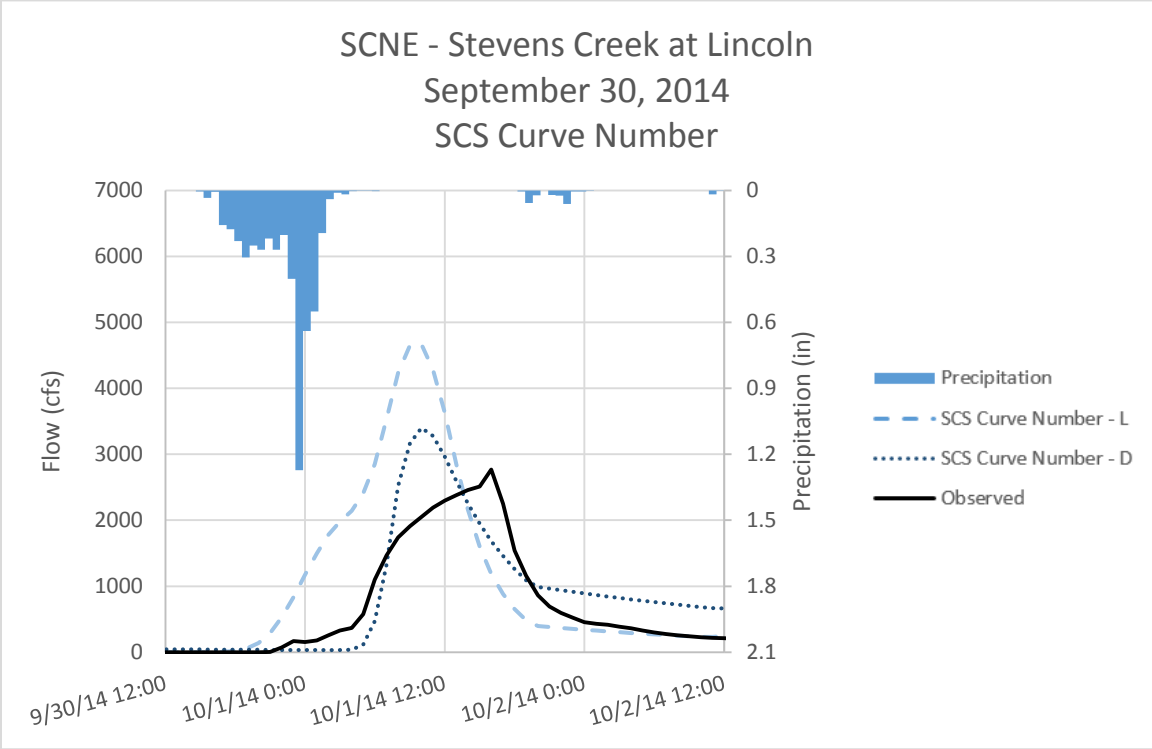

Figure D - 20. Runoff Hydrographs for SCNE – Stevens Creek at Lincoln for September 30, 2014 Event
SCS Curve Number Method – Non-Optimized Initial Conditions

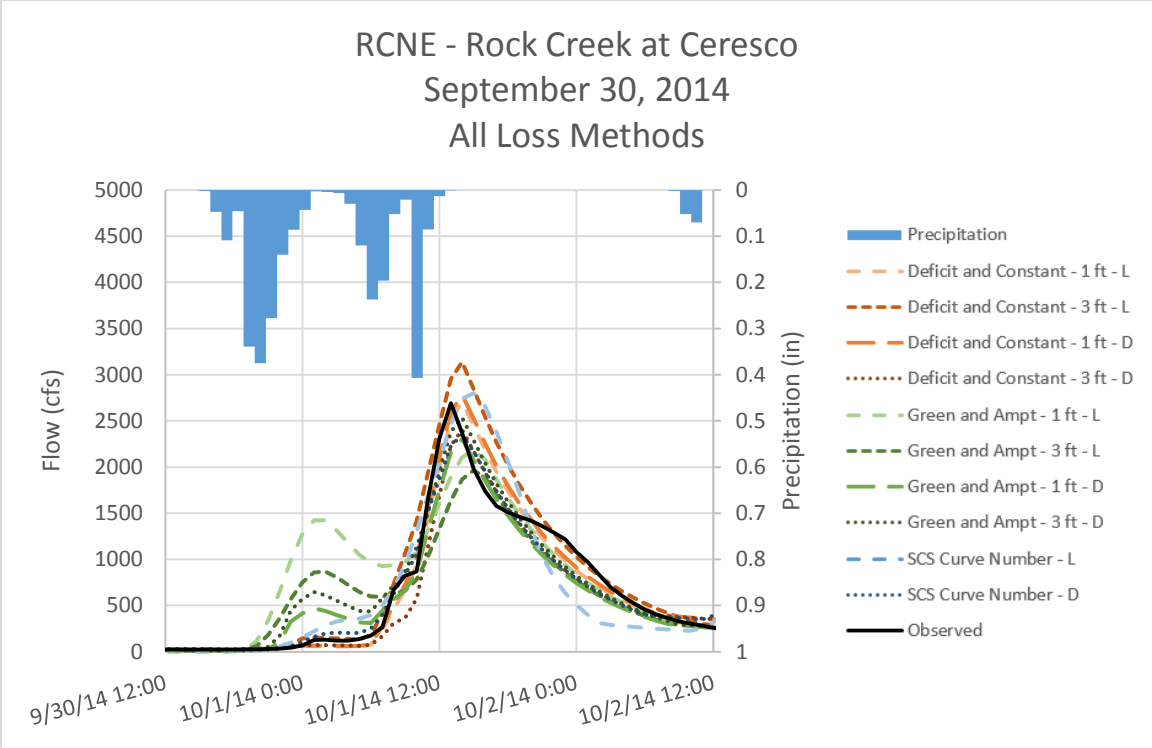

Figure D - 21. Runoff Hydrographs for RCNE – Rock Creek at Ceresco for September 30, 2014 Event All Loss Methods – Non-Optimized Initial Conditions

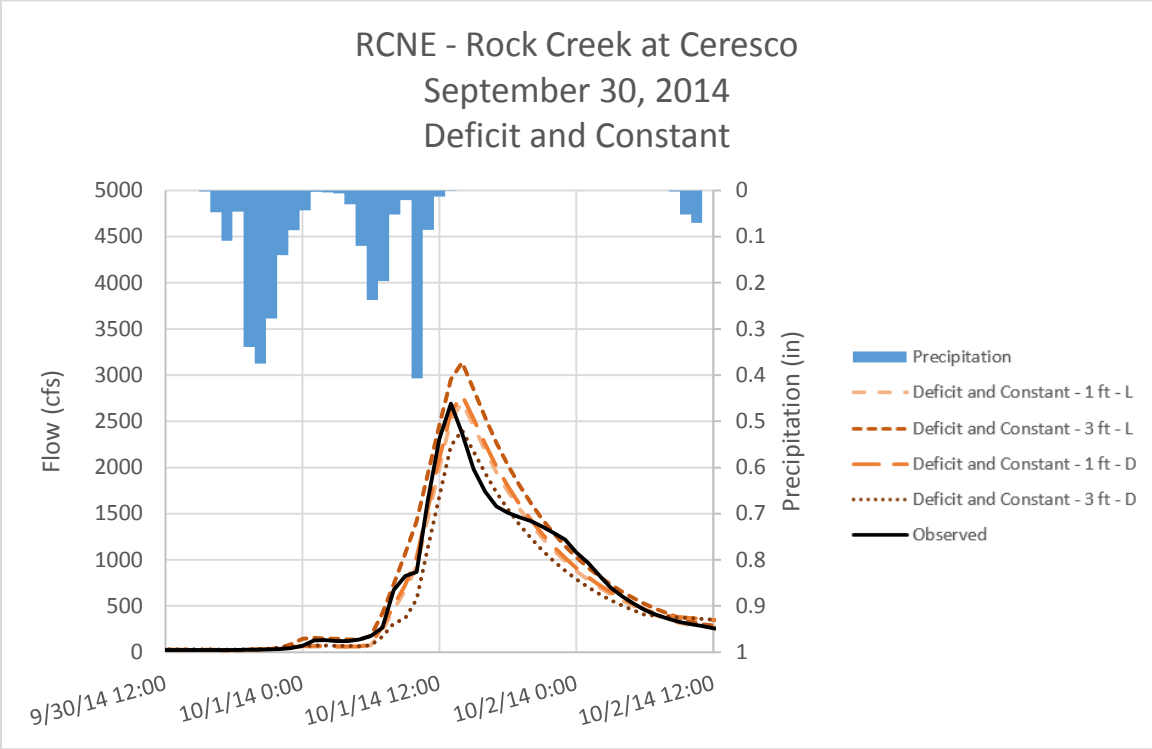

Figure D - 22. Runoff Hydrographs for RCNE – Rock Creek at Ceresco for September 30, 2014 Event Deficit and Constant Method – Non-Optimized Initial Conditions

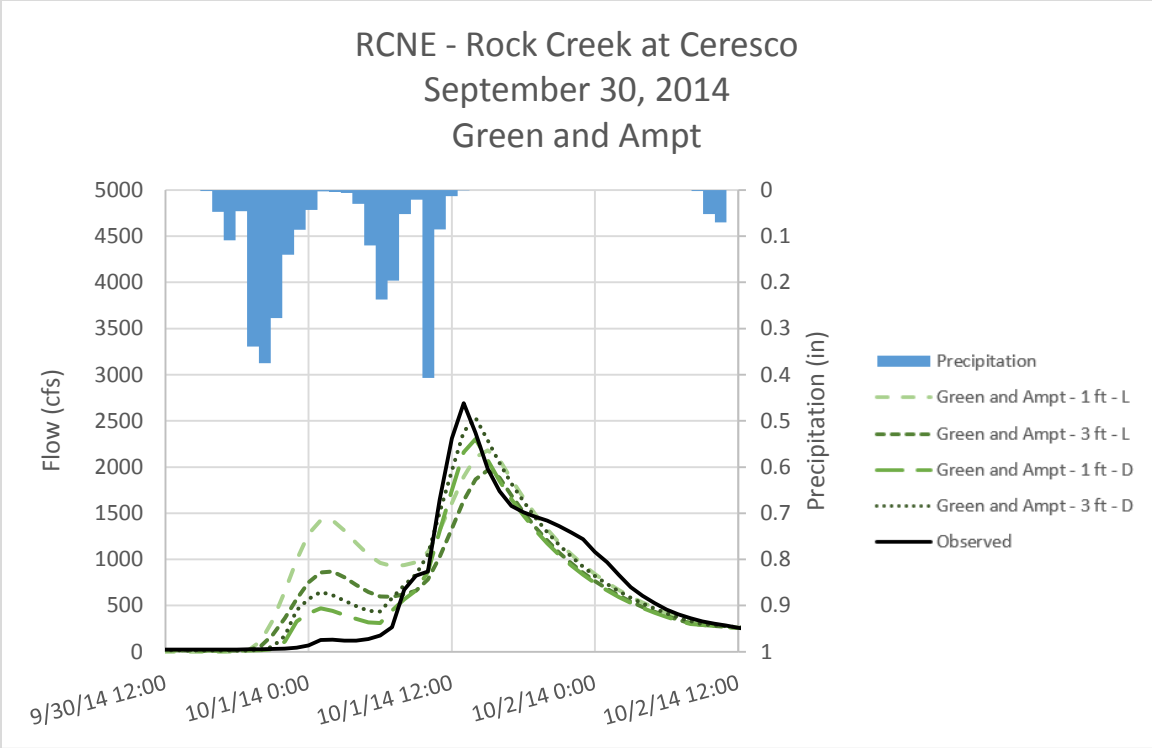

Figure D - 23. Runoff Hydrographs for RCNE – Rock Creek at Ceresco for September 30, 2014 Event
Green and Ampt Method – Non-Optimized Initial Conditions

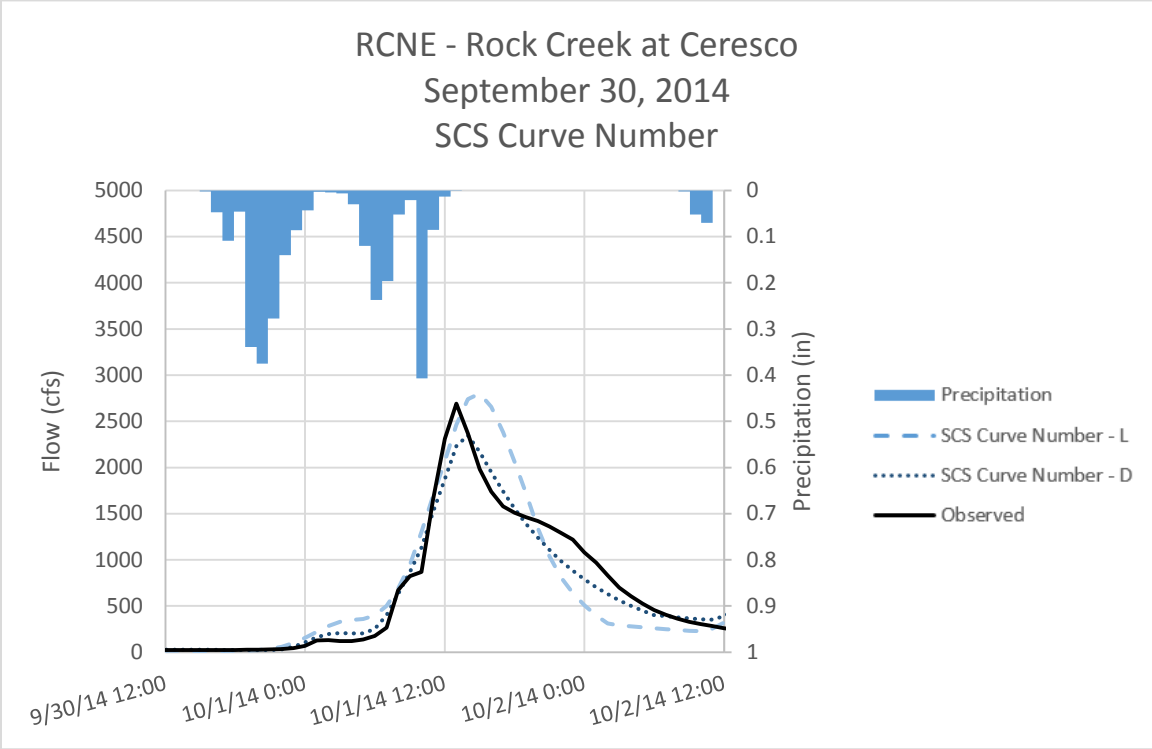

Figure D - 24. Runoff Hydrographs for RCNE – Rock Creek at Ceresco for September 30, 2014 Event
SCS Curve Number Method – Non-Optimized Initial Conditions

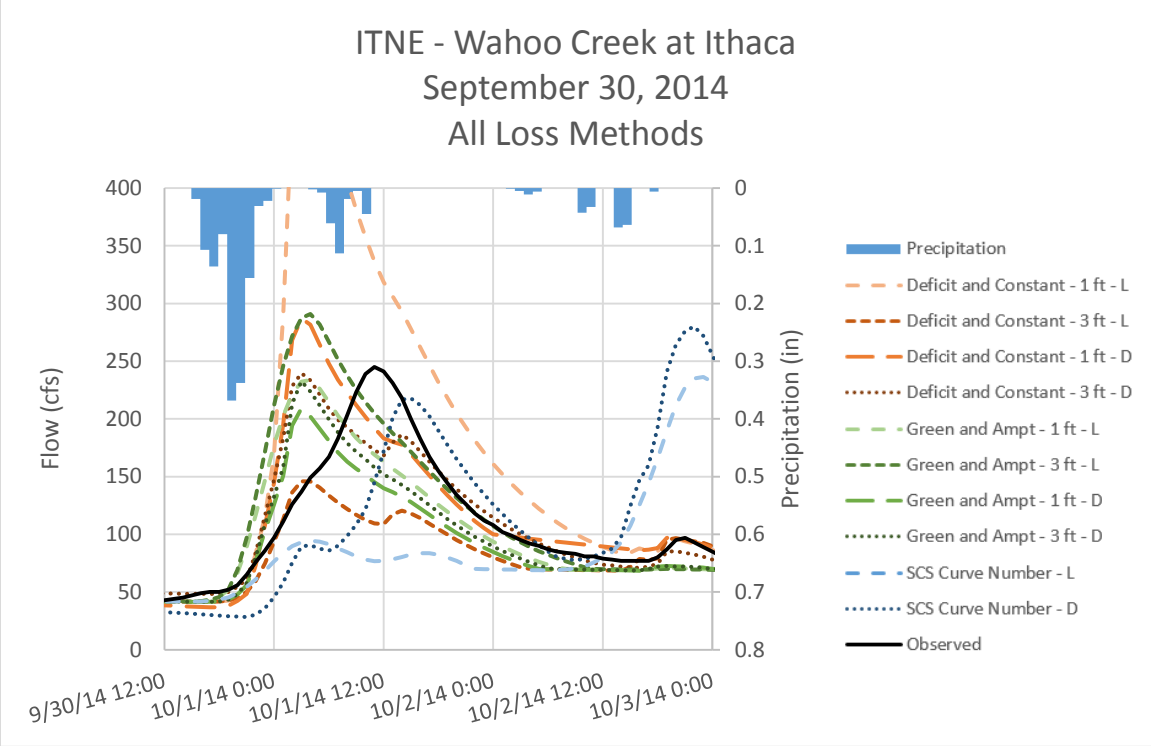

Figure D - 25. Runoff Hydrographs for ITNE – Wahoo Creek at Ithaca for September 30, 2014 Event All Loss Methods – Non-Optimized Initial Conditions

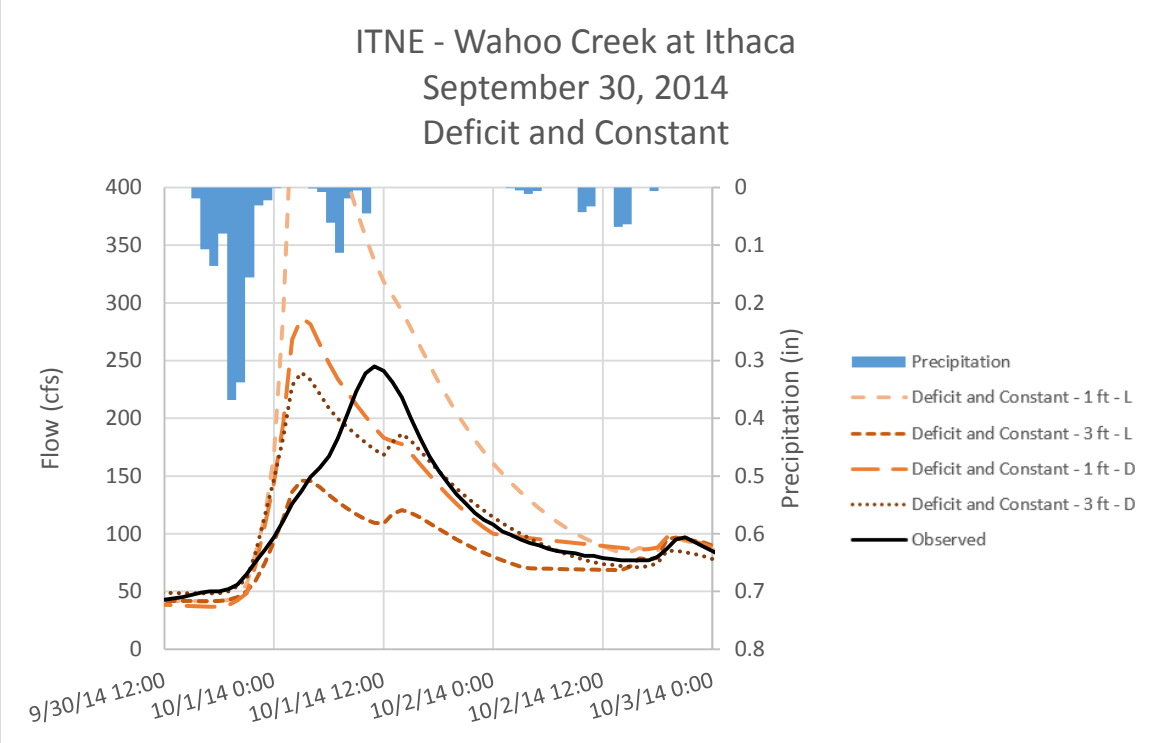

Figure D - 26. Runoff Hydrographs for ITNE – Wahoo Creek at Ithaca for September 30, 2014 Event Deficit and Constant Method – Non-Optimized Initial Conditions

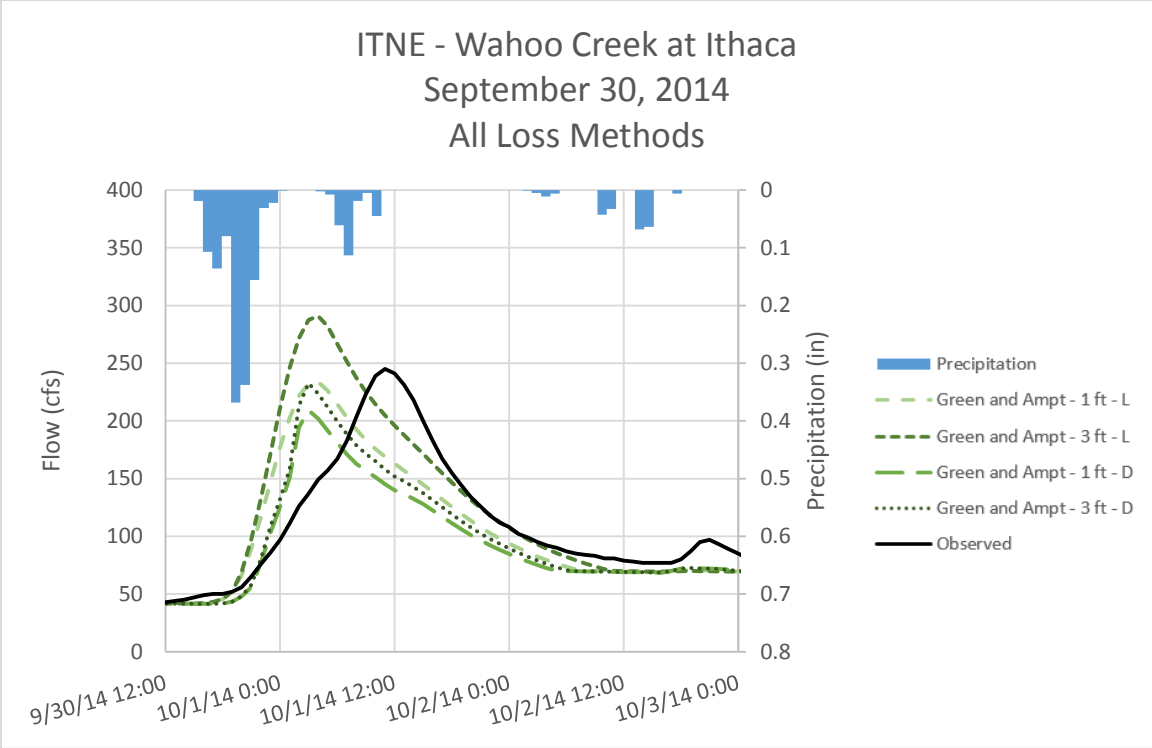

Figure D - 27. Runoff Hydrographs for ITNE – Wahoo Creek at Ithaca for September 30, 2014 Event
Green and Ampt Method – Non-Optimized Initial Conditions

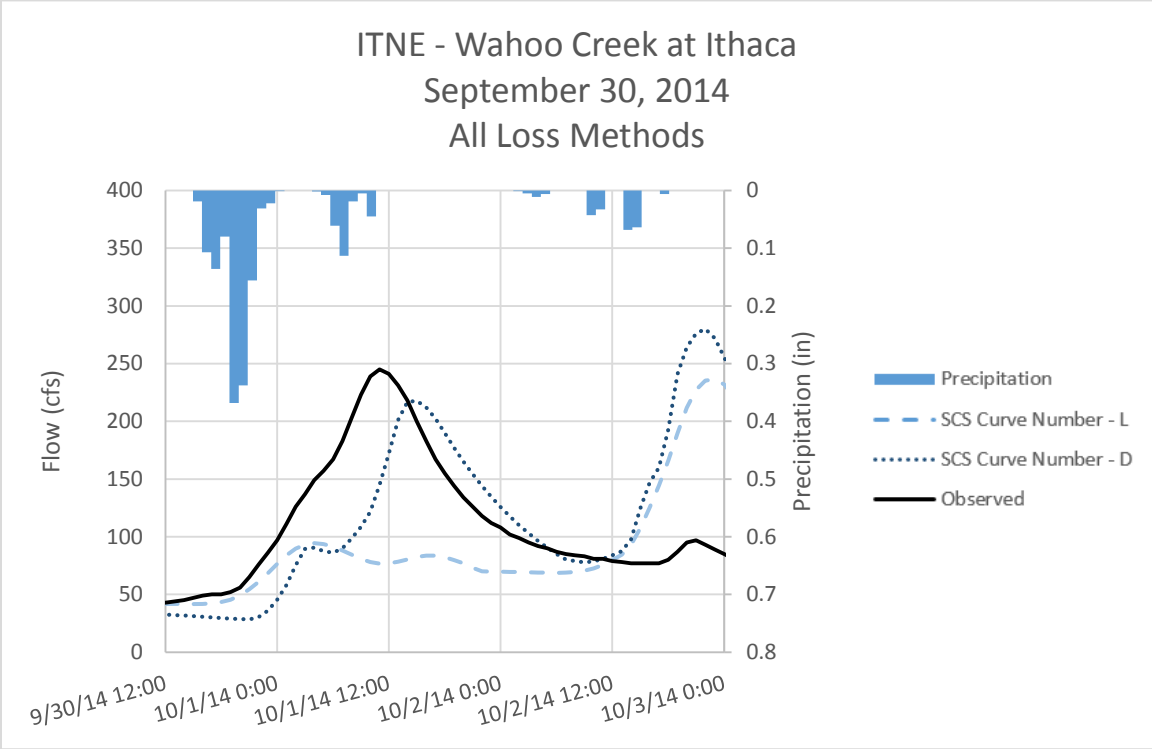

Figure D - 28. Runoff Hydrographs for ITNE – Wahoo Creek at Ithaca for September 30, 2014 Event
SCS Curve Number Method – Non-Optimized Initial Conditions

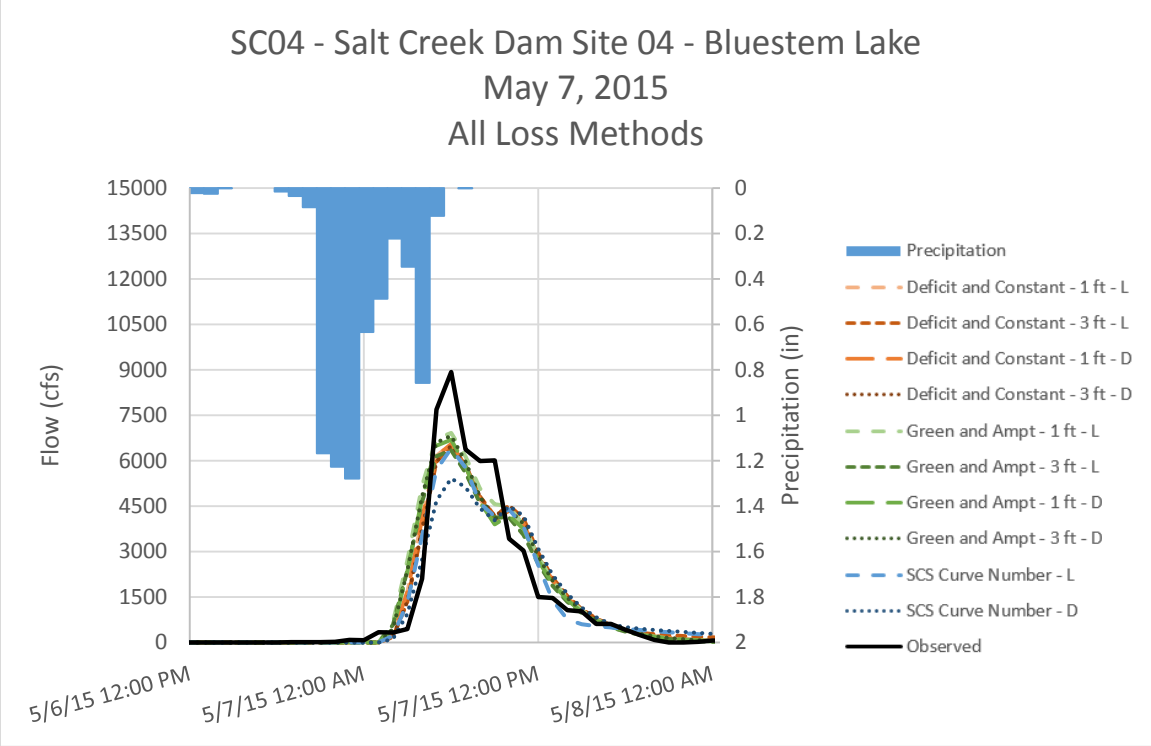

Figure D - 29. Runoff Hydrographs for SC04 - Salt Creek Dam Site 04 - Bluestem Lake for May 7, 2015 Event All Loss Methods – Non-Optimized Initial Conditions

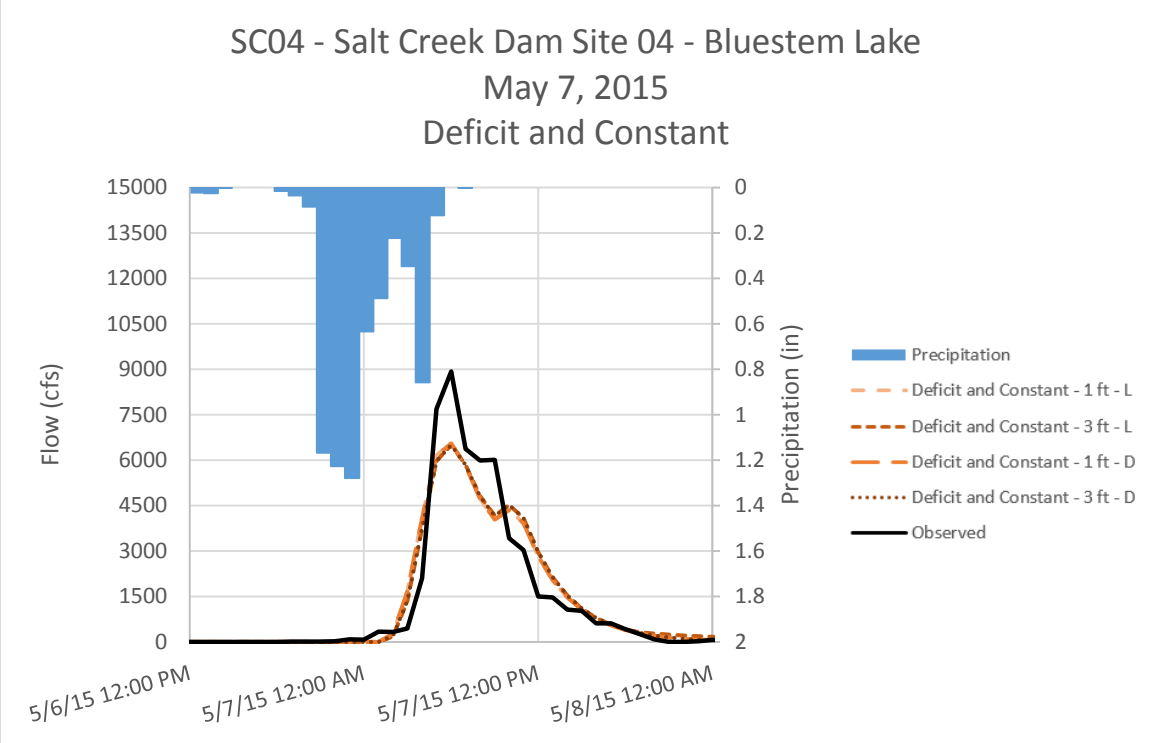

Figure D - 30. Runoff Hydrographs for SC04 - Salt Creek Dam Site 04 - Bluestem Lake for May 7, 2015 Event Deficit and Constant Method – Non-Optimized Initial Conditions

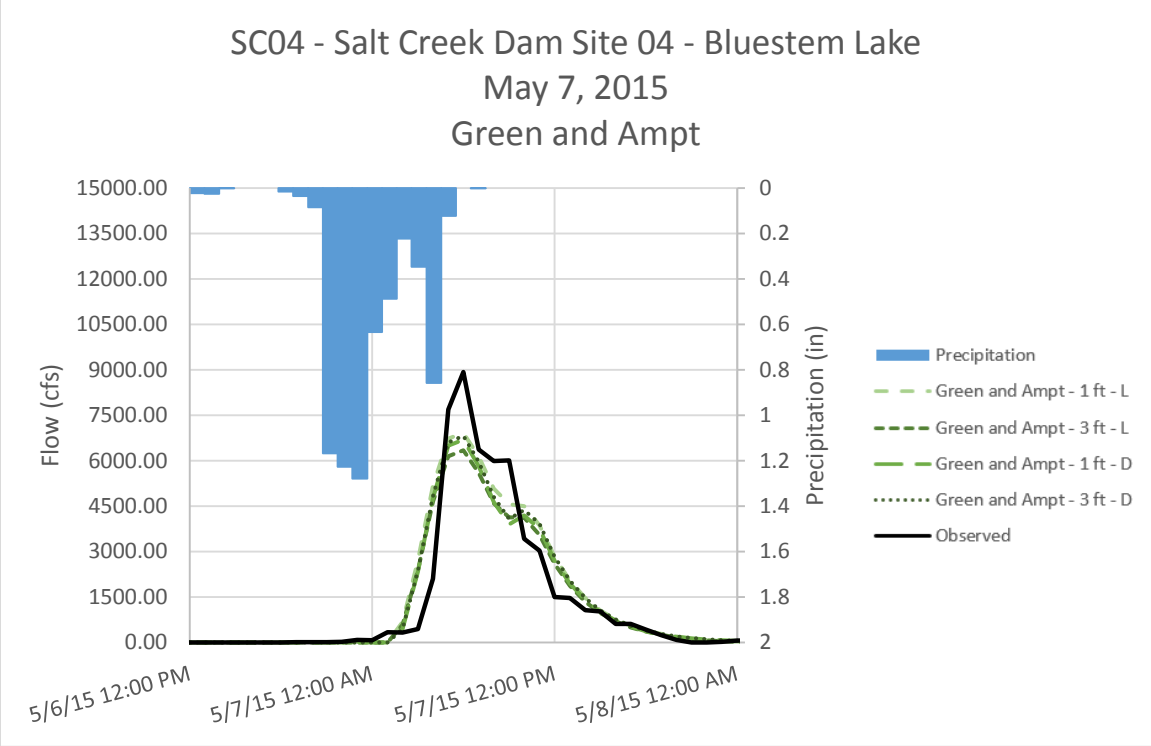

Figure D - 31. Runoff Hydrographs for SC04 - Salt Creek Dam Site 04 - Bluestem Lake for May 7, 2015 Event Green and Ampt Method – Non-Optimized Initial Conditions

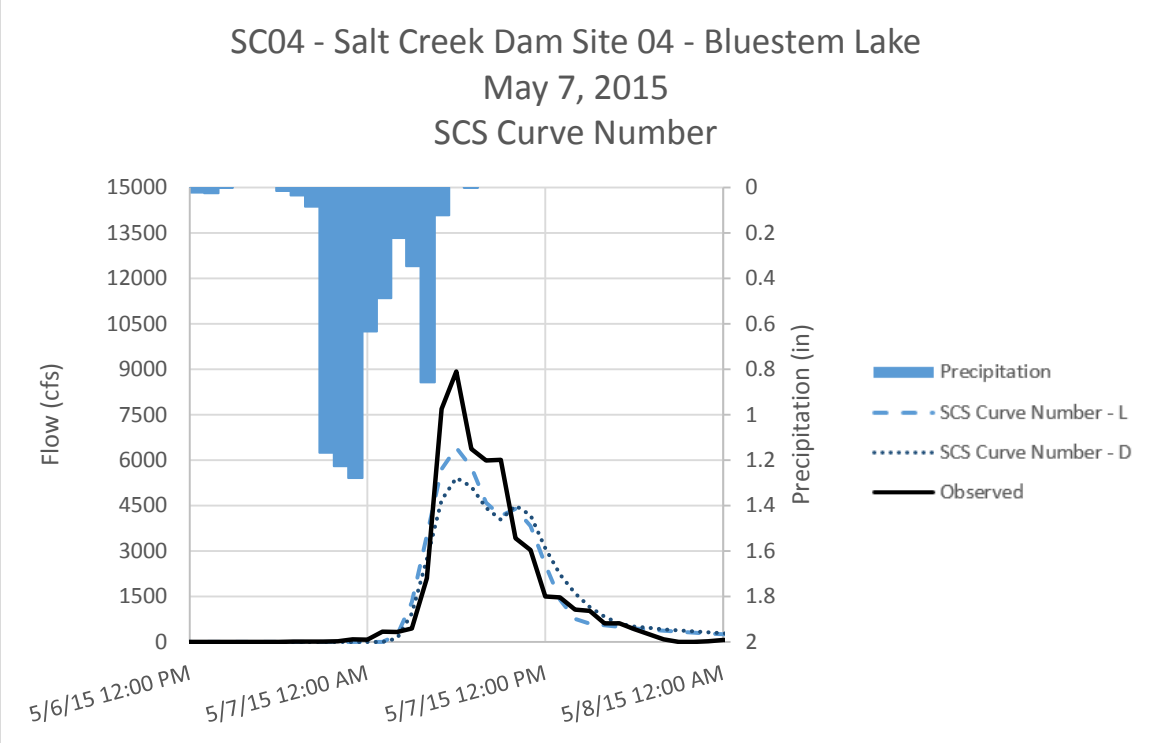

Figure D - 32. Runoff Hydrographs for SC04 - Salt Creek Dam Site 04 - Bluestem Lake for May 7, 2015 Event SCS Curve Number Method – Non-Optimized Initial Conditions

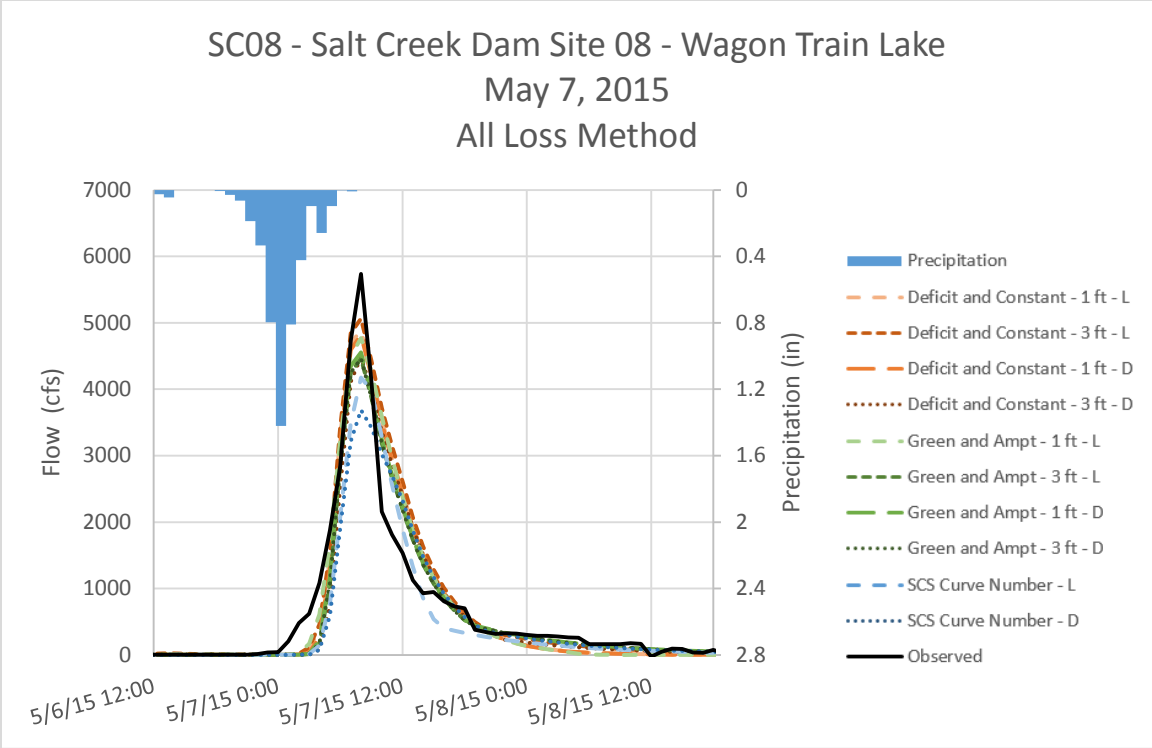

Figure D - 33. Runoff Hydrographs for SC08 - Salt Creek Dam Site 08 – Wagon Train Lake for May 7, 2015 Event All Loss Methods – Non-Optimized Initial Conditions

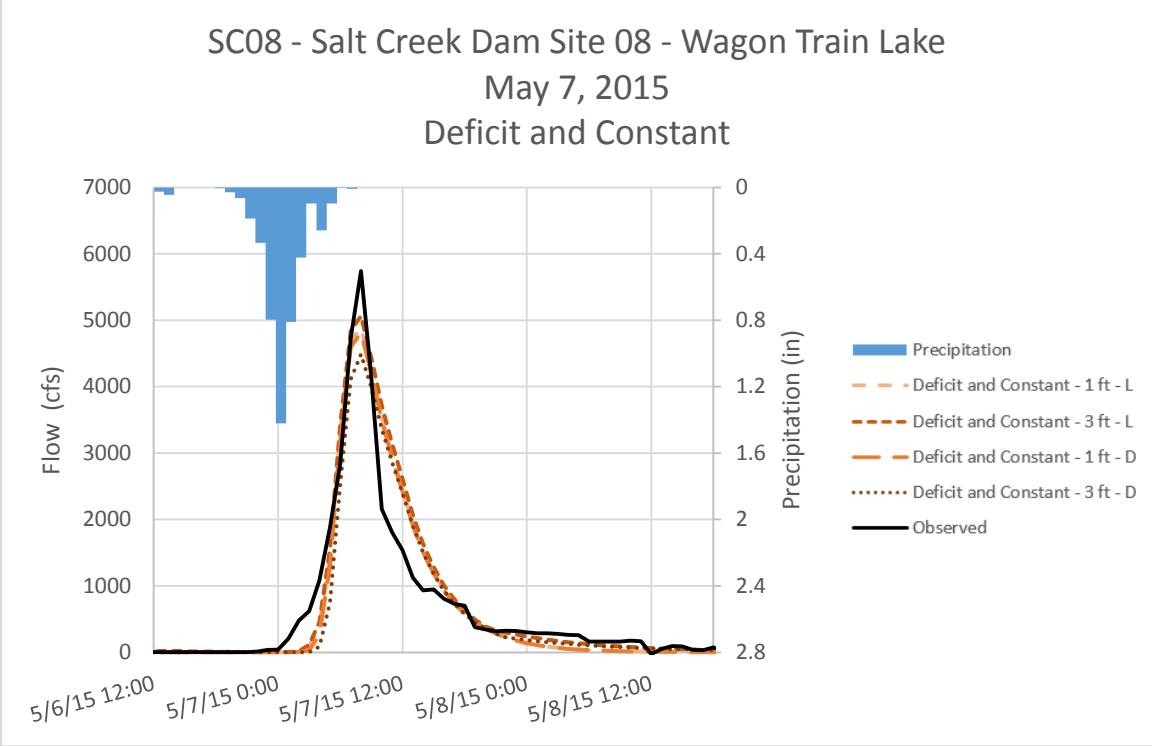

Figure D - 34. Runoff Hydrographs for SC08 - Salt Creek Dam Site 08 – Wagon Train Lake for May 7, 2015 Event Deficit and Constant Method – Non-Optimized Initial Conditions

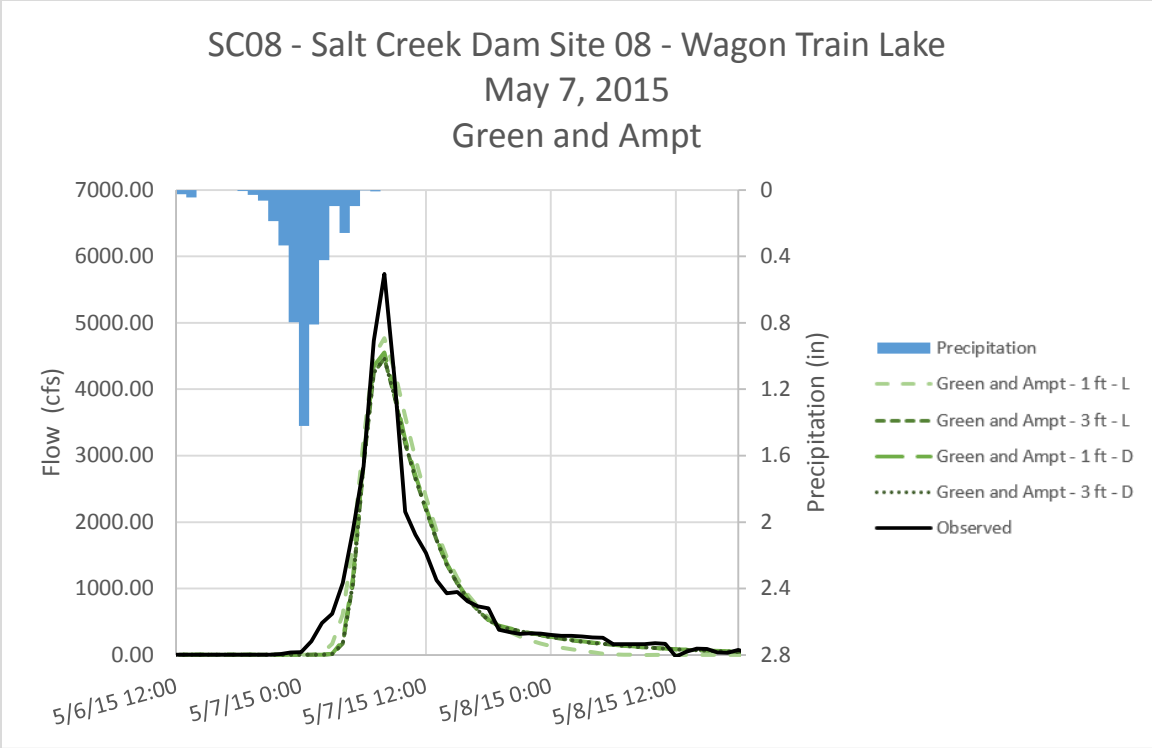

Figure D - 35. Runoff Hydrographs for SC08 - Salt Creek Dam Site 08 – Wagon Train Lake for May 7, 2015 Event Green and Ampt Method – Non-Optimized Initial Conditions

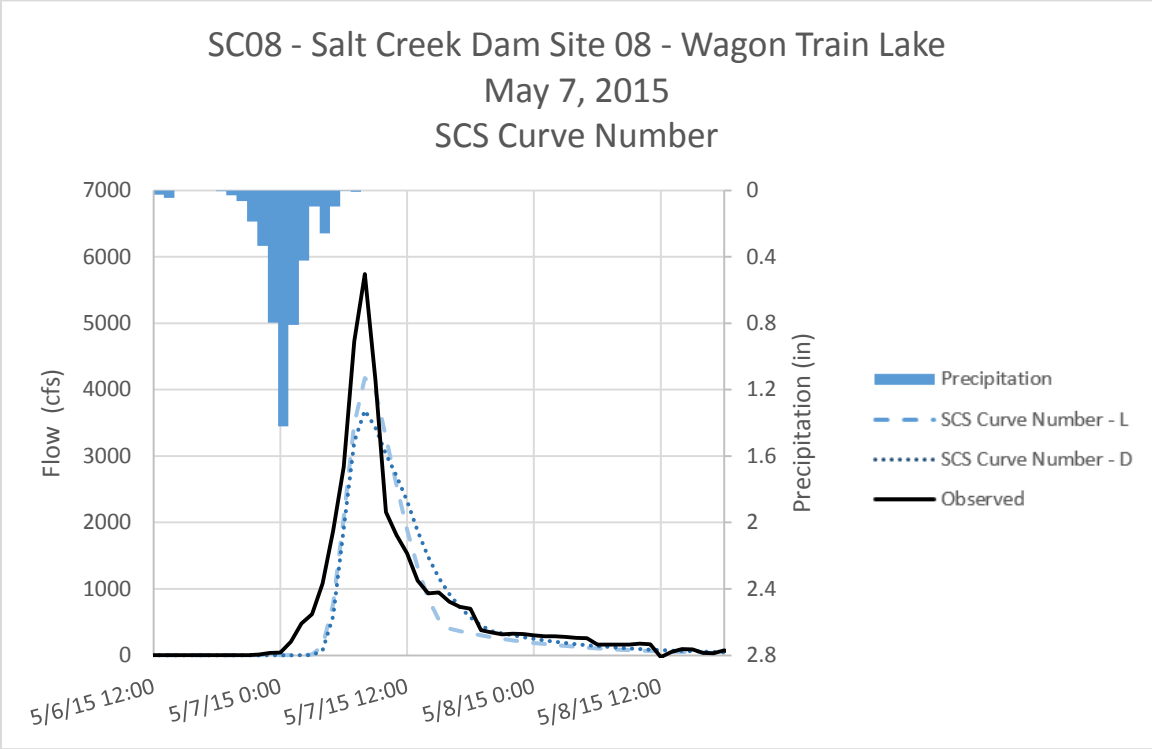

Figure D - 36. Runoff Hydrographs for SC08 - Salt Creek Dam Site 08 – Wagon Train Lake for May 7, 2015 Event SCS Curve Number Method – Non-Optimized Initial Conditions

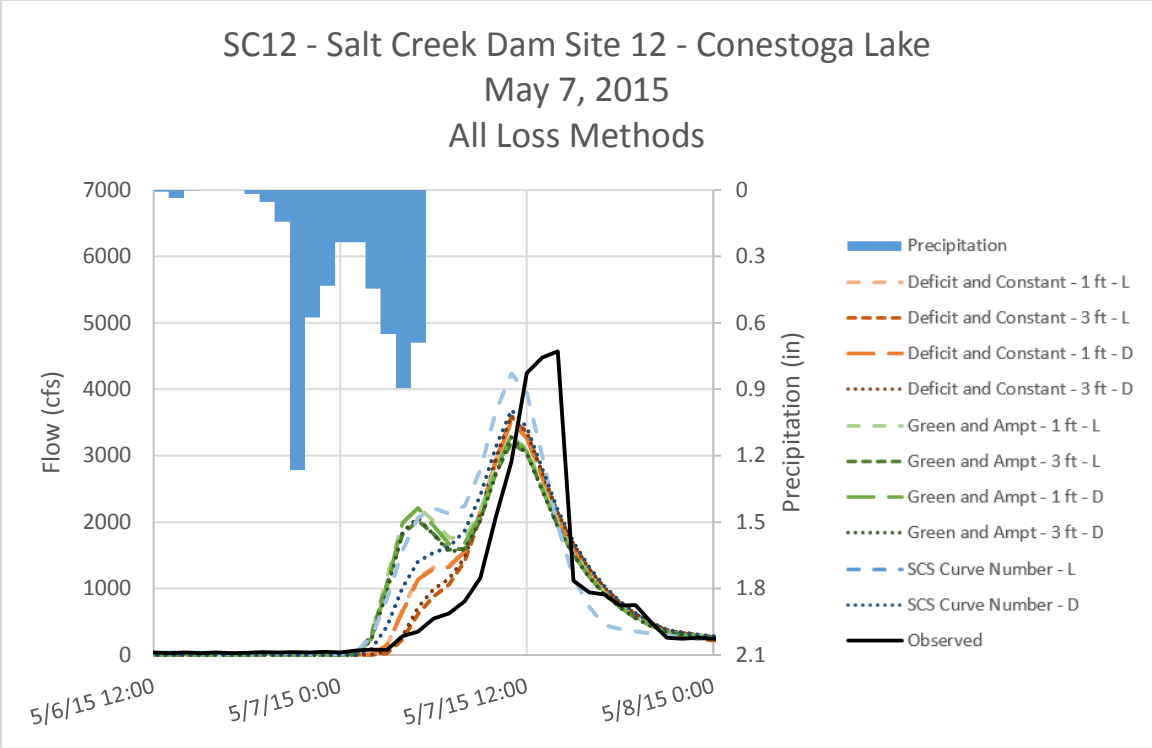

Figure D - 37. Runoff Hydrographs for SC12 - Salt Creek Dam Site 12 – Conestoga Lake for May 7, 2015 Event All Loss Methods – Non-Optimized Initial Conditions

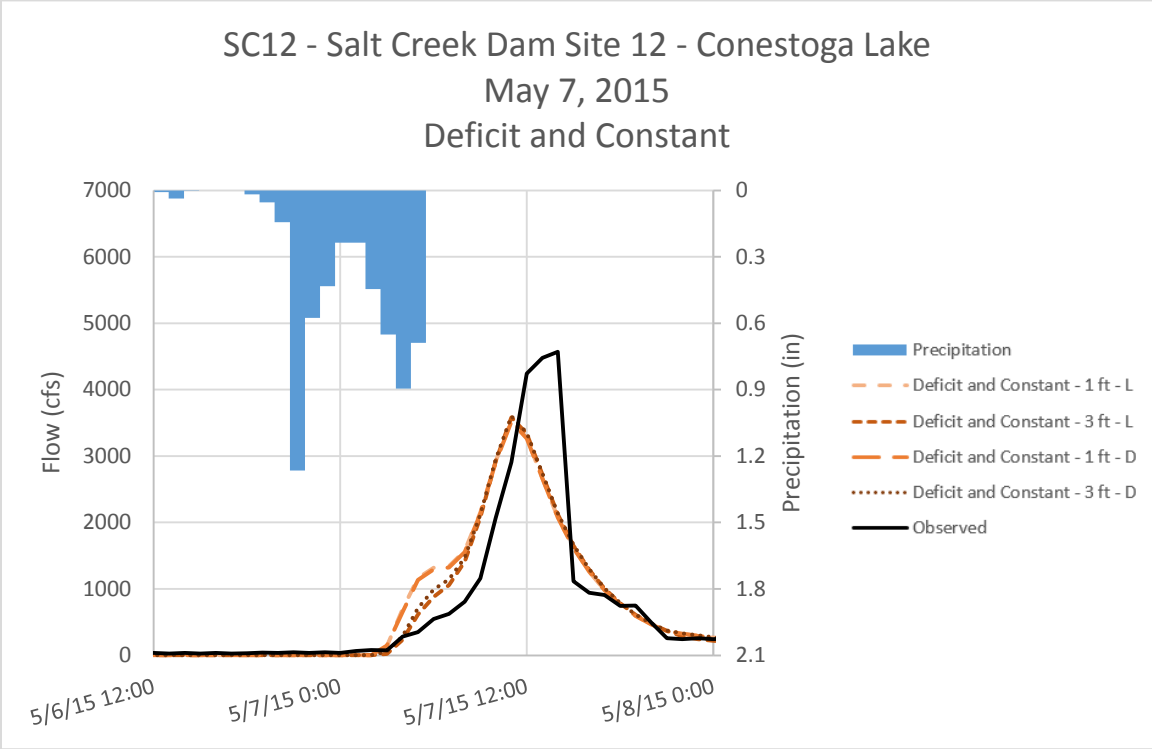

Figure D - 38. Runoff Hydrographs for SC12 - Salt Creek Dam Site 12 – Conestoga Lake for May 7, 2015 Event Deficit and Constant Method – Non-Optimized Initial Conditions

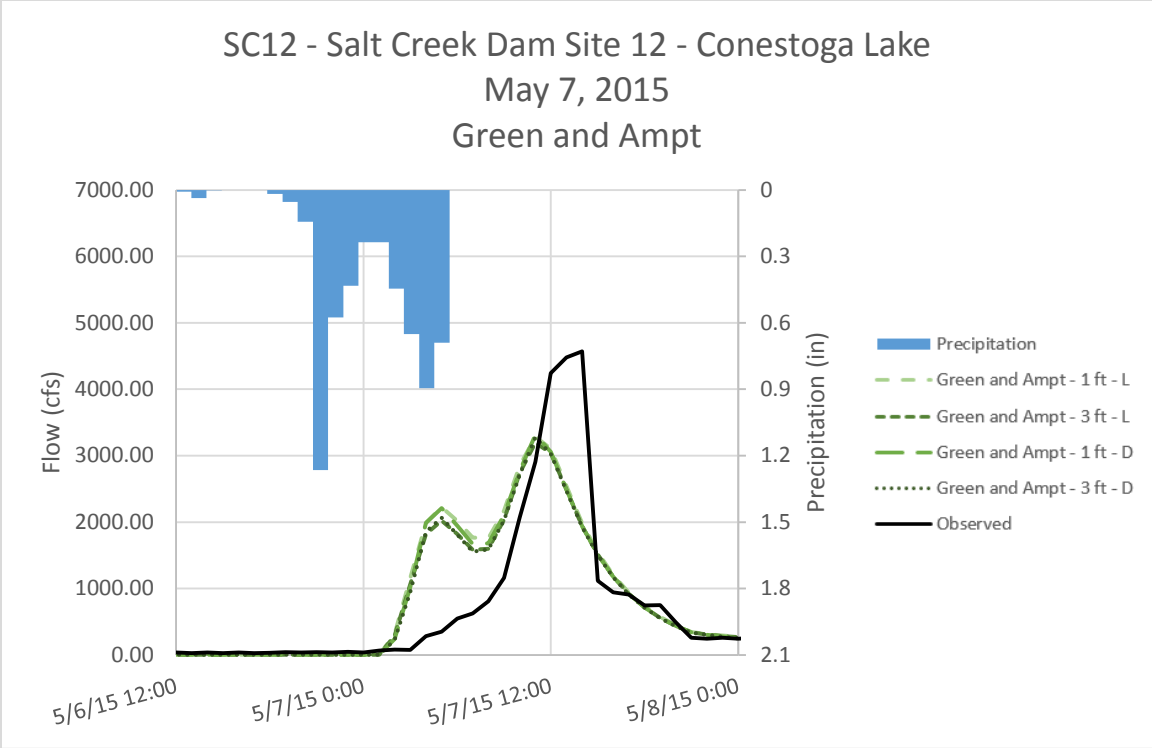

Figure D - 39. Runoff Hydrographs for SC12 - Salt Creek Dam Site 12 – Conestoga Lake for May 7, 2015 Event Green and Ampt Method – Non-Optimized Initial Conditions

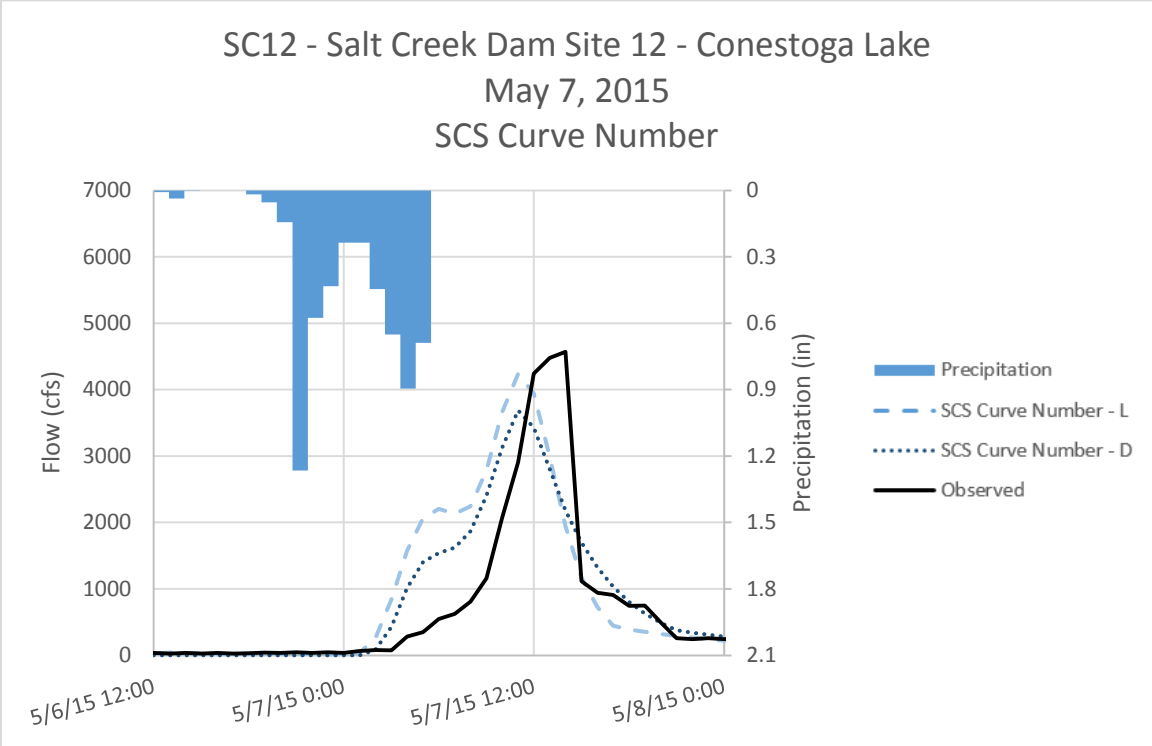

Figure D - 40. Runoff Hydrographs for SC12 - Salt Creek Dam Site 12 – Conestoga Lake for May 7, 2015 Event SCS Curve Number Method – Non-Optimized Initial Conditions

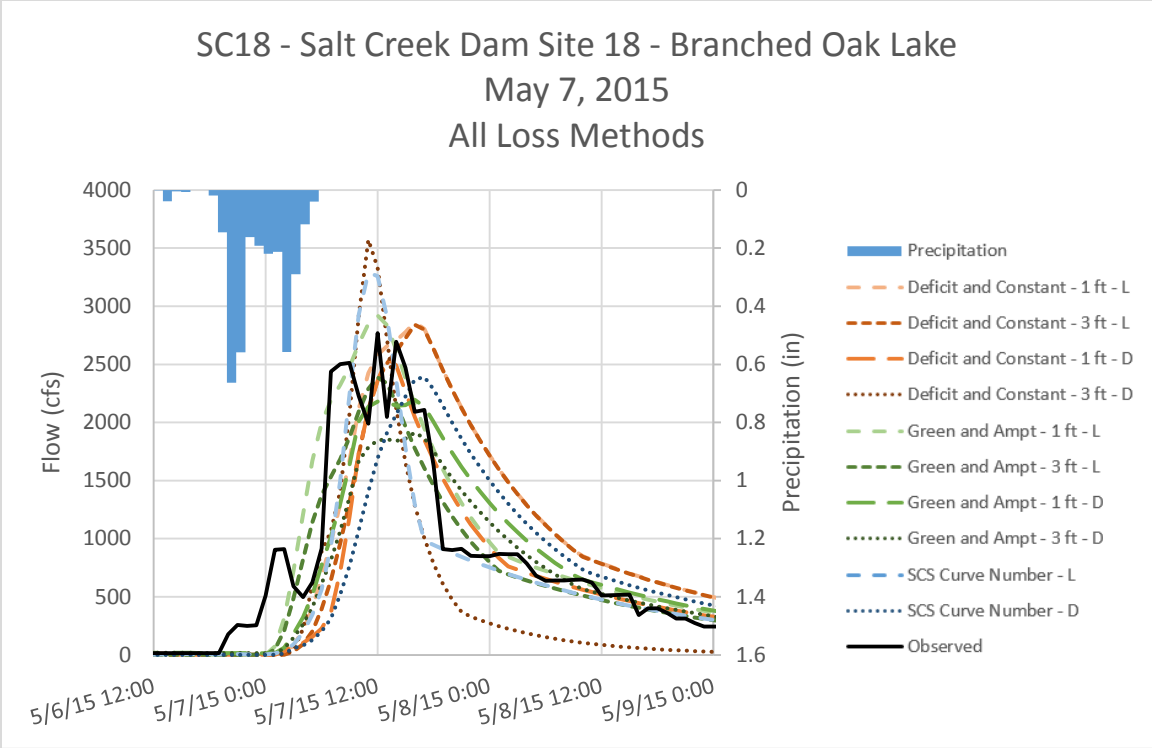

Figure D - 41. Runoff Hydrographs for SC18 - Salt Creek Dam Site 18 – Branched Oak Lake for May 7, 2015 Event All Loss Methods – Non-Optimized Initial Conditions

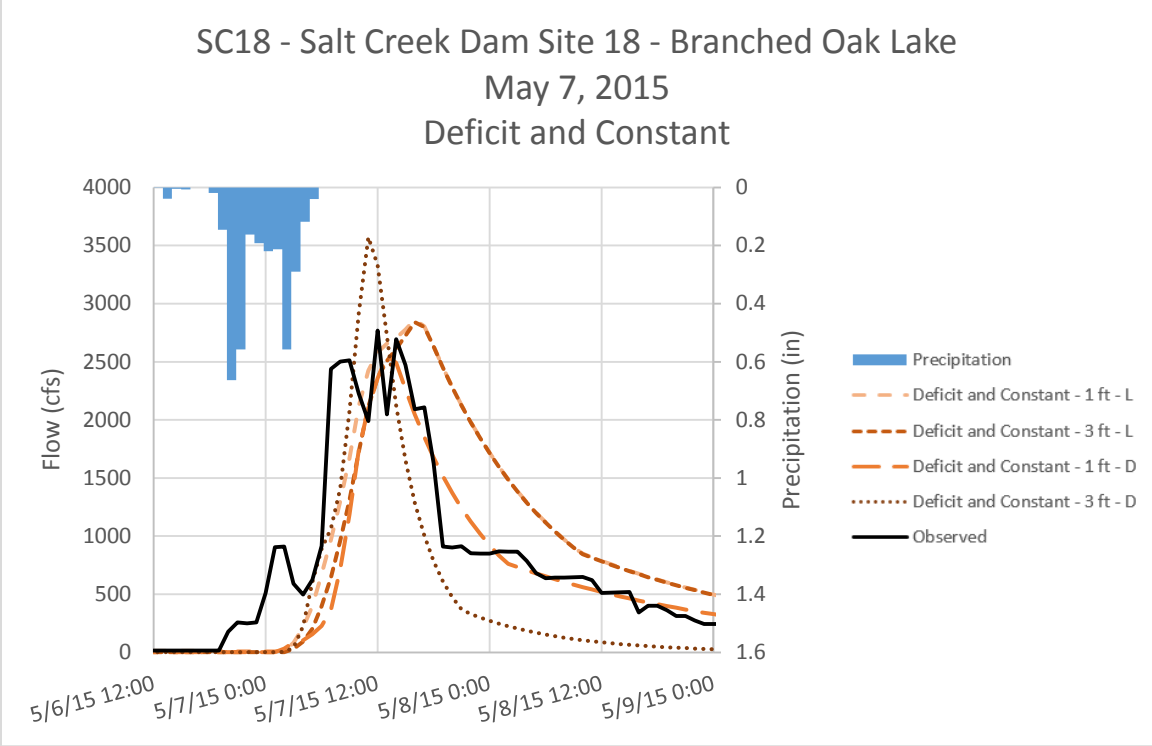

Figure D - 42. Runoff Hydrographs for SC18 - Salt Creek Dam Site 18 – Branched Oak Lake for May 7, 2015 Event Deficit and Constant Method – Non-Optimized Initial Conditions

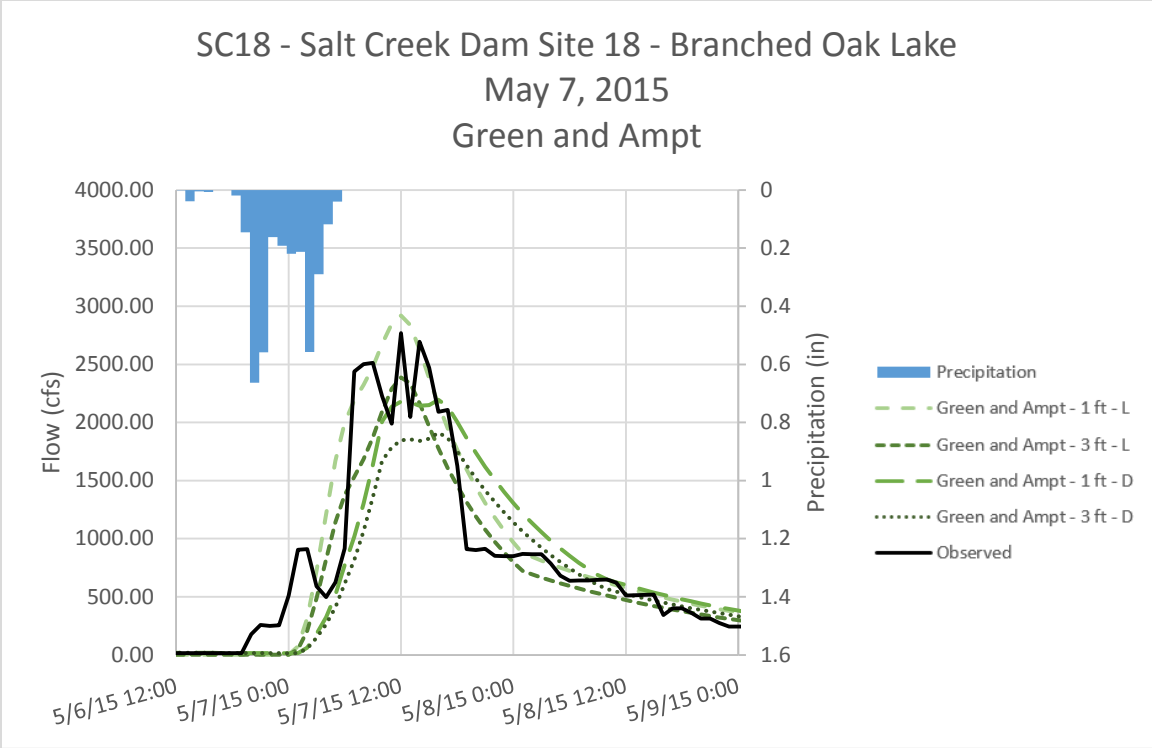

Figure D - 43. Runoff Hydrographs for SC18 - Salt Creek Dam Site 18 – Branched Oak Lake for May 7, 2015 Event Green and Ampt Method – Non-Optimized Initial Conditions

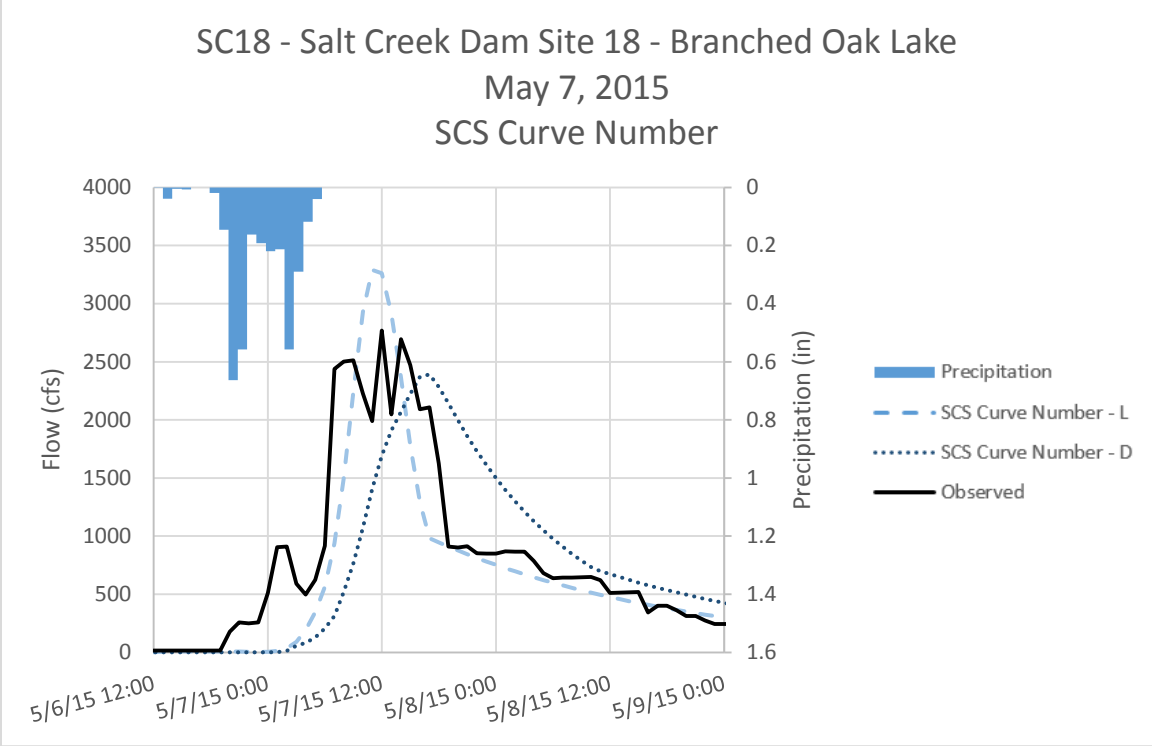

Figure D - 44. Runoff Hydrographs for SC18 - Salt Creek Dam Site 18 – Branched Oak Lake for May 7, 2015 Event SCS Curve Number Method – Non-Optimized Initial Conditions

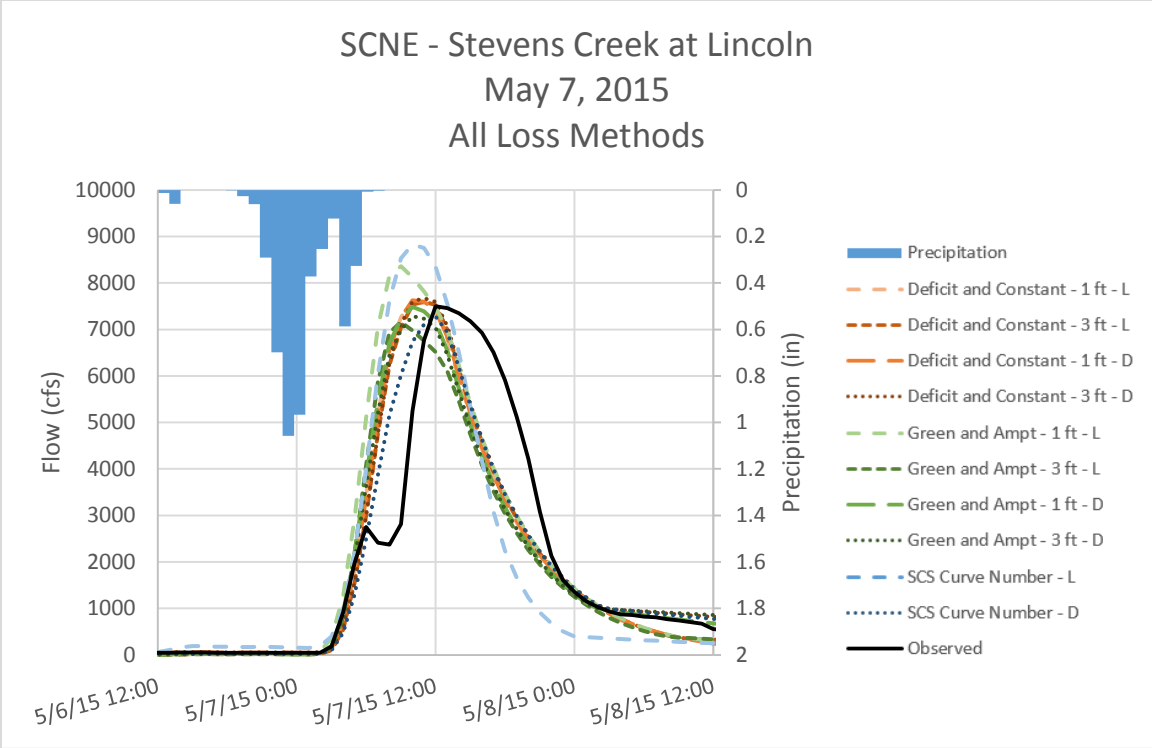

Figure D - 45. Runoff Hydrographs for SCNE – Stevens Creek at Lincoln for May 7, 2015 Event
All Loss Methods – Non-Optimized Initial Conditions

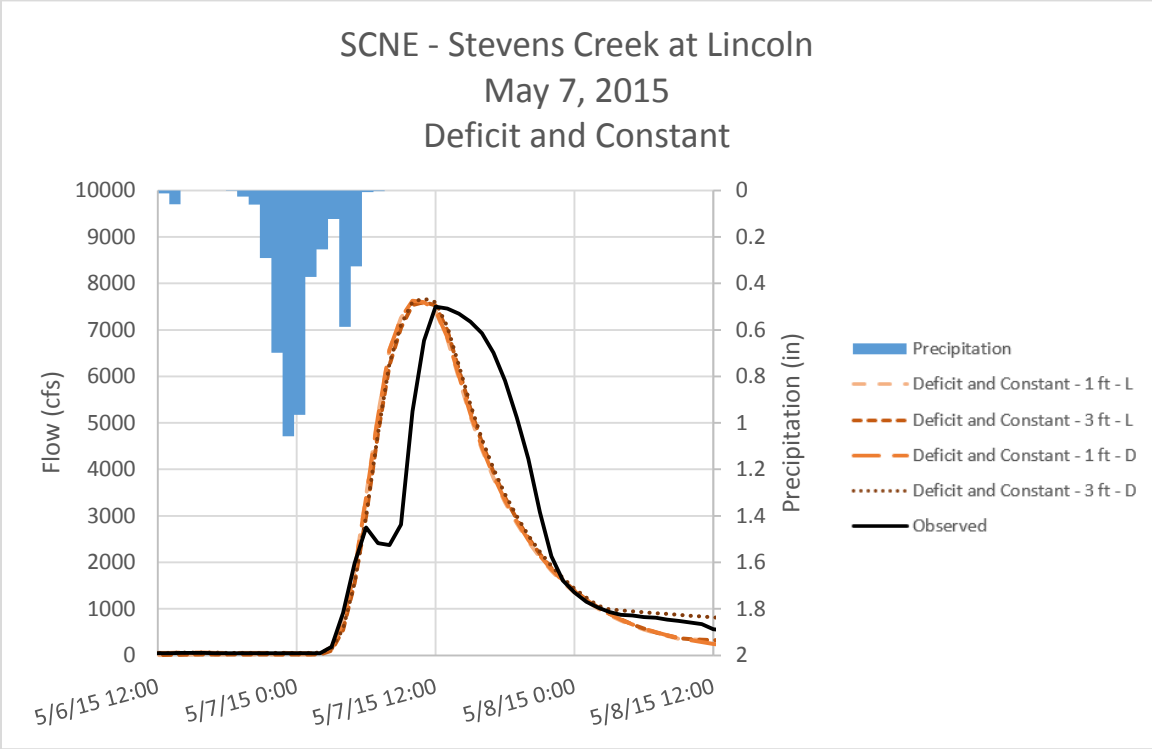

Figure D - 46. Runoff Hydrographs for SCNE – Stevens Creek at Lincoln for May 7, 2015 Event
Deficit and Constant Method – Non-Optimized Initial Conditions

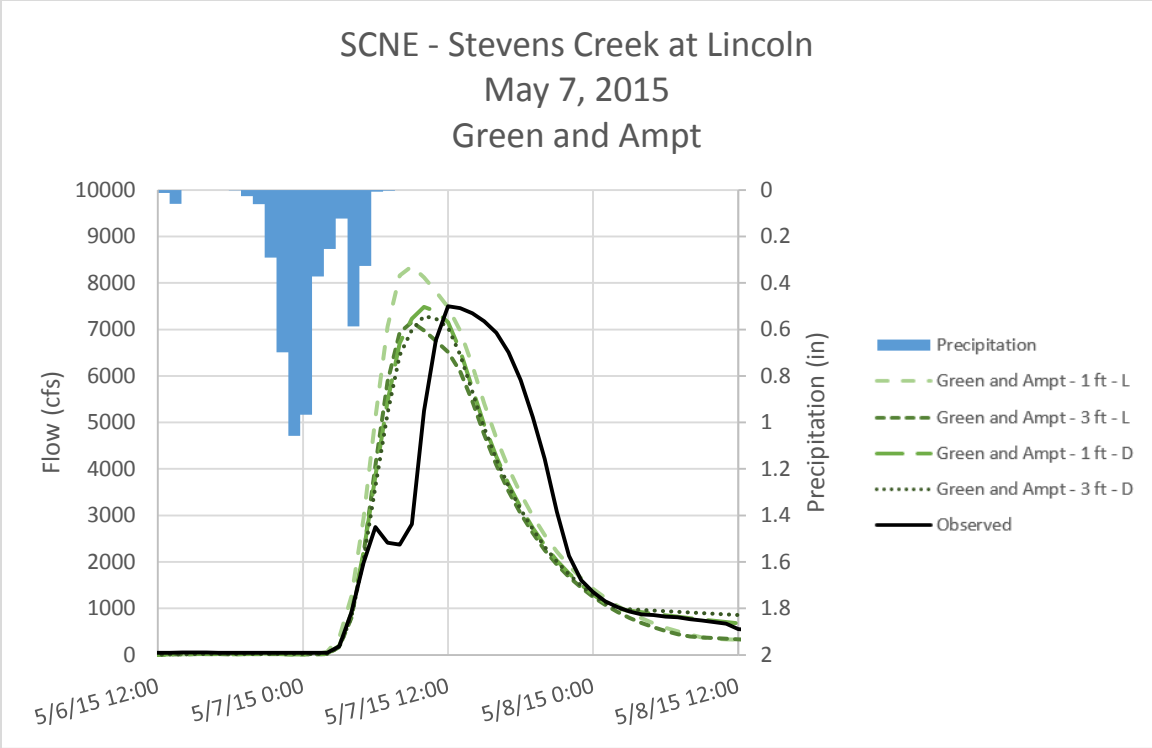

Figure D - 47. Runoff Hydrographs for SCNE – Stevens Creek at Lincoln for May 7, 2015 Event
Green and Ampt Method – Non-Optimized Initial Conditions

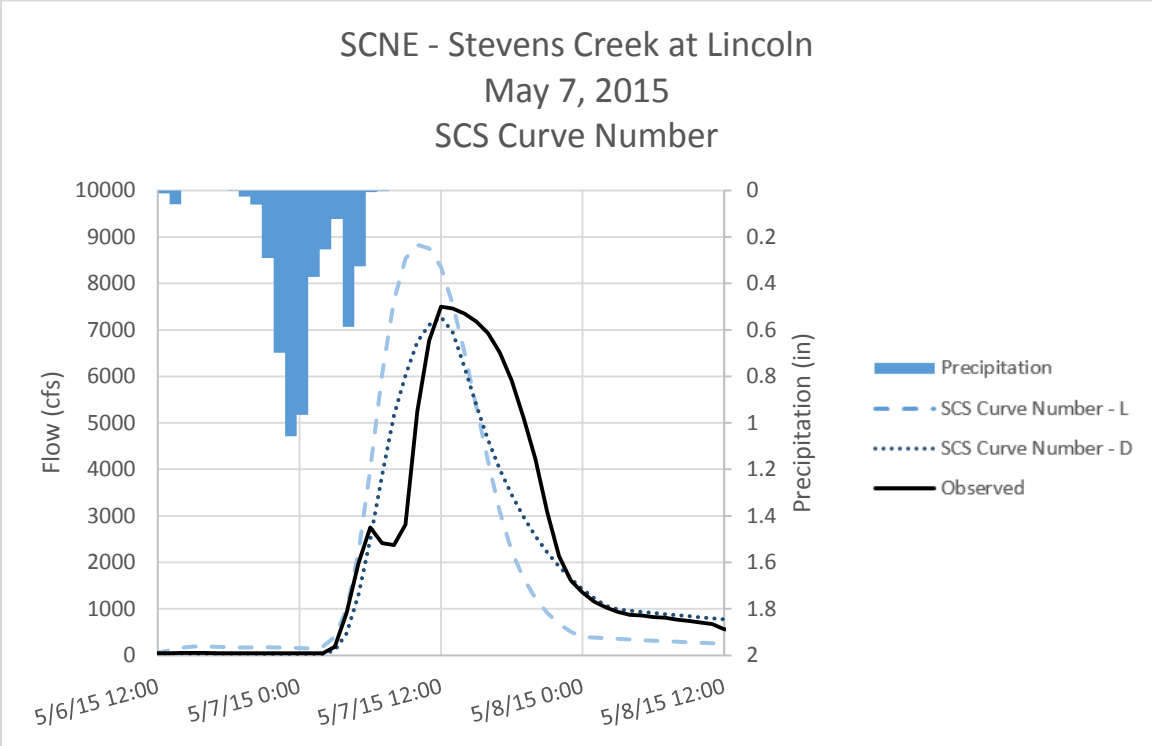

Figure D - 48. Runoff Hydrographs for SCNE – Stevens Creek at Lincoln for May 7, 2015 Event
SCS Curve Number Method – Non-Optimized Initial Conditions

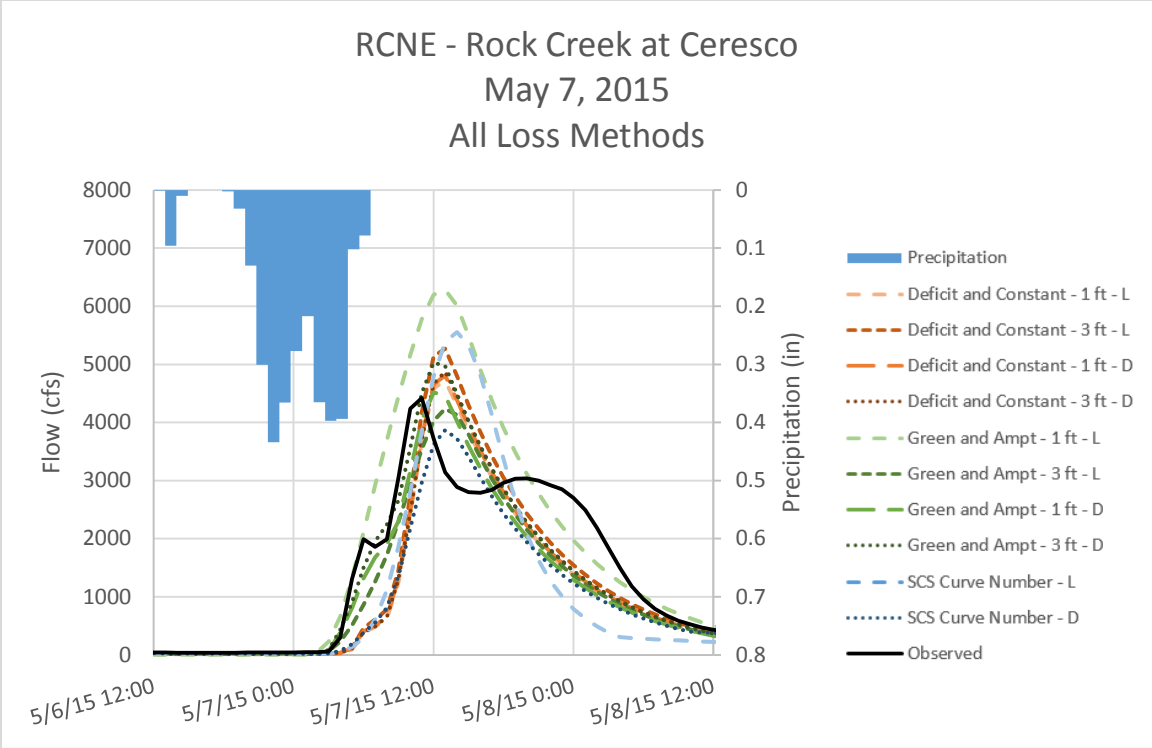

Figure D - 49. Runoff Hydrographs for RCNE – Rock Creek at Ceresco for May 7, 2015 Event
All Loss Methods – Non-Optimized Initial Conditions

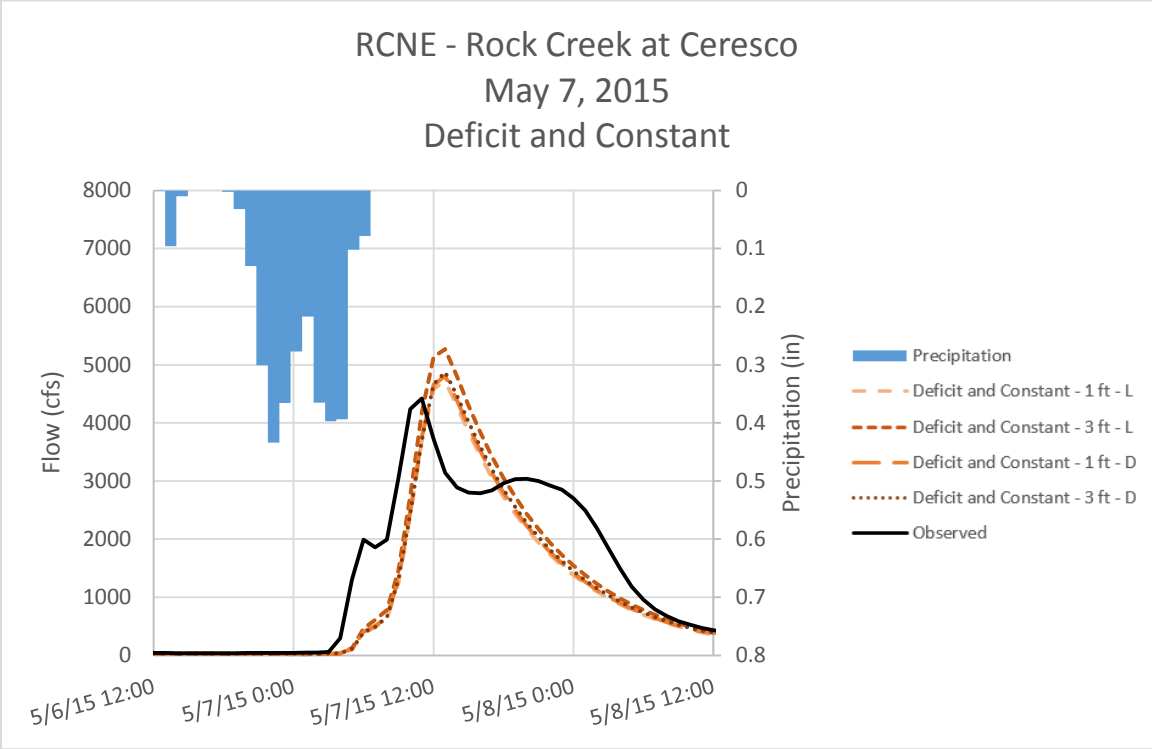

Figure D - 50. Runoff Hydrographs for RCNE – Rock Creek at Ceresco for May 7, 2015 Event
Deficit and Constant Method – Non-Optimized Initial Conditions

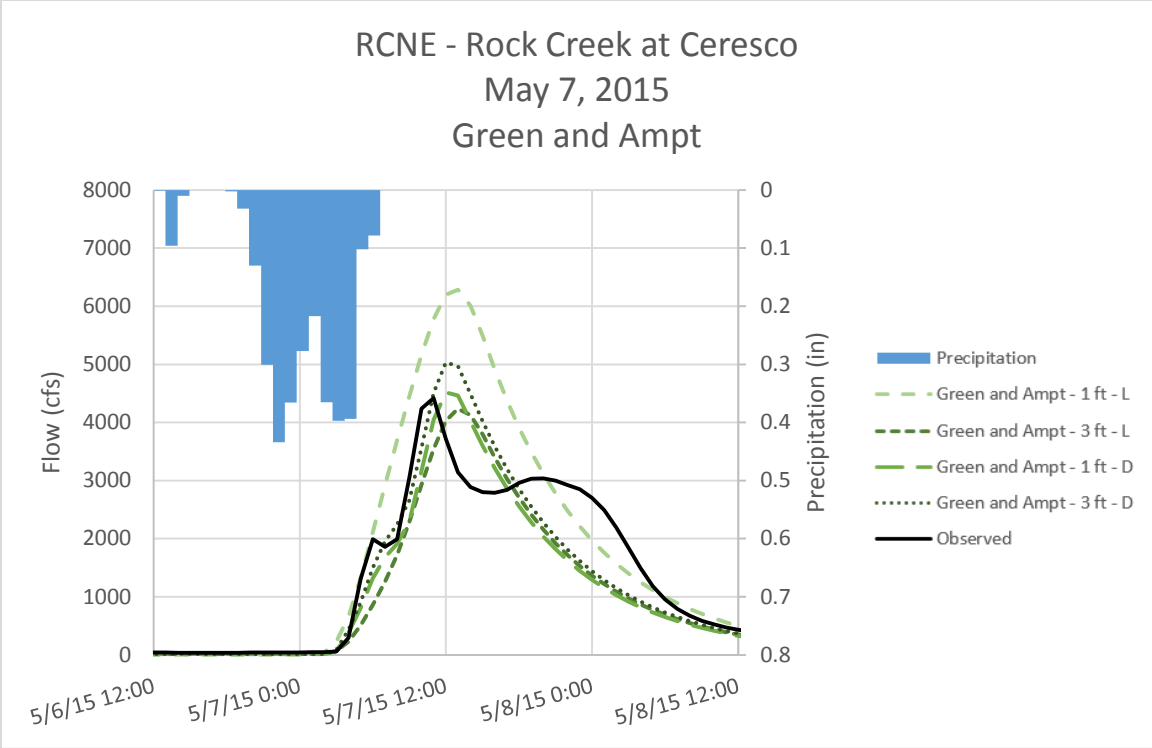

Figure D - 51. Runoff Hydrographs for RCNE – Rock Creek at Ceresco for May 7, 2015 Event
Green and Ampt Method – Non-Optimized Initial Conditions

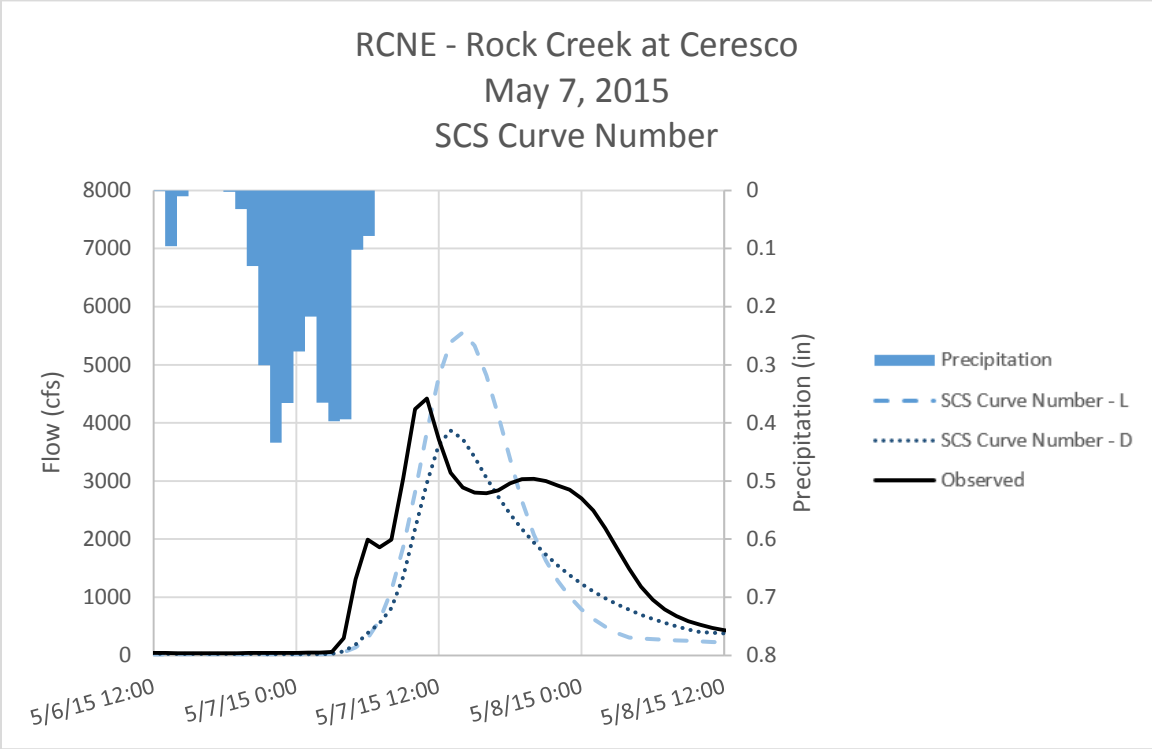

Figure D - 52. Runoff Hydrographs for RCNE – Rock Creek at Ceresco for May 7, 2015 Event
SCS Curve Number Method – Non-Optimized Initial Conditions

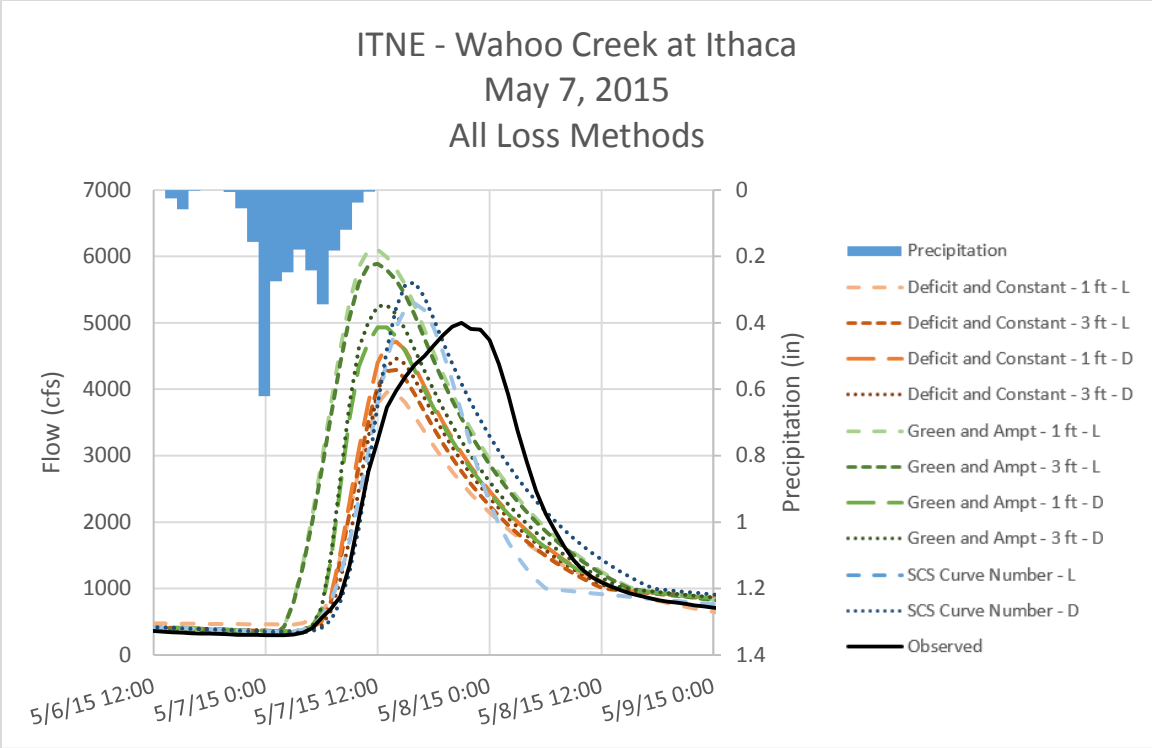

Figure D - 53. Runoff Hydrographs for ITNE – Wahoo Creek at Ithaca for May 7, 2015 Event
All Loss Methods – Non-Optimized Initial Conditions

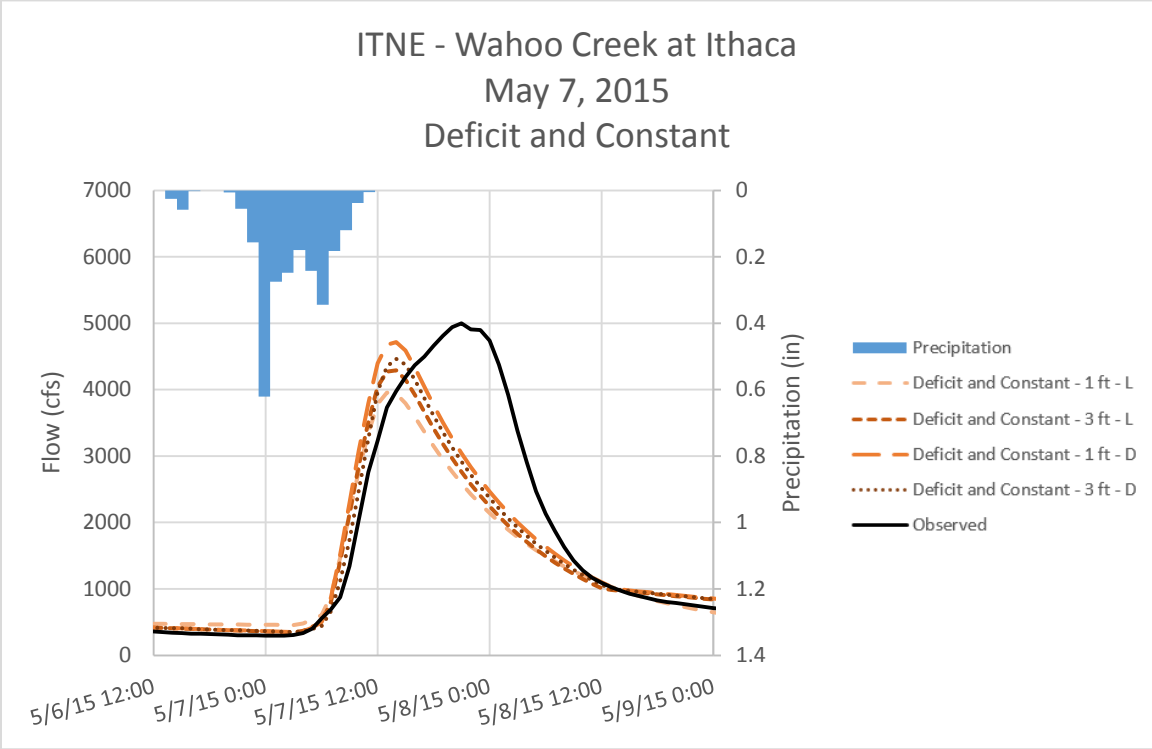

Figure D - 54. Runoff Hydrographs for ITNE – Wahoo Creek at Ithaca for May 7, 2015 Event
Deficit and Constant Method – Non-Optimized Initial Conditions

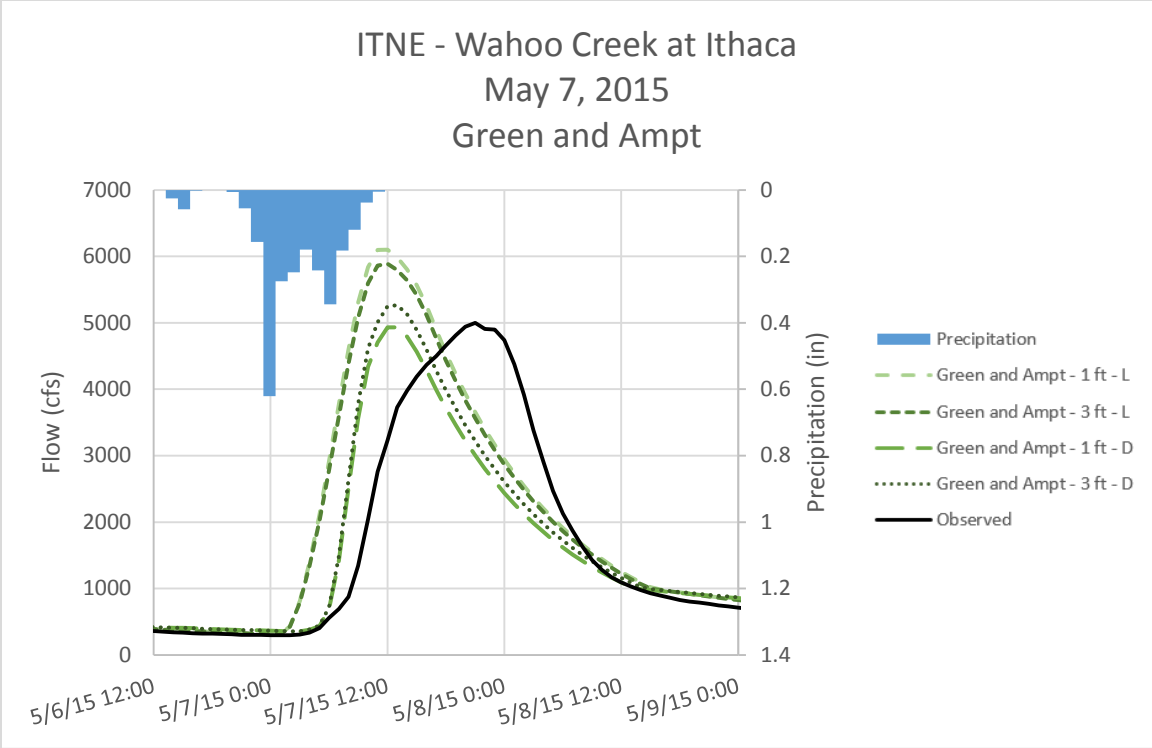

Figure D - 55. Runoff Hydrographs for ITNE – Wahoo Creek at Ithaca for May 7, 2015 Event
Green and Ampt Method – Non-Optimized Initial Conditions

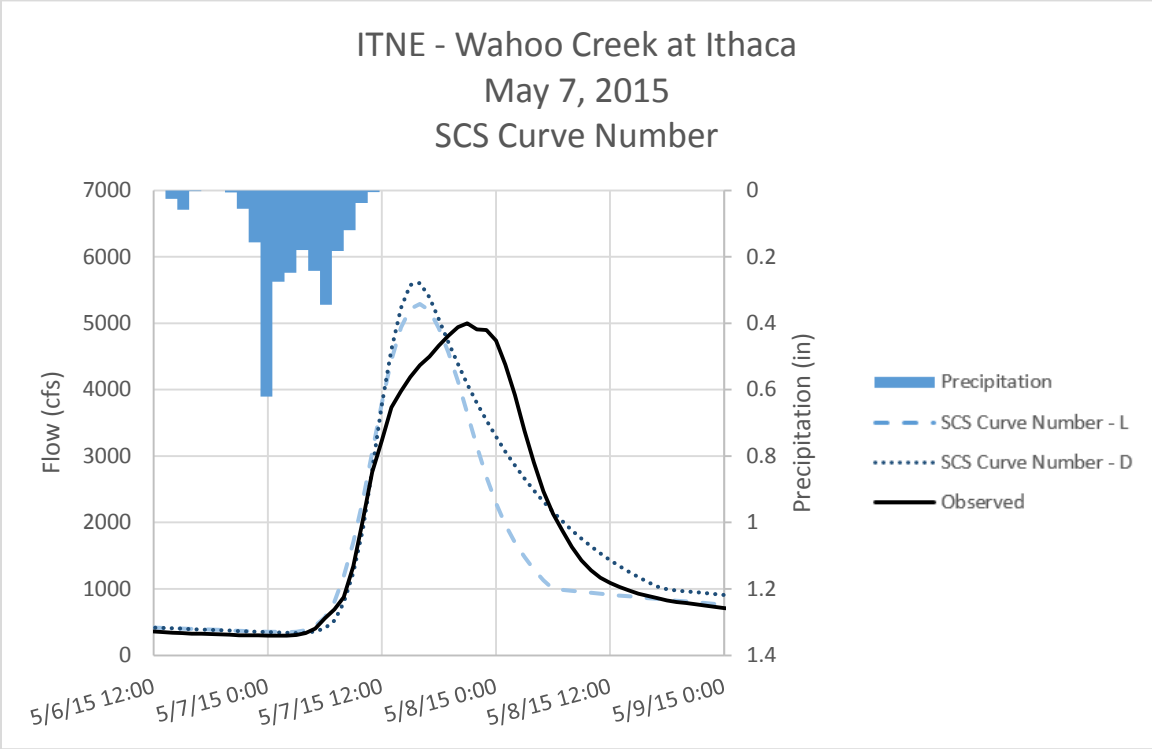

Figure D - 56. Runoff Hydrographs for ITNE – Wahoo Creek at Ithaca for May 7, 2015 Event
SCS Curve Number – Non-Optimized Initial Conditions

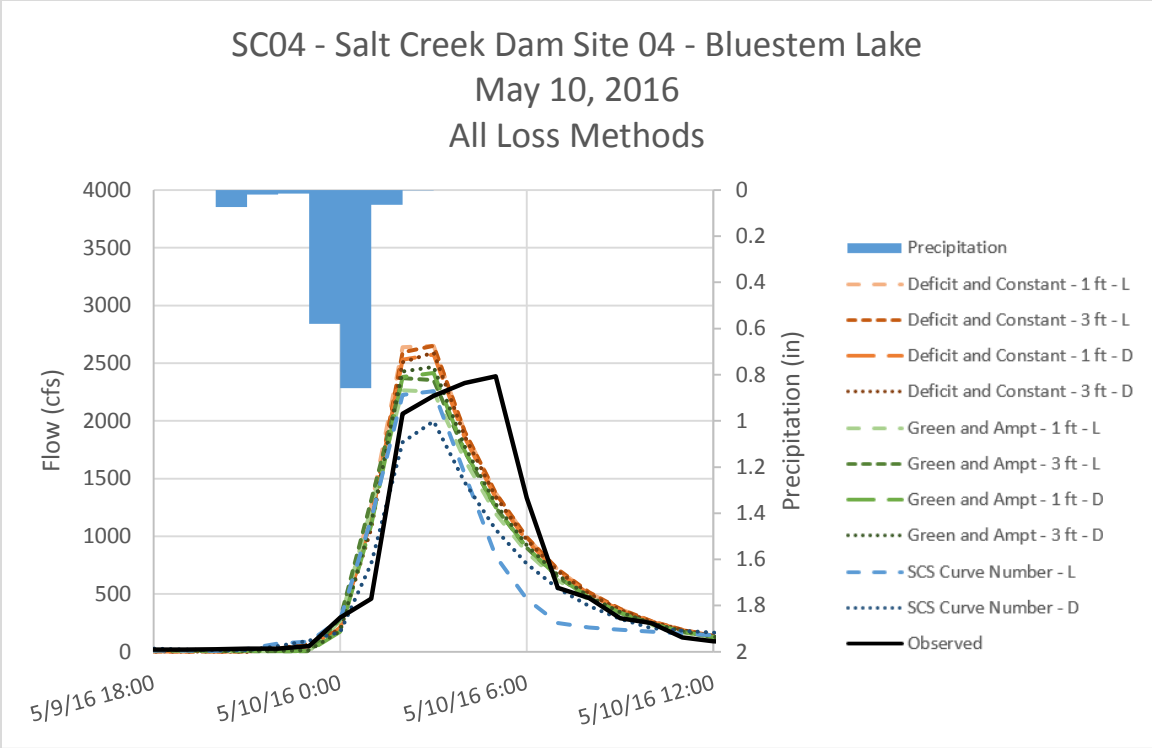

Figure D - 57. Runoff Hydrographs for SC04 - Salt Creek Dam Site 04 - Bluestem Lake for May 10, 2016 Event All Loss Methods – Non-Optimized Initial Conditions

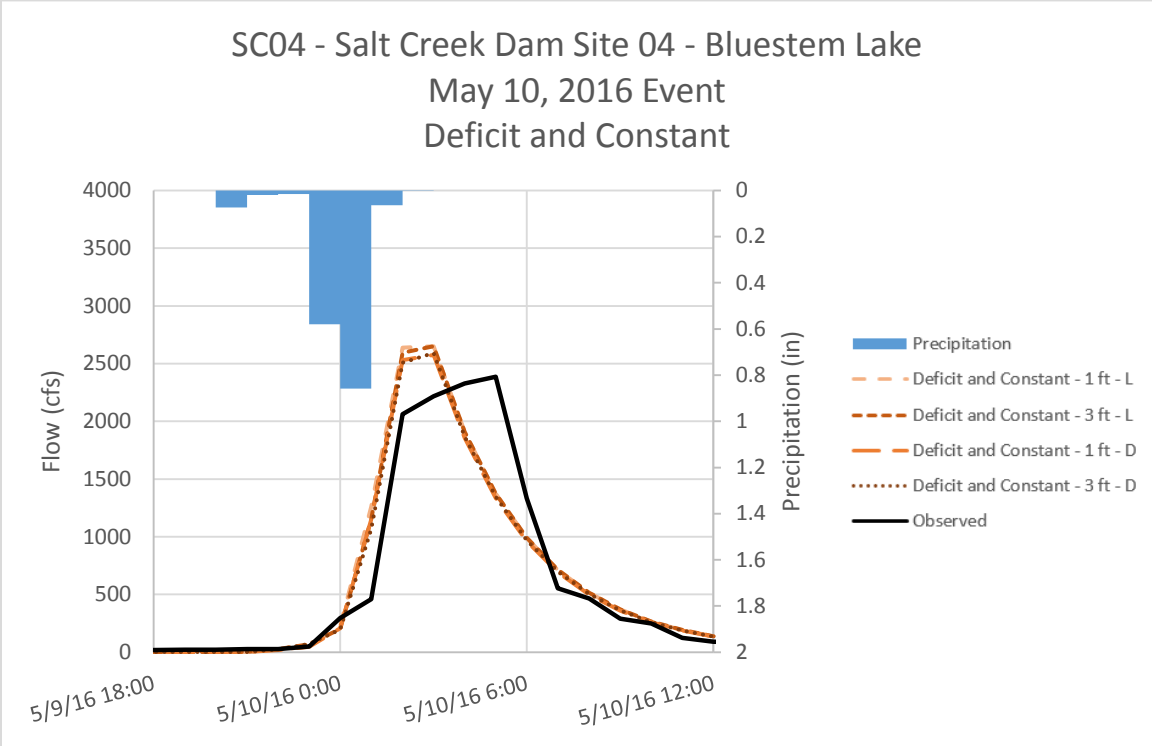

Figure D - 58. Runoff Hydrographs for SC04 - Salt Creek Dam Site 04 - Bluestem Lake for May 10, 2016 Event Deficit and Constant Method – Non-Optimized Initial Conditions

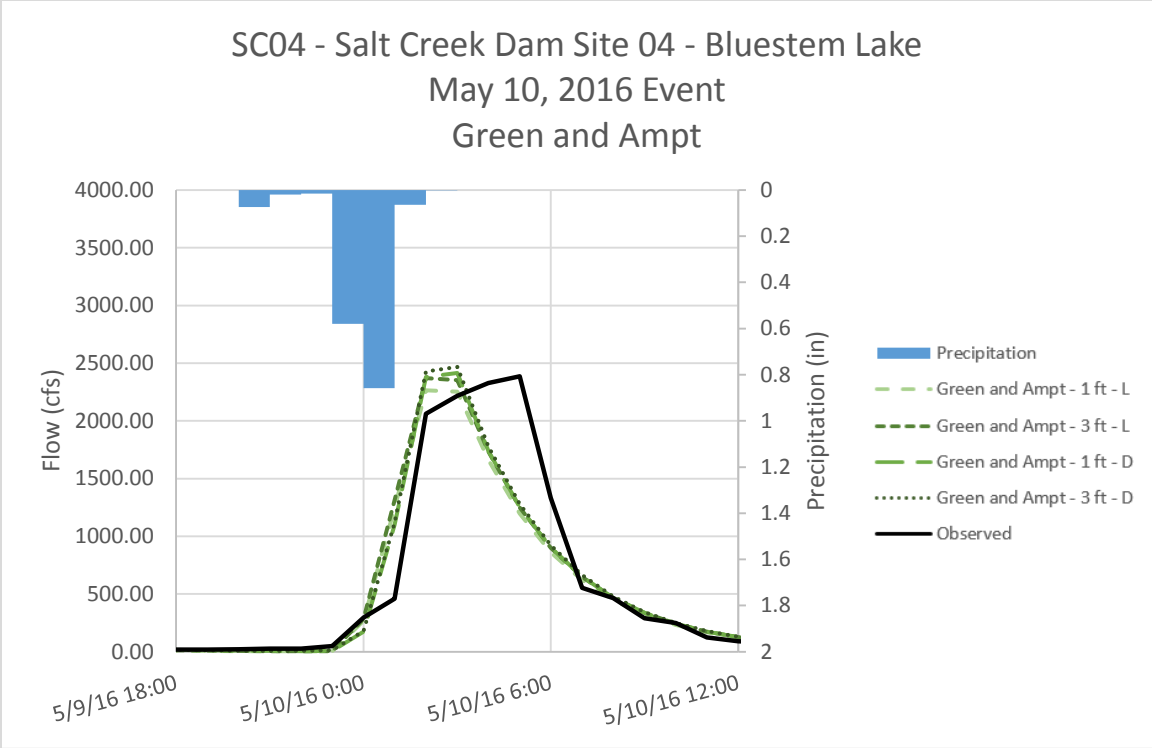

Figure D - 59. Runoff Hydrographs for SC04 - Salt Creek Dam Site 04 - Bluestem Lake for May 10, 2016 Event Green and Ampt Method – Non-Optimized Initial Conditions

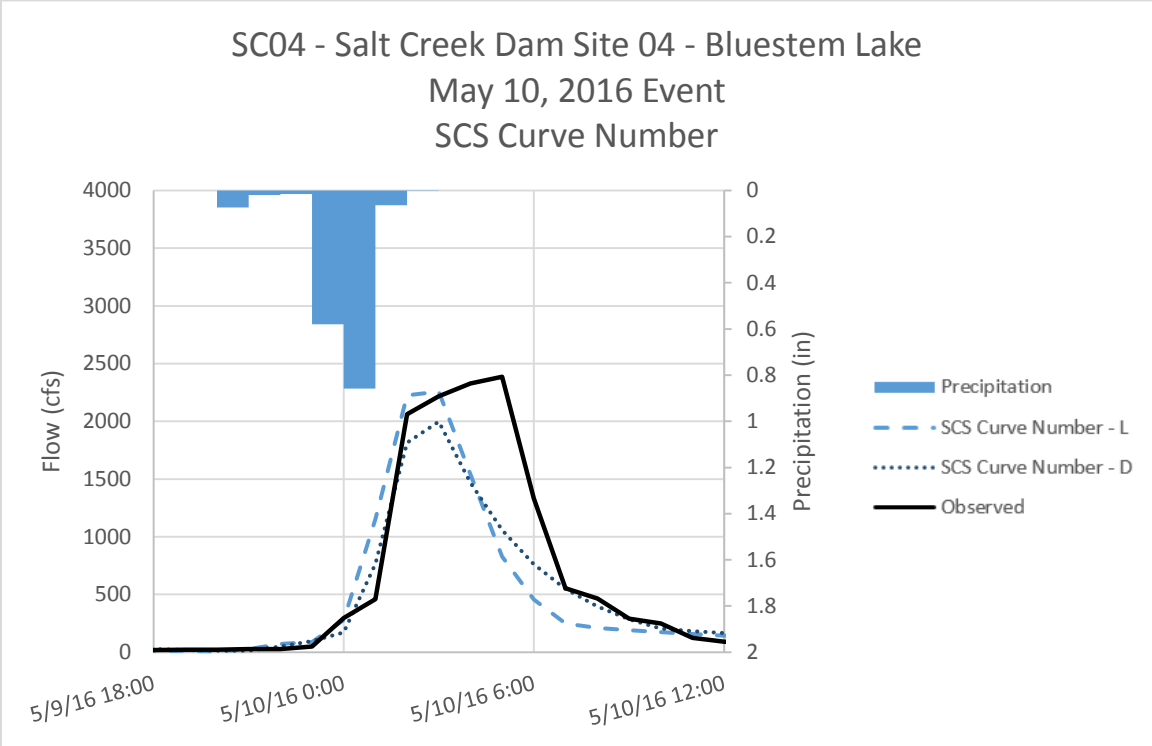

Figure D - 60. Runoff Hydrographs for SC04 - Salt Creek Dam Site 04 - Bluestem Lake for May 10, 2016 Event SCS Curve Number Method – Non-Optimized Initial Conditions

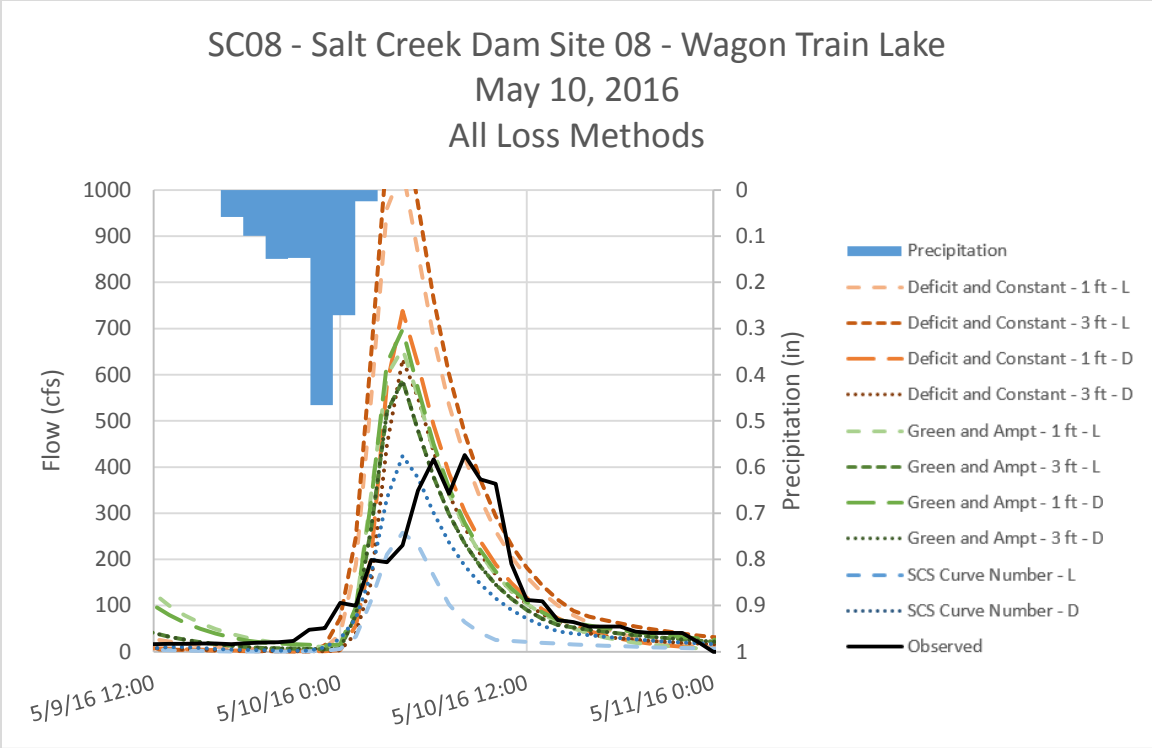

Figure D - 61. Runoff Hydrographs for SC08 - Salt Creek Dam Site 08 - Wagon Train Lake for May 10, 2016 Event All Loss Methods – Non-Optimized Initial Conditions

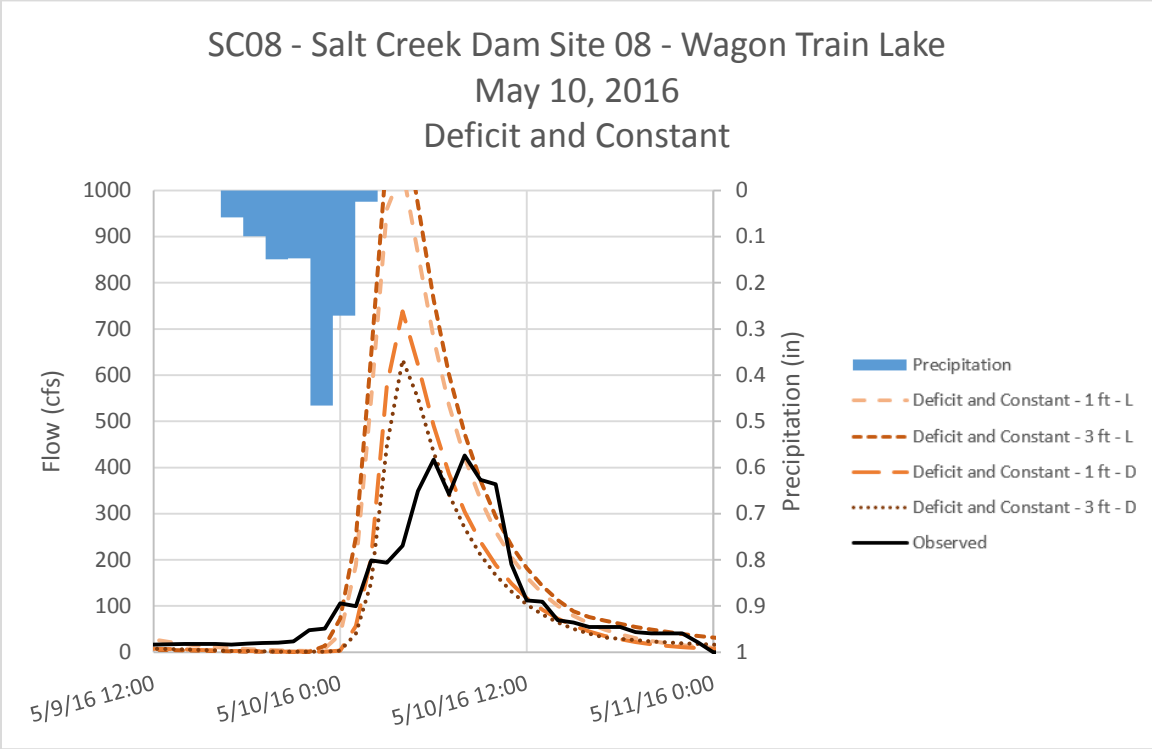

Figure D - 62. Runoff Hydrographs for SC08 - Salt Creek Dam Site 08 - Wagon Train Lake for May 10, 2016 Event Deficit and Constant Method – Non-Optimized Initial Conditions

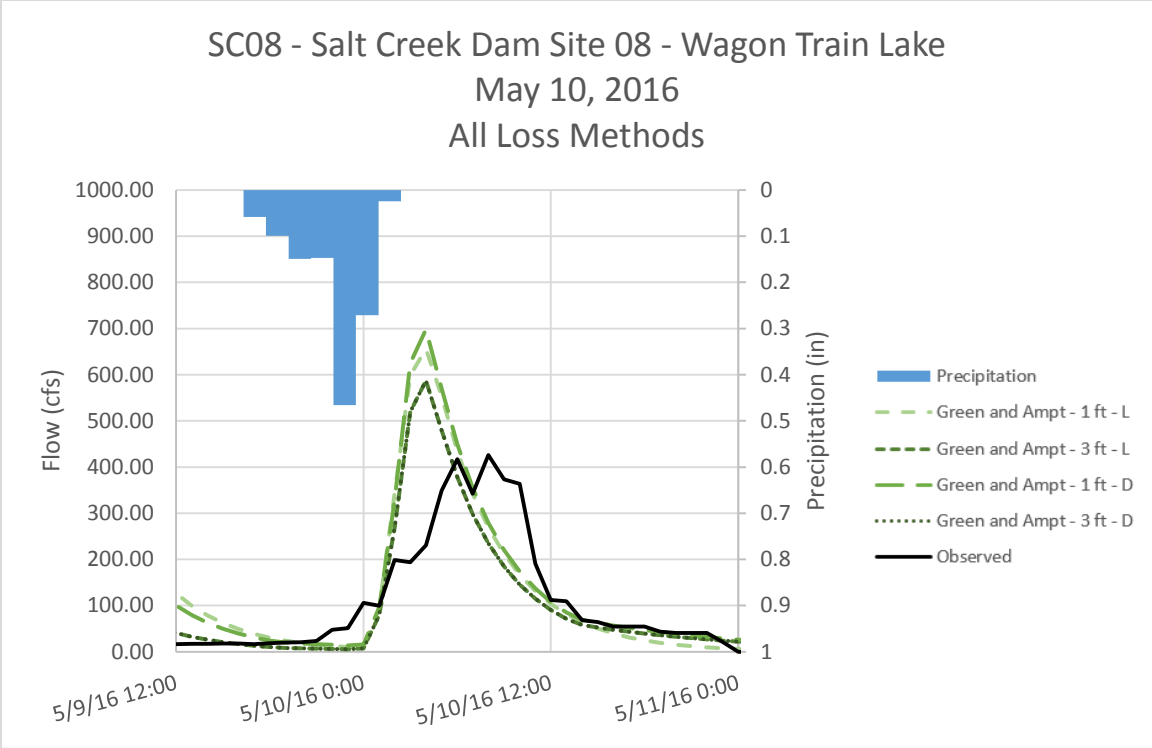

Figure D - 63. Runoff Hydrographs for SC08 - Salt Creek Dam Site 08 - Wagon Train Lake for May 10, 2016 Event Green and Ampt Method – Non-Optimized Initial Conditions

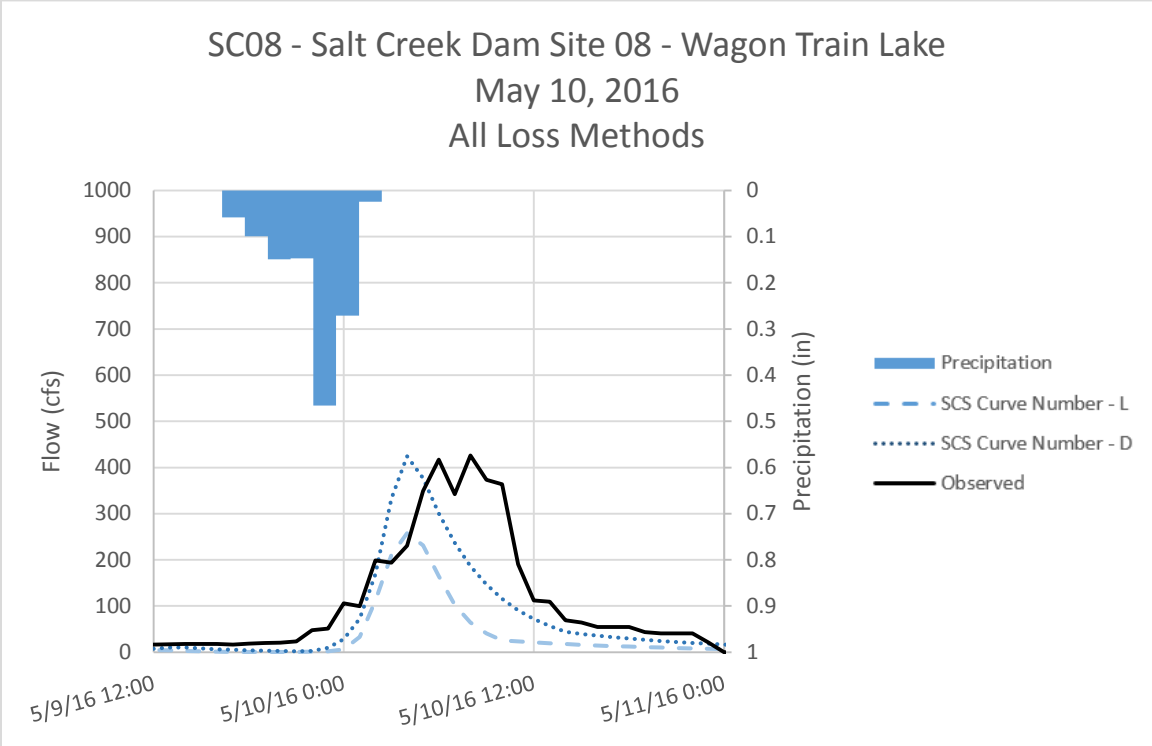

Figure D - 64. Runoff Hydrographs for SC08 - Salt Creek Dam Site 08 - Wagon Train Lake for May 10, 2016 Event SCS Curve Number Method – Non-Optimized Initial Conditions

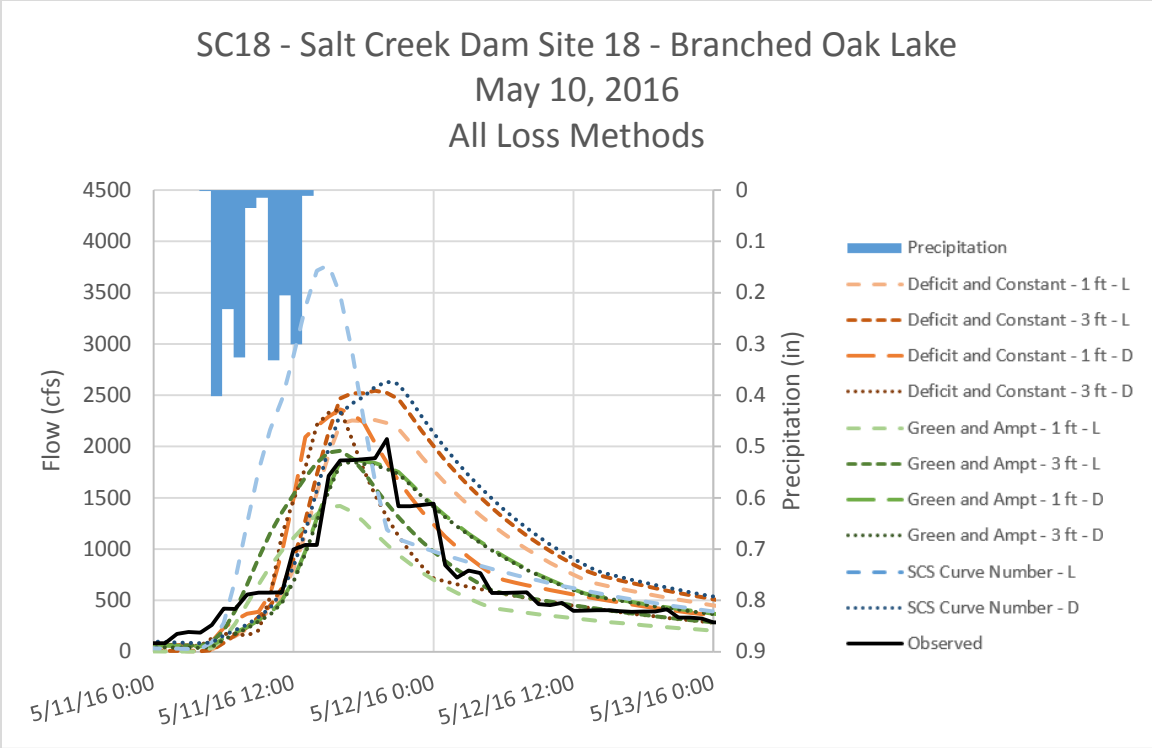

Figure D - 65. Runoff Hydrographs for SC18 - Salt Creek Dam Site 18 – Branched Oak Lake for May 10, 2016 Event All Loss Methods – Non-Optimized Initial Conditions

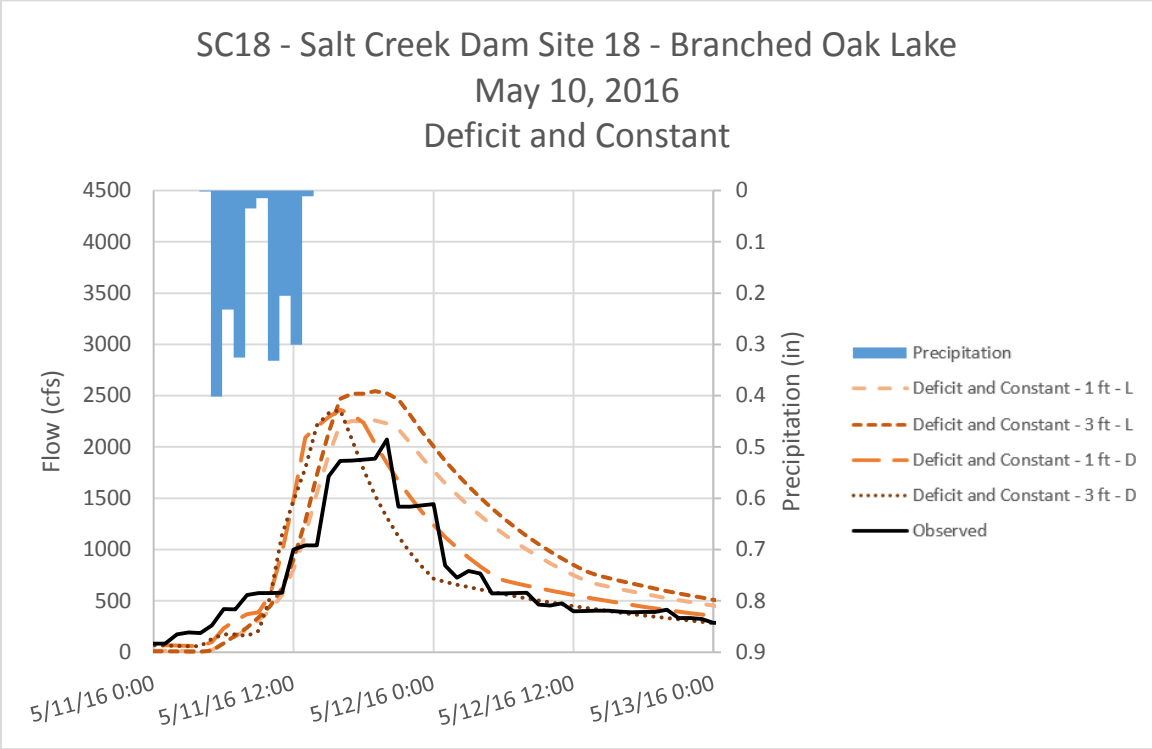

Figure D - 66. Runoff Hydrographs for SC18 - Salt Creek Dam Site 18 – Branched Oak Lake for May 10, 2016 Event Deficit and Constant Method – Non-Optimized Initial Conditions

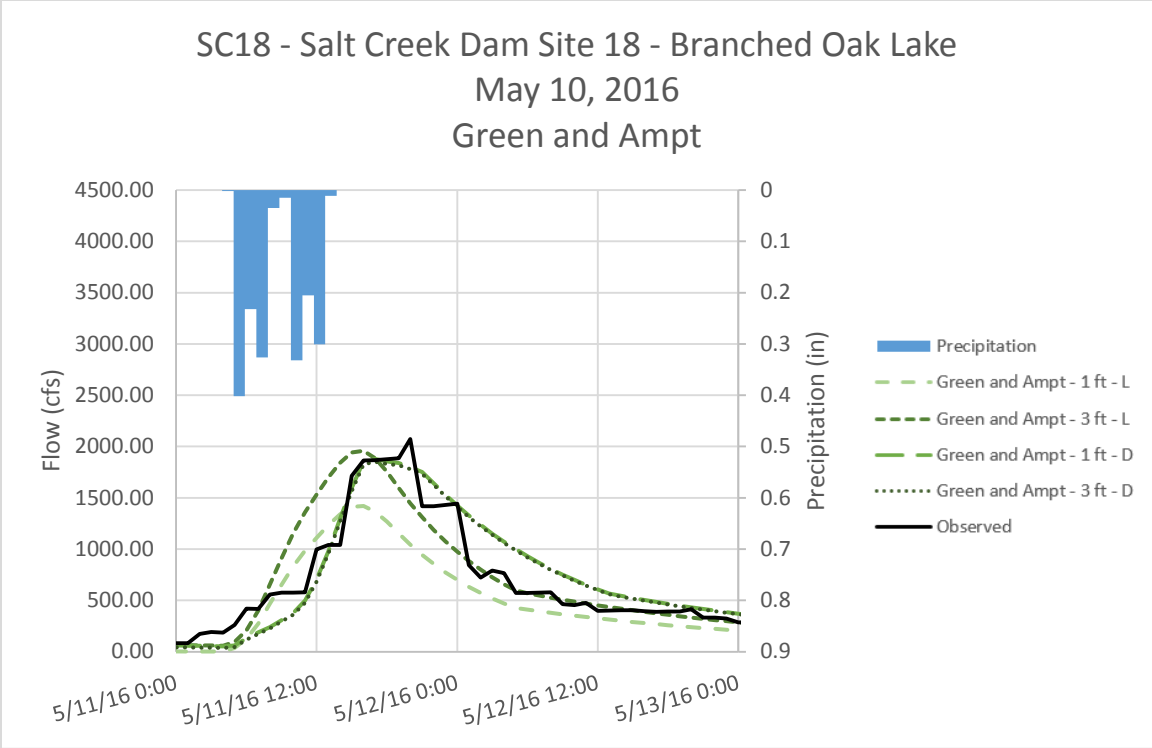

Figure D - 67. Runoff Hydrographs for SC18 - Salt Creek Dam Site 18 – Branched Oak Lake for May 10, 2016 Event Green and Ampt Method – Non-Optimized Initial Conditions

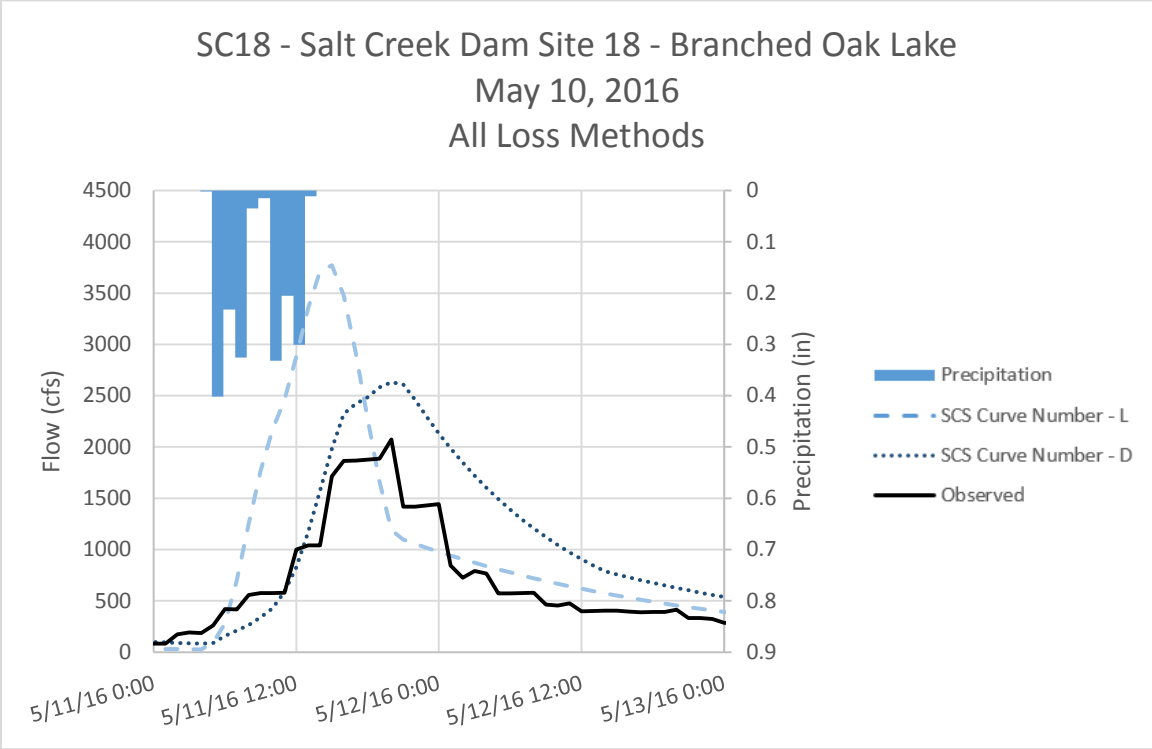

Figure D - 68. Runoff Hydrographs for SC18 - Salt Creek Dam Site 18 – Branched Oak Lake for May 10, 2016 Event SCS Curve Number Method – Non-Optimized Initial Conditions

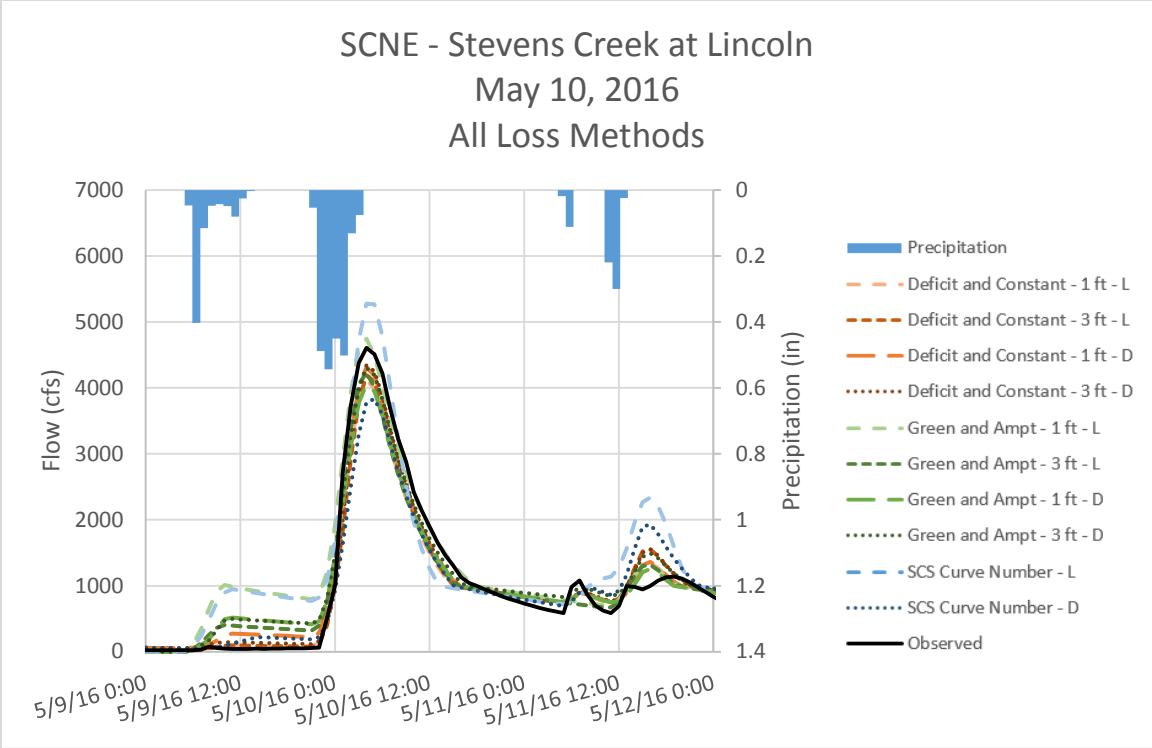

Figure D - 69. Runoff Hydrographs for SCNE – Stevens Creek at Lincoln for May 10, 2016 Event
All Loss Methods – Non-Optimized Initial Conditions

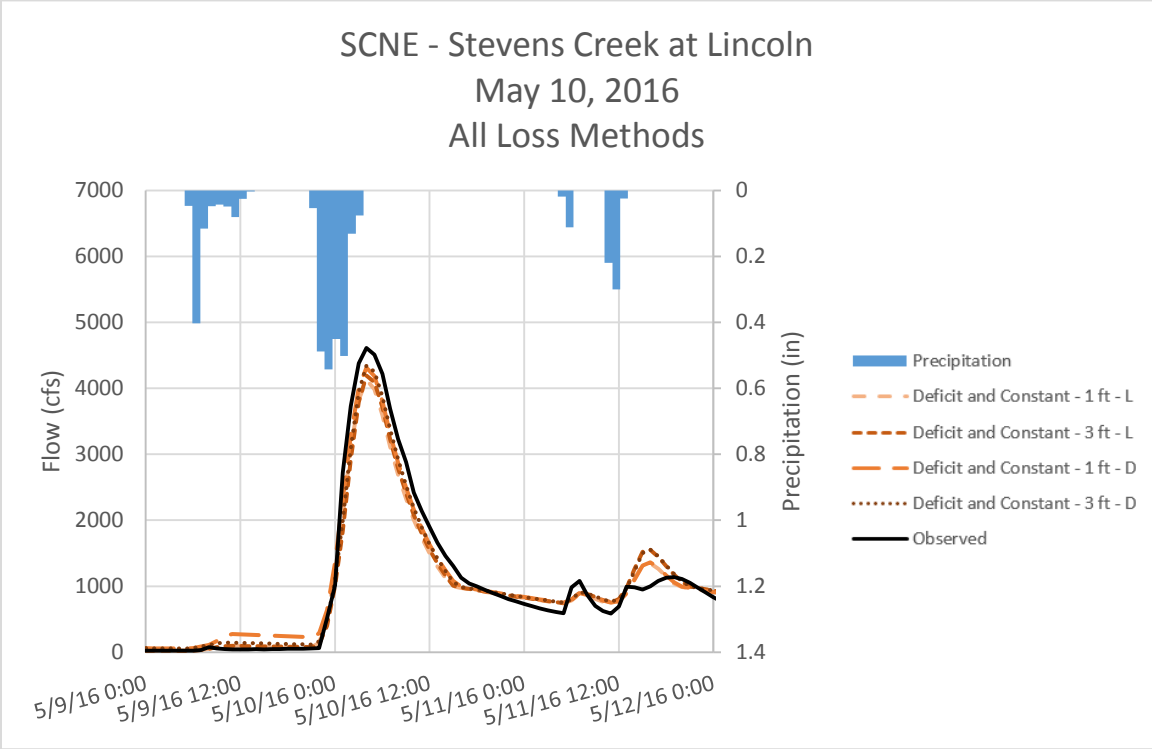

Figure D - 70. Runoff Hydrographs for SCNE – Stevens Creek at Lincoln for May 10, 2016 Event
Deficit and Constant Method – Non-Optimized Initial Conditions

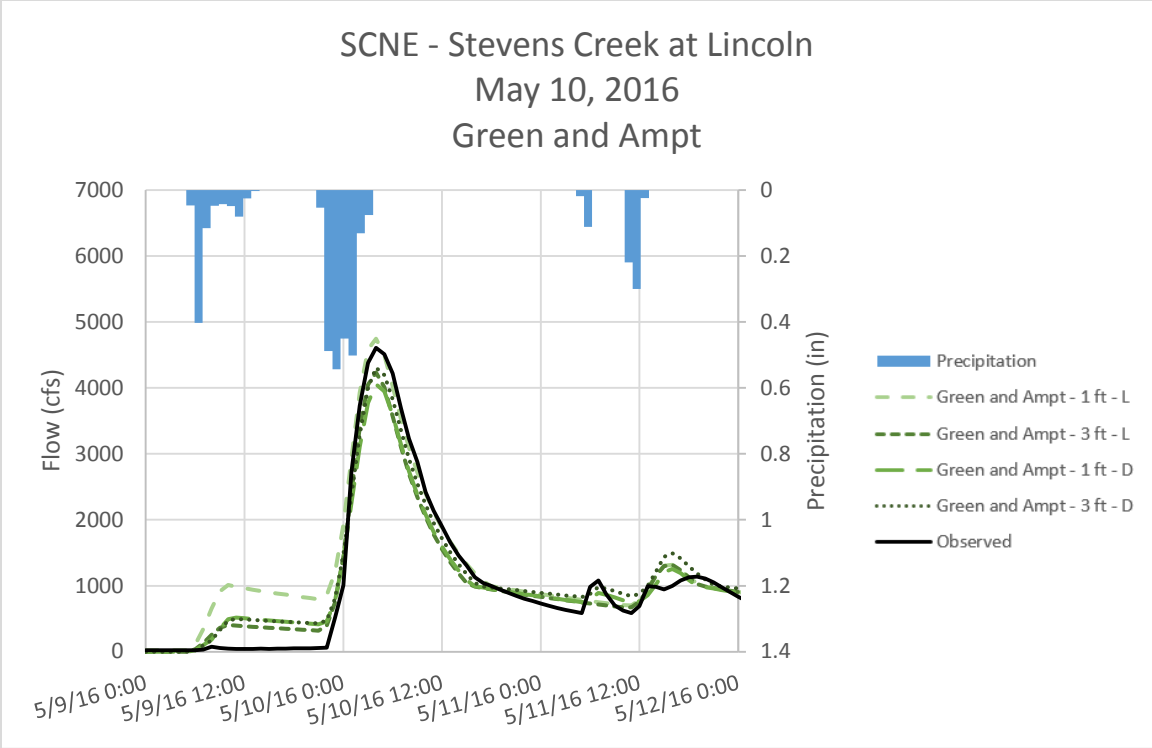

Figure D - 71. Runoff Hydrographs for SCNE – Stevens Creek at Lincoln for May 10, 2016 Event
Green and Ampt Method – Non-Optimized Initial Conditions

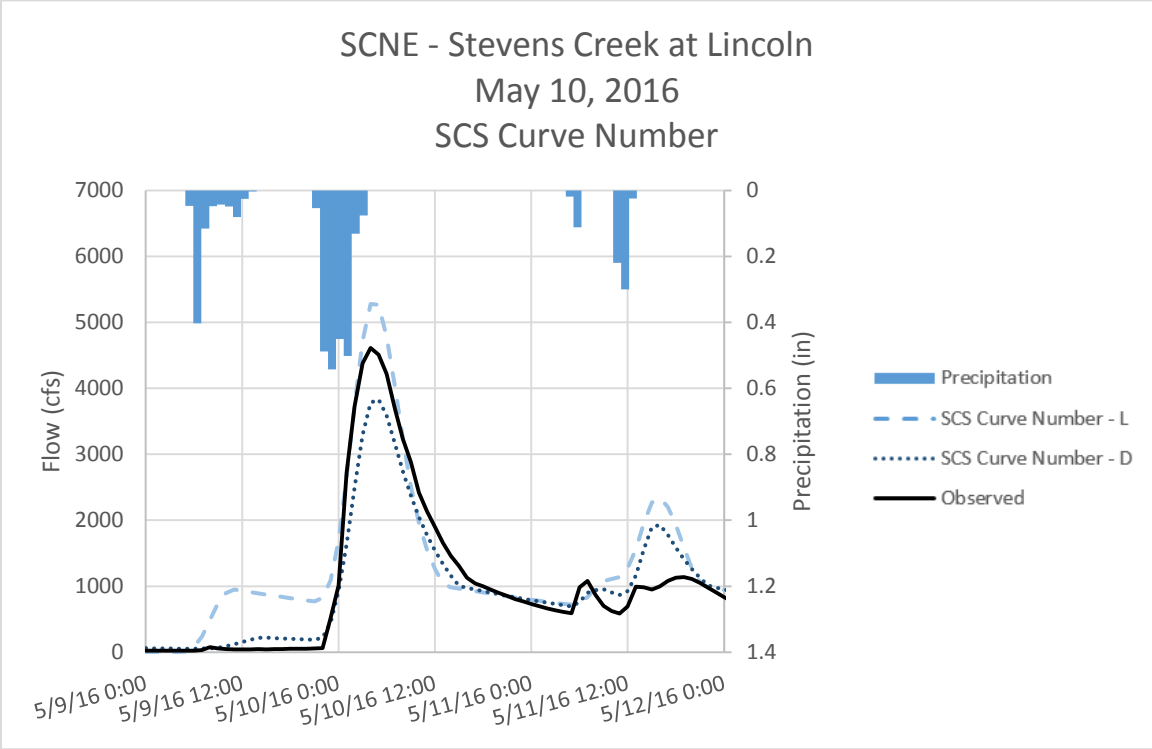

Figure D - 72. Runoff Hydrographs for SCNE – Stevens Creek at Lincoln for May 10, 2016 Event
SCS Curve Number Method – Non-Optimized Initial Conditions

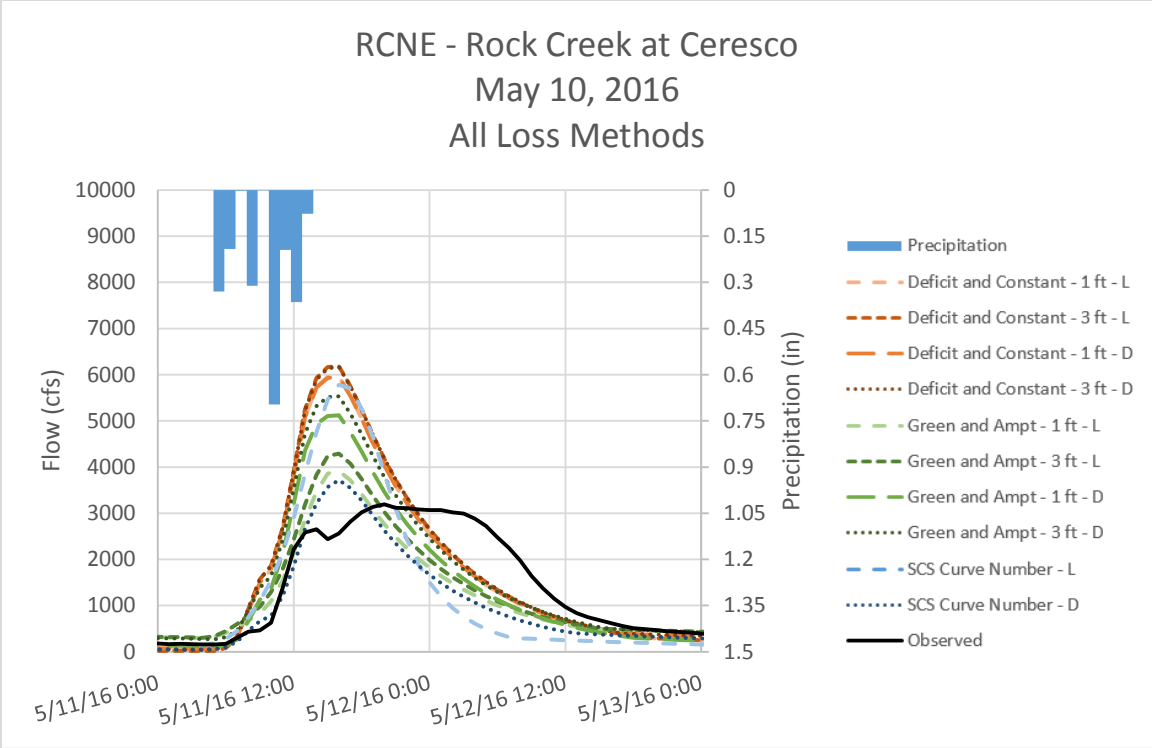

Figure D - 73. Runoff Hydrographs for RCNE – Rock Creek at Ceresco for May 10, 2016 Event All Loss Methods – Non-Optimized Initial Conditions

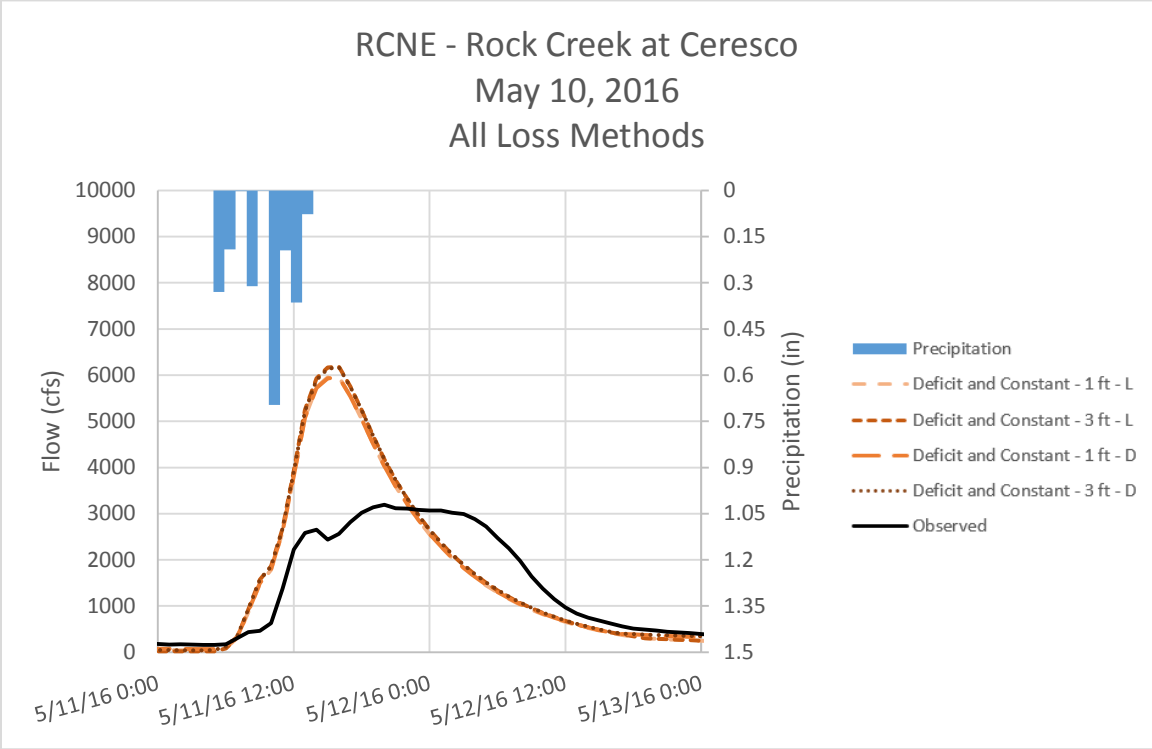

Figure D - 74. Runoff Hydrographs for RCNE – Rock Creek at Ceresco for May 10, 2016 Event Deficit and Constant Method – Non-Optimized Initial Conditions

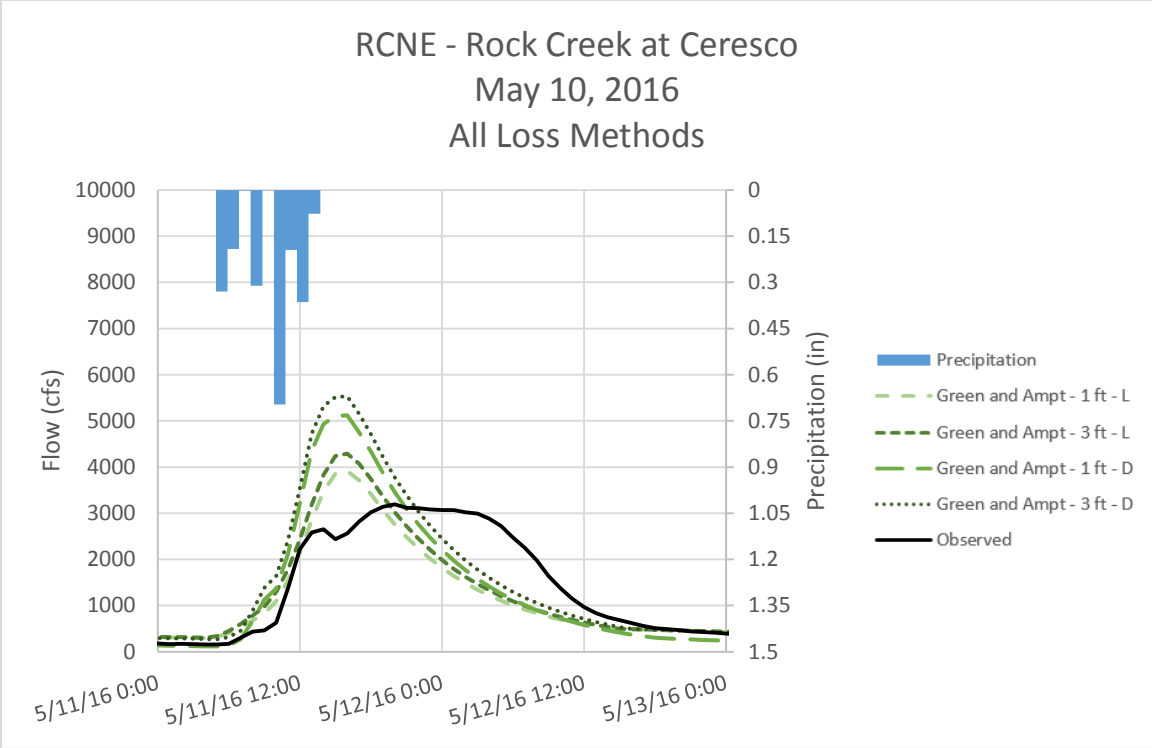

Figure D - 75. Runoff Hydrographs for RCNE – Rock Creek at Ceresco for May 10, 2016 Event
Green and Ampt Method – Non-Optimized Initial Conditions

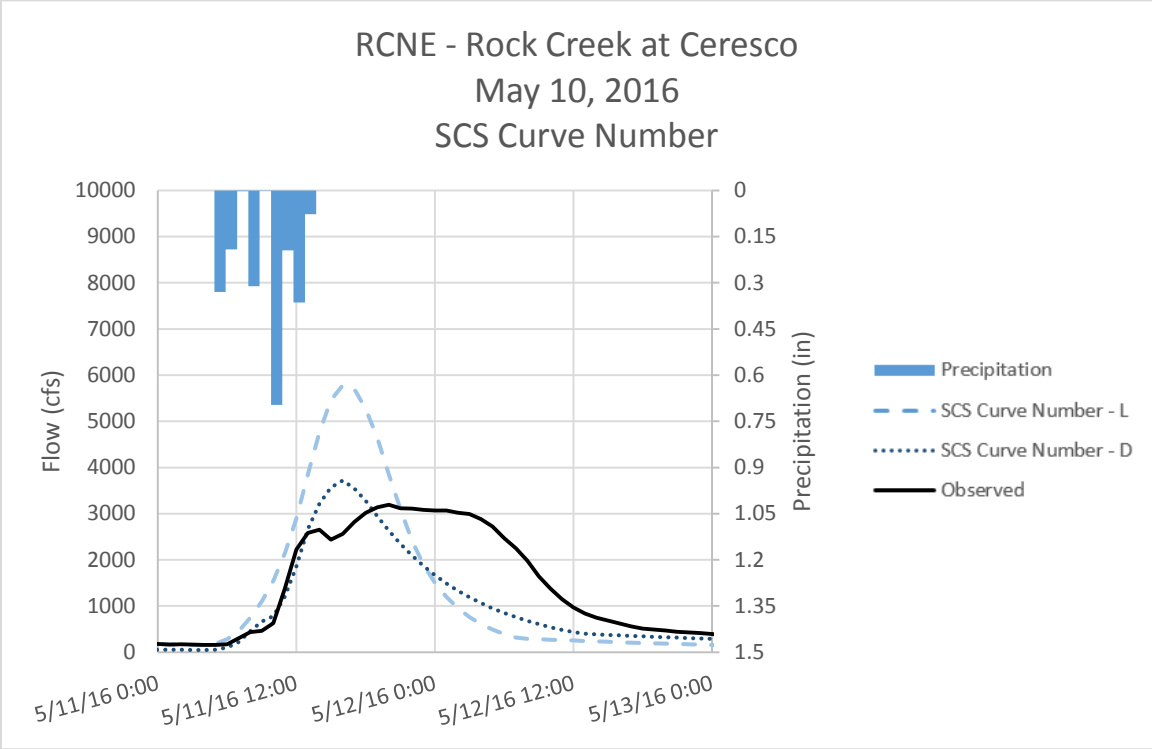

Figure D - 76. Runoff Hydrographs for RCNE – Rock Creek at Ceresco for May 10, 2016 Event
SCS Curve Number Method – Non-Optimized Initial Conditions

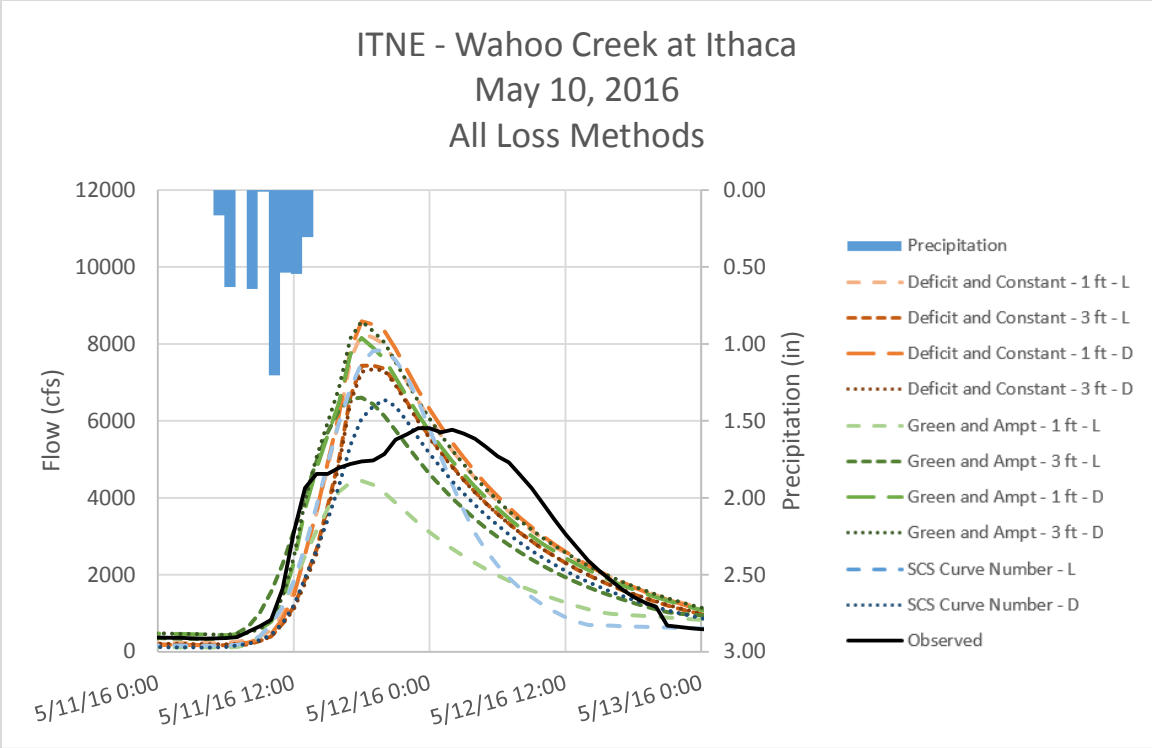

Figure D - 77. Runoff Hydrographs for ITNE – Wahoo Creek at Ithaca for May 10, 2016 Event
All Loss Methods – Non-Optimized Initial Conditions

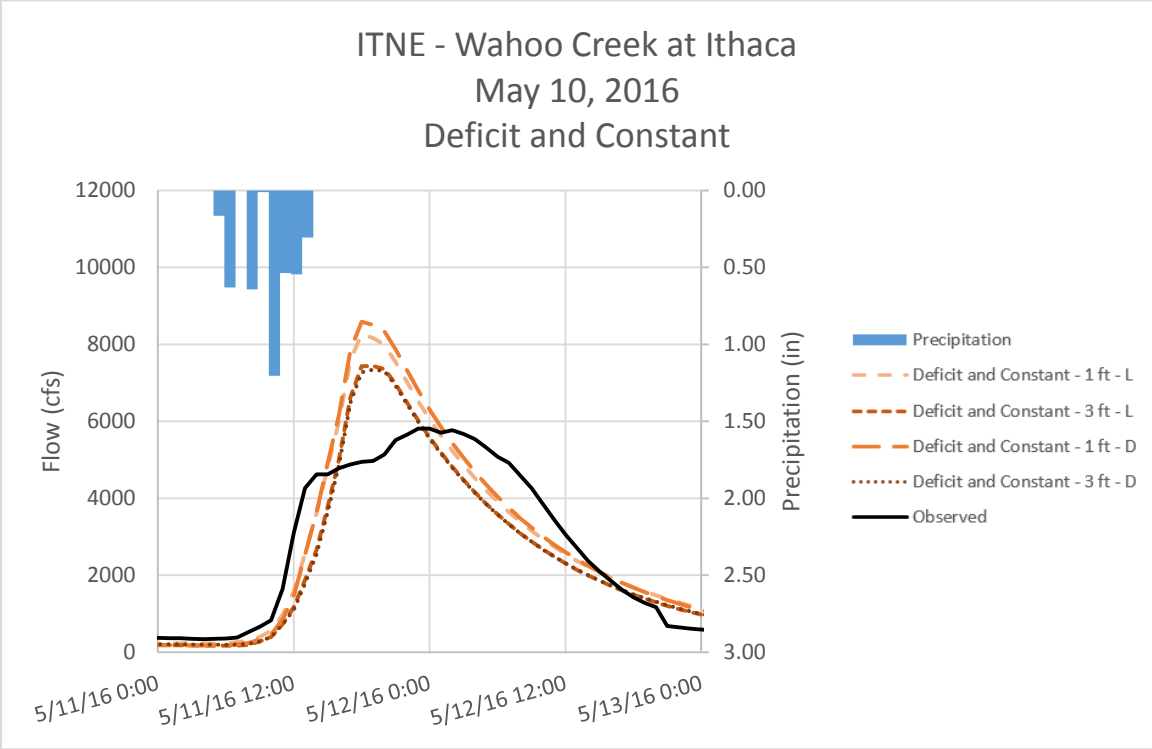

Figure D - 78. Runoff Hydrographs for ITNE – Wahoo Creek at Ithaca for May 10, 2016 Event
Deficit and Constant Method – Non-Optimized Initial Conditions

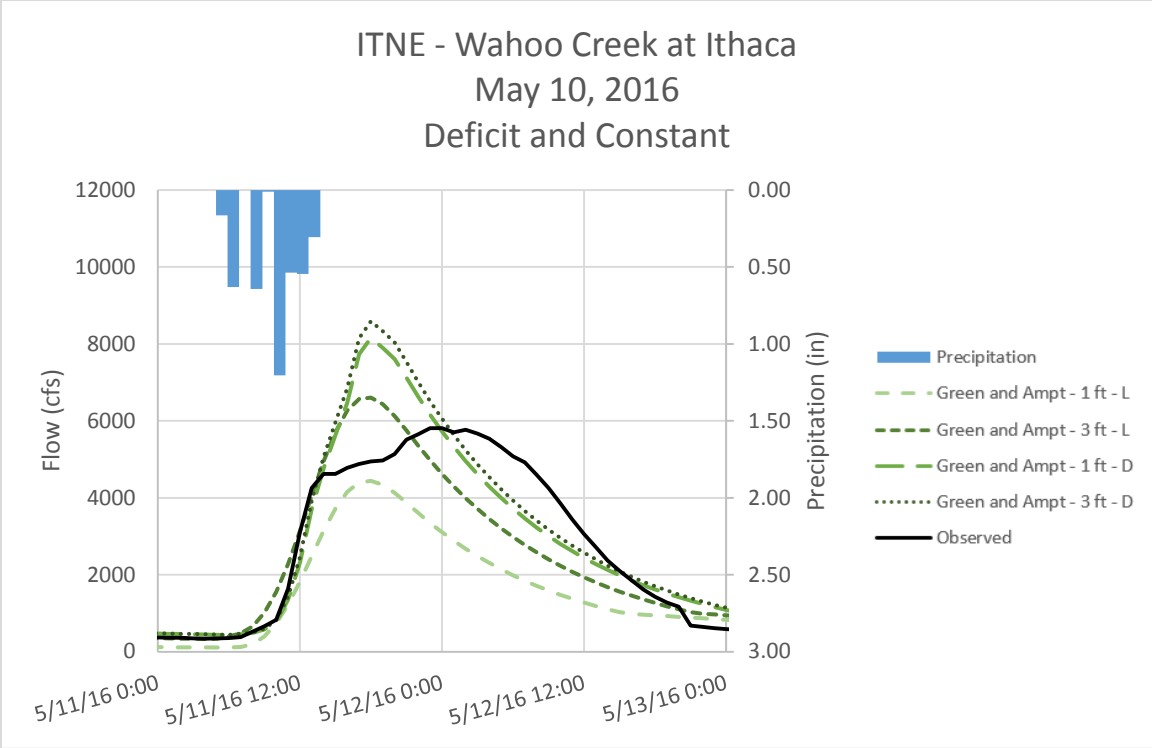

Figure D - 79. Runoff Hydrographs for ITNE – Wahoo Creek at Ithaca for May 10, 2016 Event
Green and Ampt Method – Non-Optimized Initial Conditions

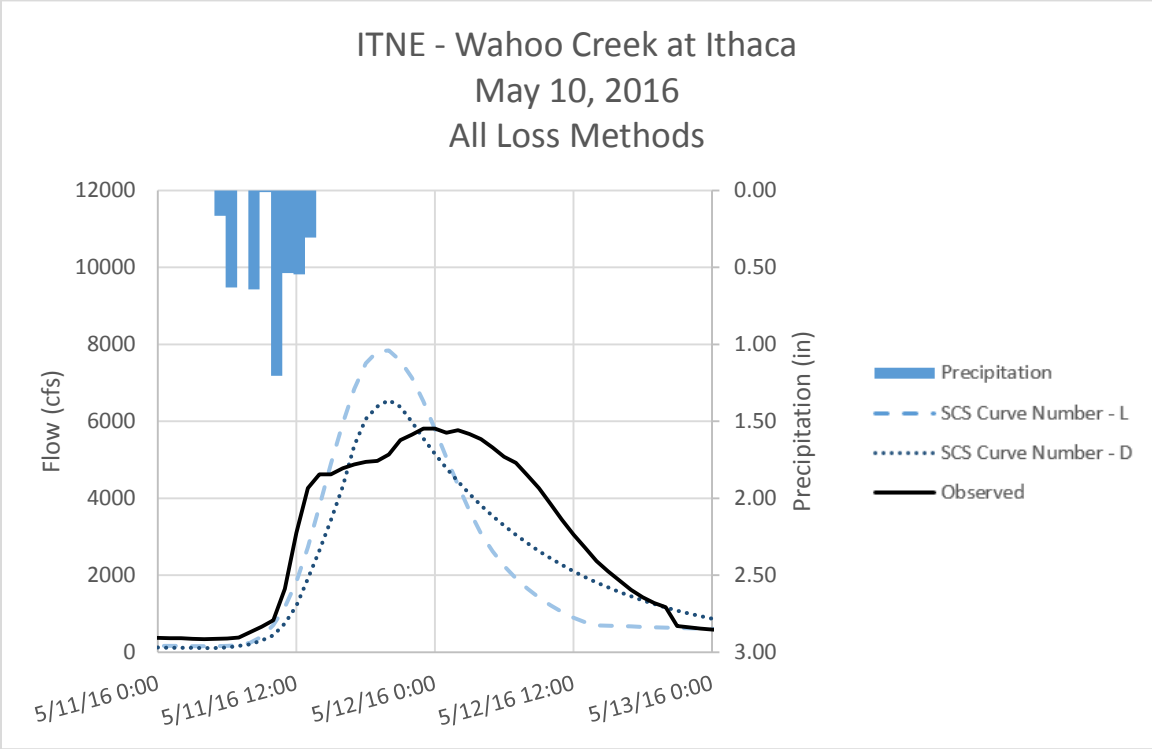

Figure D - 80. Runoff Hydrographs for ITNE – Wahoo Creek at Ithaca for May 10, 2016 Event
SCS Curve Number Method – Non-Optimized Initial Conditions